UNIVERSITAT DE BARCELONA

Unveiling novel components of the protein complex responsible for cGMP synthesis in retinal photoreceptors: role in cell physiology and disease

Santiago López Begines

Programa de Doctorado en Biomedicina

2012/2016

Unveiling novel components of the protein complex responsible for cGMP synthesis in retinal photoreceptors: role in cell physiology and disease

Memoria presentada por Santiago López Begines, licenciado en Bioquímica, para aspirar al grado de Doctor en Biomedicina. Este trabajo ha sido realizado en el Departamento de Patología y Terapéutica Experimental y en el Departamento de Ciencias Fisiológicas de la Facultad de Medicina de Bellvitge (Universitat de Barcelona)

Dirigida por,
Dra. Ana Méndez Zunzunegui
Investigadora IDIBELL
Departamento de Ciencias Fisiológicas
de la Universitat de Barcelona

Tutor,
Dr. Carles Solsona Sancho
Catedrático del Departamento de
Patología y Terapéutica
Experimental de la Universitat de
Barcelona

Santiago López Begines

Barcelona, Septiembre 2016

IDIBELL
Institut d'Investigació Biomèdica de Bellvitge

UNIVERSITAT DE BARCELONA

“Hay hombres que luchan
un día y son buenos. Hay
otros que luchan un año y
son mejores. Hay quienes
luchan muchos años y son
muy buenos. Pero los hay
que luchan toda una vida,
esos son los imprescindibles”

Bertolt Brecht

A Loreto,

a mis padres

y a mis hermanas

Table of Contents

Resumen en Español

Resumen en Español

La vía mediante la cual la luz produce señales neuronales para iniciar la percepción y discriminación de objetos, movimientos, sombras y colores comienza en la retina. La retina está formada por varias capas celulares, siendo las células fotorreceptor cono y bastón las neuronas responsables de la fototransducción. Las células fotorreceptor de la retina, conos y bastones, son neuronas altamente compartimentalizadas y especializadas en responder a la luz. La fototransducción comienza con la captación de un fotón por el pigmento visual, que desencadena una cascada de señalización por proteína G que en último término provoca la disminución de los niveles de cGMP. Esta disminución provoca el cierre de los canales dependientes de cGMP en la membrana, interrumpiendo la entrada de cationes y causando la hiperpolarización de la célula. Esta hiperpolarización disminuye la tasa de liberación de neurotransmisor en la terminal sináptica, que es la señal que se transmite a neuronas de orden superior, y en último término al cerebro. Los procesos de terminación de la respuesta una vez se ha respondido a la luz también son esenciales para el funcionamiento correcto de conos y bastones. Los fotorreceptores deben restablecer el equilibrio de oscuridad con la cinética adecuada para recuperar la sensibilidad a la luz, la capacidad de responder a nuevos estímulos visuales. Defectos genéticos tanto a nivel de activación como de terminación de la señal dan lugar a distintas formas de ceguera hereditaria.

El complejo proteico en cuya caracterización se centra este trabajo, responsable de la síntesis de GMP cíclico en conos y bastones, juega un papel clave en la terminación de la señal, y ha sido vinculado a varias formas de distrofia de retina. Para el restablecimiento del equilibrio de oscuridad, hay dos procesos importantes en la terminación de la respuesta: uno, la inactivación de los componentes enzimáticos en la cascada de activación; y dos, la restauración de los niveles de cGMP a los niveles de oscuridad por nueva síntesis. El complejo responsable de la síntesis de cGMP en conos y bastones consiste en una forma particulada de guanilato ciclasa específica de retina (RetGC1 en su isoforma más relevante), y dos proteínas que le confieren sensibilidad a calcio (las Guanylate Cyclase Activating Proteins GCAP1 y GCAP2). La actividad ciclasa es estimulada por la bajada en la concentración de Ca2+ que ocurre durante el cierre de los canales en respuesta a la luz. La estimulación de la ciclasa restaura los niveles de cGMP, y con ello la apertura de los canales y los niveles de Ca2+. El aumento en la concentración de Ca2+ inhibe a la ciclasa, cerrando el bucle. Este bucle de regulación entre cGMP y Ca2+ es fundamental en el proceso de terminación de la respuesta a la luz y en adaptación visual. Mutaciones en los genes que codifican RetGC1, GCAP1 y GCAP2 han sido ligadas a mutaciones en el complejo Amaurosis Congénita de Leber *(*LCA), Retinitis Pigmentaria *(*RP) y *Cone-Rod Dystrophies*

autosómicas dominantes (adCORD), debido a que provocan alteraciones de los niveles de cGMP en la célula, que resultan de alguna manera en una gran toxicidad.

El modelo de regulación de la actividad guanilato ciclasa por las proteínas GCAP ha sido extensamente estudiado *in vitro*, a nivel bioquímico y estructural. Sin embargo, hay muchos aspectos relevantes de la acción de este complejo en el entorno de la célula viva que se desconocen: - ¿Dónde se ensambla el complejo y cómo se transporta? – ¿Cómo se integra y se modula este complejo en la célula? – ¿Cómo conducen las mutaciones a la muerte celular?

Para abordar estas preguntas, los objetivos principales de este trabajo son: i) caracterizar los mecanismos que gobiernan la distribución subcelular de las proteínas GCAP1 y GCAP2 en células fotorreceptor, para establecer dónde se ensambla el complejo; y ii) la búsqueda de nuevos interactores moleculares del complejo RetGC/GCAPs por una aproximación proteómica, que contribuyan a entender como este complejo se ensambla, se organiza y se transporta hacia el segmento sensorial, así como su regulación *in vivo*.

Debido a que los estudios celulares en este campo se ven dificultados por la alta especialización de las células fotorreceptor, y la falta de modelos celulares en cultivo que permitan hacer estudios genéticos, bioquímicos y funcionales, un objetivo de esta tesis (precedente a los mencionados) era implementar estrategias genéticas para abaratar y acelerar los estudios de función génica *in vivo*. Para ello, el trabajo se ha centrado en implementar la electroporación de DNA *in vivo* en retina para generar transgénicos transitorios (Matsuda and Cepko, 2004), y en tratar de lograr la electroporación de DNA *in vivo* en espermatogonia primaria para la generación de transgénicos estables.

La generación de animales transgénicos estables mediante transfección por electroporación de línea germinal masculina desarrollada por S. Majumdar (NII, New Delhi, India) (Dhup and Majumdar, 2008) hubiera supuesto una herramienta genética muy potente para nuestros estudios de haber funcionado. Sin embargo, tras numerosos intentos de electroporación *in vivo* siguiendo diversos procedimientos quirúrgicos con vectores de expresión gradualmente optimizados -incluyendo la utilización de plásmidos libres de isletas CpG, el uso de secuencias aisladoras flanqueando el transgén, el acompañamiento de inhibidores de la acetilación de histonas…- no hemos observado transfección de células de espermatogonia a niveles significativos, ni logrado la producción de animales transgénicos. En último término diseñamos un experimento para determinar cuantitativamente la eficiencia con que la transfección de línea germinal por electroporación de DNA *in vivo* podía funcionar. Para ello utilizamos el gen reportero fluorescente DsRed con señal de localización mitocondrial en un vector de expresión ubíquito y robusto, libre de isletas CpG, que permitiese contabilizar los espermatozoides fluorescentes

resultantes por citometría de flujo. El porcentaje de espermatozoides fluorescentes en animales transfectados fue el 0,4% del total, en comparación al 0,15% de *background* en animales control. Concluimos que esta metodología no es viable tal como está descrita. Futuros estudios establecerán los mecanismos y procedimientos adecuados para la transfección eficiente de las células germinales.

Para la generación de ratones transgénicos transitorios en retina, hemos reproducido eficientemente la metodología desarrollada por C. Cepko (Harvard, EEUU) (Matsuda and Cepko, 2004). Mediante la electroporación subretinal de DNA *in vivo*, hemos caracterizado los determinantes moleculares para la localización subcelular de las proteínas GCAPs, estableciendo que el complejo RetGC/GCAPs se ensambla en el segmento interno del fotorreceptor antes de ser transportado hacia el compartimento sensorial. Así, para el tráfico de GCAP1 hacia el segmento externo del fotorreceptor es indispensable tanto la miristoilación de la proteína como su unión a la guanilato ciclasa. Por otro lado, la activación del complejo RetGC/GCAPs no es un requerimiento para su transporte hacia el segmento externo. Mediante electroporación subretinal en retina hemos demostrado también que la fosforilación juega un papel clave en la distribución celular de GCAP2, y que fallos en la localización de GCAP2 podrían contribuir a explicar la patofisiología de la mutación hG157R ligada a retinosis pigmentaria autosómica dominante.

Para la consecución del segundo objetivo, hemos realizado una aproximación proteómica para identificar nuevos interactores de GCAP1 que nos ha conducido al descubrimiento inesperado de la interacción directa de la inosina monofosfato deshidrogenasa (IMPDH1) con la guanilato ciclasa en el compartimento sensorial, donde tiene lugar la fototransducción. IMPDH1 es la enzima responsable del paso limitante en la síntesis *de novo* de GTP, y mutaciones en el gen impdh1 han sido asociadas a adRP y Amaurosis congénita de Leber (LCA). La interacción, que ocurre con una afinidad en el orden micromolar, involucra a los dominios de dimerización y catalítico de RetGC1 y se afecta significativamente por los mutantes asociados a ceguera en IMPDH1. Este hallazgo une la síntesis *de novo* de GTP con la conversión de GTP en cGMP, agrupando genes asociados a enfermedad anteriormente considerados no relacionados y creando un nuevo marco conceptual para el desarrollo de nuevas estrategias terapéuticas. A la vez, contribuye a reducir la aparente complejidad de las distrofias hereditarias de retina debidas a la gran heterogeneidad genética que las originan –más de cien genes distintos han sido ligados a ceguera hereditaria-, a agrupar genes asociados a enfermedad en base a su implicación en procesos metabólicos comunes. La finalidad última de esta estrategia de agrupamiento de genes en base a su función busca identificar “hubs” de daño celular.

Además de esta interacción de RetGC1 con IMPDH1, también se ha caracterizado otro interactor de la ciclasa, la Creatina quinasa B (CKB), la cual

podría está proporcionando el ATP local necesario para mantener la actividad catalítica específicamente en conos.

Este trabajo arroja luz sobre la regulación y transporte del complejo RetGC/GCAPs, así como la interconexión entre los complejos de síntesis de cGMP y síntesis *de novo* de GTP, abriendo un nuevo escenario para el tratamiento farmacológico de enfermedades que provoquen cambios en los niveles de cGMP intracelulares, los cuales de forma prolongada afectan a la supervivencia de la célula, dando lugar a cegueras congénitas.

Chapter I. Introduction

1. Introduction

1.1. The eye and the retina

1.1.1. The eye forms images of the natural world on the retina

The way in which neuronal signals are evoked by light to produce our perception of scenes with objects and background, movement, shade, and color begins in the retina. The retina in the eye acts as a self-contained outpost of the brain. It collects information, analyzes it, and hands it on to higher centers through the well-defined optic nerve pathway for further processing. The initial step in visual processing is the formation on each retina of a sharp, inverted image of the outside world. The essential for clear vision are correct focus of the image by adjustment of the thickness of the lens (accommodation), regulation of light entering the eye by the pupil diameter, convergence of the two eyes to ensure that matching images fall on corresponding points of both retinas, and eye movements that compensate for self-generated or forced movements of the head. (Nicholls J.G et al. 2012. *From Neuron to Brain.* 5th ed. Sunderland, MA. Sinauer Associates, Inc.)

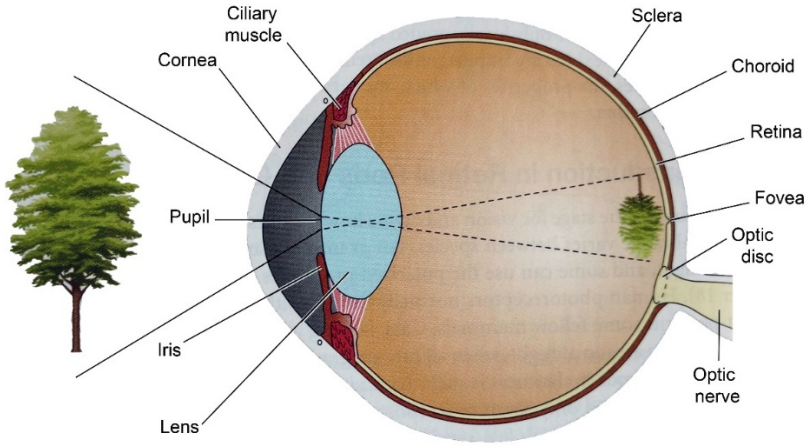

Figure I.1. Structure of the eye. Modified from Nicholls J.G et al. 2012. From Neuron to Brain. 5th ed. Sunderland, MA. Sinauer Associates, Inc.

1.1.2. Function of rod and cone photoreceptors

The retina is a neural tissue formed by five types of neuronal cells, glial cells and support cells arranged in layers (Figure I.2.A). Neuronal cells are photoreceptor cells, bipolar cells, ganglion cells, horizontal cells and amacrine cells. The Muller glia and retinal pigmented epithelium (RPE) provide trophic support to photoreceptor cells.

In vertebrates, there are two types of classical photoreceptors: rods and cones. Rods are very sensitive to light, operate at low illumination and are responsible for black and white vision during dawn and dusk. Cones are less sensitive to light but never saturate, operate during the widely varying illumination conditions of the diurnal cycle and are responsible for color vision. Both rods and cones are highly specialized and compartmentalized neurons. They have four differentiated cell regions with specific functions. The outer segment, where phototransduction takes places, contains a stack of membrane discs that are continuously renewed. The visual pigment, the protein that captures photons of light, is the most abundant protein in this compartment (at a concentration of about ~3mM, Otto-Bruc et al. 1998; Fu & Yau 2007), being embedded at disc membranes. The dense stack of discs greatly increases the probability of photon capture. An interesting difference between rods and cones is that the rod discs (except for the nascent discs at the base of the outer segment) are completely internalized and therefore physically separate from the plasma membrane, whereas the cone discs remain as folding of the plasma membrane. In fact, membrane folding at cone outer segments allows having much more surface exposed, thus facilitating substances exchange, such as chromophore to regenerate the pigment or fast calcium dynamics which are key points during light adaptation (Figure I.2.B). (Fu and Yau, 2007)

The outer segments separated by a thin connecting cilium from the inner segment. The inner segment or cell soma is the house keeping compartment of the cell. It contains the endoplasmic reticulum and the Golgi apparatus for protein synthesis, and the packed mitochondria for ATP production. All phototransduction proteins are synthesized at the inner segment, and are transported across the connecting cilium to the light sensitive compartment, the outer segment. Proximal to the inner segment is the cell nucleus, with photoreceptor nuclei aligning at the outer nuclear region. Finally, the synaptic terminal (Figure I.2.B) is where changes in membrane potential caused by light are converted to changes in the rate of neurotransmitter release to second-order neurons, therefore sensing a signal to the brain. Overall, both rods and cones respond to light by hyperpolaring, and by decreasing the rate of glutamate release at the synaptic terminal. This signal travels really fast to bipolar and ganglion cells in the direct pathway, to convey in the optic nerve for its transmission to the brain (Figure I.1 and Figure I.2.A).

Furthermore, horizontal and amacrine cells enrich the variety of connections established between photoreceptors, bipolar and ganglion cells. While photoreceptor cells “measure” the light intensity at different points of the visual image, this information is transmitted to bipolar and ganglion cells in a way in which some important integration occurs, so that the output of ganglion cells to the brain is based on contrasts of light intensity, and on movement, rather than on the light intensity of the natural world. The integration of visual information starts at the retina, and in that sense the retina is usually referred to as an “outpost” of the brain. (Rodieck,

Robert W. 1998, *The first steps in seeing.* 1st ed. Sunderland, MA. Sinauer Associates, Inc.)

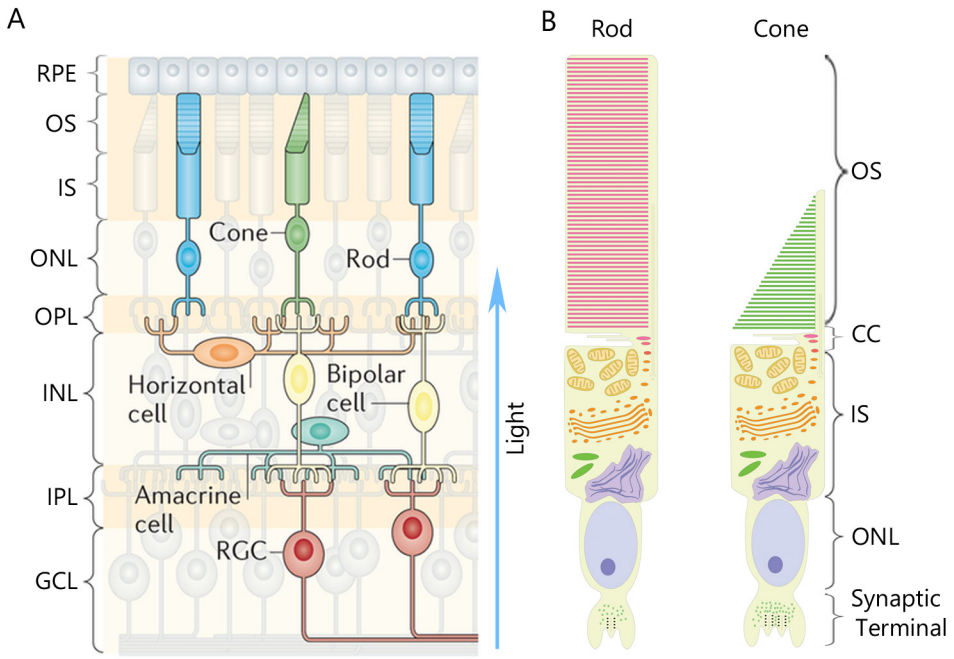

Figure I.2. Retinal layers and cell types. A. The retina is organized into three layers of cell bodies (the outer nuclear layer (ONL), inner nuclear layer (INL) and the ganglion cell layer (GCL)) and two layers of neuropil (the outer plexiform layer (OPL) and the inner plexiform layer (IPL)). Retinal neurons comprise primary sensory cells (rods and cones), interneurons (horizontal cells, bipolar cells and amacrine cells) and output neurons (retinal ganglion cells (RGCs)). Rods and cones presents a sensory compartment, outer segment (OS) and a metabolic compartment (IS). The Retinal pigmented epithelium (RPE) provides nutritional support to photoreceptors, sustains disc shedding in the constant renewal of photoreceptor outer segments and sustains the chromophore cycle. Modified from Cepko 2014. B. Rods and cones present a specialized sensory compartment, the outer segment (OS) where phototransduction takes place, a metabolic compartment (IS) where proteins are synthesized. The IS is linked to the OS through a Connecting Cilium (CC). Nucleus (ONL). Considerable differences are observed in the synaptic terminal of both types of cells.

1.2. The Light response

1.2.1. Activation phase and termination phase

Phototransduction (Figure I.3.A) is the process by which an electrical signal is produced as a result of the absorption of a photon by the visual pigment rhodopsin in photoreceptor cells. As the visual system of higher vertebrates relays in rods and cones, being rods more abundant (97% in mouse retina)(Fu and Yau, 2007), phototransduction has been better studied in rods. Rods cover the range of dim light intensities. They are extraordinarily sensitive to light, and saturate at much dimer light intensities than cones, that cover the range of bright light (Fu and Yau, 2007). The apoprotein rod opsin, a seven-transmembrane domain G-protein coupled receptor, is covalently bound in darkness to the chromophore *11-cis retinal (Cohen et al., 1992)* constituting the visual pigment rhodopsin. Absorption of a single photon by the chromophore causes its photoisomerization from *11-cis retinal* to *all-trans retinal*, triggering a conformational change in rhodopsin that confers it its active state. In its active state, rhodopsin activates transducin by promoting the exchange of GDP for GTP in transducin α-subunit, causing its separation from the βγ-transducin dimer. Gα-Transducin activates the retina-specific cGMP-phosphodiesterase (PDE) which increases its rate of hydrolysis of cGMP, reducing the cGMP levels. As a consequence of light, there is a drop in the cGMP levels. This drop of cytoplasmic cGMP, is sensed by the cGMP-gated channels in the plasma membrane. cGMP-channels are kept open in the dark, allowing the influx of Na+ and Ca2+ and keeping the cell partially depolarized. The drop in cGMP causes the closure of the channels reducing the cation influx (Na^+ and Ca^{2+}) and therefore causing the hyperpolarization of the cell (Yau and Hardie, 2009). This light-driven hyperpolarization of the cell reduces the rate of release of synaptic vesicles in the synaptic terminal, sending a signal to higher order neurons.

When the exposure to light ends (Figure I.3.B), everything that has been activated has to be inactivated in order to restore the darkness equilibrium.

For that, photoactivated rhodopsin is phosphorylated by rhodopsin kinase and arrestin binding, that “caps” rhodopsin, preventing it from further interacting with transducin. In the case of the effector complex formed by Transducin Gα and PDE in rods, inactivation resides in a GAP (GTPase activating) complex consisting of RGS9 (G protein signaling 9), an RGS9-anchoring protein (R9AP) and an orphan G protein β subunit (Gβ5), that accelerate the intrinsic GTPase activity of Gα subunit, promoting the exchange of GTP for GDP (Yau and Hardie, 2009).

Importantly, to restore the darkness equilibrium the cGMP levels have to be reestablished to the dark levels by new synthesis. The enzyme responsible for cGMP synthesis is retinal guanylate cyclase (RetGC). RetGC is regulated by Ca2+ (stimulated when the Ca2+ levels drop in response to light), by the Guanylate Cyclase Activating proteins, (GCAPs). Therefore, the drop in Ca2+ that

accompanies the light response initiates a feedback loop that counteracts the effect of light by stimulating the replenishment of cGMP, the reopening of cGMP channels, the restoration of Na^+ and Ca^{2+}influx and with it the sensitivity of the photoreceptor cell to light (Lucas et al., 2000).

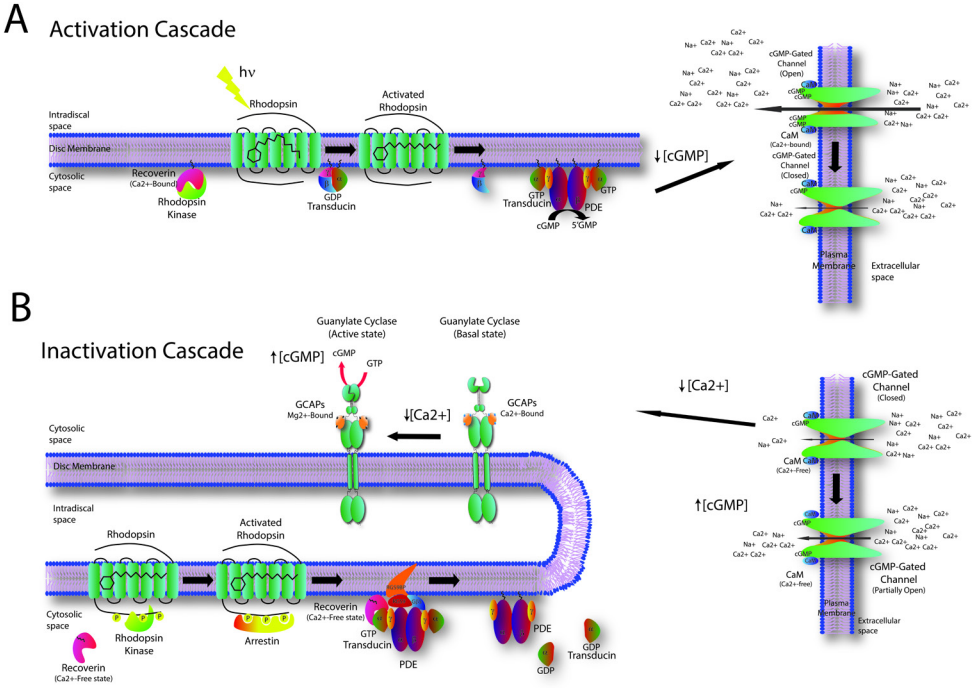

Figure I.3. Phototransduction Cascade. A. Activation cascade. The absorption of a photon by 11-cis-retinal produces its photo-isomerization to all-trans-retinal. This isomerization produces a conformational change in rhodopsin that confers it its active state, leading to the exchange of GDP for GTP in the alpha subunit of transducin. Transducin-alpha in its active state (GTP-bound) activates Phosphodiesterase (PDE), leading to an increased hydrolysis of cGMP, which reduces its intracellular concentration. The fall in cGMP leads to closure of cGMP-gated channels at the plasma membrane, decreasing the influx of cations (mostly Na^+ and Ca2+), hyperpolarizing the cell. B. Once the light extinguishes, the darkness equilibrium must be recovered. For that, every enzyme that was activated is now deactivated. Rhodopsin is deactivated by phosphorylation by rhodopsin kinase and arrestin binding. Transducin is deactivated by an enzymatic complex that catalyzes its GTPase activity. Importantly, the cGMP levels are restored to the dark levels by new synthesis. For that, guanylate cyclase enzymatic activity is stimulated by the drop in Ca2+, through some Ca2+ binding proteins called "Guanylate Cyclase Activating Proteins, GCAPs).of transducing, hydrolyzing GTP to GDP, dissociating itself from PDE and inactivating it. In the plasma membrane, Calmodulin regulate the affinity of cGMP gated channel for cGMP participating in the mechanisms of adaptation to light.

The membrane potential in photoreceptor cells is determined, in part, by the number of cGMP open channels which in turn depends on the levels of free cGMP in the cytoplasm, which is ultimately controlled by the opposing effects of cGMP-PDE and retGC. When light leads to the activation of PDE producing a drop in cGMP levels, light also sets in motion a Ca^{2+} feedback loop that activates RetGCs in order to replenish cGMP levels in the cell and ultimately restore sensitivity to photoreceptors (Lucas et al., 2000).

1.2.2. Light adaptation

Photoreceptor cells must respond to a wide range of light intensities in the natural world. As most sensory receptors, photoreceptor cells give a graded response to light, with response intensity being proportional to the stimulus intensity. However, this relationship is not fixed. Photoreceptor cells have the capacity to adjust their sensitivity to light depending on the ambient light intensity (Fain et al., 2001). This capacity is called light adaptation. In the absence of light-adaptation capacity, photoreceptor cells would respond to light linearly until all cGMP-gated channel were closed and the photoreceptor cell saturated (Fain et al., 2001). Light-adaptation is Ca2+-dependent. Light-adaptation is a Ca2+-mediated feedback signal to the phototransduction cascade that serves to counteract the effect of light –to reduce sensitivity- with higher ambient light intensities. This Ca2+-negative feedback is exerted at several points in the transduction cascade, always serving to restore light sensitivity and avoid saturation at high ambient light intensities. The most relevant molecular target of Ca2+ regulation during light adaptation is the protein complex responsible for cGMP synthesis. As Ca2+ drops during the light response –due to closure of the cGMP-gated channels interrupting Ca2+ influx-, this drop is sensed by the Ca2+-binding proteins "Guanylate Cyclase Activating Proteins" or GCAPs, that switch from an "inhibitor" to an "activator" conformational state, dramatically increasing guanylate cyclase catalytic activity.

Replenishment of cGMP allows photoreceptors to reach a steady state in which both PDE and cyclase are accelerated and in which a proportion of the cGMP-gated channels is still open, and thus available to be closed (Fain et al. 2001; Mendez et al. 2001). In other words, replenishment of cGMP serves to avoid saturation, restores sensitivity to light, making photoreceptor cells capable of responding to light again, even if in the presence of ambient light intensity. Light-adaptation is a fundamental property of rods and especially cones, absolutely required for our visual system to operate in the natural world.

1.3. The RetGC/GCAPs complex responsible for cGMP synthesis.

1.3.1. Retinal guanylate cyclase.

Guanylate cyclase proteins catalyze the formation of cGMP from GTP. Until date two main types of guanylate cyclases have been described: soluble or membrane-attachment. Soluble guanylate cyclase (sGC) is encoded by two genes, form a heterodimer and require a heme group for its function. It is the only receptor known for nitric oxide and plays an important role in regulation of blood pressure (Sharma and Duda, 2014).

Table I.1. Family of Guanylate cyclase proteins.

Soluble or Memb	***Human (Gene)***	***Mouse (Gene)***	***Aliases***	***Ligand***	***Tissue/Cells***	***Comments***
Memb.	*GCA, NPR-A (NPR1)*	*GC-A (Npr1)*	*Natriuretic peptide receptor A*	*ANP, BNP*	*Vasculature*	*Regulates hypertension*
Memb.	*GCB, NPR-B (NPR2)*	*GC-B (Npr2)*	*Natriuretic peptide receptor A*	*CNP*	*Brain, bone*	*Null alleles associates with dwarfism*
Memb.	*GCC (GUCY2C)*	*GC-C (Gucy2c)*		*Guanylyl, uroguanylyl enterotoxin*	*Intestines*	*Null alleles insentives to enterotoxins*
Memb.	*GCD (GUCY2E)*	*GC-D (Gucy2d)*	*Olfactory neuroepithelia (ONE)-GC*	*Guanylyl, urogynylyl*	*Subset of olfactory neurons*	*Pseudogene in primates*
Memb.	*RetGC1 (GUCY2D)*	*GC-E (Gucy2e)*	*RetGC1, GC1*	*GCAPs*	*Rods and cones, pineal*	*Null alleles associated with LCA-1*
Memb.	*RetGC2 (GUCY2F)*	*GC-F (Gucy2f)*	*RetGC2, GC2*	*GCAPs*	*Rods*	
Memb.	*GCG (GUCY2G)*	*GC-G (Gucy2g)*		*Unknown*	*Mouse testis, kidney*	*Pseudogene in human*
Soluble	*GUCY1A2*	*Gucy1a2*	*sGC-α2*	*Nitric Oxide*	*Endothelium*	
Soluble	*GUCY1A3*	*Gucy1a3*	*sGC-α3*	*Nitric Oxide*	*Endothelium*	
Soluble	*GUCY1B2*	*Gucy1b2*	*sGC-β1*	*Nitric Oxide*	*Endothelium*	
Soluble	*GUCY1B3*	*Gucy1b3*	*sGC-β2*	*Nitric Oxide*	*Endothelium*	*Pseudogene in human*

Modified from (Karan et al., 2010). Ligands of GC binds to the extracellular domain, except for GCAPs that are bound to the intracellular region of the protein

Membrane-attached guanylate cyclases are integral membrane proteins encoded by more than 7 genes and act as homodimers. They present an extracellular domain, a single transmembrane domain and an intracellular domain that catalyzes the conversion of GTP to cGMP (Sharma and Duda, 2014). The extracellular domain presents the binding pocket for the molecules that activate guanylate cyclase catalytic activity. In Table I.1 are summarized the guanylate cyclase characterized until date.

1.3.2. Neuronal Calcium Sensor family

Neuronal Calcium Sensor (NCS) proteins are a family of proteins that belong to the Calmodulin superfamily. These proteins detect changes in the intracellular Ca^{2+} concentration in neurons and regulate their target proteins to modify their function (Burgoyne and Haynes, 2012). NCS proteins are encoded by 14 conserved genes. All gene products have four EF-hand domains and show a limited similarity with Calmodulin (<20%). From the four EF-hand domains (helix-loop-helix domains that coordinate Ca2+), two or three are functional and able to bind Ca2+, depending of the member (figure I.4).

Their distinct properties as their own on-rate kinetics, Ca^{2+}-affinities and localization allow them to carry out non-redundant roles that do not overlap with the functions of calmodulin (McCue et al., 2010).

NCS are protein of about 22kDa that share about 30-70% of protein sequence identity. Many family members, but not all, are N-terminal myristoylated,

```
                                                  EF-Hand 1
GCAP1           MGNVM----------EGKSVEELSSTECHQWYKKFMTECPSGQLTLYEFRQFFGLKNLSP  50
GCAP2           MGQEFS-------WEEAEAAGEIDVAELQEWYKKFVMECPSGTLFMHEFKRFFKVTD-DE  52
Recoverin       MGNSKSGALSKEILEELQLNTKFSEEELCSWYQSFLKDCPTGRITQQQFQSIYAKFFPDT  60
Calmodulin      ---------------MADQLTEEQIAEFKEAFSLFDKDG-DGTITTKELGTVMRSLG-QN  43

                          EF-Hand 2                             EF-Hand 3
GCAP1           SASQYVEQMFETFDFNKDGYIDFMEYVAALSLVLKGK-VEQKLRWYFKLYDVDGNGCIDR  109
GCAP2           EASQYVEGMFRAFDKNGDNTIDFLEYVAALNLVLRGT-LEHKLKWTFKIYDKDGNGCIDR  111
Recoverin       DPKAYAQHVFRSFDSNLDGTLDFKEYVIALHMTTAGK-TNQKLEWAFSLYDVDGNGTISK  119
Calmodulin      PTEAELQDMINEVDADGNGTIDFPEFLTMMARKMKDTDSEEEIREAFRVFDKDGNGYISA  103

                                                      EF-Hand 4
GCAP1           DELLTIIQAIRAINPCS--------DTTMTAEEFTDTVFSKIDVNGDGELSLEEFIEGVQ  161
GCAP2           LELLNIVEGIYQLKKACRRELQTEQGQLLTPEEVVDRIFLLVDENGDGQLSLNEFVEGAR  171
Recoverin       NEVLEIVMAIFKMITPEDVKLLP--DDENTPEKRAEKIWKYFGKNDDDKLTEKEFIEGTL  177
Calmodulin      AELRHVMTNLG----------------EKLTDEEVDEMIREADIDGDGQVNYEEFVQMMT  147

GCAP1           KDQMLLDTLTRSLDLTRIVRRLQNGEQDEEGADEAAEAAG  201
GCAP2           RDKWVMKMLQMDMNPSSWLAQQRR---------KSAMF--  200
Recoverin       ANKEILRLIQFEPQKVKEKMKNA-----------------  200
Calmodulin      AK-------------------------------------  149
```

Figure I.4. Alignment of main NCS of retinal photoreceptor cells. In green is show the Gly2, which it is modified by myristoylation. In red, EF-hands domains. In blue, phosphorylation site of GCAP2

Table I.2. Neuronal Calcium sensor proteins and their proposed functions in mammalian systems. (Extracted from Burgoyne 2007)

Subgroup	***First appearance in evolution***	***Mammalian protein***	***Expressed human splice variants***	***Proposed functions***
A	*Yeast*	*NCS-1*	*1*	*Regulation of neurotransmission, stimulation of constitutive and regulated exocytosis, learning, short-term synaptic plasticity, Ca^{2+} channel and Kv4 channel regulation, phosphoinositide metabolism, dopamine D2 receptor endocytosis, GDNF signaling, neuronal growth and survival.*
B	*Nematodes*	*Hippocalcin*	*1*	*Anti-apoptotic, AMPA receptor recycling in LTD, MAPK signaling, learning.*
		Neurocalcin-δ	*1*	*Guanylyl cyclase activation*
		VILIP1	*1*	*Guanylyl cyclase activation's and recycling, traffic of nicotinic receptors, increase of cAMP levels and secretion*
		VILIP2	*1*	*Regulation of P/Q-type Ca^{2+}-channels*
		VILIP3	*1*	*Unknown*
C	*Fish*	*Recoverin*	*1*	*Light adaption by inhibition of rhodopsin kinase*
D	*Fish*	*GCAP1*	*1*	*Regulation of retinal guanylyl cyclase*
		GCAP2	*1*	*Regulation of retinal guanylyl cyclase*
		GCAP3	*1*	*Regulation of retinal guanylyl cyclase*
E	*Insects*	*KChip1*	*3*	*Regulation of Kv4 and Kv1.5 channels, repression of transcription.*
		KChip2	*5*	*Regulation of Kv4 and Kv1.5 channels, repression of transcription.*
		KChip3	*2*	*Regulation of Kv4 channels, presinilin processing, APP processing, repression of transcription, pro-apoptotic, regulated ER Ca^{2+}*
		KChip4	*6*	*Regulation of Kv4 channels, presenilin-processing, repression of transcription.*

what allow their association with membranes by a Ca^{2+}-myristoyl switch in some cases, hence playing a role in the regulation of their targets (Ames and Lim, 2012).

Five classes of NCS have been described in mammals, named from A to E, and summarized in table I.2.

1.3.3. Historical perspective of RetGC/GCAPs complex.

It has been known since the 70s that light lead to changes in the calcium and cGMP concentration of photoreceptor cells. Therefore, either of these two molecules could be the second messenger that carried the message from visual pigment excitations at the disk membranes to a change in membrane potential at the plasma membrane of photoreceptor outer segments. It was the identification of cGMP-gated channels in 1985 that established cGMP as the second messenger of phototransduction (Fesenko et al., 1985). At the same time, biochemical and electrophysiological studies at different laboratories established Ca2+ as a key molecule regulating the gain and the rate of recovery of the light response in the process of light adaptation. As mentioned above, retinal guanylate cyclase is the protein responsible for cGMP synthesis in phototransduction. In the early 70's, RG. Pannbaker (Pannbacker, 1973) suggested that retinal guanylate cyclase could be regulated by calcium. In the late 80's, KW Koch and L. Stryer showed that Ca2+ regulation of guanylate cyclase activity was very robust during the light response, boosting cGMP synthesis 5-20 fold when calcium went down from 1µM to 10nM (Koch and Stryer, 1988). They also showed that this Ca2+ regulation was not exerted directly to the guanylate cyclase, but through some soluble modulator. At that moment, several independent laboratories in the world started the search for this soluble protein. In the mid 90's two independent laboratories, using different experimental designs, identified two related but not identical soluble calcium binding proteins that were assigned to the neuronal calcium sensor family. They were called guanylate cyclase activating proteins 1 & 2 (GCAP1 and GCAP2)(Dizhoor et al., 1995, 1994; Gorczyca et al., 1994; Lowe et al., 1995; Palczewski et al., 1994).

GCAP proteins switch between two different conformational states: in their Ca2+-bound form in the dark, GCAP proteins inhibit cGMP synthesis (inhibitor state); while in their Ca2+-free form, acquired as the Ca2+ drops during the light response, they stimulate guanylate cyclase activity (activator state). In this way, GCAPs provide a calcium feedback regulation to guanylate cyclase, linking cGMP synthesis to Ca^{2+} concentration that serves to adjust the sensitivity of the photoreceptor to the background illumination.

Several biochemical studies then addressed the mapping of functional domains in GCAP1 and GCAP2 involved in activation or inhibition of RetGC by analysis of deletion mutants and chimeric proteins in which different regions of the

GCAP proteins were substituted by the corresponding regions of Recoverin or neurocalcin (Krylov et al., 1999; López-del Hoyo, 2014; Olshevskaya et al., 1999).

It was determined that several regions of the GCAP molecules are required for RetGC activation (Figure I.4): a) a region within the N-terminal region starting at Trp21 (numbering corresponding to GCAP1) that comprises a 5 to 7 amino acid stretch preceding EF-1, the EF-1 domain -non-functional at Ca^{2+} coordination- and some additional amino acids; b) the region between EF-hands 2 and 3, representing the "interdomain" or "hinge" region between the NH2- and COOH- terminal globular domains in the structure of GCAPs, is required for activation and determines the direction of the Ca2+-switch in GCAP2; and c) a stretch of about 20 amino acids starting at Phe156 immediately adjacent to EF-4 within the COOH-terminal domain (Krylov et al., 1999; López-del Hoyo, 2014; Olshevskaya et al., 1999).

Within these domains, the stretches of amino acids Trp21-Thr27 preceding EF-1 in the NH2-terminal region, and Thr177-Arg182 within the COOH-terminal region in GCAP1 (Krylov et al., 1999), and the corresponding regions in GCAP2, appear to be critical for RetGC activation (Olshevskaya *et al.* 1999a). Therefore, a picture is emerging in which the signal in the GCAP proteins involved in RetGC recognition is discontinuous, involving the NH2- and COOH-terminal regions. In contrast, inhibition of RetGC requires the first 9aa of GCAP1 (Krylov et al., 1999), and the EF-1 domain in GCAP2 (Olshevskaya et al., 1999)(López-del Hoyo, 2014).

Recently, the structure of GCAP1 has been resolved (Lim et al., 2013) making possible a functional characterization of the key residues implied in binding and regulation of RetGC by GCAP1 (Peshenko et al., 2014). Binding of GCAP1 to RetGC involves the EF-1 domain. The myristoyl group attached to an N-terminal glycine, is sequestered in an internal binding pocket independently of Ca^{2+}-binding state, and it is essential for GCAP1 binding to RetGC (I. V Peshenko et al., 2012). As Ca^{2+} binds to EF-hand 4, it triggers a conformational change at the N-terminus through a Ca^{2+}-myristoyl tug that controls the exposition of key residues of EF-1 and EF-2 that conform the target binding surface of GCAP1 to RetGC (Lim et al., 2014). By a thorough analysis of single residue GCAP1 mutants capacity to bind and activate RetGC, the target binding site of GCAP1 has been defined. It involves residues from EF-hand 1 (Tyr-22, Lys-23, Lys-24, Met- 26, Glu-28, Pro-30, Ser-31, Gly-32, Tyr-37, and Glu-38) and EF-hand 2 (Phe-73, Met-74, Val-77, and Ala-78) (Peshenko et al., 2014). On the other hand, binding of GCAP1 to RetGC is required but not sufficient for activation of RetGC. RetGC acts as a dimer, and a fully active cyclase domain requires the dimerization of this domain. The binding of GCAP1 enhances the dimerization of cyclase domain, but primary binding itself is not sufficient for activation. Some important secondary interactions or allosteric effects are provided in a second step once the complex with the cyclase is formed. The residues M26, K85 and W94 are localized in the patch that conforms the target

binding surface. Mutations in these residues allow GCAP1 binding to RetGC, but not its activation (Peshenko et al., 2014).

On the other hand, GCAP2 presents an alternative regulation that is absent in GCAP1. It was described that GCAP2 can be phosphorylated at Ser201 *in vitro* in a conformational Ca2+-dependent manner (Peshenko et al., 2004). Recently, our group has shown that this phosphorylation at Ser201 determines the localization of GCAP2 *in vivo*. In response to constant light exposure as Ca2+ drops, the Ca2+-free form of GCAP2 is phosphorylated at Ser201, triggering the binding of 14-3-3 to phospho-GCAP2 and its retention to the metabolic compartment, precluding its transportation to the sensory compartment (López-del Hoyo et al., 2014).

While myristoylation of GCAP1 has been described to increase the affinity of GCAP1 for RetGC (I. V. Peshenko et al., 2012), myristoylation of GCAP2 did not affect its affinity for RetGC (Olshevskaya et al., 1997). Thus, this points to a difference in the regulation of both GCAPs by myristoylation.

1.3.4. Regulation of RetGC/GCAPs complex. Role in termination of the light response and light adaptation.

Both GCAPs can bind to RetGC, but different models have been proposed for the stoiquiometry of the complex and its regulation. Actually, two opposed models have been proposed for the mechanism of action of GCAPs in the RetGC/GCAPs complex. The first one establishes that both GCAPs can bind to RetGC at the same time through two different binding sites: GCAP1 to RetGC juxtamembrane domain, and GCAP2 to RetGC C-terminal domain (reviewed in Sharma & Duda 2014). The second one, defended by A. Dizhoor, establishes that both GCAPs bind to RetGC through a common or overlapping binding site at the dimerization domain around Met823, in a mutually exclusive manner (Figure I.5)(I. V. Peshenko et al., 2015; I. V Peshenko et al., 2015).

Vertebrate photoreceptors contain two guanylate cyclases, RetGC1 and RetGC2, which share a high degree of sequence identity. RetGC1 is present at relatively high concentrations in rod and cone outer segments, whereas RetGC2 is restricted to rod outer segments in mice and humans. The relative amounts of RetGC1 and RetGC2 vary with species with a RetGC1 to RetGC2 ratio 4:1 in mouse and 30:1 in bovine photoreceptors (Molday et al., 2014).

Thus, the basis of different roles of both GCAPs relies in their Ca^{2+} sensitivities and their affinities to both RetGCs. GCAP1 has a lower affinity for Ca^{2+} ($K_{1/2}$= 130-140nM) than GCAP2 ($K_{1/2}$= 50-60nM). Levels of free Ca^{2+} inside a mouse rod range from 250mM in darkness to a 23nM in saturating light. So, during the initial fall in Ca^{2+} incurred during the photon response, many more GCAP1 molecules release their Ca^{2+} than GCAP2. The majority of GCAP2 molecules release their bound Ca^{2+} when intracellular Ca^{2+} falls to a lower degree, during saturating

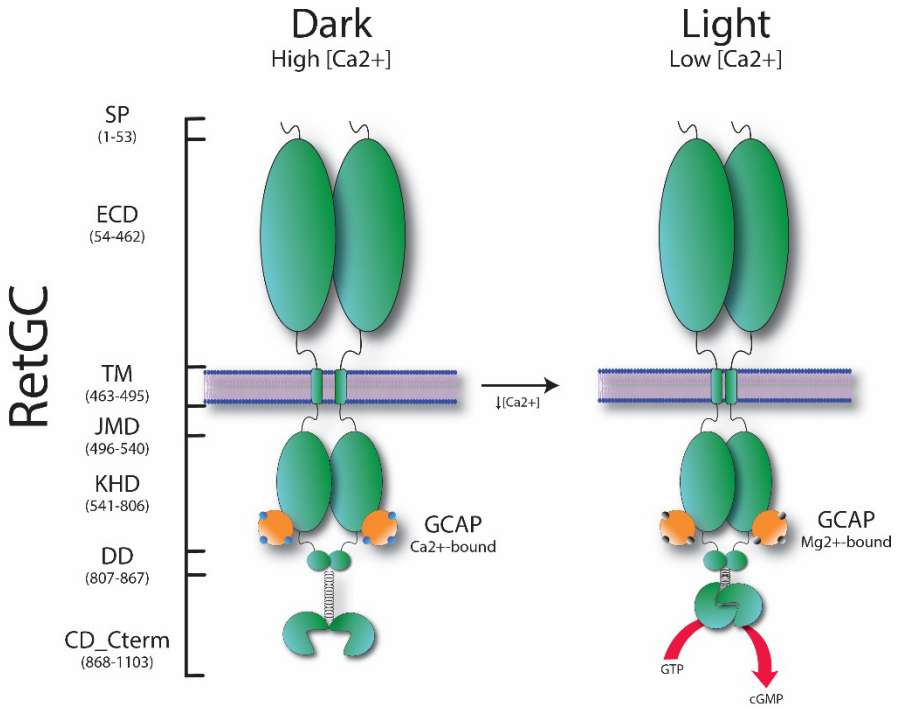

Figure I.5. Model of regulation of RetGC by GCAPs. RetGC (in green) is a transmembrane protein that functions as a dimer, permanently bound to GCAPs (in orange) by the Kinase homolog domain (KHD). GCAPs activate cGMP synthesis in light conditions, when the [Ca^{2+}] is low, by prompting the dimerization of cyclase domain (CD_Cterm). Signal Peptide (SP), Extracellular domain (ECD), Transmembrane Domain (TM), Juxtamembrane domain (JMD), Dimerization domain (DD). Number represents localization of domains in base of primary structure of RetGC.

responses to brighter light (Wen et al., 2014). GCAP1 presents higher affinity for RetGC1 than GCAP2. The population of RetGC1 presents a large fraction bound to GCAP1 and only a small fraction bound to GCAP2 (less than 20%). At the same time all RetGC2, which accounts for 25-30% of all RetGC activity, is bound exclusively to GCAP2 (I. V Peshenko et al., 2015; Peshenko et al., 2011). Taken together, RetGC2 is regulated only by GCAP2, and RetGC1 is regulated by both GCAPs, but with the majority of molecules bound to GCAP1.

The mechanistic model of GCAPs modulation of RetGC is today referred to as "*Calcium relay mechanism" (Koch and Dell'orco, 2013)* or "*Calcium recruitment mechanism" (Wen et al., 2014)*. It establishes a modulation of cGMP synthesis at two stages: when the calcium levels start to drop during the light response, GCAP1 activates RetGC in a first boost of cGMP synthesis; and only when the calcium levels drop more substantially in response to brighter or longer light exposures GCAP2

would come into play to produce a second stage of RetGC activation and second boost of cGMP synthesis.

The fine-tuning of different Ca^{2+} affinities in the complement of different GCAP proteins that characterize each species (there are up to seven different GCAP proteins in zebrafish (Scholten and Koch, 2011) would increase the overall sensitivity of the regulatory mechanism, as the joint action of different GCAPs would expand the dynamic range of responses to Ca^{2+} without losing the sensitivity that is contributed by the cooperative effect of Ca^{2+} on retinal guanylate cyclase regulation by each GCAP (Burgoyne, 2007).

1.3.5. Trafficking of RetGC/GCAPs complex. Role of RD3.

Phototransduction proteins are synthetized at the inner segment "house-keeping" compartment of the cell, and must be transported to the outer segment photosensitive compartment. Because the outer segment compartment of photoreceptor cells is constantly renewed (completely renewed each ten days in humans), this polarized vesicular trafficking occurs massively and is strictly required for photoreceptor viability. Understanding the mechanisms that govern the assembly, organization and trafficking of signaling protein complexes to the outer segment where phototransduction takes place is a main focus of the photoreceptor cell biology field; as mutations at these processes lead to inherited retinal blindness.

The RetGC/GCAPs complex is present exclusively in photoreceptor cells. Although the localization of GCAPs might vary in different species, there is a consensus that establishes thatGCAP1 is expressed in both rods and cones in high vertebrates, with a higher relative expression in cones than rods. On the other hand, GCAP2 is expressed preferentially in rods and to a much lower level in cones (Cuenca et al., 1998).

Both GCAPs distribute along the cytoplasmic space of the cell, localizing to the inner segment or metabolic compartment, the outer segment and the synaptic terminal (López-del Hoyo et al., 2012). RetGCs are localized mainly at the outer segment compartment. Retinal guanylae cyclases RetGC1 and RetGC2 have been shown to be essential for the correct localization of GCAPs and other proteins involved in phototransduction (Baehr et al., 2007; Karan et al., 2010). This observation points to a group of signaling proteins, including GCAPs and proteins more generally involved in cGMP metabolism, being transported together, around RetGCs.

Although the mechanisms underlying signaling protein trafficking to the outer segment in photoreceptor cells are still poorly understood, an analogy has been established to ciliary trafficking in other ciliated cells. This analogy is based on the fact that the outer segment derives from a primary non-motile cilium. In other ciliated cells, some "ciliary-targeting sequences" in the primary structure of proteins

have been identified that confer ciliary destination. One such "ciliary targeting sequence" is the aminoacidic sequence "VxPx". In photoreceptor cells this sequence is present in rod opsin, and it has been shown to be essential for rod opsin transport to the rod outer segment compartment (Mazelova et al., 2009). In photoreceptor cells, transport to the cilium occurs by vesicular trafficking, and different subset of vesicles might be guided to the cilium by one protein containing a "ciliary targeting sequence", acting as a guide. As an example, "rhodopsin transport carrier" vesicles have been characterized, that work their way to the cilium through protein interactions triggered by rod opsin C-terminus VxPx sequence. Most membrane-bound proteins are thought to be transported to the cilium "by default" by incorporating into cilium-fate vesicles.

RetGC1 is thought to act as a "ciliary guiding" protein. Until date no ciliary targeting signal has been identified in RetGC, however some genetic studies have shown that RetGCs are required for the transportation of a subsert of proteins to the sensory compartment. The work of W. Baehr has shown that in the RetGC1/RetGC2 double knockout mouse model a subset of phototransduction proteins fail to be transported to the outer segment in rods and cones. In rods, the GCAP proteins and the different PDE subunits depend on RetGCs for their transport to the outer segment. In cones, in addition to GCAPs and PDE subunits, transducin and GRK1 have been shown to depend on RetGCs for their correct localization to the outer segments. RetGC1 transport might also involve cone opsin transportation to cone outer segments (Baehr et al., 2007; Karan et al., 2010).

Recently, another member of the RetGC/GCAPs complex has been identified by R. Molday, emerging as a protein involved in the stabilization and transport of the complex: the protein *Retinal Degeneration 3* or RD3 (Azadi et al., 2010). This protein is encoded by a locus that has been linked to inherited blindness: to the naturally-occurring mutant strain of mice rd3, and to Leber Congenital Amaurosis 12 (LCA12) in humans. Robert Molday´s laboratory reported that the locus rd3 encodes a protein (RD3) that interacts with RetGC1, and plays an essential role in the early stage of stabilization and transport of the RetGC/GCAPs protein complex. In the rd3 mice retGC1 and RetGC2 protein levels decrease dramatically, to the point that they cannot be detected. Likewise, the localization and/or protein levels of the proteins that are co-transported with RetGC are affected.(Azadi et al., 2010).

Moreover, it has been demonstrated that RD3 interacts directly with GCAP1 and this interaction facilitates the trafficking of RetGC1 to the outer segments. Also, the RetGC/GCAPs/RD3 complex is altered by most of LCA1-linked mutations in RetGC1. (Zulliger et al., 2015).

How RD3 regulates, stabilizes or orchestrates the trafficking of the RetGC/GCAPs complex to the outer segment are still open-questions. The specific role of RD3 in the stabilization and trafficking of the RetGC/GCAPs complex is still unknown.

1.3.6. Mutations in the genes encoding the proteins in the RetGC/GCAPs/RD3 complex and disease.

Mutations in the different components of the RetGC/GCAPs/RD3 protein complex have been linked to Retinitis Pigmentosa (RP), Cone-Rod Dystrophies (CORD) and to Leber Congenital Amaurosis (LCA).

Retinitis Pigmentosa is the most common cause of photoreceptor degeneration. It presents poor night vision in early or middle life. It progresses to loss the mid-peripheral field of vision, which gradually extends and leaves many patients with a small central island of vision due to the preservation of macular cones. The most common form of RP results from a primary defect in rods, but this almost invariably leads to secondary loss of cones (Alan F. Wright et al., 2010). RP can be present autosomal dominant, autosomal recessive or X-linked segregation.

Cone-rod dystrophies (CRD) are a group of pigmentary retinopathies that have early and important changes in the macula. Cone dysfunction occurs first and is often followed by rod photoreceptor degeneration. Common initial symptoms are decreased visual acuity, dyschromatopsia, and photophobia which are often noted in the first decade of life. Night blindness occurs later as the disease progresses. Cone-rod dystrophies are a group of disorders separate from rod-cone dystrophies where the primary defect is in the rod photoreceptors with typical pigmentary changes in the peripheral retina. The progression of vision loss is generally slower in rod-cone dystrophies. Cone dystrophies comprise another group of disorders with exclusive cone involvement in which the macula often has a normal appearance in association with loss of central acuity (Cross, 2016).

Leber congenital amaurosis (LCA) is the most severe form of inherited retinal blindness. LCA is characterized and unified by the following clinical features: severe and early visual loss, sensory nystagmus, amaurotic pupils, and absent electrical signal on electroretinogram (den Hollander et al., 2008). The first signs are usually noted before the age of 6 months. These consist of a severe reduction in vision accompanied by nystagmus, abnormal pupillary responses, and photophobia. LCA is genetically heterogeneous with at least 22 known gene mutations associated with the phenotype, whose prevalence of each one may be different (Figure I.6). It is also clinically heterogeneous both within and among families, which difficults the characterization of genotype-phenotype correlations for treatment purposes (Cross, 2016). Although LCA has also been associated to other syndromes, such as Joubert syndrome, mental retardation, autism or olfactory dysfunction; some of this associations are under controversy due to the intrinsically difficulty of correct characterization and correlation between genotype and phenotype of LCA(den Hollander et al., 2008).

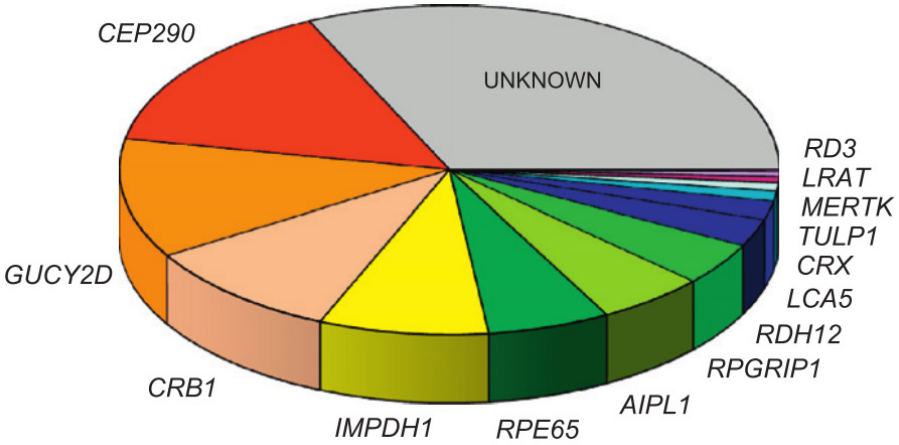

Figure I.6. Prevalence of LCA-associated mutations for 14 of the 22 causative genes. CEP290 (15%), GUCY2D (12%) and CRB1 (10%) are the most frequently mutated genes. Mutations in approximately 30% of all cases remain to be identified (den Hollander et al., 2007).

- *LCA-associated mutations to RetGC.*

Mutations in RetGC are a leading cause of LCA. About 12% of total mutations related to LCA are located in the GUCY2D gene encoding RetGC1. Until date, 41 mutations have been described in the GUCY2D gene related to LCA (Stone, 2007). From these, 18 are located in the extracellular domain of the protein (ECD); 1 is located at the transmembrane domain (TM); 8 are located in the kinase homology domain (KHD), 3 are located in the dimerization domain (DD); and 10 are located in the catalytic domain (CD). Most of these mutations are null mutations, resulting in truncated forms of the protein that are unstable (premature stop codons), or in loss of function by directly affecting the active site, the catalytic activity or dimerization capacity. However, mechanism of action of several of the mutations is still unknown. Recently, it has been proposed that some mutations mapping in the KHD and DD domains of RetGC (R768W, R795Q, R822P) lead to LCA by affecting the target binding site of GCAP1 (Jacobson et al., 2013; I. V. Peshenko et al., 2015). Although these mutations in RetGC1 were demonstrated to affect GCAP1 binding to the protein *in vitro*, it has not been demonstrated that the failure of GCAP1 binding to RetGC1 is what causes the loss of visual function and eventual cell death *in vivo*. Actually we known that GCAP1 and GCAP2 double knockout mice present largely normal retinas for up to one year of age, and almost functional responses by electroretinography (Mendez et al., 2001). Therefore, we cannot exclude that these

mutations may affect some other functional aspect of RetGC in photoreceptors *in vivo*, such as some step in its trafficking to the outer segment, its anchoring or some as-yet-unforeseen aspect of its regulation *in vivo*.

Mutations in GUCY2D gene encoding RetGC1 have also been linked to autosomal dominant CORD, namely CORD6 (Jiang et al., 2008). These mutations lead to constitutive activity of the cyclase *in vitro*, which explains its gain-of-function (autosomal dominant) nature (Wilkie et al., 2000).

- *LCA-associated mutations to RD3.*

Recently, the protein encoded by the rd3 locus (protein RD3) has been identified as a protein that interacts with the RetGC/GCAPs protein complex. The name rd3 originated from the naturally occurring strain of blind mice, the "retinal degeneration 3 mice" or "rd3 mice" that was characterized preceding the identification of the human rd3 locus linkage to LCA (type 12, LCA12). RD3 was reported to interact directly with RetGC1 in bovine rod outer segments, and proposed to be involved in stabilization and transport of the RetGC/GCAPs complex, based on the fact that in rd3mice, the level of RetGC1 is dramatically reduced at the protein level, and neither RetGC1 or the GCAP proteins can be detected at the outer segments (Azadi et al., 2010). Instead, these proteins accumulate at the inner segment compartment, indicating that their trafficking fails in the absence of functional RD3 protein. Mutations in RD3 could lead to LCA by compromising the protein stability (by causing frameshifts or large deletions in the protein, Preising et al, 2012; Perrault et al, 2013). Mutations in RD3 are mostly loss-of-function mutations that have an autosomal recessive pattern of inheritance.

Specifically, 4 mutations have been identified in the RD3 locus that yield a premature termination of the protein (R38X, E46X, E46A2bp deletion 83 X, Y60X, Preising et al, 2012; Perrault et al, 2013), all of which present autosomal recessive inheritance.

In addition, a point mutation has been linked to Retinitis Pigmentosa in a family from Spain (de Castro-Miró et al., 2014). The reason why this RD3 mutation is linked to RP instead of LCA is not known, and it stresses the need to deepen the functional characterization of the RD3 protein *in vivo*. There are clearly many aspects of RD3 putative implication in the stabilization, assembly and trafficking of the RetGC/GCAPs complexes that are still not known, as well as differences in these processes in rods and cones.

- *Disease-linked mutations in GCAPs.*

Many mutations have been reported in the genes encoding the GCAP proteins that are linked to retinal dystrophies. To date, twelve different mutations in guanylate cyclase activating protein 1 (GCAP1) have been linked to autosomal dominant cone

dystrophies, a disease characterized by the loss of color vision and central visual acuity, and to macular dystrophies (summarized in table I.3) (Dell'Orco et al., 2014; Kamenarova et al., 2013; Newbold et al., 2002, 2001; Nishiguchi et al., 2004; Palczewski et al., 2004). GCAPs stimulate RetGC catalytic activity when intracellular Ca^{2+} decreases in response to light. It is the "Ca^{2+}-empty" form of GCAPs that activate cGMP synthesis. Generally, the mutations leading to cone dystrophy affect one of the Ca^{2+} binding sites or alter protein structure in a way that impairs Ca^{2+}-binding (Figure I.7). The resulting mutant proteins remain active with increasing [Ca^{2+}], leading to constitutive activation of the cyclase independently of the lighting conditions, as reported by *in vitro* studies (Dizhoor and Hurley, 1996; Mendez and Chen, 2002). A hypothesis for how GCAP1 mutations lead to photoreceptor cell death *in vivo* has been proposed. Mutant GCAPs would cause constitutive cGMP synthesis, leading to abnormally high levels of cGMP. As a consequence, a higher fraction of the cGMP-channels would be kept open, increasing the inward current of calcium. Elevated intracellular calcium would induce apoptosis (Krizaj and Copenhagen, 2002). Two recent studies characterizing transgenic mice expressing Y99C-GCAP1 in rod photoreceptors would support this hypothesis (Olshevskaya et al., 2004; Sokal et al., 1998).

However, we have obtained evidence for other mechanisms by which mutations in GCAPs may contribute to toxicity, from studies performed in the laboratory on mutant GCAP proteins expressed on the GCAPs double knockout genetic background. We have observed that a form of GCAP2 that is severely impaired at binding Ca^{2+} [with the three functional EF-hands disrupted, (EF^{-} GCAP2)] is deleterious for the cell even when it is not active and does not traffic to the light-sensitive compartment. We expressed the EF^{-}GCAP2 mutant in rod photoreceptors of transgenic mice. While *in vitro* this mutant leads to constitutive activation of guanylate cyclase (Dizhoor and Hurley, 1996), just like the GCAP1 mutants associated to autosomal dominant cones dystrophies (Olshevskaya et al., 2004; Sokal et al., 1998), when expressed *in vivo*, we observed that this protein was inactive and accumulated at proximal compartments of the cell, likely due to misfolding. We demonstrated that this Ca2+-free form of the protein was phosphorylated at Ser201 and bound to 14-3-3 proteins in response to this phosphorylation event *in vivo*. As a result, it was retained at the inner segment compartment and precluded from distributing to rod outer segments. Its accumulation at the inner segment compartment led to its progressive aggregation, cell death and overall retinal degeneration (López-del Hoyo et al., 2014).

In summary, there are two main mechanisms by which mutations in the GCAP proteins may lead to blindness: **i)** by disrupting Ca2+-regulation of RetGC activity therefore causing constitutive guanylate cyclase activity resulting in abnormally elevated cGMP, higher-than-normal number of open channels and abnormally high entry of Ca2+, which causes cell death (Dizhoor and Hurley, 1996;

Peshenko and Dizhoor, 2007; Woodruff et al., 2007); and **ii)** by affecting protein conformation, causing cell death by mechanisms independent of cGMP metabolism but more related to those in conformational disorders (López-del Hoyo et al., 2014). Characterizing the cGMP-independent basis of toxicity will help to guide combined therapies for patients in the future.

Among GCAP1 mutations, P50L is interesting for us, because, it does not localize in an EF-hand and does not lead to constitutive activation of RetGC *in vitro*. GCAP1-P50L presents an affinity for RetGC and activation capacity similar to WT, but has been described to have lower thermal stability. So, GCAP1-P50L is a good candidate to cause toxicity by a mechanism independent of cGMP metabolism and more related to conformational disorders. This is why one of the specific aims of this thesis is to express this mutant in transient transgenic mice to analyze the effect of this mutations on the protein subcellular distribution (Chapter III), to study the physiopathology of this mutation.

On the other hand, in GCAP2 only one mutation has been described to be associated with autosomal dominant RP (Sato et al., 2005). It is localized in the EF-4 hand and could be similar to mutants localized in EF-4 in GCAP1 (like G159V) (see *table I.3)*. Based on this analogy GCAP2-G157R could result in lower affinity to Ca^{2+} and constitutive activation of RetGC. However, as described above, the Ca2+-free form of GCAP2 does not result in constitutive activation of the cyclase *in vivo* because GCAP2 (unlike GCAP1) presents additional regulation in vivo by phosphorylation (López-del Hoyo et al., 2014). The observation that the Ca^{2+}-free form of GCAP2 is phosphorylated to a much higher level than the wildtype protein, that it is retained at the inner segment by binding to 14-3-3 proteins, and its high

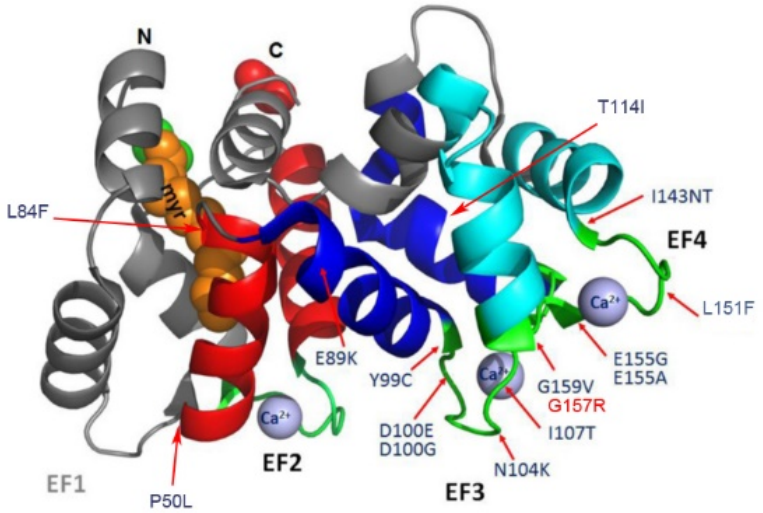

Figure I.7. Three dimensional structure of GCAP1. Disease-related residues in GCAP1 are indicated in blue. In red, residue linked to RP in GCAP2. PDB: 2R2I. (Jiang et al., 2014)

tendency to aggregate upon accumulation, lead us to speculate that this could be mechanism underlying the pathology of the GCAP2-G157R mutant. That is why one of the specific aims of this thesis is to study whether G157R mutation in GCAP2 affects the subcellular distribution of the protein, which would indicate a cGMP-independent physiopathology.

Table I.3. List of identified mutants linked to disease in GCAPs

GCAP	*Mutation*	*Localization*	*Dystrophy*	*Activity of GC*	
GCAP1	*P50L*		*AD Cone, rod-cone*	*Like WT*	*Low thermal stability*
GCAP1	*L84F*		*AD Cone, cone-rod, macular*	*Constitutive Activation*	*High Thermal stability*
GCAP1	*E89K*	*EF3*	*AD Cone*	*Constitutive Activation*	
GCAP1	*Y99C*	*EF3*	*AD Cone, cone-rod, macular*	*Constitutive Activation*	
GCAP1	*D100E*	*EF3*	*AD Cone*	*Constitutive Activation*	
GCAP1	*N104K*	*EF3*	*AD Cone*	*Constitutive Activation*	
GCAP1	*I107T*	*EF3*	*AD Cone, cone-rod, macular*	*Constitutive Activation*	
GCAP1	*T114I*	*EF3*	*AR Atypical RP*		
GCAP1	*I143NT*	*EF4*	*AD Cone*	*Constitutive Activation*	
GCAP1	*L151F*	*EF4*	*AD Cone-rod*	*Constitutive Activation*	
GCAP1	*E155GD*	*EF4*	*AD Cone*	*Constitutive Activation*	
GCAP1	*G159V*	*EF4*	*AD Cone*	*Constitutive Activation*	
GCAP2	*G157R*	*EF4*	*AD RP*		

*Compiled from (*http://www.omim.org/entry/600364*, Jiang et al., 2014, Kamenarova et al. 2013; Dell'orco et al. 2014; Newbold et al. 2001; Palczewski et al. 2004; Nishiguchi et al. 2004; Sato et al. 2005).*

Taken together, the fact that so many mutations map at the protein complex responsible for cGMP synthesis (RetGC/GCAPs/RD3) stresses the relevance to deepen our understanding of the mechanisms underlying the stabilization, assembly, trafficking to the outer segment, anchoring and functional regulation of this enzymatic complex, as well as its functional interconnexions with multienzyme complexes in interconnected metabolic pathways.

1.4. IMPDH1. Role in photoreceptor cells and its relationship to inherited blindness

1.4.1. Role of IMPDH1 in de novo synthesis of guanine nucleotides.

GTP can be synthesized *de novo*, or by a *salvage* pathway. The biosynthetic pathway for *de novo* synthesis of GTP relies on two main metabolic pathways: i) the synthesis of IMP from PRPP by the purinosome multienzyme complex, culminating in IMP synthesis, which is the common precursor for ATP and GTP synthesis (Figure I.8.A); and ii) synthesis of GTP from IMP by four enzymetic activities (Figure I.8.C).

The purinosome (Figure I.8.A) comprises six enzymes that catalyze the conversion of phosphoribosyl-pyrophosphate to inosine 5′-monophosphate (IMP). These six enzymes include one trifunctional enzyme (TrifGART: GARS, GART, and AIRS domains), two bifunctional enzymes (PAICS: CAIRS and SAICARS domains; ATIC: AICART and IMPCH domains), and three monofunctional enzymes (PPAT, FGAMS, and ASL) (French et al., 2013; Yu et al., 2014).

Four enzymes catalyze the conversion of IMP to GTP. IMPDH catalyzes the rate-limiting step of GTP synthesis, acting as the gateway to guanine nucleotides (Hedstrom, 2009). IMPDH catalyzes the conversion of IMP to Xanthine Monophosphate (XMP), with the reduction of NAD^+ to NADH. Subsequently, XMP is converted to GMP by GMP Synthetase (Figure I.8.C). Guanylate kinase phosphorylates GMP producing GDP with ATP consumption, and then GTP is produced by phosphorylation of GDP by nucleoside-diphosphate kinase.

IMP and GMP can also be synthesized directly from hypoxanthine and guanosine respectively through the action of Hypoxanthine-guanine phosphoribosyltransferase (HPGRT), that transfers the 5-phosphoribosyl group from 5-phosphoribosyl 1-pyrophosphate (PPRP) to these nucleotides (Figure I.8.B).

In this context, IMPDH plays an essential role in GTP synthesis, constituting the rate-limiting step in the pathway from IMP to GTP.

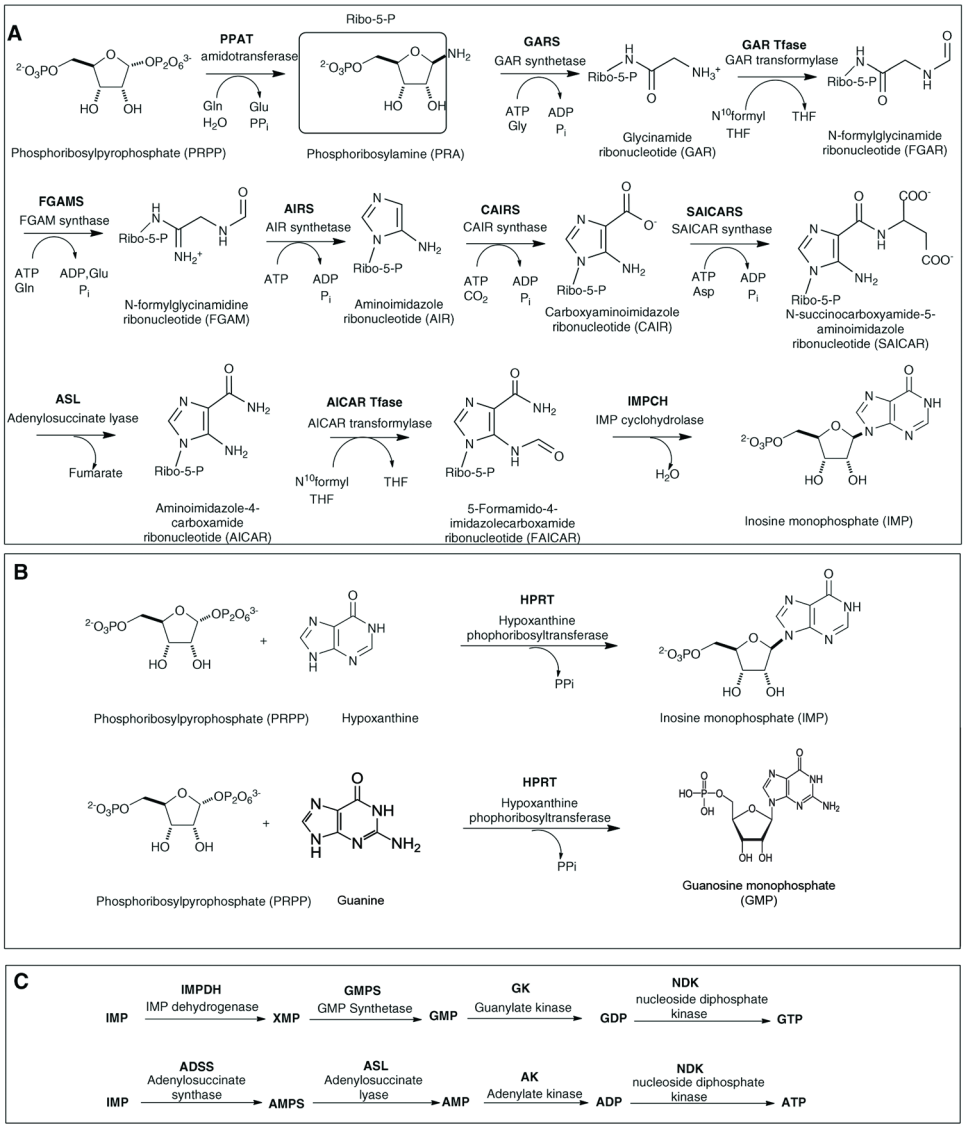

Figure I.8. Biosynthetic pathway of purines. A. Reactions catalyzed by the purinosome, common pathway in de novo synthesis of adenine and guanine nucleotides. B. Salvage pathway in purines biosynthesis. HPRT catalyzes the transfer of a phophorybosyl group to hypoxanthine, yielding IMP or to guanine, yielding GMP. C. IMP is the last common intermediate in the synthesis of ATP and GTP. GTP is synthesized from IMP by the successive enzymatic steps by IMPDH1, GMPS, GK and NDK. ATP is synthesized from IMP by the action of ADSS, ASL, AK and NDK. Modified form Zhao et al. 2013.

1.4.2. Structure of IMPDH.

Genes coding for IMPDH are highly conserved in evolution in all eukaryotes and also some prokaryotes. IMPDH is also conserved at the protein level. Like most mammals, humans have an IMPDH1 and an IMPDH2 gene. These genes encode enzymes that are 84% identical at the amino acid level and are virtually indistinguishable in its catalytic activity, but differ in its tissue expression pattern. IMPDH2 is dominant major isoform in most tissues and is up-regulated in proliferating cells and down-regulated upon differentiation. IMPDH1 is typically expressed at low levels but mRNA levels are high in tissues including retina, pancreas, brain, kidney and spleen (Thomas et al., 2012). Little or no Impdh2 expression is detectable in photoreceptors and only low levels of HPRT transcript are observed (Aherne et al., 2004). However, mice lacking IMPDH1 present only a mild retinal degeneration at 11 months old, that indicates that other non-canonical pathways may be involved in the regulation of the guanine pool in the retina.
IMPDH forms tetramers in solution, each monomer consisting of a catalytic and a regulatory domain. The catalytic domain is composed by an eight-stranded α/β barrel structure, which performs the enzymatic function, and the regulatory domain, of about 120 amino acids long, is inserted within a loop of the catalytic domain and is composed of two repeats of the cystathionine b-synthase (CBS) domain, constituting a CBS pair or Bateman domain (CBS domain or Bateman domain)(Bowne et al., 2006a; Buey et al., 2015). (Figure I.9).

CBS domains are also present in a variety of proteins such as voltage-gated chloride channels, AMP-activated protein kinase and CBS, where they regulate the protein function in response to the binding of adenosyl molecules (Buey et al., 2015). The physiological importance of CBS domains is emphasized by the fact that

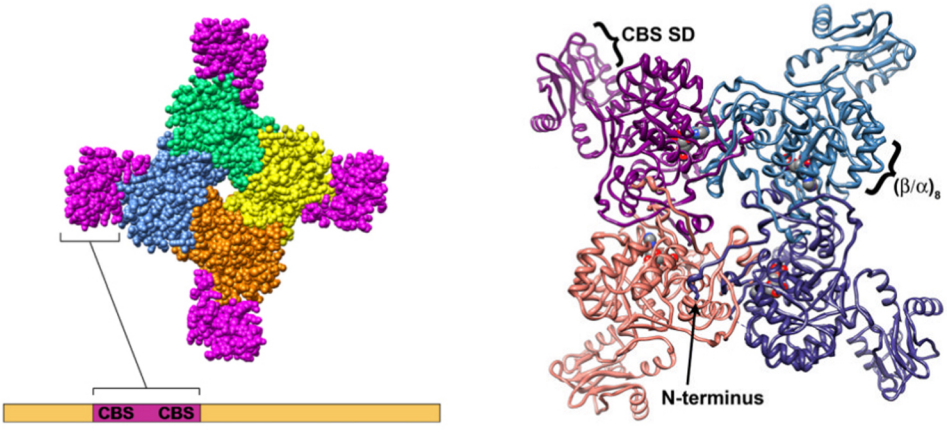

Figure I.9. Structure of IMPDH1. IMPDH1 forms a tetramer (also octamer), where catalytic domain are guided to the center of structure and CBS domains are guided out (Hedstrom, 2009; Pimkin and Markham, 2008).

mutations in these domains are associated with a variety of human hereditary diseases, such as homocystinuria, Wolff-Parkinson-White syndrome, myotonia congenital, etc. (Buey et al., 2015; Pimkin and Markham, 2008). Mutations in the CBS domain also have been linked to Retinitis pigmentosa and Leber Congenital Amaurosis (see below 1.4.3).

IMPDH1 presents a complex regulation that is not well understood with multiple mechanisms that regulate its activity in the cell.

1.4.3. Retina-specific isoforms of IMPDH: mutations linked to RP and LCA

IMPDH1 has been linked to blindness. In 2002, a mutation linked to autosomal dominant retinitis pigmentosa 10 (adRP10) was identified from a large family from Spain (Arg224Pro,(Kennan et al., 2002), Table I.4); and another mutation (Asp226Asn) in two American and one British families (Bowne *et al*, 2006b, Table I.4). Mutations R105W and N198K were later linked to rare adLCA (Bowne *et al*, 2006b, Table I.4). These mutations cluster at the CBS-"similar to cystathione-b-synthase gene"-structural domain of the protein. This is a domain that flanks the α/β barrel structure which performs the enzymatic function, dispensable for catalytic activity and whose function is not known. Furthermore, mutations in IMPDH1 are autosomal dominant, assumed to cause a "gain-of-function" rather than a "loss-of-function" phenotype, based on the observation that the IMPDH1 knockout presents only a mild retinopathy (Aherne et al., 2004). Today it is estimated that mutations in IMPDH1 account for 5-10% of autosomal dominant retinitis pigmentosa (adRP) cases (Bowne et al., 2002). Despite IMPDH1 conservation and ubiquity, the clinical manifestations of missense mutations in IMPDH1 are limited to the retina. The mechanism underlying the disease is currently unknown. It has been predicted that IMPDH1 would have some specific or distinctive function in photoreceptor cells of the retina. Extensive structural and biochemical IMPDH1 characterization has provided important insights in this respect, even if IMPDH1 unique or distinctive function in the retina is still not completely understood.

The first important insight towards understanding a retinal-specific phenotype of IMPDH1 mutations is that IMPDH1 expression levels are very high in photoreceptor cells of the retina, compared to other tissues, and that there are several retinal-specific isoforms of IMPDH1 that are produced by alternate splicing and/or alternative start sites of translation (Bowne et al., 2006a). There are four to seven major isoforms of IMPDH1 in high vertebrates, with their specific sequence and relative abundances varying between species (Bowne et al., 2006a, 2006b; Spellicy et al., 2007) (Figure I.10). Figure I.10 shows that although the canonical isoform of IMPDH1 (514aa) is the same in both humans and mice, major retinal-specific isoforms can be different (546aa in human and 603-604aa in mouse).

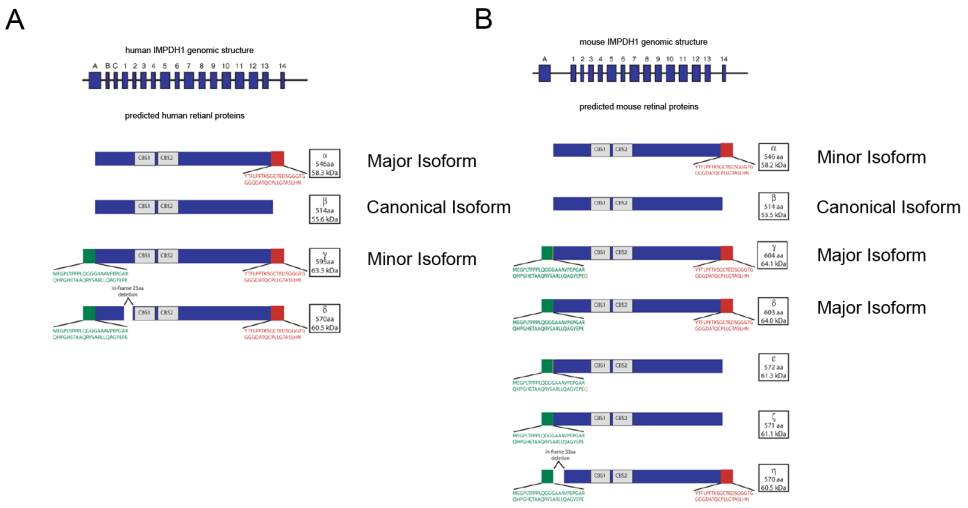

Figure I.10. Genomic structure and detected proteins in retina in A. human and B. mouse.(Spellicy et al., 2007)

Table I.4 shows the mutations in IMPDH1 that have been linked to retinal dystrophies.

Table I.4. Mutations linked to retinal degeneration found in IMPDH1.

Mutations	*Disease*	*Localization inside*	*Frequency*	*Identified population*
R105W	*LCA*			*American subject*
T116M	*adRP*	*CBS Domain*		*American subject*
N198K	*LCA*	*CBS Domain*		*American subject*
R224P	*adRP*	*CBS Domain*		*Large Spanish*
D226N	*adRP*	*CBS Domain*	*2%RP*	*American subject*
V268I	*adRP*			*American subject*
G324D	*adRP*	*Catalytic Domain*		*American subject*
H372P	*adRP*	*Catalytic Domain*		*American subject*

Compiled from Bowne et al. 2006; Kennan et al. 2002; Bowne et al. 2002

1.5. Brain-type Creatine Kinase

1.5.1. Role of Brain-type Creatine Kinase (CKB).

Creatine kinase (CK) catalyzes the reversible transphosphorylation from ATP to creatine (Cr) to yield phosphocreatine (PCr). The action of CK contributes to maintain the cellular energy homeostasis by guaranteeing stable and locally buffered ATP/ADP ratios (Andres et al., 2008; Wallimann et al., 1998).

Four isoforms of CK can be found in vertebrates: Muscle-type (M), Brain-type (B), sarcomeric mitochondrial-type (sMt) and ubiquitous mitochondrial (uMt). These enzymes are associated in two different combinations depending on tissue expression, dimeric MM-CK and octameric sMT-CK, which is expressed in differentiated sarcomeric, cardiac and skeletal muscle; and dimeric BB-CK with

octameric uMt-CK, which is expressed in brain, neuronal cells, retinal photoreceptor cells, hair cells bundles of the inner ear (Shin et al., 2007), smooth muscle, kidney, endothelial cells, spermatozoa and skin.

Both combinations of isoenzymes contribute to generate an intracellular pool of PCr, which represents a temporal energy buffer that prevent a fall on ATP levels in high cell energy requirements scenarios. Cytosolic and mitochondrial CK are specifically localized in those focus of high ATP consumption of the cell, like ATPases of different ions pumps, myosin ATPase of contractile muscle apparatus, or the calcium pumps in the sarcoplasmic reticulum. Due to the specific localization of both types of isoenzymes, and the much faster diffusion rate of PCr and Cr compared with ATP and ADP, the CK/PCr system is the energy shuttle of the cell (Andres et al., 2008).

1.5.2. ATP cycle in mitochondria.

ATP is synthetized by oxidative phosphorylation in mitochondria or by glycolysis. CK is associated to those points of ATP synthesis to generate a pool of PCr. Mt-CK is located at intermembrane space of mitochondria, and synthetize PCr from mitochondrially generated ATP. PCr leaves mitochondria by Cr-transporters. PCr is used to generate a PCr pool that is used to buffer cytosolic ATP/ADP ratios and for local ATP consumption (Figure I.11) (Andres et al., 2008; Wallimann et al., 1998).

1.5.3. Phosphocreatine cycle in muscle and neurons.

Cells with high and fluctuating energy demand, like muscle cells and neurons, which must change in seconds (or miliseconds) from an idle state to a fully active state, may increase the rate of ATP hydrolysis in several orders of magnitude within seconds, but ATP levels remains stable. Thus, these cells require the action of immediately available, fast and efficiently working energy supporting systems that connect sites of energy consumption with those of energy production via a phosphoryl transfer network (Andres et al., 2008). Diffusion coefficient of PCr is higher than ATP (Hubley et al., 1995). For this reason, the CK/PCr system plays a critical role in ATP metabolism.

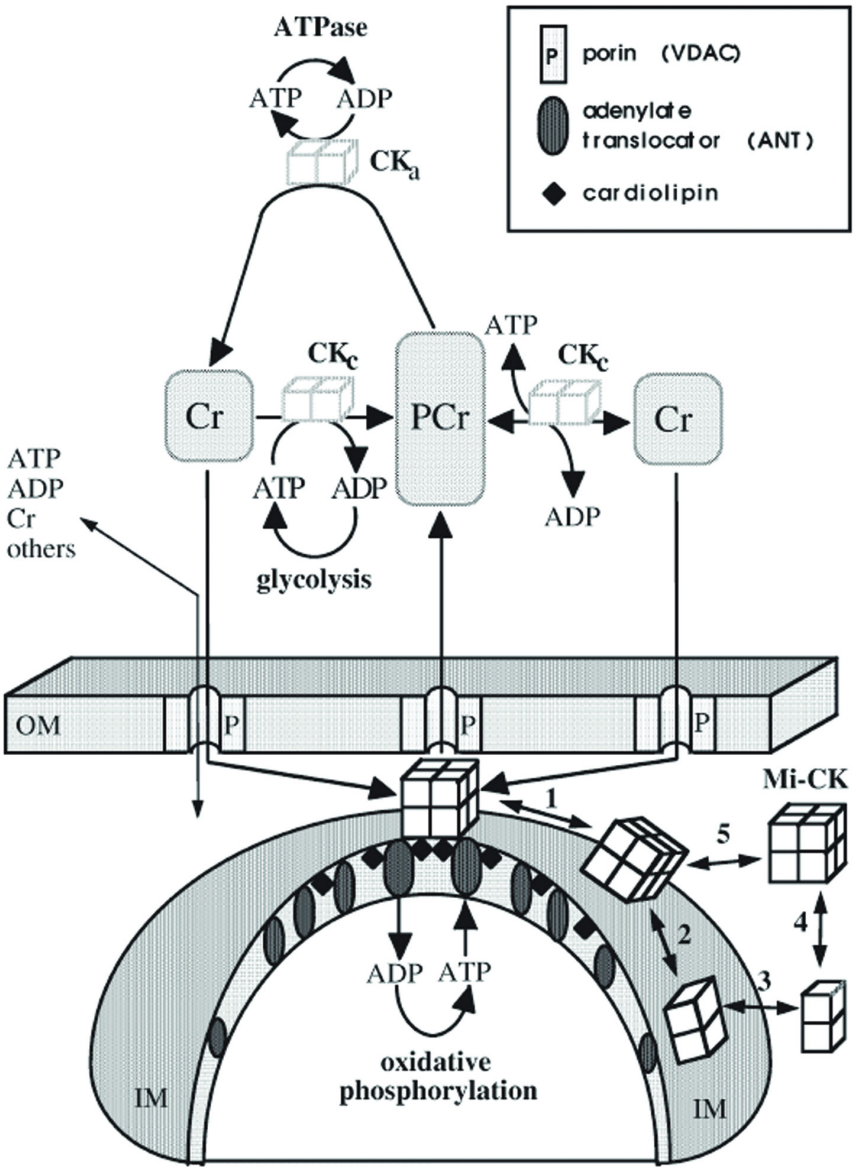

Figure I.11. Phosphocreatine/Creatine Cycle. ATP is produced by oxidative phosphorylation in the mitochondrial matrix. Mitochondrial Creatine Kinase (Mi-CK) which is bound to outer side of mitochondrial inner membrane (IM) close to outer membrane (OM) acts as a shuttle catalyzing the tranfer of a high energy phosphate group from ATP to Creatine, exporting phosphocreatine (PCr) to cytosol and maintaining the levels of ADP in mitochondrial matrix. PCr can also be produced by cytosolic Creatine Kinase (CKc) transfering a phosphate group form ATP produced by glycolysis. PCr acts as a reservoir of energy into cytosol diffuse to high energy demand places to supply ATP by local action of specifically associated creatine kinase (CKa).(From Wallimann et al. 1998)

1.5.4. Differences in energetic requirements of rods and cones

Major ATP consumers in rods and cones are the Na^+ influx through cGMP-gated channel, maintained by ATPase ion-pumps and enzymatic processes necessary for signal transduction (eg. GTP consumption by Transducin and Guanylate cyclase, visual pigment phosphorylation…). Changes on ATP homeostasis can board from $5.7 \cdot 10^7$ molecules of ATP in rod disk in darkness to zero in bright light that closes all cGMP-gated channels in a time-window of milliseconds (Okawa et al., 2008).

In darkness, rods and cones have a similar ATP consumption, as they have similar dark currents and similar amplitude and voltage-dependence of inner segment Ca^{2+} current. However, in light, cones consume much more ATP than rods. In cones, at the brightest bleaching intensity, the influx of Na^+ through cGMP-gated channels never falls further than about half that in darkness. Therefore, cones have a higher metabolic cost than rods (Okawa et al., 2008). Cones have a similar biochemical cascade to rods, but the kinetics of the response to light are faster than rods (Kawamura and Tachibanaki, 2008; Rodieck, 1998), pointing to higher ATP requirements of cones than rods.

1.6. Development of innovative methodologies for gene function studies in the retina.

1.6.1. Genetic heterogeneity of Retinal Dystrophies

Inherited retinal dystrophies, affecting one in 4000 individuals worldwide, are very heterogeneous at the genetic level and at their clinical manifestations. This great heterogeneity difficults their study and treatment. Gene defects might primarily affect rod function (causing retinitis pigmentosa, RP); cone function (cone-rod dystrophies and age-related macular degeneration); or both types of photoreceptor cells in a severe congenital form of retinal dystrophy (Leber congenital amaurosis, LCA). These disorders have autosomal recessive, autosomal dominant or X-linked patterns of inheritance and are clinically and genetically heterogeneous. Some of these genes are listed in Figure I.12 and include those that code for proteins directly involved in the light response at the light sensitive compartment but also genes encoding proteins whose function is required for the expression, stabilization, trafficking or anchoring of phototransduction proteins. This group includes transcription factors, splicing factors or proteins involved in ciliary membrane trafficking.

To study the effect of mutations in phototransduction genes is relatively straight-forward because phototransduction has been intensely studied for the last three decades. The major molecular players and enzymatic steps have been well

characterized. However, many genes that have been recently linked to retinal disorders encode proteins of unknown function that are likely involved in other central aspects of photoreceptor cell biology that are less understood. One of these is the underlying mechanisms of polarization that sustain the high degree of compartmentalization of these cells. Many genes linked to Retinitis or LCA are suspected to be involved in polarized membrane trafficking across the cilium, or in cilium biogenesis and maintenance, but their specific functions remain unknown: some gene examples are RP1, TULP1, RP9, TOPORS, RPGR, RPGRIP1, CEP290, RD3, RP2, and LCA5.

One of the difficulties to address gene function studies in photoreceptor cells of the retina resides in the high degree of specialization of these cells. There are no established cell lines that reproduce their high degree of compartmentalization. For this reason it is required the production of genetically modified mice, a crucial tool for understanding the role of a gene in biology and disease in the context of the living cell.

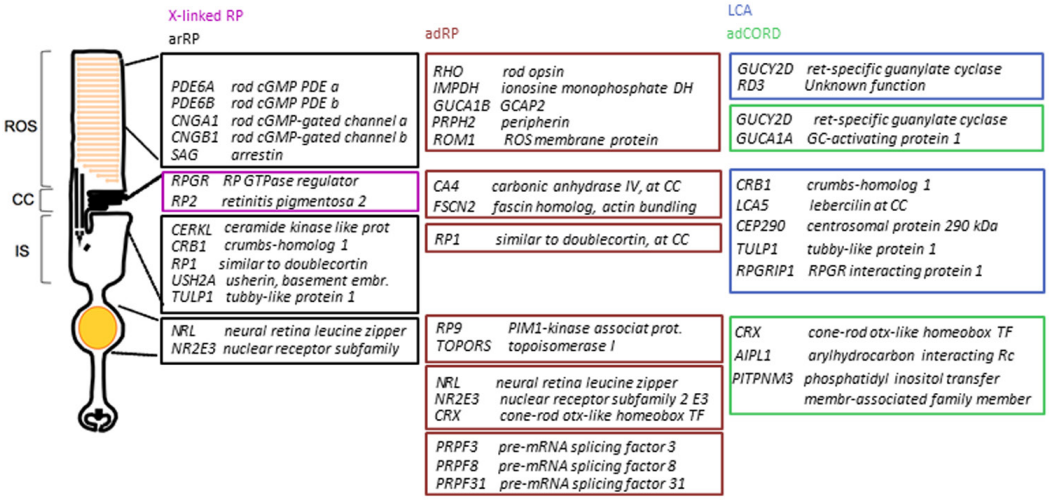

Figure 1.12. List of Retinal Dystrophies (RD) causative genes and their subcellular localization. arRP, adRP, XlRP: autosomal recessive/dominant/X-linked retinitis pigmentosa. LCA: Leber's congenital amaurosis. adCORD: autosomal dominant cone-rod dystrophy.

1.6.2. Historical perspective of Transgenic Animals.

Mankind has always wanted to modify his environment for his own benefit. The methods of modification of animals and plants have evolved with mankind itself, beginning with domestication of wild animals and plants up to reaching the era of DNA recombinant technology. Genetic engineering era began in 1972, stablishing a milestone in the evolution of this field (Figure I.13), when the first genetically modified organism was created (Cohen et al., 1972) by transfering genes from an *E.*

coli to another to confer it with new characteristics. In 1974, Rudolf Jaenisch *et al.* (Jaenisch and Mintz, 1974) got the first genetically modified mammal, but the generated mouse could not transmit the acquired characteristic to its offspring. This milestone was achieved eight years after, when the first stable transgenic mouse that passed exogenous genes to its offspring was obtained (Palmiter et al., 1982)(Figure I.13). Palmiter and collaborators injected exogenous DNA carrying the gene for human growth factor into the pronucleus of fertilized eggs, which led to generation of transgenic mice with a dramatic growth.

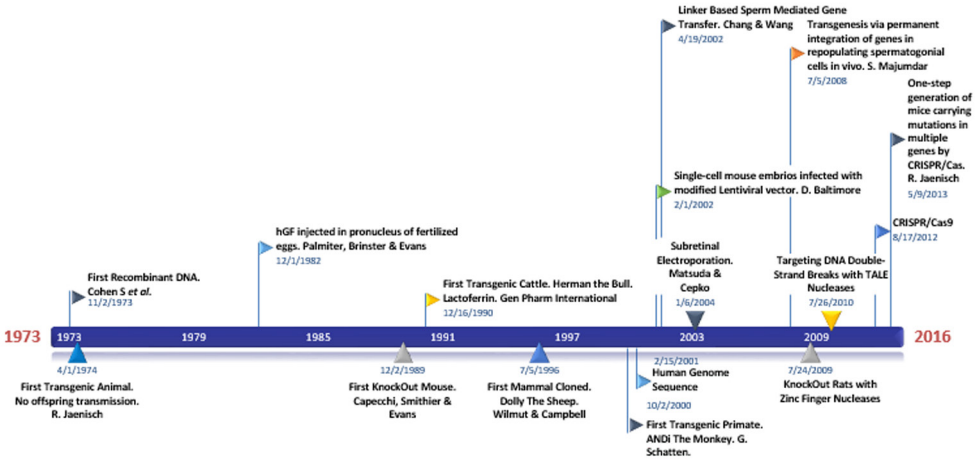

Figure 1.13. Milestone in evolution of transgenic animals.

The heterologous expression of a gene in a given cell type or tissue (generation of transgenic animals) opened great opportunities to the study of human diseases and molecular and cellular basic processes. However sometimes loss-of-function studies are required in the study of these same processes. The first loss-of-function mouse was generated in 1989 on the basis of independent work of M. Capecchi (Homologous Recombination); O. Smithier, (Homologous recombination); and M. Evans (developing procedures for injection of modified cells into embryos).

Today there are several established ways to generate transgenic animals:

- Microinjection of pronucleus of fertilized eggs. Used by Palmiter et al. to generate the first stable transgenic mouse.
- Embryonic stem cells injection. This methodology was used for generation of the first knockout mouse (Capecchi, 1989; Doetschman et al., 1987; Koller et al., 1989; Thomas and Capecchi, 1987). Nobel Prize in Physiology and Medicine in 2007.
- Virus delivering into fertilized eggs. Modified virus, that can infect but cannot replicate itself, are injected into fertilized eggs (Lois et al., 2002). This methodology

can be used for transfect directly the egg at stage of pronucleus or to transfect embryonic stem cells, improving transfection efficiency.

- Somatic cell nuclear transfer. In which the cell of a somatic cell is transferred to cytoplasmic of an enucleated egg. This technique was used for the first mammal cloned, Dolly the sheep (Wilmut et al., 1997).

New tools have arisen in more recent years, like Zinc-Finger Nucleases (ZFN), Transcription-activator like effector Nucleases (TALEN) and Clustered Regularly Interspaced Short Palindromic Repeats (CRISPR), that have enabled custom gene editing, easing and increasing efficiency of homologous recombination. Briefly, ZFN and TALEN are designed proteins, that act as dimer, composed by two domains, the nuclease domain from FokI nuclease, and a DNA recognition domain, that can be formed by three Zinc-finger, where each one recognize three base pair, or by 8-10 Talen repeats, where each subdomain recognized only one base pair. These characters have done difficult to work with ZFN or TALEN because of they involve the precise design of a nuclease protein that must be refined for its correct function (Gaj et al., 2013). On the other hand, CRISPR involve a site-directed nuclease, Cas9, whose recognition site is defined by a specific sequence of 20 nucleotides in a RNA molecule (Cong et al., 2013; Jinek et al., 2013; Mali et al., 2013; Qi et al., 2013; Wang et al., 2013; Yang et al., 2013). This fact facilitates working with this kind of nucleases and make it a powerful tool revolutionizing gene editing and transgenic animal fields.

Despite of the numerous milestones in generation of transgenic animals, these techniques already need a great amount of resources, with highly specialized facilities and staff.

Because of photoreceptor cells are highly compartmentalized and differentiated neurons, the absence of stablished cells lines that reproduce its complexity and the heterogeneity of genetic disorders linked to blindness, forces up to work *in vivo* with genetically modified animals. Owing to this has been needed the development of new transgenic tools and so by-passing the challenges of traditional transgenic mice generation.

In this work, we going to deal about stable transgenesis by transfection and electroporation of male spermatogonia *in vivo* (Matsuda and Cepko, 2004) *(Chapter II)* and transient transgenesis by subretinal electroporation *in vivo (Chapter III)* (Dhup and Majumdar, 2008; Usmani et al., 2013).

Aims

Aims

The Retinal guanylate cyclase / Guanylate Cyclase Activating Proteins (RetGC/GCAPs) complex, responsible for cGMP synthesis in rod and cone photoreceptor cells of the retina, plays a fundamental role in termination of the light response and in light adaptation. Mutations in the genes encoding these proteins or their regulators lead to different forms of inherited human blindness. The **MAIN AIM** of this work is to characterize this protein complex by identifying new protein interactors that may contribute to understand the complex assembly, trafficking, organization and modulation *in vivo*. The complexity of the visual system and the high degree of compartmentalization of photoreceptor cells is hard to reproduce in culture or reconstituted systems. Because of that, we also aimed at developing novel transgenesis methodology that would accelerate gene function analysis in the retina.

SPECIFIC AIMS:

1. Develop new methodology for the generation of stable transgenic mice rapidly and at low cost by *in vivo* DNA electroporation of the male germline, and subsequent breeding. Development of expression vectors for efficient transgene expression in retinal rods and cones (Chapters II & III).

2. Study the mechanisms governing GCAP1 and GCAP2 subcellular distribution in photoreceptor cells, by studying the molecular determinants of GCAPs distribution to rod outer segments *in vivo* (Chapter III).

    2.1. Identify new interacting partners of the RetGC/GCAPs complex by performing a pull-down assay with GCAP1 followed by liquid chromatography and tandem mass spectrometry identification of the bound proteins: biochemical and functional characterization of prime candidates (Chapters IV & V).

Objetivos

El complejo proteico formado por la guanilato ciclasa y las proteínas activadoras de la guanilato ciclasa (RetGC/GCAPs) en retina, responsable de la síntesis de cGMP en las células fotorreceptor de la retina, conos y bastones, juega un papel fundamental en la respuesta y adaptación a la luz. Mutaciones en genes que codifican para estas proteínas conducen a diferentes formas de cegueras hereditarias. El objetivo principal de este trabajo es caracterizar este complejo proteico mediante la identificación de nuevos interactores moleculares que puedan contribuir a entender como este complejo se ensambla, transporta, organiza y modula *in vivo.* La complejidad del sistema visual y el alto grado de compartimentalización de las células fotorreceptor de la retina son difíciles de reproducir en células en cultivo o en sistemas reconstituidos. Debido a esto, nuestro objetivo es también desarrollar nuevas metodologías de transgénesis que podrían acelerar el análisis de la función génica en retina.

Objetivos Específicos:

1. Desarrollar una nueva metodología para la generación de ratones transgénicos estables de forma rápida y a bajo coste mediante la electroporación *in vivo* de DNA en la línea germinal masculina y subsecuente cruzamiento. Desarrollo de vectores de expresión para la expresión eficiente de genes en retina.

2. Estudiar los mecanismos que gobiernan la distribución subcelular de GCAP1 y GCAP2 en fotorreceptores de retina, mediante el estudio de los determinantes moleculares que regulan la distribución de las proteínas GCAPS al segmento externo del fotorreceptor *in vivo.*

3. Identificar nuevos interactores del complejo RetGC/GCAPs mediante ensayos de Pull-Down con GCAP1 seguidos de la identificación de las proteínas unidas por cromatografía líquida y espectrometría de masas en tándem: caracterización bioquímica y funcional de los principales candidatos.

Results

Chapter II. Stable transgenesis by electroporation of spermatogonia.

Chapter III: Molecular determinants of localization of GCAPs

Chapter IV: Unanticipated interaction between IMPDH1 and RetGC1 proteins associated to blindness.

Chapter V: Characterization of RetGC1 association to Creatine Kinase-B in photoreceptor cells.

Chapter II. Stable transgenesis by electroporation of spermatogonia

Chapter II. Stable transgenesis by electroporation of spermatogonia.

Contributions

We are in debt to Dr. Alvaro Gimeno at the Vivarium facility for his assistance at training us in surgery protocols for mice. We also acknowledge Esther Castaño´s assistance with cell-sorting experiments and data interpretation.

My contribution to this chapter was the design and cloning of all presented expression vectors; the presented electroporation procedures with the different surgical protocols, and the extensive analysis of the progeny from electroporated mice by PCR, Southern blot and Western procedures.

Chapter II. Stable transgenesis by electroporation of spermatogonia

2.1. DNA electroporation in the germ line: rationale and basis of the procedure.

Because of the high degree of compartmentalization and differentiation of photoreceptor cells of the retina and their highly specialized function in visual transduction, there are no cell lines that completely reproduce this complexity in culture. Therefore, the study of basic processes at the first steps of seeing as well as the physiopathology underlying inherited retinal dystrophies are best studied *in vivo* using gain-of-function and/or loss-of-function animal models. Genetic studies in animal models are a powerful tool for the study of gene function in the context of the living cell. There are hundreds of different genes involved in various forms of inherited retinal dystrophies, many of them of still unknown function. Therefore, the development of new, more efficient methods for rapid gene function analyses *in vivo* would greatly benefit research on photoreceptor cells.

One limitation of genetic studies is the cost associated to generation of transgenic animals, particularly mammals such as mice. Standard procedures for transgenic production involve costly and technically demanding procedures, such as DNA microinjection into the pronuclei of fertilized eggs. These procedures involve expensive equipment for microinjection and for the culture of embryos, highly qualified staff, and the permanent maintenance of mouse colonies ready for the production of embryos, and the reception of embryos. Overall, transgenic facilities are very expensive to run, and generating transgenic mice is very costly and time-consuming. Our goal here was to implement in the laboratory a method for generation of stable transgenesis in the retina based on *in vivo* DNA electroporation into the male germ line. That way we would bypass the use of standard transgenic technical platforms, if we could bypass the need to isolate the embryos, put them in culture, or microinject them. The cost and the duration of generation of transgenic mice would be dramatically reduced, and anybody could do it.

When we first conceived the idea of using *in vivo* electroporation for transfection of DNA into the male germ line, we did a thorough revision of the literature and realized that the group of S. Majumdar, from the National Institute of Immunology at New Delhi, India, had apparently developed the methodology to generate stable transgenic mice this way (Dhup and Majumdar, 2008). Conceptually, the methodology relied on the fact that spermatogonial cells are located out of the blood-testis barrier (formed by tight junctions between Sertoli cells), at the base of seminal tubules and hence directly in contact with interstitial fluid (Figure II.1). Therefore, the injection of linearized naked DNA into the interstitial fluid of testis, followed by electroporation, should allow incorporation of the DNA into primary spermatogonial cells. Briefly, the methodology consisted on:

i) injection of linearized DNA into the interstitial fluid of testis followed by electroporation at postnatal day 30, ii) a waiting period of 35 days of normal rearing of electroporated male to allow for one cycle of spermatogenesis, and iii) breeding of the electroporated mice at p65, to obtain progenies that would carry the genetic modification ubiquitously.

To implement this methodology in the laboratory, we visited Dr. S. Majumdar´s laboratory at the National Institute of Immunology in New Delhi in August of 2012, in the collaborative frame of a project of Bilateral Cooperation Spain-India. There we observed and learned to perform the different procedures.

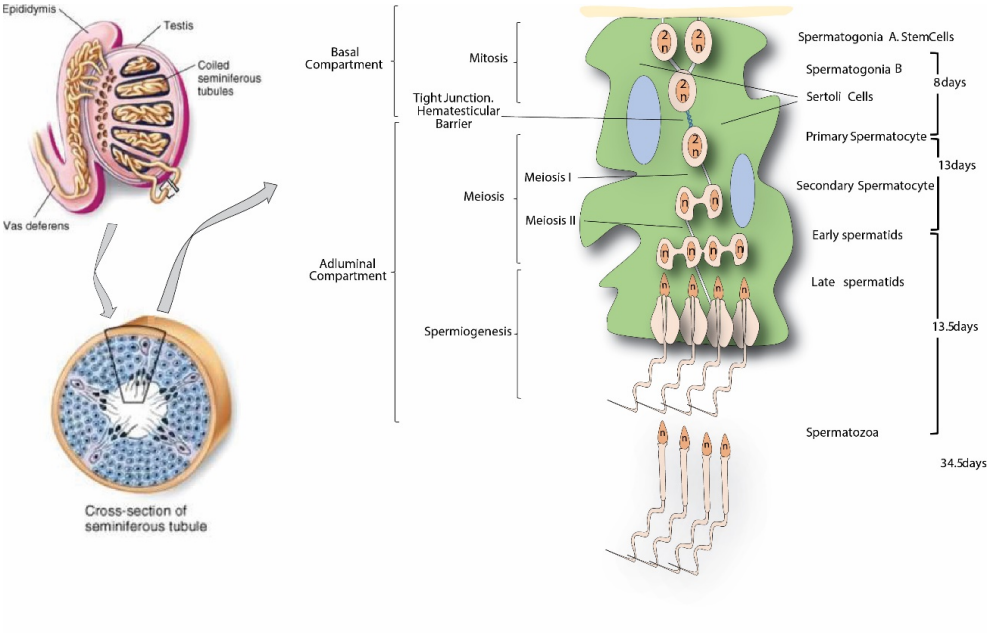

Figure II.1. Anatomy of the testis. Seminiferous tubules are coiled inside the testis. A cross-section of a seminiferous tubule shows that spermatogonia stem cells are in the periphery of the tubule, out of the blood-testis barrier (hematotesticular barrier) formed by tight-juctions of the sertoli cells. A complete cycle of spermatogenesis takes about 35 days in mouse, from differentiation of stem cells up to mature spermatozoa.

We implemented three different methods of injection over time. The first one involved the removal of one of the testis by surgery (hemicastration), while the remaining testis was injected with DNA at three different sites and then electroporated by a square-wave electroporator as described in materials and methods. The second one involved surgery to perform an opening in the wall of the scrotum to perform DNA injection and electroporation of both testis in the same procedure. Finally, the third method avoided surgery, and involved DNA injection and electroporation of both testis in the same procedure, performed through the wall

of scrotum. These methods are described in detail at the chapter of material and methods. With each change, the procedure evolved to a less-invasive method, with the goal of leaving the DNA into the interstitial fluid of the testis with the minimal possible alteration of the organism.

2.2. Progressive development of improved expression vectors for DNA electroporation in the germ line: the importance of avoiding gene silencing.

2.2.1. Results of electroporating a reporter gene under a ubiquitous promoter: use of pL_UG *plasmid.*

Our first attempt to generate stable transgenics by DNA electroporation of the male germ line was based on electroporation of 9 C57Bl/6J males with the plasmid pL_UG (#L01GLUG001XA. Signaling Gateway). This plasmid of 9Kbp expresses the reporter gene Green Fluorescent Protein (GFP) under the control of the Ubiquitin C promoter (UbiC) (Figure II.2). This plasmid drives constitutive and ubiquitous expression of GFP, and should result in the generation of mice that would emit green fluorescence upon exposure to UV-light. Electroporated C57Bl males were bred to 2-3 60-day-old females, and the obtained progeny was analyzed by exposure to UV-light, by PCR analysis and by Western Blot of different tissues.

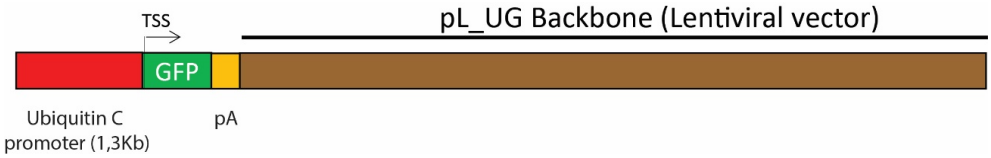

Figure II.2. Scheme map of linearized pL_UG plasmid as injected in mice. Red box represents the Ubiquitin C promoter (1.3Kb), green box represents the Green Fluorescence Protein (GFP) reporter gene, and the yellow box the polyadenylation signal. The brown box is the plasmid backbone, proceeding from the plasmid collection of the Alliance for Cell Signaling.

Figure II.3 shows a representative result of the PCR genotyping (Figure II.3A) and Western Blot (WB) analysis (Figure II.3B) of the progeny. Several PCR positive-mice are detected among the F1 (Figure II.3A, where the last lane in the panel labeled as +ctrl shows the PCR-amplified product from the electroporated plasmid). However, most of the PCR-positive mice did not show GFP expression by Western Blot analysis (Figure II.3B). We detected just one mouse that showed GFP expression in liver tissue by Western blot, even if it did so at much lower levels than a control mouse line. The positive control for Western blot was tissue obtained from an established mouse line that expresses GFP under the strong and ubiquitous CAG promoter (composed by the cytomegalovirus early enhancer element, the

promoter, first exon and first intron of chicken beta-actin gene; and the splice acceptor of the rabbit beta-globin gene (Okabe et al., 1997)). Table II.1 summarizes the results of the progeny analyzed in this experiment. The fact that we obtained several mice that were PCR-positive but did not show noticeable protein expression by Western blot, led us to hypothesize that gene silencing was likely taking place in the progeny.

Figure II.3.C shows representative testis of the electroporated mice, sacrificed at p90 after several rounds of breeding. Even 60 days after electroporation, GFP expression was clearly observed in all testis examined. Cross-sections of the testis (Figure II.3.D) highlighted isolated transfected cells with the appearance of Sertoli cells. No green spermatozoa were observed in these samples at p90, but it is not clear to us whether GFP would be expressed from the UbiC promoter in spermatozoa. Spermatozoa are highly specialized cells that express only a few selected proteins required for flagellar movement. Therefore, the absence of green signal at spermatozoa did not necessarily indicate failure of DNA integration in the germ line.

The fact that we obtained several PCR-positive mice in the progeny that did not express the protein to noticeable levels by Western blot led us to consider that gene silencing could be taking place. Therefore, experiments from here on had to take into account that gene silencing could be precluding the heterologous gene expression. Expression vectors from here on were designed to take this consideration into account.

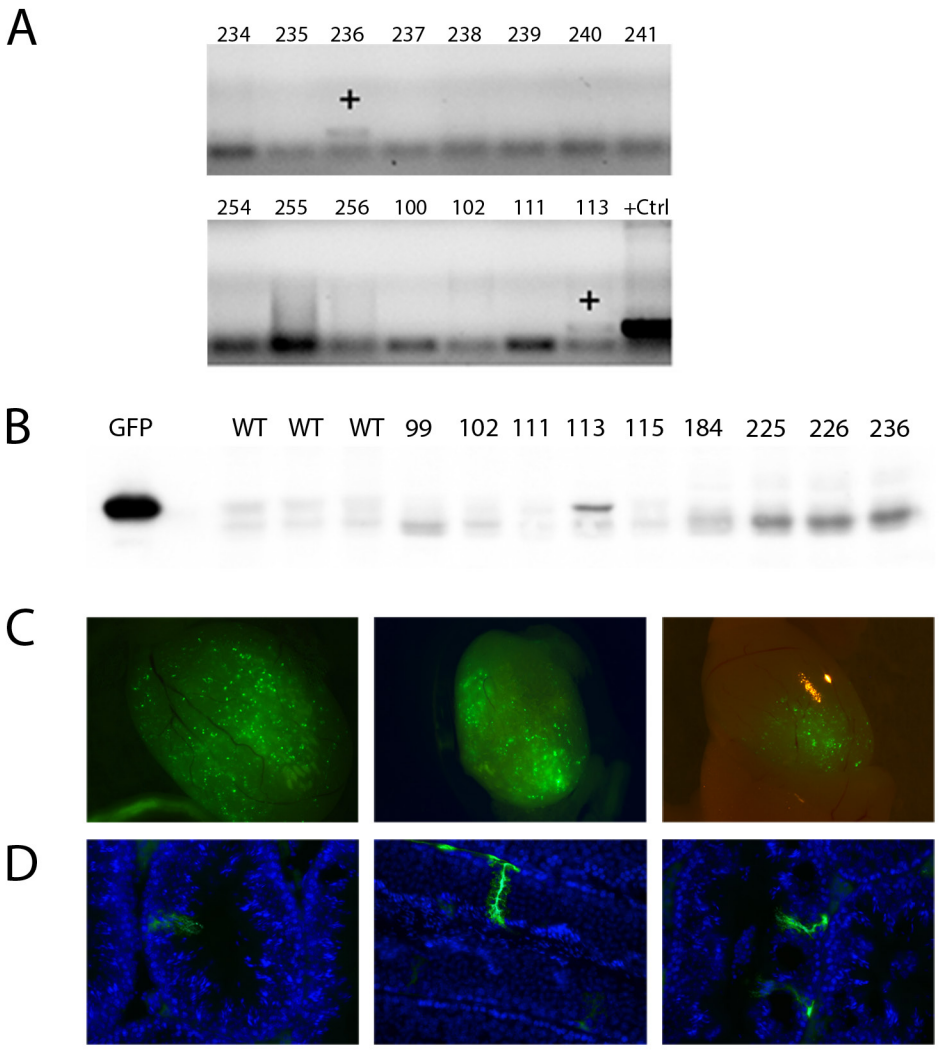

Figure II.3. Representative analysis of the progeny obtained from mice electroporated with pL_UG-GFP. A. Representative PCR analysis of the progeny, showing some PCR-positive mice. B. Western blot of liver extracts from PCR positive mice. 4µg total protein of liver homogenates were loaded in the GFP lane (positive control line, see text for details), while 40µg total protein of liver homogenates were loaded for each of the mice analyzed of the progeny. GFP expression was only observed in mouse #113. Because this lane had 10 times more amount of tissue protein than the GFP positive control, we estimate that the level of expression of GFP in mouse 113 was about 100-fold less than in the GFP established transgenic mouse. C. Testis from the electroporated mice obtained at p90 after several rounds of breeding, showing GFP fluorescence under UV-light. D. Cross-sections of electroporated testis show sporadic transfected Sertoli cells.

Table II.1 Summary of progeny analysis from mice electroporated with pL_UG

Fertile Males	Date of surgery	Date of first litter	Litters	Progeny	PCR	%PCR Positives	WB	Fluorescence with UV Light
#1	21/06/2010	13/08/2010	4	37	1			NO
#2	21/06/2010	20/08/2010	3	13	ND			NO
#3	21/06/2010	16/08/2010	3	17	ND			NO
#4	21/06/2010	16/08/2010	3	29	1			NO
#5	21/06/2010	28/08/2010	4	21	4		1?	NO
#6	21/06/2010	23/08/2010	3	17	ND			NO
#7	21/06/2010	27/08/2010	6	33	4			NO
#8	21/06/2010	16/08/2010	6	36	2			NO
8/9 (88.89%)			32	203	12	5.9	1	NO

ND- Not determined. NO- Not Observed.

2.2.2. Ruling out silencing by parental imprinting

The original paper of S. Majumdar was based on the FVB strain of mice. The FVB is an albino strain that is commonly used for generation of transgenic mice because of its prominent pronuclei in fertilized eggs and the large litter size (Jackson´s Lab). We used C57Bl in the laboratory because our research on the retina precludes us from using albino strains. It has been described that FVB and C57Bl strains, the most widely used strains in the field of transgenics, have different mechanisms of parental imprinting and gene silencing by methylation (Chaillet et al., 1995; Weichman and Chaillet, 1997). Therefore, we hypothesized that parental imprinting could be causing gene silencing in the progeny.

In order to test if parental imprinting might be responsible for gene silencing in the progeny in the C57Bl strain used in our previous experiment, four C57Bl males were injected and electroporated with plasmid pL_UG, and crossbred with FVB females. Table II.2 summarizes the results from this experiment, where only 4 PCR-positive mice were obtained in the progeny, and none of which showed detectable expression by WB or glowing fluorescence during UV-light exposure.

Table II.2 Summary of the analysis of the progeny from mice injected with pL_UG, after breeding to FVB females.

Fertile Males	Date of first litter	Litters	%Fertile males	Progeny	PCR	%PCR Positives	*Fluorescence with UV Light*
#9	13/11/2010	6		54	4		NO
#10	02/11/2010	4		42	0		NO
2/4		10	50.00	96	4	4.17	

2.2.3. Implementing the use of DNA barrier insulators to prevent gene silencing by heterochromatin condensation.

Transgene silencing in vertebrates occurs at the chromatin level. Insulators are DNA sequences that prevent inappropriate interactions between adjacent chromatin domains. Two main types of insulators have been described: those that isolate and block the activation of a promoter by an enhancer, known as *enhancer-blocking insulators*; and those that prevent gene-silencing by creating a barrier against the spread of heterochromatin, known as *barriers insulators* (Gaszner and Felsenfeld, 2006).

One of the most characterized barrier insulators is Matrix and scaffold Attachment Region (S/MAR) originally isolated from the chicken lysozyme locus (Gaszner and Felsenfeld, 2006), that are typically AT-rich sequences that are able to form barriers between independently regulated domains, by forming interactions with the nuclear matrix, allowing higher expression of transgenes independently of chromosomal position (Bode et al., 1996; Stief et al., 1989).

In order to test whether we could prevent silencing of the transgene by using barrier insulators, we performed another electroporation experiment in which linearized pL_UG was co-injected with the insulating sequences 5' S/MAR from chicken lysozyme gene, at a molar ratio of 1:2 into 6 C57Bl males. Co-injection of two sequences of DNA has been demonstrated to allow the co-integration of both sequences at the same site (Chen and Chasin, 1998). In this experiment, 72 mice were obtained in the progeny, of which 9 were PCR-positives. None of them were positive by WB or UV-light exposure. Although this was a straightforward and rapid experiment because it did not involve cloning, it could still be argued that the pL_UG plasmid backbone, of prokaryotic origin, was in the DNA cassette flanked by the DNA barrier insulators, and could in itself promote transgene silencing. Therefore we proceeded with further development of the expression vectors.

Table II.3 Summary of analysis of the progeny from mice injected with pL_UG in the presence of 5´S/MAR insulating sequences.

Fertile Males	*Date of first birth*	*Litters*	*%Fertile males*	*Progeny*	*PCR*	*%PCR Positives*	*Fluorescencewith UV Light*
#11	*14/04/2011*	*1*		*3*		*0*	*NO*
#12	*14/04/2011*	*1*		*4*		*0*	*NO*
#13	*24/03/2011*	*3*		*14*		*0*	*NO*
#14	*19/01/2011*	*8*		*51*	*9*	*17.6*	*NO*
4/6		*13*	*66.67*	*72*	*9*	*12.5*	

2.2.4. Elimination of CpG islands from the promoter sequence in expression vectors.

DNA methylation is the most common epigenetic modification that causes gene silencing. Only the cytosines adjacent to guanine (CpG sites) are substrates for methylation by methyltransferases in mammalian cells. Methylation has two distinct functions: it acts as a protection barrier from endonucleases designed to destroy foreign DNA and as a regulator of gene expression. Vertebrate CpG islands (CGIs) are short interspersed DNA sequences that deviate significantly from the average genomic pattern by being GC-rich, CpG-rich, and predominantly nonmethylated. CGIs are associated with more than three-quarters of all known transcription start sites and are defined as DNA sequences with: GC content above 50%, ratio of observed-to-expected number of CpG dinucleotides above 0.6, and length greater than 200 base pairs. (Bock et al., 2007; Deaton and Bird, 2011). Silencing of CGI promoters is achieved through dense CpG methylation. (Deaton and Bird, 2011).

An *in silico* analysis of the Ubiquitin C promoter (1287bp) by *Methyl Express Software 1.0* (#4376041. ThermoFisher Scientific) revealed that it contained a CGI of 1280bp of length. So, we decided to change the plasmid in order to avoid CpG dinucleotides in the promoter.

We acquired the plasmid pCpG from Invivogen (#pcpgf-mcs, Invivogen), which is completely devoid of CpG dinucleotides and presents a strong constitutive and ubiquitous quimeric promoter composed by the early enhancer of cytomegalovirus promoter, the human elongation factor 1 alpha core promoter and a synthetic intron in 5'UTR. A CpG-free version of SV40 polyadenylation sequence is used and two S/MAR sequences form chicken lysozyme gene flank the expression cassette. The EGFP cDNA was cloned into the multi-cloning site of this plasmid (Figure II2.4). Two C57Bl males were electroporated with this linearized DNA

(pCpGfree-GFP). A progeny of 56 pups were obtained and analyzed. No PCR-positive mice were obtained.

Figure II.4. Map of the linearized pCpGfree-GFP plasmid used in the electroporation of mice. MAR (insulator matrix-Attachment region), ZeoR (Zeomicin resistance cassette), R6K origin (Origin of replication).

Table II.4 Summary of progeny from mice injected with pCpG-EGFP

Fertile Males	*Date of first birth*	*Litters*	*%Fertile males*	*Progeny*	*PCR*	*%PCR Positives*
#15	*11/04/2013*	*8*		*44*		*0*
#16	*09/06/2013*	*2*		*12*		*0*
2		*10*	*100.00*	*56*	*0*	*0*

2.2.5. Development and testing of plasmids based on the mouse opsin promoter.

Because our objective was to develop and characterize transgenic mouse models of gain- or loss-of function in photoreceptor cells, and given that the design of the expression vector seemed crucial, we decided to focus in parallel on the development of expression vectors based on a photoreceptor-specific strong promoter. One of the most frequently used and better characterized promoters for transgenic expression in photoreceptor cells is the rod opsin promoter. Rod opsin promoter is the strongest promoter in rod photoreceptor cells and controls the expression of the most abundant protein expressed in rods, which is the visual pigment rod opsin (3mM concentration at the outer segments).

We based our vectors on the 4.4 kb version of the Mouse Opsin Promoter (MOP), which has been extensively used for transgene expression in rod photoreceptor cells by pronuclear injection (López-del Hoyo et al., 2014, 2012). In

the 90's, the MOP was extensively characterized by Melvin I. Simon and Jeremy Nathans's groups (Kumar et al., 1996; Lem et al., 1991; Nie et al., 1996; Peng and Chen, 2011; Tummala et al., 2010; Zack et al., 1991). Several regulatory elements have been characterized in this promoter (Figure II.5).

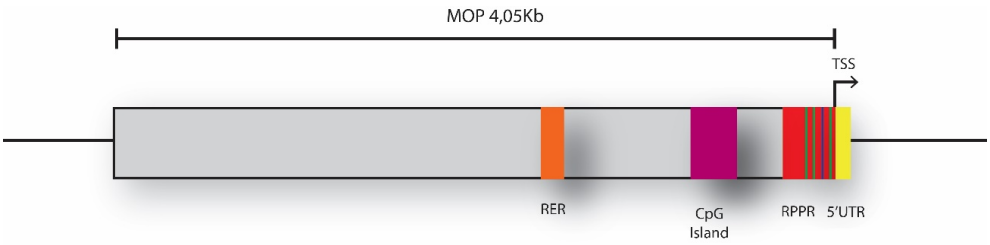

Figure II.5. Regulatory elements of the Mouse Opsin Promoter. Main elements that control the activity and expression pattern of MOP are: Rhodopsin Enhancer Region (RER, 116bp; Orange Box), CpG Island (246bp; Pink Box) and Rhodopsin Proximal Promoter Region (RPPR, 286bp; Red Box). Inside the RPPR, green lines represent the binding site of Cone-Rod-Homeobox transcription factor (Crx) and blue line represents the binding site of Neural Retina-specific Leucine zipper protein (Nrl). RER is localized at 1,446Kb upstream of Transcription Start Site (TSS) and the CpG Island at 364bp upstream of TSS. The yellow box represents the 5'UTR (85bp).

Based on the known regulatory elements of the mouse opsin promoter, we designed different promoter variants in the search for a version that could drive transgene expression efficiently upon construct incorporation in the genome, by DNA electroporation of spermatogonial stem cells. An *in silico* analysis of the MOP revealed a CpG island close to the RPPR.

As explained above, several types of DNA insulator sequences are available, that have proven successful at preventing transgene silencing and improving transgene expression efficiency in transgenic procedures by pronuclei injection. Besides S/MAR sequences, another insulator element that is widely used in the generation of transgenic mice, is the 5'HS4 sequence from the chicken β-globin locus. This sequence was characterized by G. Felsenfeld (Bell et al., 1999) and acts as a blocking barrier for heterochromatin propagation. We introduced this barrier sequence flanking the transgene cassette in some of our constructs. As detailed in materials and methods, we designed five different vectors for photoreceptor-specific transgene expression based on the mouse opsin promoter. The first one, (MOP_I in figure II.6) is a vector that we have previously used for the generation of transgenic mice by pronuclear injection (described in López-del Hoyo et al. 2012; López-Del

Hoyo et al. 2014). It comprises an expression cassette composed of the MOP 4.4Kb version, bovine GCAP2 cDNA as the gene of interest and mouse protamine 1 polyadenylation sequence, into the pBlueScript plasmid. Because this vector has been previously used to generate transgenic mice by the conventional procedure (pronuclear injection), the vector itself can be considered to be quality-proved. The second construct, (MOP_II in figure II.6) was derived from construct I by removing a 2Kb region upstream of the RER element (Matsuda and Cepko, 2004) as well as the CpG island. The third construct was based on the MOP minimal version of 286bp (MOP_III), that carries only the RPPR (Rhodopsin proximal promoter region). This version has been demonstrated to be sufficient to drive heterologous gene expression in rod photoreceptor cells (Quiambao et al., 1997; Zack et al., 1991). The fourth version was derived from construct II by introducing 5´HS4 insulator sequences flanking the transgene cassette. The fifth version contains the cassette in MOP_I flanked by S/MAR insulators in a plasmid completely devoid of CpG dinucleotides (Figure II.6).

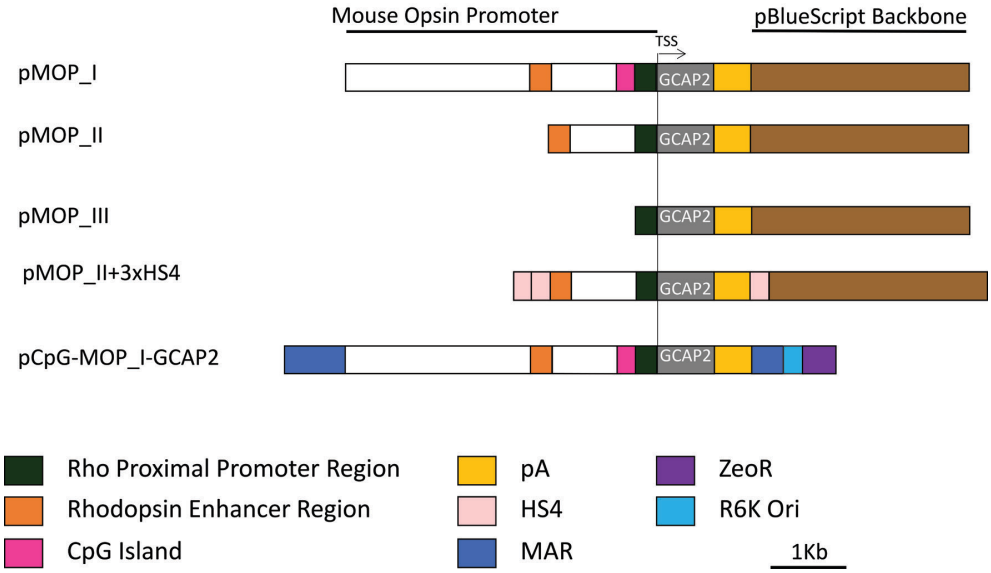

Figure II.6. Expression vectors designed for photoreceptor-specific expression, based on different versions of the mouse opsin promoter (MOP)

These vectors were injected and electroporated into GCAP1 and GCAP2 double knockout mice (Mendez et al., 2001). The goal was to express different mutant forms of the GCAP proteins in mice lacking endogenous GCAP1 and GCAP2, for a rapid assessment of the mutant phenotypes. Overall, we injected 32 males with the different constructs based on the MOP promoter. Of the 32 operated males 24 were fertile (75%). These 24 mice produced a total of 809 pups, grouped

Table II.5. Electroporation of plasmids based on the mouse opsin promoter

Vector	Type of surgery	Fertile Males	Date of surgery	Date of first litter	Litters	%Fertile males	Progeny	PCR	%PCR Positives
pMOP_I	H	5/5			26	100.00	172	42	24.4
		#21	04/05/2011	03/07/2011	7		65	24	36.9
		#22	04/05/2011	26/06/2011	5		26	7	26.9
		#23	04/05/2011	25/06/2011	7		40		0.0
		#24	04/05/2011	10/07/2011	6		37	11	29.7
		#25	04/05/2011	09/09/2011	1		4		0.0
pMOP_I	H	2/6			7	33.33	33	0	0.0
		#26	03/07/2012	06/10/2012	2		7		0.0
		#27	03/07/2012	21/10/2012	5		26		0.0
pMOP_III	H	2/2			13	100.00	85	24	28.2
		#28	03/06/2011	27/07/2011	3		18		0.0
		#29	03/06/2011	27/07/2011	10		67	24	35.8
pMOP_II	H	1/2			16	50.00	77	28	36.4
		#30	11/08/2011	19/10/2011	16		77	28	36.4
pMOP_II+ HS4	H	3/5			27	60.00	188	38	20.21
		#31	11/08/2011	13/11/2011	12		77	34	44.2
		#32	19/03/2012	17/05/2012	8		57	4	7.0
		#33	19/03/2012	19/06/2012	7		54		0.0
pCpG-MOP_I	H	3/4			11	75.00	64	39	60.9
		#34		30/09/2013	5		28	17	60.7
		#35		30/09/2013	2		9	3	33.3
		#36		08/10/2013	4		27	19	70.4
pCpG-MOP_I	T	8/8			27	100.00	190	2	1.05
		#37		15/09/2013	4		28		0.0
		#38		15/09/2013	5		30	2	6.7
		#39		14/04/2013	6		31		0.0
		#40		22/04/2013	4		22		0.0
		#41		12/06/2013	1		9		0.0
		#42		01/06/2013	2		23		0.0
		#43		31/05/2013	2		24		0.0
		#44		07/06/2013	3		23		0.0
Total		24/32			127		809	173	21.4

Surgery Type: H, Surgery with Hemicastration and injection of a single testis, T, trans-scrotum; S, surgery and injection of both testis (See Methods)

in 127 litters. More than 30 mice were analyzed for each of the five constructs. Of the 809 pups in the progeny, 173 mice were PCR-positive (21.4%). However, none of them expressed detectable levels of the transgene by Western blot (see below). Table II.5 summarizes these rounds of experiments.

Despite of the large number of PCR-positive mice detected at the genotyping level in the F1 (Figure II.7.A), none of them showed expression of the GCAP2 protein when analyzed by Western blot (Figure II.7.B).

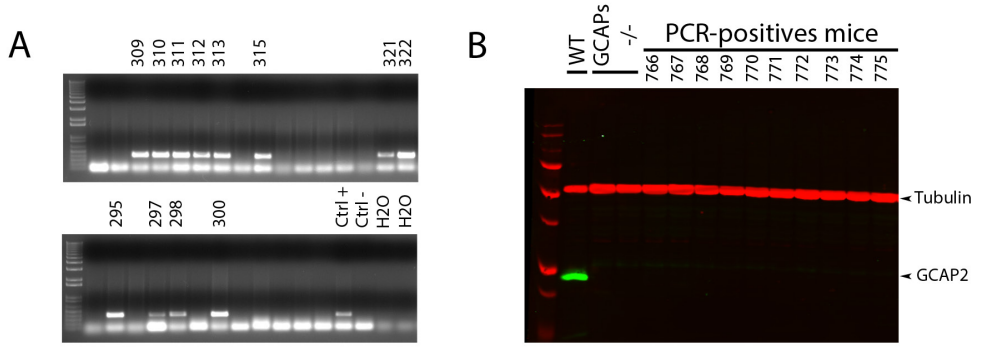

Figure II.7. Electroporation of expression vectors based on the MOP results in PCR positive mice in the progeny that do not express the protein by Western blot. A. Representative PCR genotyping of the transgene. Conventional transgenic line as Positive control. GCAPs knockout as negative control. B. Representative WB shows that PCR-Positive mice lack expression of GCAP2.

Therefore, in all of our attempts to generate transgenic mice by DNA electroporation, regardless of the promoter used or the presence or absence of insulator sequences, we invariably obtained PCR positive mice (which indicated integration of the heterologous DNA), that failed to express the heterologous protein to detectable levels. One possible explanation for these results was that the heterologous DNA was integrated in the genome (hence mice are PCR positive), but silenced epigenetically (no protein expression). Another possible explanation was that PCR positive results were not indicating an integration of the transgene, but were rather false positives. In order to distinguish between these two possibilities we decided to assess whether there had been integration of the transgene in PCR-positive F1 mice by Southern blot analysis of genomic DNA.

Genomic Southern blots are typically used in the genotyping and sorting of transgenic founders and their progeny during the establishment of transgenic lines, because pronuclei injection of heterologous DNA can result in multiple integration sites. A transgenic mouse with multiple integration sites of the transgene will segregate the transgene in each round of breeding, introducing experimental variability. This is why it is very relevant to carefully characterize transgene integration in founder mice, by Southern blot.

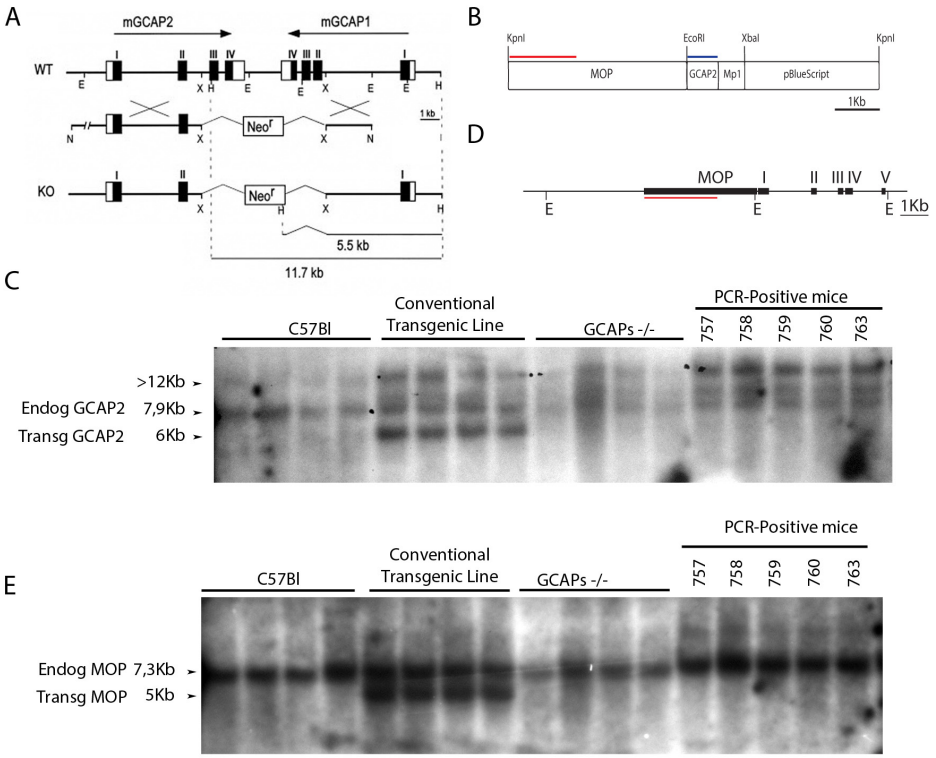

Figure II.8. Characterization by Southern Blot of progeny from electroporated males. A. Genomic structure of double Knockout GCAPs (modified from Mendez et al. 2001*). Exons II, III and IV from GCAP1 and III and IV from GCAP2 were substituted by Neo expression cassette. E (EcoRI), H (HindIII), X (XbaI). B. Structure of transgene employed in generation of transgenic mice by electroporation. For conventional transgenic mice, the same construct was used but without pBlueScript backbone, so KpnI-XbaI fragment. In red, probe against rhodopsin promoter; in blue probe against bGCAP2 cDNA. C. Southern blot genomic DNA digested with EcoRI of C57Bl, Conventional transgenic line (MOP-GCAP2-Mp1), double knockout GCAPs and PCR positive mice. Membrane was incubated with GCAP2 probe that recognize a band of about 6Kb in Conventional transgenic line that represent the fingerprint of this line. The visible band in C57Bl and conventional transgenic line of 7,9Kb represent of binding of probe to genomic DNA of GCAP2, lacked in double knockout GCAPs. The misleading band of >12Kb present in PCR-positive mice was also present in conventional transgenic line. D. Structure of genomic DNA of Rhodopsin. In red probe against MOP. E. Southern blot genomic DNA digested with EcoRI of C57Bl, Conventional transgenic line (MOP-GCAP2-Mp1), double knockout GCAPs and PCR positive mice. Membrane was incubated with MOP probe that recognize a band of about 5Kb in Conventional transgenic line that represent the fingerprint of this line with this probe. Endogenous MOP was detected as a band of 7,3Kb presented in all lines. Additional band was not detected in PCR-positive mice.*

When mouse genomic DNA is digested using a restriction enzyme and separated in an agarose gel, a probe mapping at the transgene might identify an internal band corresponding to the digestion of the transgene or its multiple sequential integrated copies (typically common to all integration sites); and also a unique band including the "flanking region of the transgene" which will be revealing of unique integration sites, therefore "fingerprinting" each founder mouse.

We performed a Southern blot analysis of selected PCR-positive mice, to investigate whether there was integration of the transgene. To assist in the identification of bands corresponding to the transgene (versus the endogenous GCAP genes or the endogenous rhodopsin promoter), we also included C57Bl (WT) mice, and GCAPs-/- mice. Furthermore, we also included the genomic DNA from a transgenic mice established by pronuclei injection with the same construct, to prove that at the technical level we were able to identify the proper bands (see loci maps and probe location in Figure II.8).

Although in a first approximation by Southern Blot, an apparent differential band was detected (Figure II.8.C) using a probe against GCAP2, an ulterior bona fide characterization using probes against MOP, showed that this band was also present in both in double knockout GCAPs and in C57Bl (Figure II.8.B).

Therefore, these results show that: i) PCR-positive mice could result from contamination and did not necessarily prove DNA integration; or ii) that integration sites are not that easily revealed by Southern blot, may be because of a low copy number. One putative interpretation is that DNA integration at spermatogonia fails because of a highly compacted chromatin (although spermatogonia are cells mitotically active and under continuous division). Alternatively, as already mentioned integrations could be taking place with a low transgene copy number that are hard to detect by Southern blot.

We designed two rounds of experiments to address these two possibilities: one, we designed electroporation experiments with the use of histone deacetylase inhibitors, to prevent the tight compaction of DNA; and two, we developed an expression vector with a strong fluorescent marker that we know for sure that would be expressed and detected in spermatozoids (the Mito-dsRed), based on its localization to mitochondria (necessarily active in sperm cells), that would allow detection of transfected sperm cells by flow cytometry.

2.2.6. Use of Histone deacetylases Inhibitors to prevent the compaction of DNA.

Histone proteins are responsible for the compaction of DNA. Histones are basic proteins with high affinity for DNA. The degree of compaction of DNA is determined by the degree of acetylation of histones, that is, acetylation of histones diminish their affinity for DNA.

Histone deacetylases (HDAC) are the enzymes responsible for removing of acetyl-groups from lysine in the NH2-terminus of histones, and therefore increase the affinity of histones for DNA. HDACs allow histones to wrap DNA more tightly (Dokmanovic et al., 2007).

Valproic acid (VPA) has been described to act as an inhibitor of HDAC allowing dynamic changes through decondensation of chromatin structure and enhance the sensitivity of DNA to nucleases and intercalating agents (Dokmanovic et al. 2007; Huangfu et al. 2008; Marchion et al. 2005; Felisbino et al. 2011).

We therefore tried a VPA treatment of mice immediately preceding DNA electroporation. Four C57Bl mice at p30 were treated with VPA (5mg VPA in 100ul of saline buffer was administered by peritoneal injection every 12h for 60h preceding the injection and electroporation with pCpGfree-GFP DNA (Backliwal et al., 2008; Marchion et al., 2005). In two of the four injected mice, the injected DNA contained 3mM of VPA. See table II.6 for a summary of the results obtained in these experiments.

Table II.6 Summary of progeny from mice injected with pCpG-EGFP+VPA

DNA+ VPA	*Type of surgery*	*Fertile Males*	*Date of surgery*	*Date of first litter*	*Litters*	*%Fertile males*	*Progeny*	*PCR*
		4/4			*6*	*100.00*	*83*	*0*
Yes	*T*	*#19*	*19/07/2013*	*15/09/2013*	*5*		*39*	
Yes	*H*	*#17*	*19/07/2013*	*15/09/2013*	*5*		*31*	
No	*T*	*#20*	*19/07/2013*	*15/09/2013*	*1*		*9*	
No	*H*	*#18*	*19/07/2013*	*23/09/2013*	*1*		*4*	

Surgery Type: H, Surgery with Hemicastration and injection of a single testis, T, trans-scrotum; S, surgery and injection of both testis (See Methods)

2.2.7. Quantification of the efficiency of heterologous DNA transfection of spermatozoa by *in vivo DNA electroporation by flow cytometry*.

A single transfected spermatogonial stem cell can generate many spermatozoids, by clonal expansion first by mitosis and later by meiosis. Spermatozoids are haploid specialized cells that bring the male genetic information to female haploid cells. Spermatozoids can be easily isolated by dissection of the epididymis and its incubation in a glucose-rich culture medium for some minutes.

Spermatozoids swim out of the epididymal tissue to the medium, where they are collected. Because of the high specialization of spermatozoids, they have a highly condensed nucleus, and a reduced cytoplasm with minimal expression of proteins. However, spermatozoids contain a large number of mitochondria that ensure the energy supply for flagellar movement. It has been reported that, although detection of a standard fluorescent protein in spermatozoids is difficult due to the reduced size of the cytoplasm and low level of expression of cytoplasmic proteins, the detection of fluorescent spermatozoids is feasible by transfecting fluorescent fusion proteins with a mitochondrial localization signal (Hibbitt et al., 2006; Huang et al., 2000).

Therefore, we designed an **ultimate experiment** that would allow us to conclusively answer the questions: **-Can transgene integration take place in spermatogonial cells by DNA *in vivo* electroporation, and be preserved at sperm cells?**, **-With what efficiency?**

We cloned the fusion protein DsRed and a mitochondrial localization signal into the vector pCpG-free from Invivogen (Figure II.9), which is completely devoid of pCpG islets and in which the transgene cassette is flanked by MAR DNA barrier insulators.

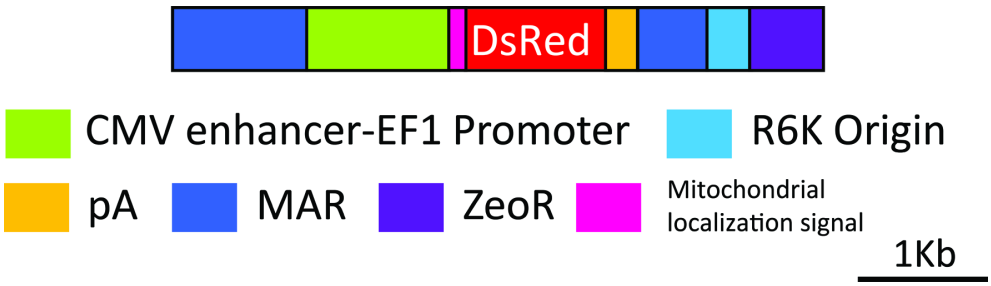

Figure II.9. Schematic representation of pCpG-mitoDsRed

Ten C57Bl males at p30 were injected and electroporated with this "ultimate" expression vector (both testis).Two non-injected C57Bl mice were carried as negative controls. Between 35 and 50 days post-electroporation (after a whole cycle of spermatogenesis), the epididymis of both testis were dissected and spermatozoids were collected. The amount of fluorescent spermatozoids was determined by flow cytometry. Table 2.7 shows a summary of the total events detected by flow cytometry, and the percentage of red fluorescent events from the total.

Total events were counted in a channel detecting Hoechst 33342 (Excitation/Emission 350/460 nm) which stains live cells (R1). The events detecting DsRed fluorescence were counted in a different channel (563/582nm) (R6) (Figure II.10.A). The percentage of total events detected in R6 versus R1 is plotted in Figure

II.10.B and it ranges from 0.06 to 1.43% in 18 determinations, with a mean value of 0.40%. The mean value obtained for this parameter in wildtype mice (non-electroporated negative control mice) is 0.15.

Figure II.10.C to J show transversal sections of the electroporated testis, showing isolated Sertoli cells and what appear to be Leydig cells with red fluorescent mitochondria, which proves the reporter gene expression from the vector, and that technically the electroporation of DNA in testis worked.

Therefore, we can conclude that the efficiency of this technique is extremely low, with our numbers indicating that **at best 1 mouse out of 250 mice in the progeny** of an electroporated male would be transgene positive.

Table II. 7. Summary of events detected by Flow cytometry

Mouse ID	*Testis*	*Total event Counts*	*DsRed events*	*%*
1	*R*	*79920*	*676.5*	*0.85*
1	*L*	*99535*	*812.5*	*0.82*
3	*R*	*49725*	*711*	*1.43*
3	*L*	*74088*	*689*	*0.93*
4	*R*	*70438*	*195*	*0.28*
4	*L*	*62026*	*173*	*0.28*
5	*R*	*39955*	*158.33*	*0.40*
5	*L*	*40395*	*154.66*	*0.38*
6	*R*	*99639*	*102*	*0.10*
6	*L*	*91105*	*55*	*0.06*
8	*R*	*4286*	*30*	*0.70*
8	*L*	*23934*	*189*	*0.79*
11	*R*	*42470*	*89.5*	*0.21*
11	*L*	*27625*	*57*	*0.21*
12	*R*	*96929*	*182*	*0.19*
12	*L*	*97417*	*313*	*0.32*
13	*R*	*95508*	*75*	*0.08*
13	*L*	*87187*	*106*	*0.12*
Total		***1182182***	***4768.5***	***0.40***
Ctrl	*R*	*97683*	*85*	*0.09*
Ctrl	*L*	*35942*	*63*	*0.18*
Ctrl	*R*	*97742*	*89*	*0.09*
Ctrl	*L*	*99563*	*247*	*0.25*
Total		***330930***	***484***	***0.15***

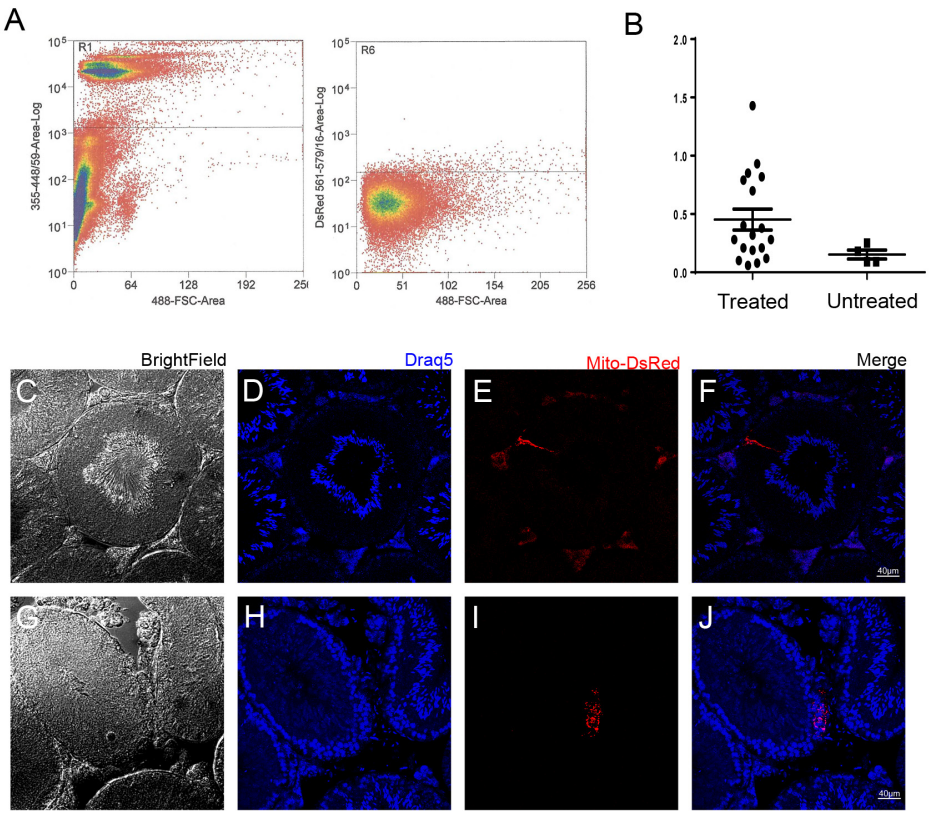

Figure II.10. Flow cytometry quantification of the efficiency of transfection in the protocol of DNA in vivo electroporation of testis. A. Isolated spermatozoids marked with Hoechst 33342 were sorted by flow cytometry (R1) and then sorted for presence of DsRed (R6). B. Percentage of events detected in R6 (DsRed positives) with respect to R1 (Hoechst positives) in electroporated mice (Treated) and control (Untreated). C-J. Cross-section of transfected testis. Nucleus are stained with Draq5. Red signal is seen mainly outside of seminiferous tubule or in sertoli cells.

2.3. Discussion.

Conceptually, the generation of transgenic animals by electroporation of spermatogonial stem cells *in vivo* offered a novel promising genetic strategy for gene function analysis, by making the generation of stable transgenic animals affordable and fast. Conceivably, this method could allow by-passing conventional transgenic facilities and their associated cost.

Testis Mediated Gene Transfer (TMGT) or *Sperm Mediated Gene Transfer* (SMGT) -the transfer of exogenous gene to male gonadal tissue or gametal cells

Table II.8. Summary of electroporated mice and progeny analyzed (Continuation in next page)

			Surgery				Mice
Vector	Insulator	HDAC	Type	Voltage (V)	N	Testis injected	Strain of males
pL_UG	No		H	60	4x2	1	C57Bl
pL_UG	No		H	60	4x2	1	C57Bl
pL_UG	MAR		H	60	4x2	1	C57Bl
pCpG-GFP	MAR		T	40	4x2	2	C57Bl
pCpG-GFP	MAR	VPA	S	40	4x2	2	C57Bl
pCpG-GFP	MAR	VPA	T	40	4x2	2	C57Bl
MOPI	No		H	60	4x2	1	GCAPs KO
MOPIII	No		H	60	4x2	1	GCAPs KO
MOPII	No		H	60	4x2	1	GCAPs KO
MOPII-HS4	HS4		H	60	4x2	1	GCAPs KO
pCpG-MOP	MAR		H	40	4x2	1	GCAPs KO
pCpG-	MAR		T	40	4x2	2	GCAPs KO

HDAC: Histone deacetylase Inbibitor. Surgery Type: H, Surgery with Hemicastration and injection of a single testis, T, trans-scrotum; S, surgery and injection of both testis.

have already been tried, for gene therapy purposes or the generation of transgenic animals. There is controversy in the literature regarding the feasibility, efficiency and underlying molecular mechanisms of these techniques. with controversial results about efficiency and mechanism of action (Parrington et al., 2011).

Table II.8 summarizes all the electroporation experiments. Eight different constructs were electroporated, based on two different ubiquitous promoters and three versions of the strong photoreceptor-specific rod opsin promoter. Plasmids devoid of CpG islets were used, and transgene cassettes were flanked by two different types of DNA barrier insulators. DNA electroporation were performed by three different experimental procedures, learnt at the laboratory from which this methodology originated. Out of more than 1.300 mice analyzed from the progeny of 57 electroporated mice, 15% were PCR positive at the genotyping level (198 mice). However, transgene expression could not be detected at the protein level in any of the 198 PCR-positive mice. From our last experiment using the DsRed reporter gene with mitochondrial localization we can conclude that the maximal efficiency with which this technology could be working is 0.40%. That is, out of 250 mice from the progeny of an electroporated male, one transgenic animal might be expected. We conclude that this methodology is not practically feasible as performed.

Table II.8. Continued from previous page

Mice					Screening		
Strain of Females	*Total males*	*Fertile Males*	*Litters*	*%Fertile males*	*Progeny*	*PCR*	*%PCR Positives*
C57Bl	*9*	*8*	*32*	*88.89*	*203*	*12*	*5.91*
FVB	*4*	*2*	*10*	*50.00*	*96*	*4*	*4.17*
C57Bl	*6*	*4*	*13*	*66.67*	*72*	*9*	*12.50*
C57Bl	*2*	*2*	*10*	*100.00*	*56*	*0*	*0.00*
C57Bl	*2*	*2*	*6*	*100.00*	*35*	*0*	*0.00*
C57Bl	*2*	*2*	*6*	*100.00*	*48*	*0*	*0.00*
GCAPs KO	*11*	*7*	*33*	*63.64*	*205*	*42*	*20.49*
GCAPs KO	*2*	*2*	*13*	*100.00*	*85*	*24*	*28.24*
GCAPs KO	*2*	*1*	*16*	*50.00*	*77*	*28*	*36.36*
GCAPs KO	*5*	*3*	*27*	*50.00*	*188*	*38*	*20.21*
GCAPs KO	*4*	*3*	*11*	*75.00*	*64*	*39*	*60.94*
GCAPs KO	*8*	*8*	*27*	*100.00*	*190*	*2*	*1.05*
Total	*57*	*44*	*204*	*77.19*	*1319*	*198*	*15.01*

The conceptual basis of DNA electroporation of spermatogonia cells relies on the fact that spermatogonial stem cells are outside the blood-testis barrier and in direct contact with the interstitial fluid. Therefore, they should be readily accessible by DNA injected in the interstitial fluid (Dhup and Majumdar, 2008). Despite of that, the fact is that in our extensive trials we observed transfected Sertoli and Leydig cells, but no transfected spermatogonial cells. Our interpretation of the results is that spermatogonial cells *in vivo* are not easily transfected by heterologous DNA because they likely have unique mechanisms in place to protect the integrity of their genomic DNA. In this sense, adenovirus-mediated gene transfer has been reported to work on Sertoli and Leydig cells, but not on spermatogonial or sperm cells. (Kojima et al., 2008, 2003).

Furthermore, as an immuneprivileged tissue, testis can trigger innate immune responses through *Toll-like Receptor* 4 expressed in Sertoli cells in response to tissue damage or viral or bacterial infections (Shang et al., 2011; Zeuner et al., 2015). A deeper knowledge of the protective mechanisms guarding the genome of germ cells might be required in order to design a DNA transfection strategy. Alternatively, transfection of messenger RNAs to transient expression of CRISPR/Cas9 to get knockout or stable transgenic may be attempted.

Chapter III: Molecular determinants of localization of GCAPs

Chapter III: Molecular determinants of localization of GCAPs

3.1. Rationale

Retinal guanylate cyclase (RetGC) and guanylate cyclase activating proteins (GCAPs) constitute the protein complex responsible for cGMP synthesis in rods and cones of the vertebrate retina. With cGMP being the second messenger in phototransduction, these proteins play a central role in the physiology of the light response. In response to light, photoexcitation of the visual pigment in rods and cones triggers a G-protein-mediated enzymatic cascade that results in stimulation of cGMP hydrolysis by cGMP phosphodiesterase (cGMP-PDE), a reduction of the cGMP levels, and the closure of cGMP-gated channels at the plasma membrane. Closure of these channels causes the hyperpolarization of the cell and a reduction of neurotransmitter release at the synaptic terminal, which is the signal transmitted to higher order neurons (Burns and Arshavsky, 2005). Timely recovery of the darkness equilibrium and the sensitivity to light in rods and cones after photoexcitation requires the replenishment of cGMP to its dark-adapted levels. cGMP levels are restored by the stimulation of cGMP synthesis that is inherent to termination of the light response. This is mediated by the GCAP proteins stimulation of RetGC catalytic activity in response to the reduction in the intracellular Ca2+ that ensues the closure of cGMP-channels upon photoexcitation (Mendez et al., 2001).

Multiple structural and biochemical studies have characterized the mode of regulation of RetGC catalytic activity by the two main GCAP isoforms in high mammals: GCAP1 and GCAP2 (Dizhoor and Hurley, 1996; Ermilov et al., 2001; J.-Y. Hwang and Koch, 2002; Laura et al., 1996; Peshenko et al., 2014, 2004; Peshenko and Dizhoor, 2004). These proteins are thought to be permanently bound to RetGC (a homodimer of GCAPs bound to a homodimer of RetGC) at rod outer segments, and regulate cyclase activity by switching between two conformational states: a Ca2+-bound “inhibitor” state, characteristic of the dark-adapted state, that inhibits cyclase activity; and a Ca2+-free, Mg2+-bound “activator” state, acquired as the Ca2+ levels drop during the light response, that activates cyclase catalytic activity. Based on a slight difference in the Ca2+ sensitivities of GCAP1 and GCAP2 (Koch and Dell’orco, 2013; Wen et al., 2014), and in the reported kinetics of the light response of mice expressing GCAP1 or GCAP2 individually (Howes et al., 2002; Mendez et al., 2001), a “Ca2+-relay model” of RetGC regulation by GCAPs has been proposed (Koch and Dell’orco, 2013). According to this model cGMP synthesis would be boosted in two stages during termination of the light response. GCAP1, less sensitive to Ca2+ than GCAP2, would be the first to acquire its activator conformation as the Ca2+ level decreases during the light response, being responsible for the first boost of cGMP synthesis. GCAP2 would contribute to

cGMP synthesis in a second stage, as the Ca2+ levels decrease even further, in response to brighter or more prolonged light exposures.

While the mode of regulation of RetGC by GCAPs has been extensively investigated, much less is known about the mechanisms that regulate the protein complex assembly and its subcellular distribution in the context of living cells. RetGC1, an integral membrane protein, appears to be confined to the outer segment compartment and the synaptic terminal of rods and cones. Its distribution to these compartments is expected to rely on vesicular polarized trafficking, although the mechanisms underlying this trafficking remain elusive (Baehr et al., 2007; Karan et al., 2010). The soluble proteins GCAP1 and GCAP2, however, appear to fill the cytosolic space of photoreceptor cells, being abundant also at the inner segment and perinuclear region. This distribution does not simply result from equalization of their concentrations in the cytosol. Two independent lines of studies point to a regulated subcellular distribution of the GCAP proteins. First, it has been reported that GCAP1 and GCAP2 fail to distribute to the rod outer segment compartment in the absence of functional RetGC (Baehr et al., 2007; Karan et al., 2010), or when the stability of RetGCs is compromised in the absence of functional RD3 (Azadi et al., 2010). This line of results indicates that GCAP1 and GCAP2 distribution to rod outer segments depends on RetGC. Second, GCAP2 subcellular distribution post-synthesis has been proposed to be regulated by phosphorylation at Ser201 and 14-3-3 binding, depending on the illumination state of the cell (López-del Hoyo et al., 2014). Taken together, these are strong indications that GCAP1 and GCAP2 subcellular distribution is dependent on RetGC1, at the same time that it is strictly regulated.

It is not known, however, whether GCAPs dependence on RetGCs for their distribution to rod outer segments implies a direct interaction. GCAPs direct binding to RetGC (i.e. complex assembly at the inner segment) might be a prerequisite for their incorporation into vesicle transport carriers with ciliary destination. Alternatively, GCAPs might simply incorporate by default to vesicle transport carriers that are somehow dependent on functional RetGC for their ciliary fate, in the same way that PDE6 subunits in rods, and cone PDE alpha and transducin subunits in cones depend on RetGC for their trafficking to the cilium (Baehr et al., 2007; Karan et al., 2010). The residues in GCAP1 that are involved in primary binding to the cyclase, versus those involved in its activation, have been precisely mapped in a recent structural-functional study (Lim et al., 2013; Peshenko et al., 2014). This mapping has allowed us to address whether GCAP1 direct binding to RetGC1 is required for GCAP1 distribution to the outer segment by using a genetic approach. In this study we expressed a GCAP1 mutant impaired at RetGC1 binding (K23D), and one that preserved binding but was impaired at RetGC1 activation (W94A) as transient transgenes in the rods of GCAP1/2 double knockout mice. Then we assessed their subcellular distribution. We here report that precluding GCAP1

binding to RetGC1, but not its activation, prevented its distribution to rod outer segments.

Conversely, GCAP1 and GCAP2 are myristoylated at Gly2 at the NH2-terminus. Whether myristoylation affects GCAPs subcellular distribution in living photoreceptors has not been addressed. An emerging number of reports have involved the lipid moiety of acylated membrane-associated proteins in regulation of protein trafficking or its restricted diffusion. In photoreceptors, several acylated proteins involved in phototransduction interact with lipid-binding proteins that regulate their localization. Lipid-binding proteins in photoreceptors include PrBP/δ and UNC119. The protein PrPB/δ encoded by the Pde6d gene functions as a prenyl binding protein that binds to the three catalytic subunits of PDE (α, β in rods and α′ in cones), two G protein-coupled receptor kinases (GRK1 and GRK7) and the rod and cone γ subunits of transducin. These proteins are synthesized in the cytosol, posttranslationally prenylated at the COOH-terminus by soluble prenyl transferases, and docked to the ER surface for further processing. Following ER processing, these proteins are targeted to the outer segment disk membranes where phototransduction takes place. PrPB/δ has been proposed to extract these proteins from the ER to allow their incorporation to transport carrier vesicles (Zhang et al., 2012). In the absence of PrPB/δ, GRK1 and PDEα′ fail to be transported to rod and cone outer segments, affecting photoreceptor physiology. UNC119A is an acyl-binding protein that shows specificity for the lauroylated and myristoylated N-termini of G-protein α-subunits. It is involved in Tα redistribution between rod outer segment and proximal compartments during light- and dark-adaptation periods (Constantine et al., 2012; Zhang et al., 2011). Collectively, the concept is emerging that acylation of membrane-associated proteins regulates their subcellular distribution, and therefore our interest in studying the role of GCAP1 and GCAP2 myristoylation in rods and cones.

We have recently proposed a unique mechanism of regulation of GCAP2 subcellular distribution. This mechanism is based on light-dependent phosphorylation at Ser201 followed by the binding of 14-3-3, that sequesters the protein at the inner segment compartment (López-del Hoyo et al., 2014). This mechanism was proposed based on observations made on a transgenic line expressing a GCAP2 mutant locked in its Ca2+-free conformation, EF^{-}GCAP2. In this study we provide a genetic demonstration that phosphorylation at Ser201 effectively determines the subcellular distribution of the wildtype GCAP2 protein. The S201D GCAP2 mutant is retained at the inner segment, and does not distribute to rod outer segments. As we had predicted in our previous study, a disease-linked mutation in GCAP2 (Sato et al., 2005), G157R, results in a significant fraction of GCAP2 retention at the inner segment in a high number of cells. This mislocalization, based on GCAP2 toxicity at the inner segment when accumulated

at its activator conformational state (López-del Hoyo et al., 2014) is likely the basis of the pathophysiology of the associated retinitis pigmentosa disorder.

In summary, in this study we set to characterize the molecular determinants of protein localization in GCAP1 and GCAP2. We conclude that GCAP1 distribution to rod outer segments requires its capacity to bind to RetGC1, but not the capacity to activate it. It also requires the NH2-terminal myristoyl group. In contrast, GCAP2 does not require myristoylation, and its distribution is regulated by light, via phosphorylation at Ser201 and 14-3-3 binding. The only disease-linked mutation in GCAP2 (hG157R GCAP2), (Sato et al., 2005), alters GCAP2 subcellular distribution in vivo, which likely explains its toxicity (López-del Hoyo et al., 2014).

3.2. Results

3.2.1. Study of the molecular determinants of GCAP1 subcellular distribution in vivo.

In order to study the molecular determinants of GCAP1 subcellular distribution in vivo, we expressed the wildtype GCAP1 protein and selected mutants as transient transgenes in the rods of GCAP1/GCAP2 knockout mice. Transgene expression vectors were based on the Mouse Opsin Promoter (MOP, 4.4-Kb version). The expression cassette consisted of the MOP, the human GCAP1 cDNA and the mouse protamine polyadenylation sequence. Plasmids were injected in the subretinal space in newborn pups and transfected by *in vivo* DNA electroporation (see Methods).

Transgenic expression of wildtype GCAP1 in rods resulted in a GCAP1 distribution between the inner and outer segment of 50:50% (Figure III.1B). This percentage of GCAP1 distribution to rod outer segments was calculated from the analysis of GCAP1 signal distribution in 17 individual cells (Appendix I Figure 2, and Figure III.1.M), where rhodopsin staining was used to label the rod outer segment layer. This pattern of localization reproduced the pattern of endogenous GCAP1 localizacion in murine rods (López-del Hoyo et al., 2012).

To assess whether the myristoyl group at GCAP1 NH2-terminus is required for GCAP1 distribution to rod outer segments *in vivo*, we expressed the mutant G2A-GCAP1. This mutant was massively retained at the inner segments, with its distribution to rods precluded, (Figure III.1.E-F). This protein distribution was consistent in 13 individual cells analyzed (Appendix I Figure 2, Figure III.1.M). This result indicates that myristoylation of GCAP1 is required for its distribution to rod outer segments *in vivo*.

To address whether GCAP1 localization to rods depends on GCAP1 direct binding to RetGC1, we expressed a mutant form of GCAP1 impaired at RetGC1 binding. A recent structure-function analysis of GCAP1 established a fine mapping of the residues involved in binding to RetGC1, at the target binding surface of

GCAP1. The residues involved in binding are located at EF-hand 1 (Tyr-22, Lys-23, Lys-24, Met- 26, Glu-28, Pro-30, Ser-31, Gly-32, Tyr-37, and Glu-38) and EF-hand 2 (Phe-73, Met-74, Val-77, and Ala-78) (Lim et al., 2013; Peshenko et al., 2014). Lys23 is one of the key residues at the binding interface, and its mutation to aspartic acid precludes GCAP1 binding to RetGC1. Therefore we expressed K23D-GCAP1 as a transgene in rods. Similar to G2A-GCAP1, the K23D-GCAP1 mutant accumulated at the inner segment, and failed to be transported to rod outer segments (Fig1 H, I). This observation was made in 13 individual cells (Appendix I Figure 3). This result provides the first demonstration that GCAP1 must be assembled with RetGC1 at the inner segment compartment in order to be transported to the outer segment. Curiously, it also excludes the possibility that GCAP1 diffuses freely in the cytosolic space between the inner and outer segment compartments.

Is GCAP1 activation of the cyclase required for its transport to rod outer segments? The aforementioned structure-funtion study established that GCAP1 binding to RetGC is needed but not sufficient for its activation. RetGC1 acts as a dimer, and a fully active cyclase domain requires the dimerization of this domain. The binding of GCAP1 enhances the dimerization of the cyclase domain, but primary binding itself is not sufficient for activation. Some important secondary interactions or allosteric effects are provided in a second step once the complex with the cyclase is formed. Three residues that are localized in the patch that conforms the target binding surface, M26, K85 and W94, have shown to be important for this second step. Mutations in these key residues are able to bind to RetGC, but not able to activate it (Peshenko et al., 2014). We transfected W94A-GCAP1 into rods, and observed that its pattern of localization reproduced that of the wildtype protein (Figure III.1.K-L), in ten individual cells (Figure III.1.M and Appendix I Figure 3).

Taken together, our results show that GCAP1 distribution to rods does not take place by simple diffusion. GCAP1 transport to rods depends on GCAP1 binding to retGC1, although this binding does not involve RetGC1 activation. Strikingly, myristoylation of GCAP1 is required for this transport, which suggests that myristoylation of GCAP1 might trigger the binding of a myristoyl-binding protein required for some step in the trafficking process (e.g. the extraction of GCAP1 from the ER and its “loading” on RetGC1 at transport carrier vesicles, see Discussion).

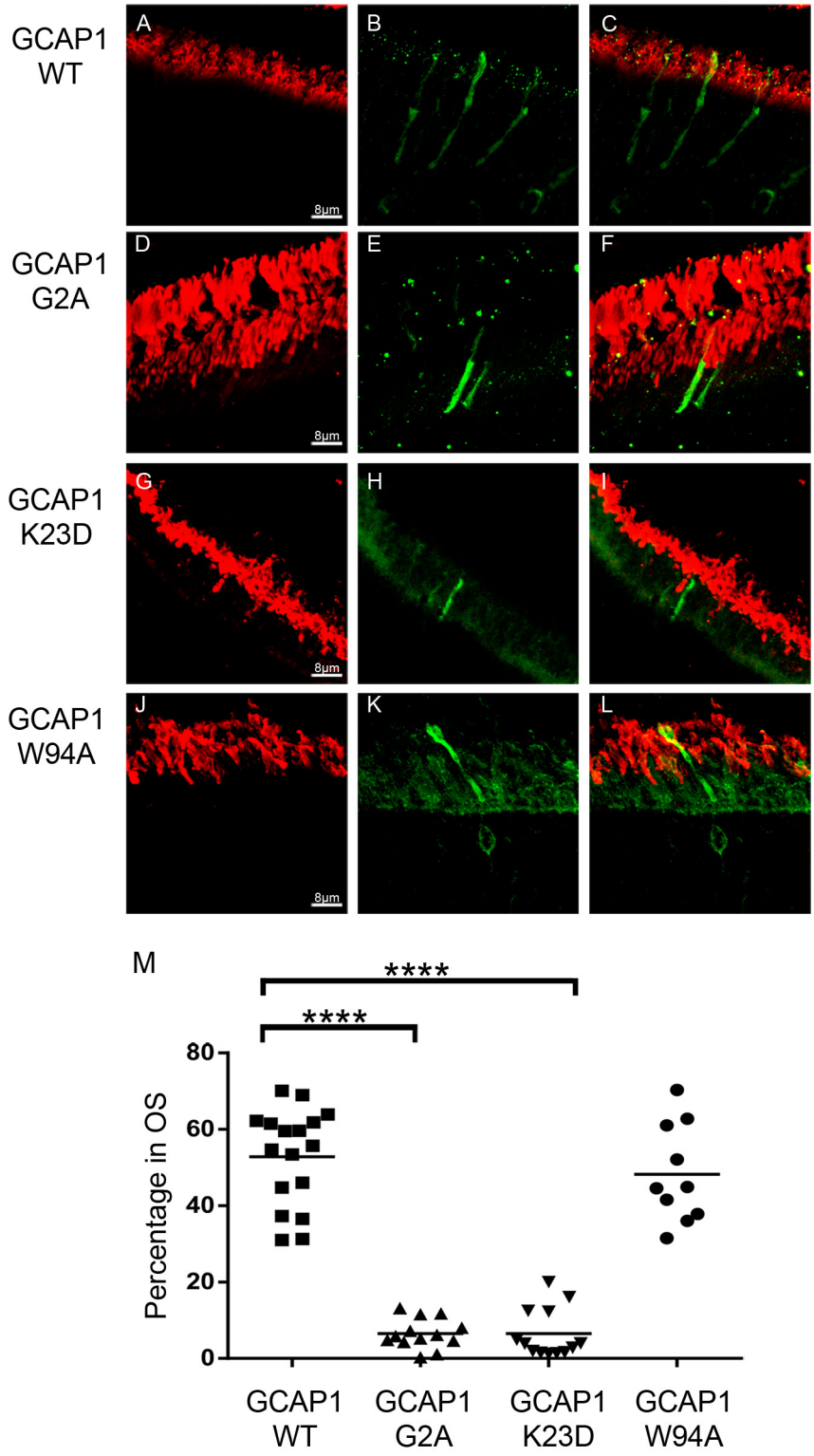
GCAP1
WT
GCAP1
G2A
GCAP1
K23D
GCAP1
W94A
A
B
C
D
E
F
G
H
I
J
K
L
8µm
M
****
****
Percentage in OS
80
60
40
20
0
GCAP1
WT
GCAP1
G2A
GCAP1
K23D
GCAP1
W94A

Figure III.1. Molecular determinants of GCAP1 distribution to rod outer segments in vivo. Wildtype and different mutant forms of GCAP1 were expressed as transient transgenes in the rods of GCAP1/GCAP2 knockout mice. Mosaicism results from the in vivo DNA electroporation method of transfection. GCAP1 WT (green signal in B-C) distributed 50%:50% between the inner and outer segment compartments. G2A-GCAP1 (D-F) and K23D-GCAP1 (G-I) were retained at the inner segment, as if their distribution to rod outer segments was precluded . W94A_GCAP1 (J-L) reproduced the wildtype localization. In red, rhodopsin mAb1D4. In green, GCAP1 pAb. M. Percentage of GCAP1 signal at the outer segment compartment (from the combined signal at outer and inner segments). Horizontal bars represent mean values. Mean±SEM were: *WT (*■) 52.86±3.08, n=17; G2A (▲) 6.49±1.08, n=13; K23D (▼) 6.47±1.77, n=13; W94A (●) 48.26±4.06, n=10. T-test was used to determine statistical significance versus WT. In G2A mutant and K23D mutant, p-value <0.0001.

3.2.2. Molecular determinants of GCAP2 subcellular localization in photoreceptor cells.

Similarly to GCAP1, when GCAP2 was transfected into GCAP1/GCAP2 knockout rods, it distributed to about 50%:50% between the inner and outer segment compartments [mean value of 52.58% ± 3.09 of GCAP2 localization in rod outer segment, of the total GCAP2 signal at outer and inner segments], in 16 individual cells (Figure III.2.B-C and Figure III.2.M, Appendix I Figure 4). This mimicked the endogenous localization of GCAP2 in wildtype mice (López-del Hoyo et al., 2014).

In order to test whether myristoylation of GCAP2 affected its subcellular distribution, we transfected rods with G2A-GCAP2. Abolishing myristoylation of GCAP2 did not have the "all or nothing" effect observed for GCAP1. However, GCAP2 distribution to rod outer segments was diminished by 20% in the absence of myristoylation, with statistical significance (Figure III.2.E-F, and Figure III.2.M, T-test P=0.01, 11 and 16 cells analyzed, see Appendix I Figure 4). Therefore, our results point to a facilitation of GCAP2 localization to rod outer segments by the myristoyl group, even if not strictly required.

We could not test whether GCAP2 binding to retGC1 is a prerequisite for its trafficking to rod outer segments, because the residues involved in GCAP2 binding to RetGC1 have not been mapped. However, we have previously reported that GCAP2 subcellular distribution presents additional regulatory steps, not present in GCAP1. We have reported that in wildtype mice raised under standard 12h dark:12h light cycles, about 50% of GCAP2 is phosphorylated at S201. It is the Ca2+-free form of GCAP2 that is phosphorylated more efficiently, and this phosphorylation results in 14-3-3 binding, that retains the protein at the inner segments (López-del Hoyo et al., 2014). Our study rigorously demonstrated the phosphorylation of EF-

GCAP2 (locked in its Ca2+-free conformational state), and how it resulted in protein sequestration by 14-3-3 proteins. However, we did not directly prove in our previous study that phosphorylation of wildtype GCAP2 causes its retention at the inner segment compartment. We here transfected rods with the Ser201Gly and Ser201Asp GCAP2 mutants, to study the effect of introducing a negative charge at position 201 in subcellular localization. The results show that the constitutive mimic of the phosphorylated form S201D-GCAP2 is retained at the inner segments (Figure III.2.H-I), while S201G-GCAP2 is not (Figure III.2-K, L). Taken together, these results are perfectly consistent with the model of GCAP2 subcellular localization that we have previously proposed (López-del Hoyo et al., 2014), but also point to the myristoyl group facilitating GCAP2 distribution to rod outer segments, likely by facilitating some step in the trafficking process that remains to be described.

Figure III.2. Molecular determinants of localization of GCAP2. Wildtype and mutant GCAP2 constructs were used to transfect the rods of GCAP1/2 knockout mice. GCAP2 WT (B-C) distributed between the inner and outer segment compartments to about 50%:50%. G2A-GCAP2 (E-F) distribution to rod outer segments diminished by 20%, but was not completely impaired. S201D-GCAP1, a constitutive mimick of phosphorylated GCAP2 was mainly retained at the inner segments (H-I), while S201G-GCAP2 (G-I) reproduced the wildtype localization. In red, rhodopsin mAb 1D4, in green, GCAP2 pAb. M. Percentage of signal at rod outer segments (expressed as a fraction of the combined signal in outer and inner segments). Horizontal bars represent the mean. Values Mean±SEM. WT (●) 52.58±3.09, n=16; G2A (■) 41.63±1.68, n=11; S201D (▲) 6.99±2.75, n=9; S201G (▼) 48.01±3.18, n=15. T-test was used to determine statistical significance versus WT. In G2A mutant, p-value <0.01; in S201D mutant, p-value <0.0001.

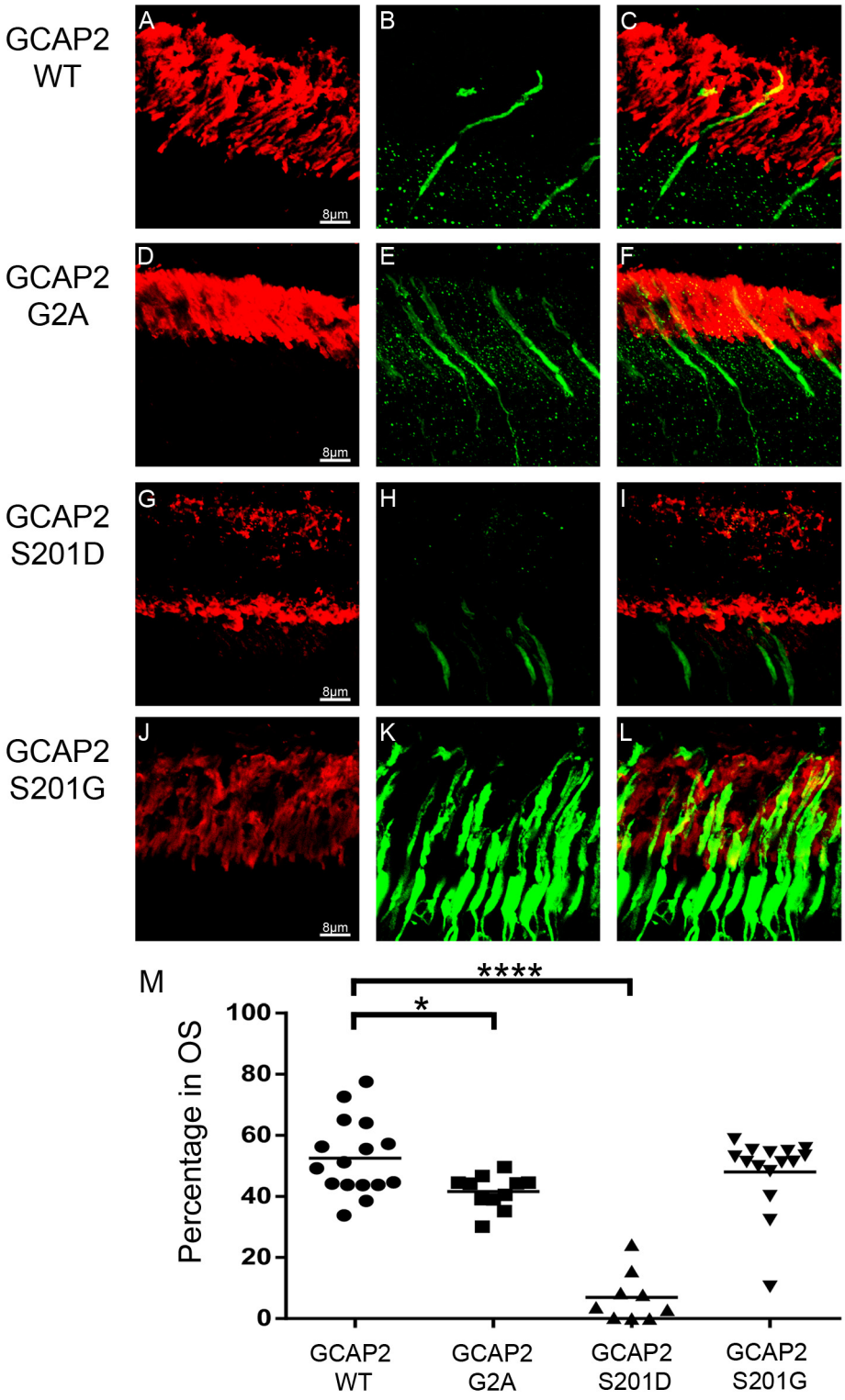
GCAP2
WT
GCAP2
G2A
GCAP2
S201D
GCAP2
S201G
A
B
C
D
E
F
G
H
I
J
K
L
8µm
M
****
*
Percentage in OS
100
80
60
40
20
0
GCAP2
WT
GCAP2
G2A
GCAP2
S201D
GCAP2
S201G

3.2.3. Subcellular localization of CORD mutation P50L-GCAP1

More than ten mutations in GUCA1A encoding GCAP1 have been linked to autosomal dominant cone rod dystrophy (adCORD) (Dell'Orco et al., 2014; Kamenarova et al., 2013; Newbold et al., 2001; Nishiguchi et al., 2004; Palczewski et al., 2004). Most mutations decrease the Ca2+ binding affinity of the protein, either directly or indirectly, ultimately resulting in an alteration of the Ca2+ sensitivity of cyclase activity. Mutations mostly result in constitutive activation of the cyclase catalytic activity in most of the physiological range of Ca2+ concentrations. However, P50L-GCAP1 is an exception. This mutation does not appear to affect the GCAP1 Ca2+ regulation of guanylate cyclase activity in vitro (Newbold et al., 2001). Due to its localization towards the NH2-terminal part of the protein, near the binding surface with RetGC1, we set to examine the effect of this mutation in GCAP1 subcellular localization *in vivo*.

P50L-GCAP1 was transient expressed as a transgene in the rods of GCAP1/2 knockout mice. The analysis of these mice showed that the P50L mutation did not affect GCAP1 subcellular distribution. P50L-GCAP1 showed a subcellular localization similar to the wildtype protein (Figure III.3).

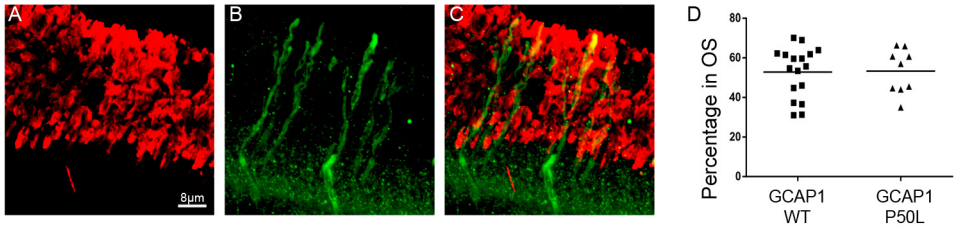

Figure III.3. Subcellular distribution of P50L-GCAP1. Transient expression of P50L-GCAP1 in the rods of GCAP1/2 knockout mice shows a subcellular distribution of the mutant (A-C) similar to the wildtype protein. In red, rhodopsin mAb 1D4. In green, GCAP1 pAb. D. Percentage of GCAP1 signal at rod outer segments (expressed as a fraction of the combined signal in outer and inner segments). Horizontal bars represent the mean. Values Mean±SEM. *WT (■)* 52.86±3.08, n=17; P50L (▲) 53.29±3.74, n=9.

3.2.4. An autosomal dominant Retinitis Pigmentosa mutation in GUCA1B encoding GCAP2 affects its subcellular distribution.

Only one mutation has been described in the GUCA1B gene encoding GCAP2: hG157R. It has been linked to autosomal dominant retinitis pigmentosa (Sato et al., 2005). The pathophysiology of this mutation is currently unknown. In order to study whether this mutation could affect GCAP2 subcellular distribution,

we expressed the equivalent mutation in the bovine GCAP2 isoform, bG161R-GCAP2 as a transient transgene in mouse rods of the GCAP1/2 knockout.

An analysis of the subcellular localization of bG161R-GCAP2 in 32 independent cells revealed two different populations of transfected cells. Approximately a third of analyzed cells (29%) (Figure 4. Group 1) presented a subcellular localization that resembled that of the wildtype protein, while near of two-thirds (71%) of analyzed cells retained GCAP2 at the inner segment (Figure III.4. Group 2).

This result indicates that the G161R mutation in bGCAP2 (equivalent to hG157R) likely conferred the protein a conformational structure that resembled to some extent that of the Ca2+-free state. Based on our previously proposed model of GCAP2 distribution, it is likely that this protein was retained at the inner segment by constitutive phosphorylation at Ser201 and 14-3-3 binding. This finding emphasizes the relevance of this regulatory mechanism of GCAP2 distribution in retinal disease.

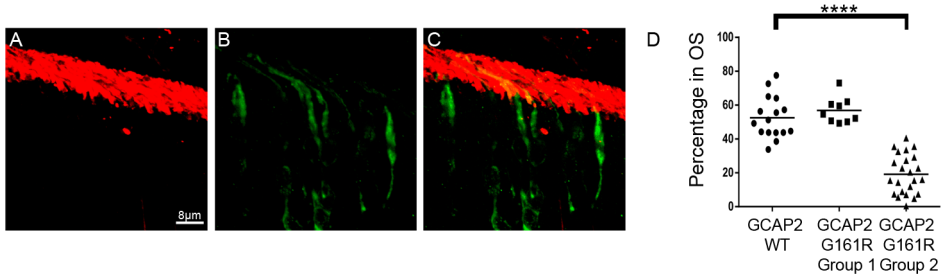

Figure 4. Subcellular distribution of bG161R-GCAP2 in transfected rods of GCAP1/2 knockout mice. Two different groups of cells could be distinguished among bG161R-GCAP2 expressing cells. Group 1 (29%) presented a distribution that ressembled that of the wildtype protein; while group 2 (71%) presented substantial retention of the protein at the inner segment. In red, rhodopsin mAb 1D4, in green, GCAP2 pAb. D. Percentage of signal at the outer segments (expressed as percentage of the combined GCAP2 signal at inner and outer segments). Horizontal bar represents the mean. Values Mean±SEM. *WT* (●) 52.58±3.09, n=16; Group1 (■) 56.89±2.57, n=9; Group2 (▲) 19.16±2.44, n=23. *p-value <0.0001*

3.3. Discussion.

In this study, we pursued the characterization of the molecular determinants of subcellular localization of Guanylate Cyclase Activating Proteins GCAP1 and GCAP2 in photoreceptor cells of the retina. GCAPs are Neuronal Calcium Sensor (NCS) proteins that play an important role during termination of the light response and light adaptation (Mendez et al., 2001). GCAPs present 4 conserved EF-hand domains for Ca2+-coordination, although EF-hand 1 is not functional at binding Ca2+. EF-1 is instead involved in GCAPs binding to RetGC1. GCAPs are

myristoylated at Gly2 at the NH2-terminus. In this study we have evaluated whether key residues in GCAP1 required for RetGC1 primary binding (K23) or post-binding activation (W94) are required for GCAP1 distribution to rod outer segments. The subjacent question was whether GCAPs post-synthesis need to assemble to their molecular target at the rod outer segment, RetGC1, in order to be transported to this compartment. We have also evaluated the effect of myristoylation in GCAP1 and GCAP2 subcellular distribution. The study was based on a genetic approach. We expressed the wildtype and mutant proteins as transient transgenes in the rods of GCAP1/GCAP2 knockout mice.

Our results show that K23D-GCAP1 fails to be transported to rod outer segments, while W94A-GCAP1 presents a normal distribution (Figure III.1). These results constitute the first direct demonstration that GCAP1 needs to bind to retGC1 at the inner segment, post-synthesis, in order to be transported to rod outer segments. Cyclase activation, however, is not required for transportation. These results are consistent with previous indirect reports that GCAP1 and GCAP2 fail to be transported to rod outer segments in the absence of a functional RetGC, in the RetGC1/2 knockout mice (Baehr et al., 2007; Karan et al., 2010) or the rd3 mice (Azadi et al., 2010). Therefore, we can conclude that the RetGC1/GCAP1 complex is assembled at the inner segment and is transported as a complex. This transport is expected to rely on polarized vesicular trafficking. Our results are also consistent with previous studies in that it discards free passive diffusion of GCAP1 and GCAP2 between the inner and outer segment compartments.

By expressing G2A-GCAP1 and G2A-GCAP2 in rods, we have observed that precluding the myristoylation of GCAPs *in vivo* had a substantial effect on their subcellular localization. Unmyristoylated GCAP1 was substantially retained at the inner segment (Figure III.1). Unmyristoylated GCAP2 distributed to rod outer segments, although to a lesser extent than the myristoylated protein (20% less in G2A-GCAP2 versus GCAP2, Figure III.2). This effect of the myristoyl group *in vivo* came as a surprise. The resolved structure of GCAP1 shows that the myristoyl group, attached to NH2-terminal Gly2, is permanently buried inside a hydrophobic pocket in the protein, independently of the Ca^{2+}-bound state (Lim et al., 2013). GCAP1 and GCAP2 do not exhibit the "Ca2+-myristoyl switch" reported for recoverin (J. Hwang and Koch, 2002; I. V. Peshenko et al., 2012). In recoverin, the fatty acid is extruded from the hydrophobic pocket in response to Ca2+ binding, and contributes to membrane attachment (Ames et al., 1997; J. Hwang and Koch, 2002). In contrast, crystallographic and NMR studies have documented that the myristoyl group in GCAP1 and GCAP2 is maintained inside the hydrophobic pocket both in the "inhibitory" and the "activator" states, not being exposed (Lim et al., 2013; Stephen et al., 2007). Recently it has been proposed that the myristoyl group in GCAP1 serves to adjust the Ca2+-binding affinity and the extent of cyclase activation by establishing a dynamic connection between the two semiglobullar parts

of the protein, that link conformational changes driven by Ca2+-binding at EF-4, to changes at the RetGC recognition surface in GCAP1 (Lim et al., 2013; Peshenko et al., 2014). The apparent affinity of myristoylated GCAP1 for RetGC was determined to be 5-fold higher than that of unmyristoylated GCAP1, using a RetGC activation assay (I. V. Peshenko et al., 2012).

Our result that unmyristoylated GCAP1 is mostly retained at the inner segment might be interpreted in two ways: i) that unmyristoylated GCAP1 shows a very diminished binding affinity for RetGC1, and therefore it is the binding to RetGC1 that fails; and ii) that the myristoyl group mediates an as-yet-undescribed additional step in polarized membrane trafficking: e.g. by involving the role of a lipid-binding protein such as UNC119 (Figure III.5). This putative intermediate step

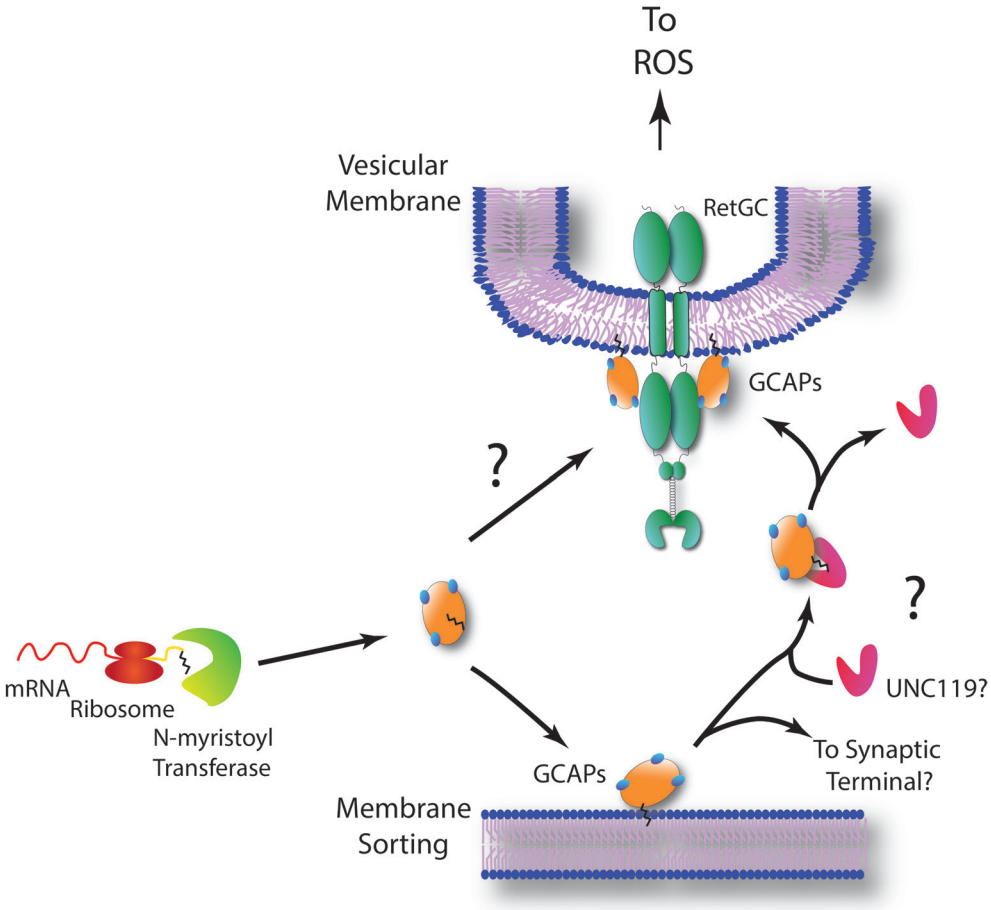

Figure III.5. Model of vesicular transport of GCAP1. Newly synthetized and myristoylated GCAP1 could: i) directly bind to RetGC or ii) be anchored to a sorting membrane compartment from where it would be extracted by an acyl-binding protein (i.e. UNC119) prior to its binding to RetGC at the vesicular membrane.

could serve to extract GCAP1 from a sorting membrane organelle in the secretory pathway, that may define its destination (Figure III.5). Future experiments will be addressed to distinguish between these two possibilities. We will determine the difference in the dissociation constant of myristoylated and unmyristoylated GCAP1 for RetGC1, by measuring the steady state binding of recombinant proteins by Surface Plasmon Resonance (SPR). On the other hand, we will investigate whether myristoylated GCAP1 binds to UNC119 (identified in our proteomic databases from GCAP1 pull-down assays) *in vitro* and *in vivo*.

Interestingly, there are similitudes and differences in the mechanisms determining the subcellular distribution of GCAP1 and GCAP2 in photoreceptor cells. We could not address whether GCAP2 requires its binding to RetGC1 for its transport to the rod outer segment, because its RetGC1 binding surface has not been characterized in detail (Ames et al., 1999). Previous studies indirectly point to the requirement of GCAP2 association to RetGC1 for its transport to rod outer segments (Baehr et al., 2007; Karan et al., 2010). The effect of precluding myristoylation in GCAP2 was much less than in GCAP1. Biochemical studies have determined that myristoylation of GCAP2 has only a minor effect on Ca2+ binding affinity and the extent of cyclase activation, compared to GCAP1 (J.-Y. Hwang and Koch, 2002; J. Hwang and Koch, 2002). The myristoyl in GCAP2 may serve to thermally stabilize the protein (Schröder et al., 2011).

Importantly, GCAP2 subcellular distribution is regulated by phosphorylation. In wildtype mice reared in standard cyclic light, 50% of GCAP2 is phosphorylated at Ser201. This phosphorylation triggers the binding of 14-3-3 proteins, that sequester the protein at the inner segment. GCAP2 is preferentially phosphorylated in its Ca2+-free conformation (predominant in light-adapted states). In this study, we further validate this model of regulation, by showing that a mutant that is a constitutive mimic of phosphorylated GCAP2 at position 201 (Ser201Asp-GCAP2) is retained at the inner segment. Simply precluding phosphorylation at this position (Ser201Gly) results in an inner:outer segment distribution of 50%:50% similar to the wildtype protein. This is consistent with our previous interpretation that the maximal distribution to the rod outer segment of GCAP2 is about 50% (López-del Hoyo et al., 2014).

A mutation in GUCA1B encoding GCAP2 has been linked to retinitis pigmentosa, hG157R (Sato et al., 2005). This residue is localized in EF-hand 4, and is therefore expected to diminish GCAP2 Ca2+ binding affinity. This reduced Ca2+ sensitivity of guanylate cyclase regulation could result in constitutive cyclase activity at the physiological range of calcium concentrations as the basis of the pathology. However, we have reported that a GCAP2 mutant blocked in its Ca2+-free conformation fails to be transported to the rod outer segments, leading to a severe retinal degeneration by a mechanism that is independent of cyclase activation. Toxicity in this case results from EF^{-}GCAP2 accumulation at the inner segment, and

is independent of cGMP metabolism (López-del Hoyo et al., 2014). We here show that the equivalent bovine mutation to hG157R (bG161R) causes retention of GCAP2 at the inner segment in 71% of transfected photoreceptors. In about 29% of transfected rods GCAP2 distributes normally. The two different populations of bG161R-GCAP2 transfected cells might result from variability of GCAP2 expression levels among cells. For some reason, GCAP2 expression levels have been shown to vary significantly from cell to cell, in previous genetic studies (Makino et al., 2012; Mendez et al., 2001). Ultimately our result shows that the human mutation leads to GCAP2 retention at the inner segment in a high fraction of cells, and we have already demonstrated that its accumulation at this compartment in an unstable conformation results in severe toxicity. We are currently investigating the molecular basis of this toxicity.

In this study we have also analyzed the effect of P50L-GCAP1 mutation on subcellular distribution. The reason is that P50L is the only characterized mutation in GCAP1 that does not result in a significative change in Ca2+ sensitivity of guanylate cyclase activity, and constitutive cGMP synthesis. We reasoned that it could affect protein trafficking, and lead to toxicity by accumulating at the wrong compartment. However, transgenic expression of P50L-GCAP1 in rods resulted in normal distribution. Therefore, we conclude that the P50L mutation in GCAP1 does not affect its subcellular distribution.

Taken together, our results show that the RetGC/GCAPs complex is assembled at the inner segment, and transported to the rod outer segment as a protein complex. This initial study sets the ground to investigate the mechanisms regulating the assembly, transport and *in vivo* regulation of the RetGC/GCAPs, a central protein complex in photoreceptor physiology and the basis of many inherited retinal disorders.

Chapter IV: Unanticipated interaction between IMPDH1 and RetGC1 proteins associated to blindness

Chapter IV: Unanticipated interaction between IMPDH1 and RetGC1 proteins associated to blindness.

Contributions

I cloned all mutants of IMPDH1, stablished protocols for expression and purification of recombinant proteins IMPDH1 and RetGC, isolated bovine ROS for proteomic and biochemical studies and performed such studies (proteomic data analysis, pull-down and immunoprecipitation of IMPDH1 and GCAP1, size-exclusion chromatography, and Surface Plasmon Resonance (SPR)).

Antibodies against IMPDH1 and RetGC1, expression and purification of MBP-RetGC1 fusion fragments proteins for SPR and Pull-down; immunostaining figures IV.4 & 5, acquisition, together Jordi Andilla at ICFO (Institute of photonic sciences), and quantification of figure IV.5 were performed by Anna Plana.

We acknowledge the assistance of Dr. Marta Taulés at the molecular interaction analysis facility of CCiTUB with the Surface Plasmon Resonance (SPR, Biacore) system as well as her assiatnce in the interpretation of the results. We kindly aknowlege the implication of Dr. Josep Maria Estanyol and Dr. Maria José Fidalgo at the Proteomic facility of CCiTUB in the processing of the different samples by LC-MS/MS and their guidance with data analysis.

My contribution to this Chapter was the cloning of all expression vectors for the different recombinant proteins, establishing the protocols for purification of GCAP1, GCAP2, RetGC1 and IMPDH1, the isolation of bovine rod outer segment preparations for pull-down assays and biochemical studies, and the presented GCAP1 pull-down assays, crossed immunoprecipitation protocols, size-exclusion chromatography experiments and Surface Plasmon Resonance analysis. In addition, I implemented the pair-wise label-free quantitative analysis of the proteomic databases..

Chapter IV: Unanticipated interaction between IMPDH1 and RetGC1 proteins associated to blindness.

4.1. Rationale

Inherited retinal dystrophies, that affect 1 in 4000 individuals, are characterized by a vast clinical and genetic heterogeneity. Gene defects might primarily affect rod function and lead to retinitis pigmentosa (RP); cone function and cause cone-rod dystrophies (CORD) or macular degeneration (MD); or both types of photoreceptors in a severe form of inherited blindness manifested in early childhood (Leber congenital amaurosis, LCA). These disorders have autosomal recessive, autosomal dominant or X-linked patterns of inheritance and are genetically and functionally very diverse. Retinitis pigmentosa is caused by mutations in over 58 different genes; cone-rod dystrophies by mutations in 19 genes, while 24 different genes have been linked to LCA (www.sph.uth.tmc.edu/RetNet). Mutations may affect genes encoding signaling proteins directly or indirectly involved in the light response, regulators of gene expression, chaperones, trafficking proteins or structural proteins required for photoreceptor development and viability (Daiger et al., 2015; den Hollander et al., 2008; Stone, 2007). This genetic and functional diversity has hampered the study of these disorders. An in-depth comprehension of the physiological pathways in which these proteins are involved would allow to group them according to common signaling pathways or cellular processes, and greatly assist in the design of novel therapies.

One such functional group is constituted by the proteins involved in cyclic guanosine 3′,5′-monophosphate (cGMP) metabolism. Cyclic GMP is the second messenger in visual transduction. Light sets in motion an enzymatic cascade that ultimately results in hydrolysis of cGMP, a reduction of cGMP levels, closure of the cGMP-gated channels at the plasma membrane (permeable to Na+ and Ca2+) and the hyperpolarization of the cell, which is the signal transmitted to higher order neurons (Burns and Arshavsky, 2005). Free cGMP levels therefore determine the transmembrane potential of rods and cones at any moment. At any illumination condition, cGMP levels are determined by the rate of synthesis by guanylate cyclases and the rate of hydrolysis by cGMP-phosphodiesterase (PDE6) (Gross et al., 2015, 2012). The enzymes responsible for cGMP synthesis in human photoreceptors are retinal guanylate cyclases RetGC1 and RetGC2 (also known as GC-E and GC-F), with RetGC1 being the more abundant isoform in rods and cones and the one relevant for disease (Lowe et al., 1995; Peshenko et al., 2011; Shyjan et al., 1992; Sokal et al., 2003; Yang et al., 1995). Specific subtypes of PDE6 are responsible for cGMP hydrolysis in rods and cones (Bender and Beavo, 2006; Gillespie and Beavo, 1988).

Mutations that cause alterations in the levels of cGMP are very deleterious for photoreceptor cells. Autosomal recessive mutations in the GUCY2D gene encoding RetGC1 have been linked to Leber Congenital Amaurosis type I (LCA1), accounting for 6-12% of LCA cases in the USA and Northern Europe (Jacobson et al., 2013; Perrault et al., 1996). Loss-of-function mutations in RetGC1 are thought to impair visual transduction by causing the closure of cGMP-channels due to the lack of cGMP synthesis (Baehr et al., 2007). LCA1 is considered an "equivalent-light" disorder because visual impairment and progressive cellular damage are thought to result from the permanent closure of the channels and ensuing hyperpolarization of the cell, which is much the same situation that results from excessive or prolonged light exposure (Fain, 2006). The physiopathology underlying LCA12 caused by mutations in RD3 is likely to be very similar, since RD3 has been shown to be required for RetGC1 stability and transport to the outer segments (Azadi et al., 2010; Molday et al., 2013).

On the other hand, mutations in other loci that result in abnormally elevated levels of cGMP are also deleterious for photoreceptor cells. The enzyme responsible for cGMP hydrolysis in rods is the heterotetrameric phosphodiesterase 6 (PDE6), made up of an alpha, a beta and two gamma subunits (Bender and Beavo, 2006). The genes PDE6B and PDE6A encoding PDEα and PDEβ were the second and seventh loci identified as associated to arRP (Huang et al., 1995; McLaughlin et al., 1993); and mutations in PDEG encoding PDEγ were subsequently described (Dvir et al., 2010). Naturally occurring or gene-targeted strains of mice functionally deficient in PDE6B, PDE6A or PDE6G have revealed that abnormally high cGMP levels underlies the retinal degeneration in these scenarios (Bowes et al., 1990; Farber, 1995; Sakamoto et al., 2009; Tsang et al., 1996). That is, mutations in any subunit of PDE6 that ultimately impair light-stimulated cGMP hydrolysis lead to an increase of cGMP levels that results in cell damage. The same phenotype results from arLCA and adCD-associated mutations in aryl hydrocarbon receptor interacting protein like-1 (AIPL1), a photoreceptor specific protein required for the stability, assembly and membrane association of PDE in rods and cones (Kolandaivelu et al., 2009; Ramamurthy et al., 2004). Elevated cGMP levels are predicted to be deleterious for cones as well. Mutations in PDE6C and PDE6H encoding the cone-specific α and γ subunits of PDE6 have been linked to autosomal recessive cone dystrophy (arCD) and achromatopsia, respectively (Kohl et al., 2012; Thiadens et al., 2009). Although not functionally demonstrated *in vivo*, the mutations are predicted to decrease cone PDE activity and trigger a pathophysiological mechanism similar to that affecting rods (Chang et al., 2009). Gain-of-function mutations in GUCY2D gene encoding RetGC1 and GUCA1A gene encoding guanylate cyclase activating protein 1 (GCAP1) have also been reported, linked to adCORD (Hunt et al., 2010; Payne et al., 1998; Wilkie et al., 2000). Most of these mutations lead to constitutive activity of the cyclase *in vitro*, and to accumulating levels of cGMP in rod outer segments

when expressed in animal models (Olshevskaya et al., 2004; Sokal et al., 1998; Woodruff et al., 2007). In brief, mutations in nine different genes have been identified that cause inherited retinal dystrophies by altering the cGMP levels, which leads to severe toxicity in rods and/or cones. Regulation of cGMP metabolism is vital for rod and cone photoreceptors.

An additional gene involved in guanine nucleotide metabolism has been linked to blindness: IMPDH1, encoding inosine monophosphate dehydrogenase 1. This enzyme catalyzes the rate-limiting step in de novo GTP synthesis by converting inosine monophosphate (IMP) to xanthosine monophosphate (XMP) with the reduction of NAD. Mutations in IMPDH1 linked to adRP10 were identified in 2002 from a large family from Spain [Arg224Pro, (Kennan et al., 2002)] and two American and one British families [Asp226Asn, (Bowne et al., 2002)], and together account for 5-10% of adRP cases (Tam et al., 2008). Mutations R105W and N198K were later linked to rare adLCA (Bowne et al., 2006b). Three of these mutations map at the CBS -"similar to **c**ystathione-**b**-**s**ynthase gene"- structural domain of the protein, that is dispensable for catalytic activity and whose function is unclear. IMPDH1 mutations are expected to have a "gain-of-function" rather than "loss-of-function" phenotype, since the IMPDH1 presents only a mild retinopathy (Aherne et al., 2004). Despite IMPDH1 conservation and ubiquity, the clinical manifestations of missense mutations in IMPDH1 are limited to the retina. IMPDH1 gene expression analysis has revealed retinal-specific transcripts generated by alternative splicing and alternative start sites of translation (Bowne et al., 2006a); and structural and biochemical characterization of IMPDH1 unveiled its capacity to bind single-stranded nucleic acids (McLean et al., 2004) and its tendency to aggregate (Aherne et al., 2004). However, the specific or distinctive function of IMPDH1 in photoreceptor cells that underlies the pathophysiology in adRP10 and adLCA remains unclear.

In this study we show an unanticipated association of IMPDH1 with the RetGC1/GCAPs complex responsible for cGMP synthesis at the outer segment of photoreceptor cells. We prove that there is a direct interaction between RetGC1 and IMPDH1 in the micromolar range of affinity that requires the dimerization domain of RetGC1 and is modulated by the CBS domain of IMPDH1. This interaction is affected by IMPDH1 mutations linked to adRP10 and arLCA. This study outlines the RetGC1/GCAPs complex as part of a multienzyme complex comprising enzymes in de novo synthesis of GTP, setting a new scenario for the interpretation of IMPDH1 and RetGC1 mutations linked to inherited retinal dystrophies.

4.2. Results

4.2.1. A search for new GCAP1 binding proteins revealed new interactors of the RetGC1/GCAPs complex responsible for cGMP synthesis in rods and cones.

A proteomic approach was originally devised to identify new molecular targets of the calcium sensor protein GCAP1 in photoreceptor cells, in order to expand our understanding of the integrated Ca2+-mediated adaptation response to light, a fundamental process in photoreceptor cell physiology. To that goal, a recombinant form of GCAP1 fused to a Histidine tag was expressed in bacteria, purified, and covalently linked to magnetic beads. Pull-down assays were performed from bovine rod outer segment preparations (bov ROS) solubilized in 1% Triton X100. Parallel pull-down assays were performed under Ca^{2+} or EGTA conditions, to identify proteins with preferential affinity for the Ca^{2+}-bound or Ca^{2+}-free form of GCAP1 (Figure IV.1). Bound proteins in both conditions were identified by liquid chromatography and mass spectrometry and subjected to label-free quantitative analysis. For each identified protein, the equation in Figure IV.1 determined the fold-change ratio in relative abundance in the two experimental conditions, based on the spectral count ((Old et al., 2005), see Methods). The distribution of fold-change values in the Ca^{2+} versus EGTA condition is shown in the scatter plot in Figure IV.1, in which dots represent individual proteins in alphabetical order. Only those proteins that were unequivocally assigned based on unique peptides were considered (332 proteins, Table IV.I). Nearly 80% of these proteins were found in the -3 to +3 -fold-change range (light shaded area, Figure IV.1). These included the highly abundant cytosolic proteins that typically constitute the background in proteomic analysis: glycolytic enzymes (e.g. GAPDH, pyruvate kinase), cytoskeletal proteins (e.g. actin, spectrin, tubulin, vimentin), chaperones, ribosomal proteins and keratins. Highly abundant proteins in bov ROS, such as the visual pigment rhodopsin, the cGMP-gated channel, cGMP-phosphodiesterase, rhodopsin kinase, arrestin, phosducin and other signaling proteins in the light response were also identified in this range. However, many of these proteins were also identified with similar spectral counts in a negative control pull-down assay performed with Ran, a soluble protein of a similar size to GCAP1 (data not shown). Therefore, most proteins in this range were not considered for further analysis in this study, despite the fact that the bonafide GCAP1 molecular target, retinal guanylyl cyclase 1 (RetGC1), was also found in this group [27 peptides (35 spectra) in the Ca^{2+} condition; 16 peptides (18 spectra) in the EGTA condition, fold-change of 0.18]. We here focused on proteins that bound preferentially to one of the conformational states of GCAP1.

We found 37 proteins with a fold-change$_{Ca2+/EGTA}$ > 3 (scatter plot in Figure 1). These proteins that showed a clear preference for the Ca^{2+}-bound form of GCAP1

are listed in Table IV.1. On the other side, 34 proteins showed a fold-change$_{Ca2+/EGTA}$ < -3, Table IV.2. These tables include the spectral counts in the negative control pull-down with Ran under identical Ca^{2+} or EGTA conditions. While the proteins that preferentially bound the Ca^{2+}-empty (Mg^{2+}-bound) form of GCAP1 were mostly identified in the control pull-down, most of the proteins that showed preferential binding affinity for the Ca^{2+}-bound form of GCAP1 appeared highly specific. As a sample, heat shock protein 90 alpha (HSP90α) was identified with 33 peptides (53 spectra); creatine kinase B (CKB) with 19 peptides (114 spectra); and annexin A6 (ANXA6) with 23 peptides (30 spectra); while none of these proteins were identified in the control pull-down assay under the same Ca2+ conditions. Interestingly, we found several proteins known to play essential roles in photoreceptor cell physiology. For instance, we identified four of the eight subunits of the Chaperonin Containing TCP-1 complex (CCT, also called TCP-1 Ring Complex, TriC), that is known to be required for the morphogenesis of the rod outer segment compartment (Posokhova et al., 2011), which points to a role of this complex on the assembly of the RetGC1/GCAPs complex . We also found five proteins associated to Bardet-Biedl Syndrome (BBS), a disorder affecting 1/100.000 individuals caused by defects in primary cilia biogenesis, that curses with retinal dystrophy in addition to deafness, obesity, diabetes and polydactyly (Sheffield, 2010). The identified proteins BBS2, BBS4, BBS7 and BBS9 (Table I) form part of the BBSome, a conserved protein complex found within primary cilia enriched at the ciliary base and presumably involved in ciliary protein trafficking, while Leucine zipper transcription factor-like 1 (LZTFL1, Table IV.1) is a BBSome-interacting protein that regulates ciliary localization of the BBSome. These results point to the BBSome involvement in RetGC1/GCAP1 ciliary trafficking. .

Most interestingly, three proteins involved in de novo synthesis of GTP were identified robustly in a highly specific manner: inosine monophosphate dehydrogenase 1 (IMPDH1: 18 peptides, 24 spectra); guanylate kinase 1 (GUK1, 11 peptides, 24 spectra) and the bifunctional purine biosynthesis protein PURH (ATIC gene, 19 peptides, 20 spectra).

In this study we focused on the characterization of IMPDH1 association to the RetGC1/GCAP1 complex because mutations in IMPDH1, the enzyme that catalyzes the rate-limiting step in de novo synthesis of GTP, have been linked to very severe inherited retinal dystrophies for more than ten years, of so far unclear pathophysiology.

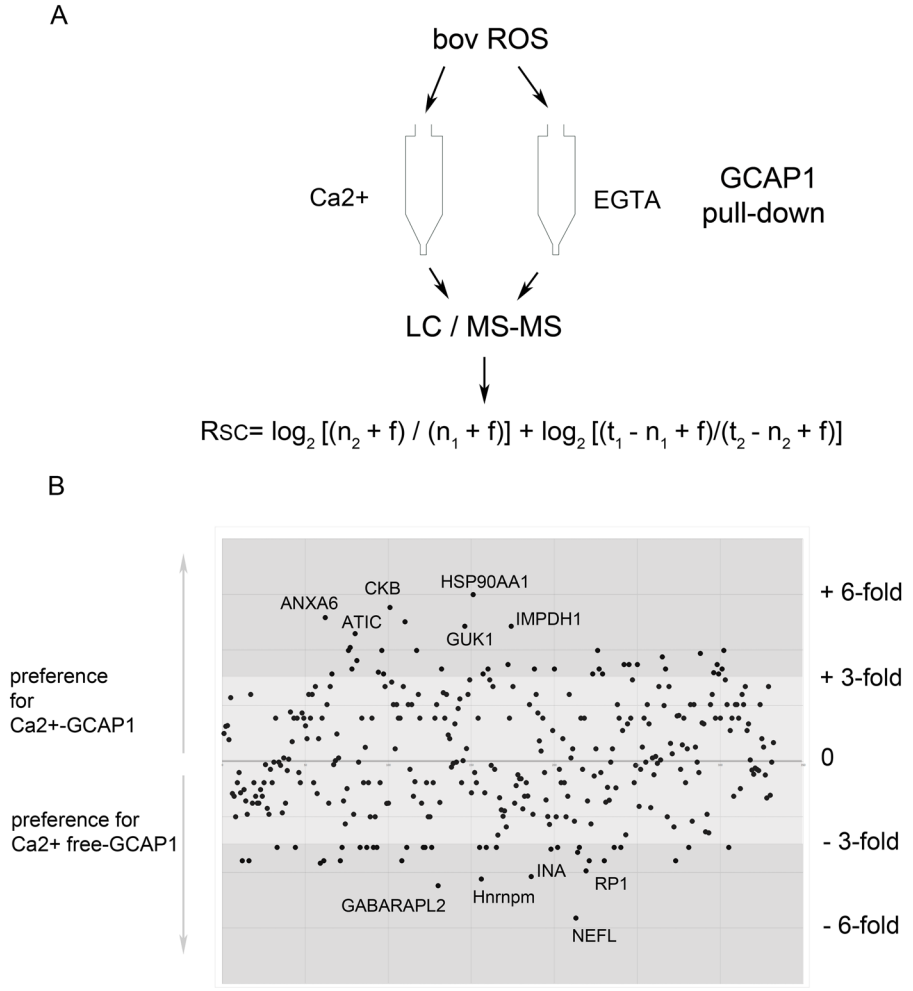

***Figure* IV.*1*. *Identification of GCAP1 binding partners by pull-down assays followed by liquid chromatography and mass spectrometry. A**. Sketch of the procedure. Recombinant GCAP1 was cross-linked to Epoxi Dynabeads, and parallel pull-down assays were performed from bov ROS solubilized in 1% Triton X100, under Ca2+ or EGTA conditions. Elution fractions were subjected to liquid chromatography and mass spectrometry (LC-MS/MS) analysis. Proteomic databases were filtered so that only proteins with at least a unique peptide were retained. A label-free quantitative comparative analysis was performed between Ca2+ and EGTA samples, according to*(Old et al., 2005)*, by applying the equation shown, where, for each protein, R_{SC} (Ratio from Spectral Count) is the log_2 ratio of abundance between Samples 1 (Ca2+) and 2 (EGTA); n_1 and n_2 are spectral counts for the protein in Samples 1 and 2, respectively; t_1 and t_2 are total numbers of spectra*

over all proteins in the two samples; and f is a correction factor set to 0.5. ***B.*** *Scatter plot of* R_{SC}-$_{Ca2+/EGTA}$ *(Fold-change* $_{Ca2+/EGTA}$*) for the list of proteins identified in both samples. Each dot represents an individual protein, in alphabetical order of protein identifier. Its position represents the preference for the Ca2+-bound form or the Ca2+-free form of GCAP1. Protein identifiers are shown for proteins at very high and very low fold-change values: ANXA6, annexin A6; ATIC, 5-aminoimidazole-4-carboxamide ribonucleotide formyltransferase/IMP cyclohydrolase; CKB, creatine kinase B; GUK1, Guanylate Kinase 1; HSP90α, Heat Shock Protein 90 alpha; IMPDH1, inosine monophosphate dehydrogenase 1; GABARAPL2, Gamma-aminobutyric acid receptor-associated protein-like 2; Hnrnpm, Heterogeneous nuclear ribonucleoprotein M; INA, alpha-internexin; NEFL, neurofilament light polypeptide; RP1, Retinitis Pigmentosa 1.*

Table IV.1. Proteins identified by LC-MS/MS in GCAP1 pull-down assays from bovine rod outer segment preparations in Ca2+ or EGTA conditions, that show a higher affinity for the Ca^{2+}-bound form of GCAP1

				GCAP1 pull Down				**Neg. Conrol Ran**	
				Ca^{2+} condition		**EGTA condition**		**Ca^{2+} condition**	
Protein	**ID**	**Gene name**	**Fold Change**	**N. SC**	**NP**	**N. SC**	**NP**	**N. SC**	**NP**
Heat Shock Protein 90 α	*Q76LV2*	*HSP90AA1*	*5.99*	*53*	*33*	*0*	*0*	*0*	*0*
Creatine Kinase B	*Q5EA61*	*CKB*	*5.53*	*114*	*19*	*1*	*1*	*0*	*0*
Annexin A6	*P79134*	*ANXA6*	*5.17*	*30*	*23*	*0*	*0*	*0*	*0*
Dihydropyrimidinase-related protein 3	*Q62188*	*Dpysl3*	*5.02*	*27*	*16*	*0*	*0*	*0*	*0*
Inosine -5′-monophosphate dehydrogenase 1	*A0JNA3*	*IMPDH1*	*4.85*	*24*	*18*	*0*	*0*	*0*	*0*
Guanylate kinase	*P46195*	*GUK1*	*4.85*	*24*	*11*	*0*	*0*	*0*	*0*
Bifunctional purine biosynthesis protein PURH	*Q0VCK0*	*ATIC*	*4.59*	*20*	*19*	*0*	*0*	*0*	*0*
Bardet-Biedl Syndrome protein homolog 4	*Q1JQ97*	*BBS4*	*4.09*	*14*	*12*	*0*	*0*	*3*	*3*
Bardet-Biedl Syndrome protein homolog 2	*Q9CWF6*	*Bbs2*	*3.98*	*13*	*9*	*0*	*0*	*2*	*2*
Phosducin	*P19632*	*PDC*	*3.98*	*13*	*10*	*0*	*0*	*4*	*2*
Eukaryotic elongation factor 2	*Q3SYU2*	*EEF2*	*3.98*	*13*	*13*	*0*	*0*	*0*	*0*
T-complex protein 1 theta	*Q3ZCI9*	*CCT8*	*3.98*	*13*	*13*	*0*	*0*	*0*	*0*
Copine-1	*Q8C166*	*Cpne1*	*3.98*	*13*	*8*	*0*	*0*	*0*	*0*
Sodium/Potassium/ Calcium exchanger 1	*Q28139*	*SLC24A1*	*3.87*	*12*	*10*	*0*	*0*	*3*	*2*
Retinaldehyde binding protein 1	*P10123*	*RLBP1*	*3.75*	*11*	*10*	*0*	*0*	*1*	*1*
Calmodulin	*P62157*	*CALM*	*3.62*	*10*	*8*	*0*	*0*	*0*	*0*

Rab GTPase-binding effector protein 2	A4FUG8	RABEP2	3.48	9	9	0	0	0	0
T-complex protein 1 beta	Q3ZBH0	CCT2	3.48	9	9	0	0	0	0
Protein PTHB1	Q811G0	Bbs9	3.48	9	9	0	0	3	2
Putative adenosylhomocysteinase 2	Q80SW1	Ahcyl1	3.48	9	9	0	0	0	0
Hydroxyacylglutathione hydrolase, mitochondrial	Q3B7M2	HAGH	3.48	9	7	0	0	0	0
Bardet-Biedl syndrome 7	Q8K2G4	Bbs7	3.32	8	8	0	0	0	0
Myc box-dependent-interacting protein 1	O08539	Bin1	3.32	8	6	0	0	0	0
Glucose-6-phosphate isomerase	Q3ZBD7	GPI	3.32	8	6	0	0	0	0
Hexokinase-1	P27595	HK1	3.32	8	7	0	0	0	0
Leucine zipper transcription factor- like protein 1	Q3ZBL4	LZTFL1	3.32	8	7	0	0	0	0
Phosphoglycerate kinase 1	Q3T0P6	PGK1	3.32	8	8	0	0	0	0
Retinoid isomerohydrolase	Q28175	RPE65	3.32	8	6	0	0	0	0
T-complex protein 1 gamma	Q3T0K2	CCT3	3.32	8	8	0	0	0	0
Cone cGMP-specific 3',5'-cyclic phosphodiesterase subunit alpha'	P16586	PDE6C	3.20	23	21	1	1	0	0
Syntaxin-binding protein 1	P61763	STXBP1	3.18	53	28	3	3	0	0
Copine-2	P59108	Cpne2	3.13	7	6	0	0	0	0
Platelet-activating factor acetylhydrolase	Q29460	PAFAH1B3	3.13	7	6	0	0	0	0
Aspartyl aminopeptidase	Q2HJH1	DNPEP	3.13	7	7	0	0	0	0
T-complex protein 1 subunit δ	Q2T9X2	CCT4	3.13	7	7	0	0	0	0
Peptidyl-prolyl cis-trans isomerase NIMA-interacting 1	Q5BIN5	PIN1	3.13	7	4	0	0	0	0

Table IV.2: Proteins identified by LC-MS/MS in GCAP1 pull-down assay from bovine rod outer segment preparations, that show a higher affinity for the Ca2+-free form of GCAP1.

				GCAP1 pull-down				***Neg ctrl (Ran)***	
				Ca2+ condition		***EGTA condition***		***EGTA condition***	
Protein	***ID***	***Gene name***	***Fold Change***	***N. SC***	***N P***	***N. SC***	***N P***	***N. SC***	***N P***
Neurofilament light polypeptide	*P02548*	*NEFL*	*-5.64*	*0*	*0*	*14*	*13*	*25*	*16*
Gamma aminobutyric acid	*P60519*	*GABARAPL2*	*-4.48*	*0*	*0*	*6*	*5*	*0*	*0*
Heterogeneous nuclear	*Q9D0E1*	*Hnrnpm*	*-4.24*	*0*	*0*	*5*	*5*	*0*	*0*
Lamin-B1	*P14733*	*Lmnb1*	*-4.15*	*1*	*1*	*15*	*13*	*0*	*0*
Oxygen-regulated protein 1	*Q8MJ05*	*RP1*	*-3.95*	*0*	*0*	*4*	*4*	*43*	*27*
Alpha-internexin	*Q08DH7*	*INA*	*-3.67*	*2*	*2*	*18*	*17*	*34*	*19*
40S ribosomal protein S9	*A6QLG5*	*RPS9*	*-3.58*	*0*	*0*	*3*	*3*	*0*	*0*
Partner of Y14 and mago	*A6QPH1*	*WIBG*	*-3.58*	*0*	*0*	*3*	*3*	*0*	*0*
ATP synthase subunit epsilon, mitochondrial	*P05632*	*ATP5E*	*-3.58*	*0*	*0*	*3*	*2*	*0*	*0*
40S ribosomal protein S27	*Q2KHT7*	*RPS27*	*-3.58*	*0*	*0*	*3*	*3*	*0*	*0*
Ankyrin repeat domain-containing protein 33B	*Q3U0L2*	*H11*	*-3.58*	*0*	*0*	*3*	*3*	*0*	*0*
Pleckstrin homology domain-containing family A member 7	*Q3UIL6*	*Plekha7*	*-3.58*	*0*	*0*	*3*	*3*	*0*	*0*
RNA-binding protein 14	*Q5EA36*	*RBM14*	*-3.58*	*0*	*0*	*3*	*3*	*0*	*0*

Dihydrolipolylysine-residue acetyltransferase component of pyruvate	*Q8BMF4*	*Dlat*	*-3.58*	*0*	*0*	*3*	*3*	*3*	*2*
Neurofilament medium polypeptide	*O77788*	*NEFM*	*-3.27*	*1*	*1*	*8*	*7*	*15*	*11*
Microtubule-associated protein 4	*P36225*	*MAP4*	*-3.15*	*6*	*6*	*33*	*21*	*7*	*6*
Protein lin-7 homolog C	*Q0P5F3*	*LIN7C*	*-3.09*	*1*	*1*	*7*	*5*	*0*	*0*
60S ribosomal protein L4	*Q58DW0*	*RPL4*	*-3.09*	*0*	*0*	*2*	*2*	*0*	*0*
Abl interactor 1	*Q8CBW3*	*Abi1*	*-3.09*	*0*	*0*	*2*	*2*	*0*	*0*
ATP synthase subunit f, mitochondrial	*Q28851*	*ATP5J2*	*-3.09*	*0*	*0*	*2*	*2*	*11*	*2*
Caskin-1	*Q6P9K8*	*Caskin1*	*-3.09*	*0*	*0*	*2*	*2*	*0*	*0*
Charged multivesicular body protein 2a	*Q9DB34*	*Chmp2a*	*-3.09*	*0*	*0*	*2*	*2*	*2*	*2*
Coatomer subunit epsilon	*Q28104*	*COPE*	*-3.09*	*0*	*0*	*2*	*2*	*0*	*0*
Complement component 1 Q subcomponent-binding protein, mitochondrial	*Q3T0B6*	*C1QBP*	*-3.09*	*0*	*0*	*2*	*1*	*5*	*3*
Disks large homolog 4	*Q62108*	*Dlg4*	*-3.09*	*0*	*0*	*2*	*2*	*6*	*6*
Eukaryotic translation initiation factor 2 subunit 1	*P68102*	*EIF2S1*	*-3.09*	*0*	*0*	*2*	*2*	*0*	*0*
Eukaryotic translation initiation factor 2 subunit 2	*Q5E9D0*	*EIF2S2*	*-3.09*	*0*	*0*	*2*	*2*	*0*	*0*
Fibroblast growth factor 2	*P03969*	*FGF2*	*-3.09*	*0*	*0*	*2*	*2*	*0*	*0*
Heterog. nuclear-ribonucleoprotein D0	*Q60668*	*Hnrnpd*	*-3.09*	*0*	*0*	*2*	*2*	*0*	*0*

Heterogeneous nuclear ribonucleoprotein C1/C2	*Q9Z204*	*Hnrnpc*	*-3.09*	*0*	*0*	*2*	*2*	*0*	*0*
Histone deacetylase 4	*Q6NZM9*	*Hdac4*	*-3.09*	*0*	*0*	*2*	*1*	*0*	*0*

4.2.2. IMPDH1, a protein involved in de novo synthesis of GTP, associates with the RetGC1/GCAPs complex in rod outer segment preparations.

IMPDH1 is the enzyme that catalyzes the rate-limiting step in de novo GTP synthesis, by converting inosine monophosphate (IMP) to xanthosine monophosphate (XMP). The robust identification of IMPDH1 in the pull-down assay with GCAP1 indicates either a direct interaction with GCAP1 or an indirect association to GCAP1 by a direct interaction with RetGC1 or some other component in the protein complex responsible for cGMP synthesis. Despite GCAP1 cytosolic distribution in the different photoreceptor cell compartments (López-del Hoyo et al., 2012) and IMPDH1 reported abundance at the inner segments (Bowne et al., 2006a), our results pointed to IMPDH1 association with GCAP1 in the photoreceptor outer segments, because pull-down assays were performed on bov ROS.

In order to validate IMPDH1 association to GCAP1 and/or the RetGC1/GCAPs complex we performed co-immunoprecipitation assays in bovine whole retinal homogenates and bov ROS (Figure IV.2). Immunoprecipitation of GCAP1 led to co-immunoprecipitation of IMPDH1 in bovine retinal homogenates, as well as in bov ROS (Figure IV.2A). Immunoprecipitation of IMPDH1 in whole retinal homogenates led to co-immunoprecipitation of RetGC1 (Figure IV.2B), although co-immunoprecipitation of GCAP1 could not be detected, likely because of anti-IMPDH1 pAb antibodies interfering with the binding surface (not shown).

To circumvent immunoprecipitation limitations presented by antibody binding to the region of protein-protein interaction, we expressed and purified the canonical isoform of IMPDH1 in order to perform pull-down assays. IMPDH1 pull-down assays from whole retinal homogenates revealed the binding of RetGC1 (Figure IV.2C). When bovine ROS were used in IMPDH1 pull-down assays, RetGC1 was detected to an even higher extent (Figure IV.2C). Taken together, these results indicate that IMPDH1 associates to GCAP1 and RetGC1 in native tissue.

To further confirm this protein association in native tissue and to study whether it involved any of the other proteins identified quantitatively in the pull-down assays (e.g. HSP90α and CKB) bov ROS solubilized in 1% dodecyl maltoside were fractionated by size exclusion chromatography. A 3.5µm-bead size column with a separation range of 10kDa-1500kDa was used, and collected fractions were

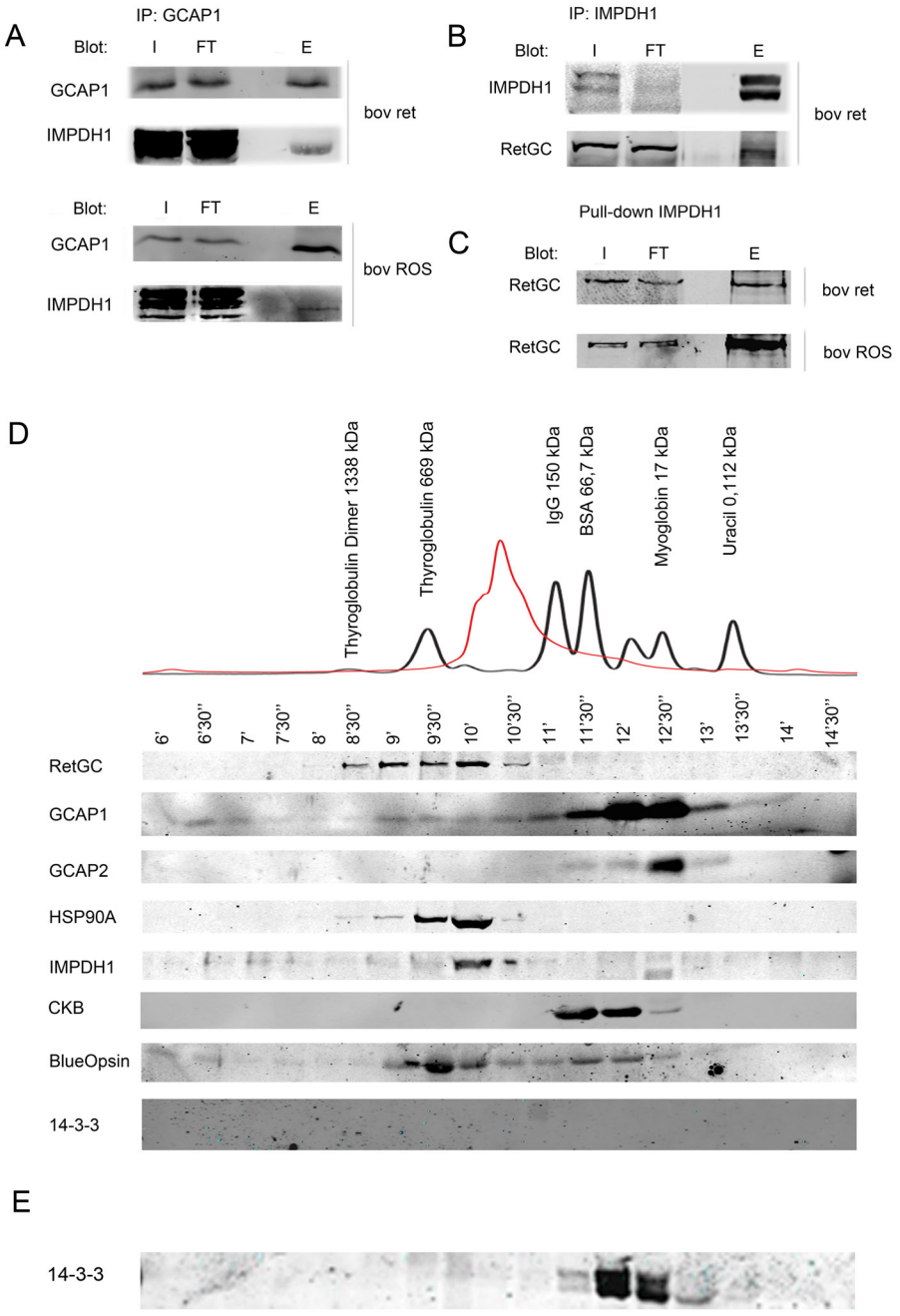

Figure IV.2. IMPDH1 is associated to RetGC1/GCAP1 in native retinal tissue. A. Co-immunoprecipitation of IMPDH1 with GCAP1 in bovine whole retina homogenates (upper panel) and bovine rod outer segments (bov ROS, lower panel). I, Input; FT, flow-through; and E, elution fractions. There are five IMPDH1 isoforms in the retina, that result from alternative splicing or alternative translation start sites(Bowne et al., 2006a) *appreciated in the input lanes. B. RetGC1 co-immunoprecipitates with IMPDH1 in bovine retinal homogenates. C. Pull-down assays with IMPDH1 (canonical bovine isoform) from bovine retinal homogenates*

(top) or bov ROS (bottom) reveal the association of RetGC1. D. RetGC1, HSP90α and IMPDH1 co-elute during the fractionation of bovROS by size-exclusion chromatography (3.5µm-bead size column with a separation range of 10kDa-1500kDa), at the 10min fraction corresponding to 500-600kDa. Black line, chromatogram of the protein standards. Red line, chromatogram of bov ROS. E. 14-3-3 proteins, very abundant at photoreceptor inner segment compartments, are detected in SEC fractionation of whole bovine retinal homogenates. Therefore, their absence in bov ROS preparations indicates that inner segment contamination of the samples was minimal.

at a fraction at minute 10, corresponding to a molecular weight of about 500-600 kDa. Although GCAP1 localized mostly at fractions corresponding to its monomeric and dimeric forms, it was also detected at the 10min fraction with RetGC1, IMPDH1 and HSP90α. Besides, it is well known that the interaction of GCAP1 with RetGC1 is disrupted by detergents. Other proteins that were identified robustly in the pull-down assay with a clear preference for Ca2+-GCAP1 (e.g. CKB) did not co-migrate noticeably with RetGC1. This does not necessarily indicate that CKB does not associate with the RetGC1/GCAP1 complex, since low affinity or fast kinetic interactions could be lost during this process.

To rule out contamination of bov ROS preparations with inner segment proteins, we incubated the membrane with an antibody against 14-3-3 protein isoforms, which are very abundant at the inner segment but excluded from the outer segment compartment (López-del Hoyo et al., 2014). The absence of 14-3-3 isoforms in the sample indicated that contamination of inner segments in the bov ROS was minimal. 14-3-3 isoforms were clearly detected in SEC fractionation experiments from whole retinal homogenates (Figure IV.2E). We also tested whether cone outer segments were present in the preparation. Immunodetection of blue opsin indicated that our starting material included at least a fraction of cone outer segment organelles.

Taken together, these results show that IMPDH1 associates with the RetGC1/GCAP1 complex at the outer segment of rods and/or cones.

4.2.3. IMPDH1 shows preferential localization to rods, being abundant at the inner segment but also present at rod outer segment compartments.

In order to study whether IMPDH1 co-localizes with the RetGC1/GCAPs complexes in retinal sections, we generated a rabbit antibody against the recombinant canonical form of IMPDH1. This antibody (pAb) was highly specific for IMPDH1. When assayed on bovine retinal sections, this anti-IMPDH1 pAb yielded a specific signal at the photoreceptor cell layers that was much stronger at rods than at cones (e.g. Figure IV.3, E-G). IMPDH1 primarily accumulated at the proximal part of the inner segment layer and at the base of the outer segment of rods, as well as at the perinuclear region and at the synaptic terminal of rods and cones (Figure IV.3). At the base of rod outer segments, the IMPDH1 signal partially overlapped with rhodopsin (Figure IV.3, A-D). At cones, the most clear co-localization of IMPDH1 with GCAP1 was observed at the pedicles, whereas IMPDH1 signal at the inner and outer segment of cones was much weaker than at rods, although perceptible (Figure IV.3, E-H, and N). At rods, IMPDH1 co-localized with GCAP2 mostly at the proximal part of the inner segments, at the base of the outer segments and at the synaptic terminals (Figure IV.3, I-L, and O). When images of IMPDH1 staining were acquired in a confocal microscope requiring much less light excitation [Leica hybrid detector (HyD)] photobleaching was heavily reduced and images could be acquired at a higher zoom, maximizing discernment of subcellular detail. In these images (Figure IV.3, M), IMPDH1 was also observed to be enriched at processes stemming from the outer limiting membrane, that we attribute to the microvilli of Muller cells, and at connecting ciliums.

Co-immunolocalization assays of IMPDH1 and RetGC1 could be performed with our highly specific polyclonal antibodies (both made in rabbit), by conjugating the anti-IMPDH1 antibody with a 488nm-fluorophore. Images were acquired at increasing magnification (Figure IV.4). When low excitation light was used for image acquisition of a frame encompassing all photoreceptor layers, IMPDH1 was most abundant at the inner segment layer and outer plexiform layer, and highlighted the connecting cilium of cones and rods - two rows of “spikes” - and the microvilli of Muller cells (Figure IV.4A). Consistent with previous reports, RetGC1 staining was predominant at the outer segment layer, stronger at cones than at rods (Figure IV.4B). Using a higher excitation light and higher zoom, IMPDH1 enrichment at the inner segment layer and connecting cilium was even more evident, but immunostaining was also noticeable at the outer segment compartment and the nuclei of photoreceptors (Figure 4D). The anti-RetGC1 antibody stained the outer segment compartment of cones and rods (Figure IV.4E). Co-localization of IMPDH1 with RetGC1 at the connecting cilium of several rods and cones appeared evident (Figure IV.4F). A higher zoom framing the outer segment layer showed partial co-localization of IMPDH1 and RetGC1 at this compartment (Figure IV.4,

G-I), and Supplementary Figure 1. A colocalization analysis of RetGC1 and IMPDH1 restricted to the rod outer segment layer revealed that 71% of IMPDH1 colocalizes with RetGC1 (SEM=10%, n=4 images, with each image being the average of four consecutive planes from the same z-stack, Figure IV.5).

A hallmark of IMPDH1 immunolocalization staining is the detection of subcellular fiber-like structures, characterized in cells in culture (Chang et al., 2015). These structures might appear as punctuate and small spicule-shaped structures termed "cytoophidia"; or as larger mature structures termed "rods and rings", suggested to form when de novo purine synthesis is positively regulated (Chang et al., 2015). We routinely observe both types of structures in bovine retinal sections, typically covering the cytosolic space of rods and scarcely but also present in the cytosol of cones (e.g. Figure IV.3E, I). Whether their formation shows a correlation with dark-adaptation or light exposure of the eyes, and their functional implications await further studies.

Collectively, our immunolocalization studies show co-localization of IMPDH1 and RetGC1 at photoreceptor outer segments, being particularly strong at the connecting cilium.

Figure IV.3. Immunolocalization of IMPDH1 in bovine retinal sections. IMPDH1 localization was assayed in bovine retinal cryosections by indirect immunofluorescence (green signal in A, E, I, M, N, O), that were also stained for: rhodopsin at the rod outer segments (B); GCAP1, that highlights cones due to its higher level of expression in cones than rods, but present in both cells at the outer segment, inner segment and synaptic terminal compartments (F); and GCAP2, that highlights rods, with a strong signal at the outer segment, inner segment and synaptic terminals (J). IMPDH1 is present at both rods and cones, with the rod signal being much more intense. It distributes along the whole cytosolic space of the cell, being particularly enriched at the inner segment, the base of the outer segment at what appears to be the connecting cilium, as well as filamentous structures resembling the microvilli of Muller cells, the perinuclear region at the outer nuclear layer and the synaptic terminal of rods and cones (A, E, I). IMPDH1 co-localizes with rhodopsin at the base of the outer segment (C); with GCAP1 at the base of cone outer segments (G) and cone pedicles (N); and with GCAP2 at rod inner segments (K) and rod spherules (O). Image acquisition using a much lower excitation light and higher zoom (Leica HyD hybrid detector, Leica SP5 confocal microscope) allows a better discernment of stained subcellular processes (M). Scale bar is 25µm in A to L, 10µm in M, N and O. OS, outer segment; IS, inner segment; ONL, outer nuclear layer; OPL, outer plexiform layer.

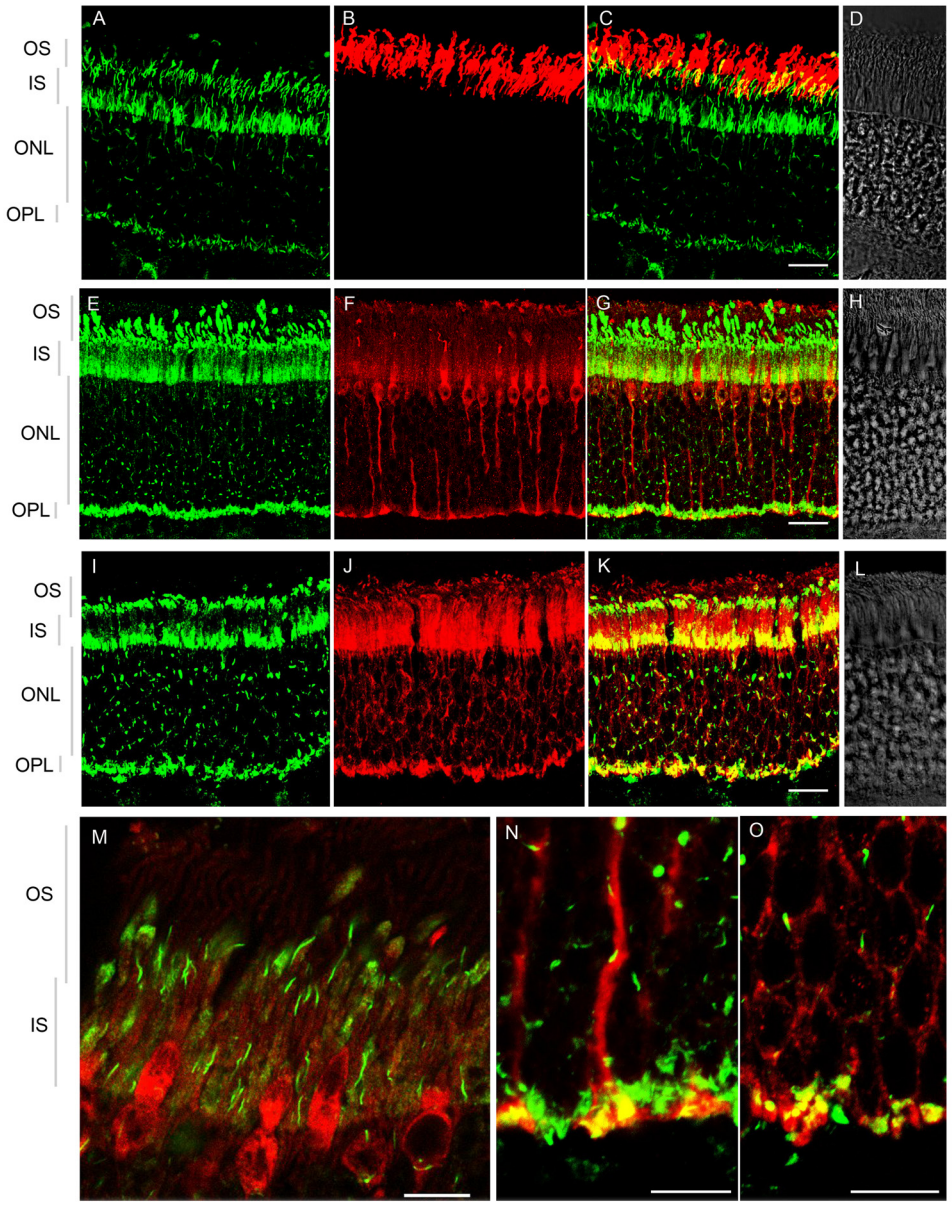
A
B
C
D
OS
IS
ONL
OPL
E
F
G
H
OS
IS
ONL
OPL
I
J
K
L
OS
IS
ONL
OPL
M
N
O
OS
IS

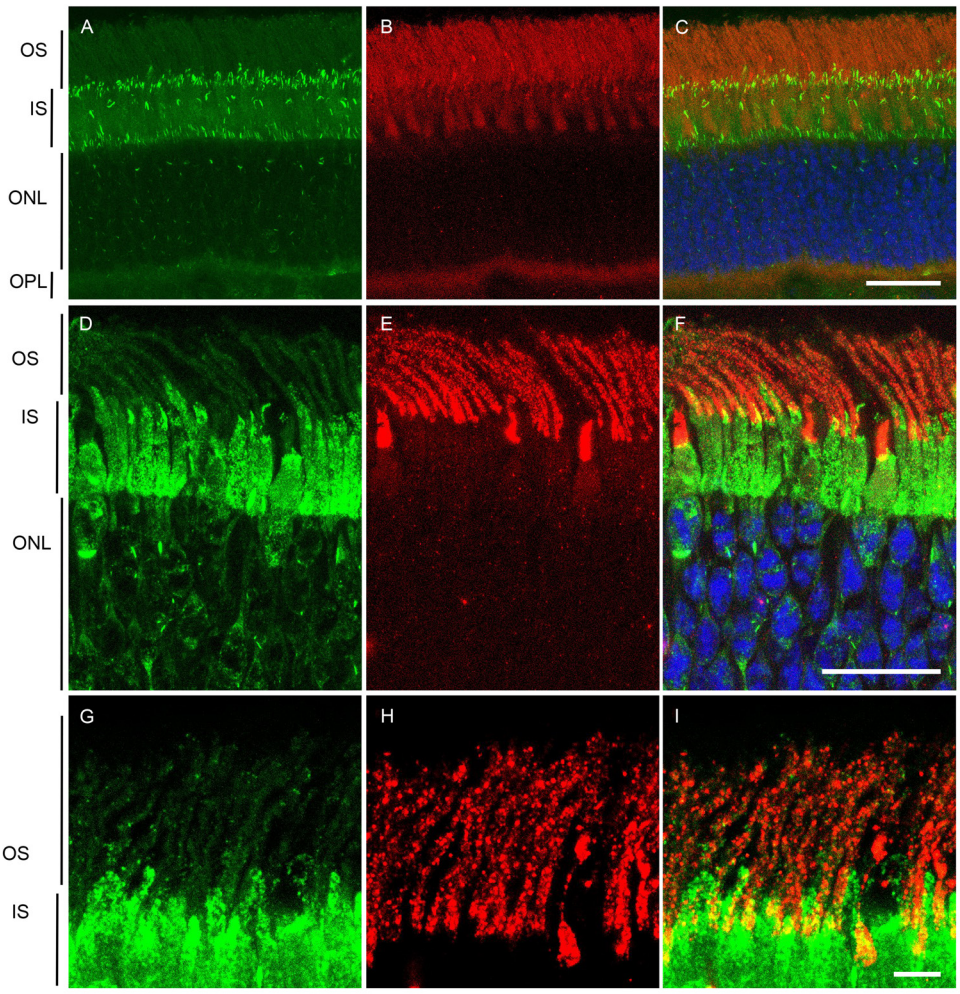

Figure IV.4. Analysis of subcellular co-localization of IMPDH1 and RetGC1. Immunolocalization of IMPDH1 in bovine retinal cryosections with an anti-IMPDH1 pAb conjugated with Alexa 488 (green signal); and of RetGC1 with an anti-RetGC1 pAb with an anti-rabbit IgG-Alexa 555 (red signal). Images at panels A-C were acquired at low excitation light in a frame encompassing all photoreceptor layers, to show that IMPDH1 is most abundant at the inner segment layer, and to remark that IMPDH1 signal highlights the rod connecting cilium (upper row of "spikes"); cone connecting cilium (more discontinued middle row of "spikes"); and Muller cell microvilli (filamentous structures at lower row), at panel A. RetGC1 signal typically highlights cone outer segments, but is also noticeable at rod outer segments and synaptic terminals (panel B). RetGC1 and IMPDH1 co-localization is barely perceptible in the merged image at this gain (C). Images were acquired at increasing excitation light and increasing zoom in order to assess co-localization (panels D-F, and panels G-I). Although much weaker than at the inner

segments, IMPDH1 was also present at rod outer segments (D, G), where it co-localized with RetGC1 (F, I). IMPDH1 signal is brighter and co-localizes with RetGC1 at the connecting cilium of rods and cones (F, I). Scale bar is 25µm in A to F, and 10µm in G to I. OS, outer segment; IS, inner segment; ONL, outer nuclear layer; OPL, outer plexiform layer.

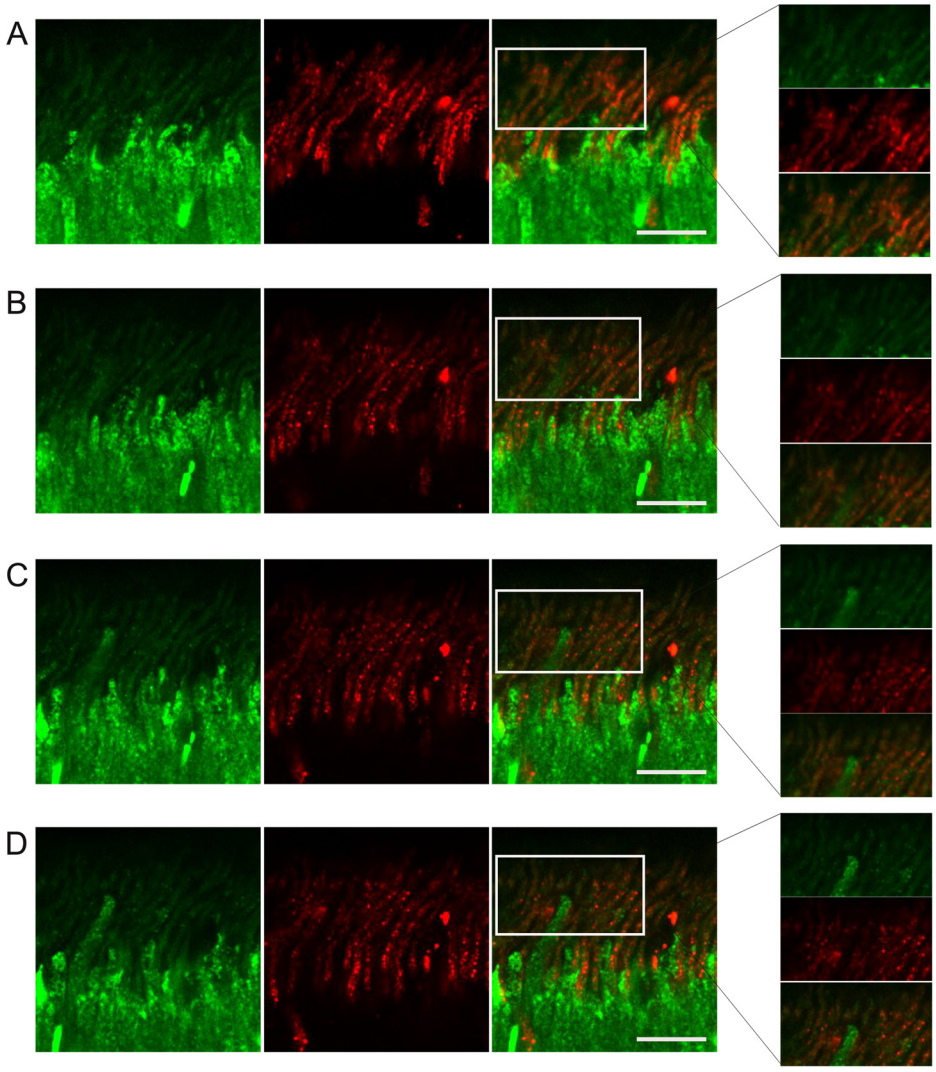

E

Z-Stacked planes	M1	M2	tM1	tM2
31-35 (A)	1	1	0.68	0.51
36-40 (B)	1	1	0.89	0.85
41-45 (C)	1	1	0.74	0.59
46-50 (D)	1	0.99	0.97	0.89
media	1	0.998	0.82	0.71
SEM	0	0.003	0.07	0.1

M1: proportion Ch1 coinciding to Ch2
M2: proportion Ch2 coinciding to Ch1
tM1: M1 after threshold
tM2: M2 after threshold

Figure IV.5. Percentage of RetGC1-IMPDH1 colocalization at the rod outer segment layer. Co-immunostaining of RetGC1 (red) and IMPDH1 (green) in a bovine retinal section. Images were acquired at 100x magnification, applying a 5x zoom. Each panel is the average image of four consecutive planes from the same z-stack, labelled as planes 31-35 (A); planes 36-40 (B); planes 41-45 (C), and planes 46-50 (D) from an original stack of 55 planes. A ROI was selected restricted to the rod outer segment layer. E. Table showing Manders' coefficients for Coloc2 analysis.

4.2.4. A direct interaction between IMPDH1 and RetGC1 is mediated by RetGC1 dimerization/catalytic domain and modulated by IMPDH1 CBS domain.

In order to study whether the observed association of IMPDH1 with the RetGC1/GCAPs complex involved a direct interaction between IMPDH1 and RetGC1, and to map the region of RetGC1 involved in the interaction, we expressed three protein fragments covering the RetGC1 cytosolic domain. RetGC1 is a type I transmembrane polypeptide that contains an extracellular domain (ECD), a transmembrane domain (TM) and a cytosolic domain (Figure IV.6.A). The ECD of RetGC1 is intradiscal and dispensable for guanylyl cyclase catalytic activity. It is the cytosolic region of the protein that contains the catalytic domain (CD) and a kinase homology domain (KHD) involved in the interaction with GCAP1 and therefore critical for Ca2+-regulation of the enzyme (Laura et al., 1996). The KHD and CD are separated by a dimerization domain (DD), which is also required for cyclase activity, as RetGC is only functional as a dimer. Expression of the whole cytosolic domain of RetGC1 was deemed practically unfeasible due to its instability in solution, even when attempted with different protein tags to promote solubility. Therefore, we expressed the human RetGC1 cytosolic domain in two fragments: JMD/KHD (residues M496-K806) and DD/CD (N807-S1103), expressed as fusion proteins with maltose binding protein (MBP). A fragment containing the CD domain in the absence of the DD was also expressed: CD (G868-S1103). Residue numbers refer to human RetGC1 (NP_000171; GI: 4504217).

Pull-down assays were performed from whole bovine retinal homogenates solubilized in 1% dodecyl maltoside. The JMD/KHD protein fragment pulled-down IMPDH1, HSP90α and Tr α at low but detectable levels (Figure IV.6.B left panels). This fragment also pulled-down GCAP1 as expected, although the low levels detected are in agreement with previous reports that the presence of detergents destabilize the RetGC1-GCAP1 interaction. The DD/CD protein fragment did not pull-down GCAP1, but pulled-down IMPDH1, CKB, HSP90α and Tr α to a much higher extent than the JMD/KHD fragment (Figure 5B middle panels). When only the catalytic domain (CD fragment) was used for pull-down, the amount of IMPDH1 protein bound diminished substantially, and those of CKB, HSP90α and Tr α

diminished dramatically (Figure IV.6.B right panels), which indicates that the dimerization domain is required for the association of RetGC1 with IMPDH1, as well as with CKB, HSP90α and Tr α. These results are more apparent at the histogram plot in Figure IV.6.C, that represents the fraction of bound protein to each RetGC1 region, determined from each immunoblot for each pull-down assay (protein density in the elution fraction expressed as a function of protein density in the input). Taken together, our results show that IMPDH1, CKB, HSP90α and Trα associate to RetGC1, and that the region of RetGC1 that contributes the most to this association is the DD/CD region, indicating that RetGC1 dimerization is likely required for these interactions.

Because the most prevalent adRP10 mutations in IMPDH1 map at the CBS domain, we investigated whether this domain was involved in the interaction. The CBS -"similar to **c**ystathione-**b**-**s**ynthase gene"- structural domain of the protein is a domain that flanks the α /β barrel structure which performs the enzymatic function, dispensable for catalytic activity and of function unknown. We expressed and purified the canonical form of bovine IMPDH1 fused to thioredoxin (Trx-IMPDH1), and a deletion mutant lacking both copies of the CBS domain (Trx-IMPDH1ΔCBS). Pull-down assays were performed with Trx-IMPDH1 or Trx-IMPDH1ΔCBS on whole bovine retinal homogenates solubilized in 1% dodecyl maltoside. IMPDH1 pulled-down RetGC1 on solubilized whole retinal homogenates (Figure 5D, left panel). In two independent experiments, we determined that IMPDH1ΔCBS induced the binding of RetGC1 to a 1,68-fold higher extent than IMPDH1 (histogram in Figure IV.6,D). These results indicate that the CBS domain in IMPDH1 interferes with the association of IMPDH1 with RetGC1 in native tissue, likely serving to modulate this interaction depending on the protein functional state.

To test whether RetGC1 and IMPDH1 established a direct interaction, we mixed recombinant-expressed RetGC1-DD/CD with IMPDH1 and performed an immunoprecipitation of IMPDH1 to test for co-immunoprecipitation of RetGC1-DD/CD. To rule out unspecific binding of RetGC1-DD/CD to the Ab-immobilized beads, a fixed amount of RetGC1-DD/CD was mixed with variable amounts of IMPDH1, and an excess of anti-IMPDH1 Ab-beads was used for immunoprecipitation in all samples. RetGC1 was co-immunoprecipitated in the assay to the extent of IMPDH1 immunoprecipitation (Figure IV.7.A).

To further prove this direct interaction and to measure its affinity, we monitored the interaction by surface plasmon resonance (SPR). Affinity measurements were carried out with a fixed concentration of RetGC1-DD/CD or RetGC1-JMD/KHD coupled to the chip (used as ligands), and a range of concentrations of IMPDH1 passed in solution (analyte). An affinity analysis was performed based on steady-state binding levels, by direct analysis of a plot of amount of complex (maximal response in resonance units, RU) as a function of IMPDH1 concentration, assuming a 1:1 binding model (Figure IV.7.B). A dissociation constant of 2.09 x 10^{-6} M was

obtained for the RetGC1-DD/CD fragment of the cyclase, and 5.05 x 10^{-6} M for the RetGC1-JMD/KHD fragment. This result confirms that the interaction is direct, and that the DD/CD fragment of the cyclase contributes more to the interaction than the JMD/KHD, even though a more substantial difference in the dissociation constants was expected based on Figure IV.7 (see Discussion).

Taken together, our results show that RetGC1 establishes a direct interaction with IMPDH1 in the micromolar (physiological) range of affinity, mediated mostly by the dimerization/catalytic domain of the protein and likely modulated by IMPDH1 CBS domain.

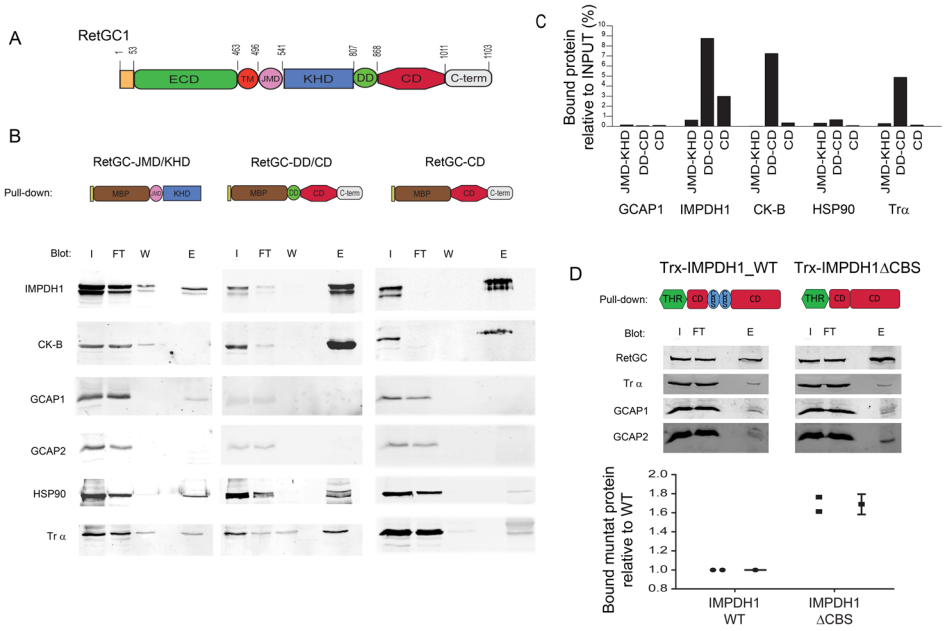

Figure IV.6. Regions of RetGC1 and IMPDH1 involved in the interaction. A. Organization of RetGC1 in protein domains: ECD, extracellular domain; TM, transmembrane domain; KHD, kinase homology domain; DD, dimerization domain; CD, catalytic domain. B. Pull-down assays from solubilized bovine retinas were performed with different RetGC1 protein regions fused to Maltose Binding Protein (MBP), as indicated by the diagrams. Input (I); flow-through (FT); washing (W) and elution (E) fractions from pull-down assays were resolved by SDS-PAGE and immunoblotted for the indicated proteins. The DD/CD region of RetGC1 was substantially more efficient at binding IMPDH1 in pull-down assays than the JMD/KHD region. The dimerization domain of RetGC1 substantially contributes to

RetGC1 binding to IMPDH1, creatine kinase B, HSP90α and Transducin α. C. Quantification of pull-down results in the mapping of RetGC1 domains involved in the interaction. The histograms for each protein represent the percentage of bound protein relative to the input, to the indicated RetGC1 region (quantitated from a density analysis of the bands in the elution and input lanes in the corresponding panels, correcting for dilution factors and suppressing the mean background). D. Effect of the IMPDH1 CBS domain in IMPDH1 interaction with RetGC1. Pull-down assays were performed from solubilized bovine retinas with IMPDH1 (bovine canonical isoform) or IMPDHΔCBS, lacking both copies of the CBS domain. I, input; FT, flow-through; E, elution fractions. The binding of RetGC1 to IMPDH1 or IMPDH1ΔCBS was compared by densitometry of the RetGC1 band in the elution fraction (after input normalization and suppression of background). The dot plot shows single measurements taken from IMPDH1 (●) and IMPDH1ΔCBS (■) in two independent experiments, and the mean. Bars represent the range of measurements. RetGC1 showed a higher affinity (1.68-fold higher) for IMPDHΔCBS than for IMPDH1.

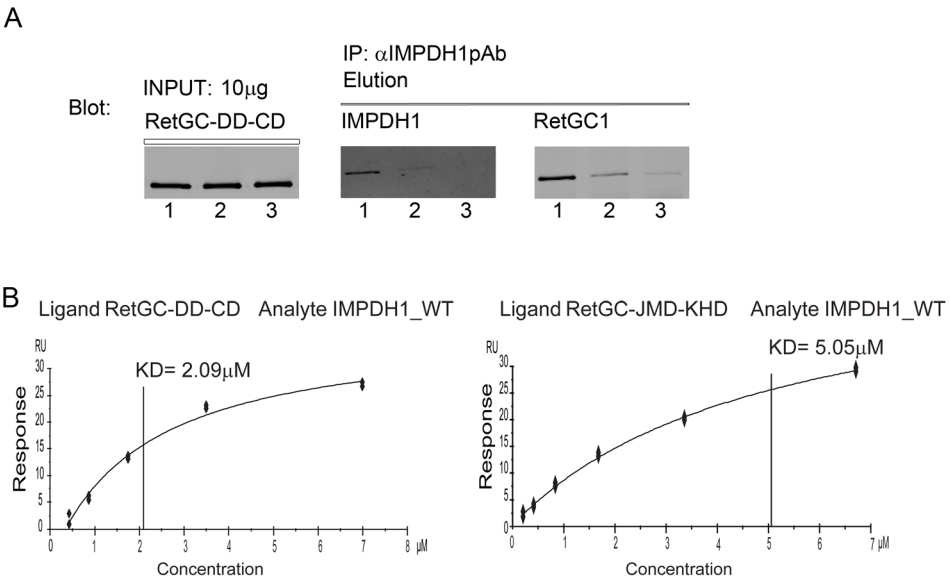

Figure IV.7. IMPDH1 and RetGC1 show a direct interaction with micromolar affinity. A. Decreasing amounts of recombinant Thr-IMPDH1 (10, 1 and 0.1μg) were mixed with a fixed amount of recombinant MBP-RetGC1-DD/CD (10μg, Input), and IMPDH1 in each sample was immunoprecipitated to completion with an excess amount of anti-IMPDH1 pAb- protein G-beads (Elution, IMPDH1 immunoblot). The level of RetGC1 co-immunoprecipitation (Elution, RetGC1 immunoblot) was determined by the level of IMPDH1 in the sample, which rules out unspecific binding of RetGC1 to the beads. B. Surface Plasmon Resonance (SPR) analysis of the interaction affinity. The RetGC1-DD/CD or RetGC1-JMD/JHD fragments of the cyclase were used as ligands covalently attached to the

sensor chip; and the Trx-IMPDH1 protein was passed in the mobile phase as an analyte at 2-fold serial dilutions from a 6.71µM stock solution. The affinity of the interaction was determined from measurement of steady-state binding levels as a function of analyte concentration, from multi-cycle experiments performed with duplicates. For analysis of the steady-state binding data, a model of 1:1 binding was assumed (4-parameter fitting, T200 Biacore analysis software), and the chi-square value defining the closeness of the fit (describing the deviation between the experimental and fitted curves) was 1.57 RU2 for RetGC1-DD/CD (Rmax = 44.1 RU) and 0.167 RU2 for RetGC1-JMD/KHD (Rmax = 50.5 RU). Chi-square values are typically considered acceptable when they are less than 10% of the experimental maximal response.

4.2.5. An adRP10 mutation and a rare LCA mutation in IMPDH1 alter its interaction to RetGC1.

Mutations R224P and D226N in IMPDH1 have been associated to autosomal dominant retinitis pigmentosa (adRP), whereas mutations R105W and N198K have been linked to autosomal dominant rare Lebers Congenital Amaurosis (adLCA). The basis of the pathology associated to these mutations has not been established. To investigate whether these mutations affect IMPDH1 interaction with RetGC1, we expressed thioredoxin fusion forms of IMPDH1 canonical isoform and the individual mutants: R105W, N198K, R224P and D226N. Pull-down assays were performed by using a normalized amount of IMPDH1 protein (Figure IV.8. input), using whole bovine retinal homogenates solubilized in 1% dodecyl maltoside. The amount of RetGC1 bound by each mutant was expressed as a function of the RetGC1 bound by wildtype IMPDH1 (Figure IV.8. histogram). Values are the mean from three independent experiments, with error bars representing the standard error. The RP10 mutation R224P substantially impaired binding of RetGC1 to IMPDH1, that occurred only to 42% of RetGC1 binding to wildtype IMPDH1. In contrast, LCA mutation N198K enhanced the interaction, promoting RetGC1 binding to a 1.57-fold higher extent than normal. Mutations R105W and D226N did not show statistically significant changes in RetGC1 binding when compared to wildtype IMPDH1.

Taken together, these results show that adRP10 mutation R224P substantially diminished IMPDH1 interaction to RetGC1, whereas adLCA mutation N198K significantly enhanced it, emphasizing the physiological relevance of this interaction.

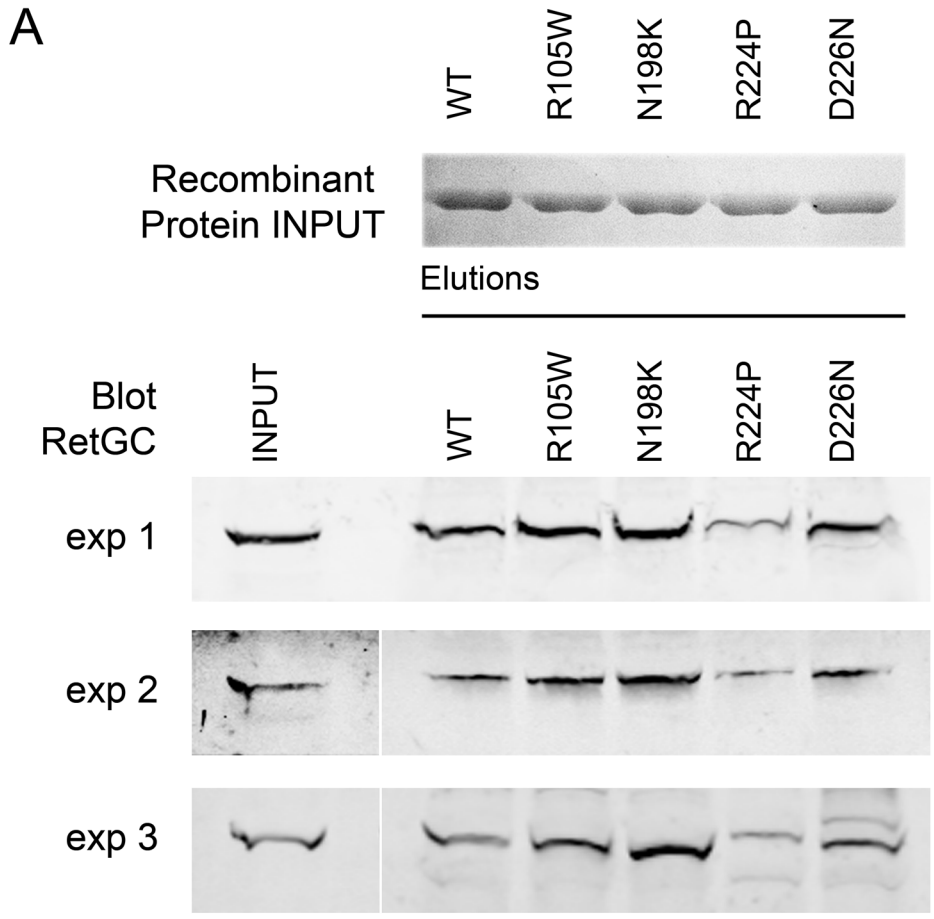
A
WT
R105W
N198K
R224P
D226N
Recombinant Protein INPUT
Elutions
Blot RetGC
INPUT
WT
R105W
N198K
R224P
D226N
exp 1
exp 2
exp 3

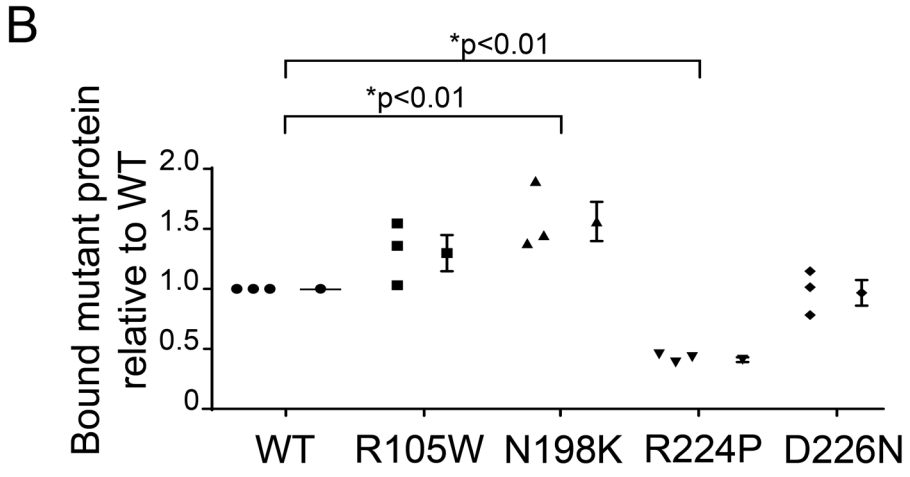
B
*p<0.01
*p<0.01
Bound mutant protein relative to WT
2.0
1.5
1.0
0.5
0
WT
R105W
N198K
R224P
D226N

Figure IV.8. Effect of IMPDH1 mutations associated to adRP10 and LCA in IMPDH1-RetGC1 interaction. A. IMPDH1 mutants associated to adLCA (R105W and N198K); and adRP10 (R224P and D226N) were expressed and purified as thioredoxin fusion recombinant proteins, and used in pull-down assays from solubilized bovine retinas. Aliquots of IMPDH1-immobilized resin corresponding to an identical amount of coupled IMPDH1 in each sample (wildtype and R105W, N198K, R224P, and D226N individual mutants, -recombinant protein input panel-) were used as baits. The level of RetGC1 pulled-down by each mutant from a bovine retinal extract is shown in the lower -elution- panel. B. The amount of RetGC1 bound by each mutant was calculated by densitometry of the corresponding RetGC1 bands, and expressed for each mutant as a function of the RetGC1 bound by wildtype IMPDH1 (lane WT). The dot plot shows measurements taken from three independent experiments. Statistical analysis was done with one-way ANOVA, and Dunnett's test to multiple comparisons (α=0.05; p<0.01). Mean±SE; WT (●) 1±0; R105W (■) 1.312±0.15; N198K (▲) 1.576±0.16; R224P (▼) 0.42±0.02; D226N (◆) 0.98±0.11.

4.3. Discussion

In this study we report the identification of new binding partners of Guanylate Cyclase Activating Protein 1 (GCAP1) in the retina that led to the unexpected discovery of a direct interaction between IMPDH1 and RetGC1. Inosine monophosphate dehydrogenase 1 (IMPDH1) is the enzyme in the first and rate-limiting step in de novo synthesis of GTP. It is abundantly expressed in the retina, and mutations in the impdh1 gene have been associated to autosomal dominant Retinitis Pigmentosa (adRP) and Leber Congenital Amaurosis (adLCA), (Bowne et al., 2006b, 2002; Kennan et al., 2002). Retinal guanylate cyclase 1 (RetGC1) is responsible for cGMP synthesis in rods and cones. Mutations in the GUCY2D gene encoding RetGC1 have been linked to arLCA and autosomal dominant cone rod dystrophy (adCORD), (Boye, 2015; Dizhoor, 2000; Hamel, 2007; Hunt et al., 2010). Therefore the RetGC1-IMPDH1 interaction reveals a link between cGMP synthesis and de novo GTP supply in photoreceptor cells. This opens a new scenario for the interpretation of the pathophysiology of blindness-causative mutations in IMPDH1 and RetGC1, and it draws attention to the enzymes involved in guanine nucleotide biosynthesis as putative blindness-associated or modifier genes for future genetic studies.

Identified GCAP1 binding partners important for photoreceptor cell physiology. IMPDH1 was one of the proteins identified in a search for novel interactors of the calcium sensor GCAP1, a protein that binds to RetGC1 to confer it Ca2+-sensitivity. Parallel pull-down assays were performed with GCAP1 in its Ca2+-free or Ca2+-bound forms from bov ROS, and identified proteins were

analyzed by a label-free quantitative approach. The goal was to identify proteins with preferential affinity for one of GCAP1 conformational states, on the basis of discerning putative binding targets from the background. This pursued discrimination was particularly successful for proteins showing a fold-change$_{Ca2+/EGTA}$ >3 (Table IV.1).

Among the GCAP1 putative binding partners we identified four of the eight subunits of the Chaperonin Containing TCP-1 complex (CCT complex). This complex is necessary for the folding of several key signaling and structural proteins in rod outer segment formation, according to the analysis of a mouse model with suppressed CCT activity (Posokhova et al., 2011). While GCAP1 or RetGC1 were not identified among the folding substrates in these mice, our data would call for a revision of RetGC1 and GCAP1 specific alterations in this mouse model, as we predict that they are CCT substrates.

Intriguingly, we also found five proteins associated to Bardet-Biedl Syndrome (BBS), a syndromic retinopathy affecting 1/100.000 individuals that curses with deafness, obesity and diabetes (Sheffield, 2010). Enrichment of the BBSome and LZTFL1 proteins in our GCAP1 pull-down assay may be explained by the reported association of the BBSome to the CCT complex (Posokhova et al., 2011). Alternatively, it may point to the BBSome involvement in RetGC1/GCAP1 trafficking to the cilium. In this respect, it will be worth to assess whether there are specific alterations in the levels of RetGC1 and GCAP1 at the rod outer segment compartment of available knockout models in BBSome components (Zhang et al., 2013), and the Lztfl1 knockout mice (Jiang et al., 2016).

Table I also included signaling proteins that were likely identified because they are co-transported with the RetGC1/GCAPs complex by vesicular trafficking to the cilium. This is the case for PDE6C (cone PDE6 alpha), that fails to reach the cone outer segment compartment in RetGC1/RetGC2 double knockout mice (Baehr et al., 2007). Other proteins that fail to distribute to the outer segment in the absence of functional RetGC1 and RetGC2 in photoreceptors are rod PDE6 and cone transducin (Baehr et al., 2007). Different subunits of PDE6 and rod transducin were identified in our pull-down assay with a high number of spectra (Table IV.2), but did not meet the criteria to be included in Table IV.1 because their fold-change$_{Ca2+/EGTA}$ did not reach our arbitrary threshold. Since RetGC1 itself did not meet Table I criteria (Table IV.2), it is likely that Table IV.2 contains many bonafide interactors of free GCAP1 or the RetGC1/GCAP1 complex, that will be further investigated in future studies. We focused this study on demonstrating uncontrovertibly the association of IMPDH1 with the RetGC1/GCAP1 complex, to infer putative functional implications in the pathophysiology of blindness.

Characteristics of IMPDH1 direct interaction with RetGC1. IMPDH1 was identified robustly and specifically in the GCAP1 pull-down assay performed on bov

ROS (Figure IV.1). IMPDH1 was not identified in GCAP1 pull-down assays performed on whole bovine retinal homogenates that resulted in similar overall sample depth at LC-MS/MS protein identification (data not shown). Subsequently we showed that recombinant IMPDH1 (bovine canonical isoform) efficiently pulled-down RetGC1 from bovine rod outer segment samples (Figure IV.2), demonstrating that IMPDH1 association was to the RetGC1/GCAP1 complex, rather than -or in addition to- free GCAP1. Furthermore, we showed that IMPDH1 co-migrated almost entirely with RetGC1 during size-exclusion chromatography fractionation of bov ROS, at a fraction that also contained HSP90α another protein identified in table I (Figure IV.2). Co-migration of HSP90α with RetGC1 was consistent with HSP90α binding to recombinant RetGC1 DD-CD domains in pull-down assays from bovine retinas (Figure IV.6). These results point to HSP90 association to RetGC1. This chaperone has been involved in the stabilization or assembly of other multi-enzyme signaling protein complexes, including the "purinosome" involved in de novo GTP biosynthesis (French et al., 2013). Therefore, HSP90 may be an important auxiliary chaperone in the assembly or organization of the RetGC1/GCAP1 heterotetramers in higher order multi-enzyme complexes.

We here demonstrate that IMPDH1 association to the RetGC1/GCAP1 complex is through a direct interaction with RetGC1, that involves the dimerization and catalytic domains of RetGC1. The dissociation constant of this interaction was determined to be in the micromolar range by surface plasmon resonance (SPR) (Figure IV.7), which is within the physiological range for protein-protein interactions. The region of RetGC1 that contributed most to the interaction comprised the dimerization and catalytic domains, at the C-terminus (DD/CD/COOH region), Figure IV.6. So, IMPDH1 interaction with RetGC1 primarily involved a region of RetGC1 different from the region reported for GCAP1 interaction (JMD-KHD) (I. V. Peshenko et al., 2015; I. V Peshenko et al., 2015), which our pull-down assays faithfully reproduced (Figure IV.6). Dimerization of RetGC1 is likely required for IMPDH1 interaction, because removing the DD domain substantially reduced IMPDH1 binding (Figure IV.6). Other proteins that associate to this complex, like CKB, HSP90α and Trα, followed the same trend (Figure IV.6). The higher contribution of the DD/CD region than the JMD/KHD region to IMPDH1 interaction was also reflected in the SPR experiments, that yielded dissociation constants of K_D = 2.09μM for RetGC1-DD/CD and K_D = 5.05μM for RetGC-JMD/KHD. We would have expected a bigger difference between the K_D values based on the 8-fold higher amount of IMPDH1 binding to the DD/CD than the JMD/KHD region in pull-down assays (Figure IV.6.C). However, pull-down assays were performed on native tissue (whole retinal homogenates) where enzymatic steps (e.g. phosphorylation) or auxiliary proteins (e.g. GCAP1, RD3, HSP90) may influence the interaction. Given that it is ultimately the

quaternary structure of RetGC1 that configures the mapping interface, all cytosolic RetGC1 domains may contribute to it to different extents.

Subcellular localization of the IMPDH1-RetGC1 interaction. Previous immunolocalization studies of IMPDH1 in murine retinal sections reported IMPDH1 localization primarily at photoreceptor inner segment and outer plexiform layers (Bowne et al., 2006a; Tam et al., 2008) by using an antibody to canonical IMPDH1 C-terminus. Our immunolocalization studies, performed on bovine retinal sections with an affinity purified anti-IMPDH1 pAb raised against the whole bovine canonical isoform (see methods) were basically consistent with these reports. In bovine retinal sections we also observed that IMPDH1 was predominant at the inner segment and outer plexiform layers (Figure IV.3), being much more abundant at rods than at cones at the inner segment layer, but equally enriched at rod and cone synaptic terminals (Figure IV.3). Nevertheless, we could now make use of more advanced confocal microscope configurations that substantially increase sensitivity to gain more insight into subcellular detail. We here report that IMPDH1 is enriched at the connecting cilium of both rods and cones (Figure IV.4) and at microvilli of Muller cells (Figure IV.3M). More importantly, we also show that IMPDH1 is also present at the rod outer segment compartment, where its signal is much weaker than at inner segments but noticeable; and where it partially co-localizes with RetGC1 (Figure IV.4, Figure IV.5). We also observed strong co-localization at the connecting cilium of rods and cones (Figure IV.4). These findings are in accordance with the identification of IMPDH1 in the proteome of the bovine rod outer segment compartment (Kwok et al., 2008), and consistent with our identification of IMPDH1 as a GCAP1 interactor in a pull-down assay performed on bov ROS (Figure IV.1, Table IV.1).

Physiological implications of IMPDH1-RetGC1 interaction: an emerging protein network with relevance in the pathophysiology of blindness.

IMPDH1 is the enzyme in the first and rate-limiting step in de novo synthesis of GTP from IMP, by converting inosine monophosphate (IMP) to xanthosine monophosphate (XMP) (Figure IV.9). XMP is further converted to GMP, GDP and GTP by Guanosine 5′-monophosphate synthase (GMPS), Guanylate Kinase (GK) and Nucleoside-diphosphate kinase (NDK), Figure IV.9. However, the precise contribution of de novo synthesis of GTP to overall GTP supply is not clear, since GTP can also be produced by the salvage pathway via the conversion of free purine bases (guanine, hypoxanthine) to their corresponding nucleotides by phosphoribosylation by the enzyme hypoxanthine-guanine phosphoribosyl transferase (HGPRT), Figure IV.9. It is not known how much each pathway contributes to GTP supply. In dividing cells the salvage pathway sustains normal growth, but it is the regulation imposed on de novo synthesis that has a great effect upon growth rate during malignant transformation (Zhao et al., 2013). In

photoreceptor cells of the retina the individual contributions have not been characterized in detail, but it has been proposed that de novo GTP synthesis is responsible for the bulk of GTP supply, based on the strong expression of IMPDH1 compared to HGPRT at the transcript level (Aherne et al., 2004). IMPDH1 (IMPDH2 isoform is not detected in the retina (Aherne et al., 2004)), is therefore a relevant enzyme because the retina is one of the most energy-consuming tissues of the body, and photoreceptor cells have a high requirement for GTP in the visual transduction cycle (Burns and Arshavsky, 2005; Pugh and Lamb, 1990; Wensel, 2008). Impdh1-/- mice display a slowly progressive form of retinal degeneration, in which visual function becomes gradually compromised. Interestingly, a progressive reduction in the a- and b-wave amplitudes of scotopic electroretinogram responses precedes by several months any noticeable photoreceptor cell loss, which likely indicates a disturbance in cGMP biosynthesis by progressive GTP depletion (Aherne et al., 2004). This IMPDH1 loss-of-function phenotype is consistent with de novo GTP synthesis being required for GTP conversion to cGMP (Figure IV.9); but the retinopathy is too mild to explain the much more severe phenotype in adRP10 patients (Aherne et al., 2004). Properties of IMPDH1 mutations other than their effect on enzymatic activity have been invoked to explain the human disorder (see below).

What is the physiological significance of IMPDH1-RetGC1 interaction? We propose that the interaction implies an integration of guanine nucleotide metabolic pathways (Figure IV.9), based on a number of indications. First, in the GCAP1 pull-down assay we also identified guanylate kinase (GK) and the bifunctional enzyme AICAR transformylase/IMP cyclohydrolase (ATIC gene, PURH protein), Table IV.1. GK catalyzes the third step in GTP synthesis from IMP, whereas PURH catalyzes the ninth and tenth steps in de novo purine synthesis (last two arrowheads in the pathway from PRPP (Phosphoribosyl pyrophosphate) to IMP), Figure IV.9. Interestingly, a case of an infant with severe neurological defects and congenital blindness has been reported to be caused by a mutation in the ATIC gene (Marie et al., 2004). Second, descriptions of dynamic, reversible formation of multi-enzyme complexes in nucleotide metabolism are emerging, that portray the channeling of nucleotide flux under integrated control (Havugimana et al., 2012; Zhao et al., 2015). It is tempting to speculate that the complex responsible for cGMP synthesis in photoreceptor cells might associate to other multi-protein complexes in higher order assemblies, for an integrated regulation of guanine nucleotide supply depending on the light and nutritional state of the cell. Third, we do not contemplate that IMPDH1 interaction with RetGC1 responds to a ciliary co-transport requirement, because IMPDH1 expression levels or localization are not affected in the rd3 mice, deficient in RetGC1 ciliary transport (data not shown). Overall, we believe that the IMPDH1-RetGC1 interaction reflects an interplay between cGMP synthesis and GTP supply (Figure IV.9). Further studies based on the electrophysiological analysis of the effect

of IMPDH inhibitors on rod responses to light will be necessary to prove this interpretation.

What are the implications for the pathophysiology of inherited retinal dystrophies? Since the first reports of IMPDH1 mutations causing adRP10, it was proposed that IMPDH1 should have a distinctive function or property in the retina, to explain the retina-specific phenotype of a protein that is ubiquitously expressed (Bowne et al., 2002; Kennan et al., 2002). IMPDH1 expression level is much higher in the retina than other tissues, and unique retinal isoforms are predominant, that result from alternative splicing and alternate start sites of translation (Bowne et al., 2006a). The adRP-associated mutations Arg224Pro and Asp226Asn do not reduce catalytic activity (Aherne et al., 2004; Mortimer and Hedstrom, 2005). Both mutations are located in the second cystathione beta synthase (CBS) domain of IMPDH1, whose function is not clear yet. It has been reported that the IMPDH1 CBS domain binds to single-stranded nucleic acids, and that this binding capacity is diminished by adRP10 IMPDH1 mutations. However, the particular aspect of RNA metabolism that could be influenced by IMPDH1 or its physiological effect have not been described (McLean et al., 2004; Mortimer and Hedstrom, 2005; Xu et al., 2008). More convincing, given the dominant-negative effect of IMPDH1 mutations on the adRP10 phenotype, is the proposal that IMPDH1 pathology may rely on the observed IMPDH1 tendency to aggregate (Aherne et al., 2004; Tam et al., 2010, 2008; Wang et al., 2011). We here show that the CBS domain is not required for IMPDH1 binding to RetGC1, but that it likely modulates the interaction, as the IMPDH1ΔCBS mutant showed significantly enhanced binding to RetGC1 (Figure IV.6). Our results also show that R224P substantially decreases binding, while N198K significantly enhances binding to RetGC1 (Figure IV.8). Collectively, we show that IMPDH1 mutations associated to adRP10 and adLCA alter IMPDH1 binding to retGC1. This implies that mutations in IMPDH1 with an autosomal dominant pattern of inheritance may cause the pathophysiology by interfering with RetGC1 localization or function. An even more relevant implication of a functional coupling of IMPDH1 and RetGC1 (that is, between de novo GTP synthesis and GTP conversion to cGMP) is the fact that specific inhibitors of IMPDH could be tested to treat the inherited retinal dystrophies: associated to mutations that lead to constitutive guanylate cyclase activity (mutations in GUCY2D encoding RetGC1 associated to adCD (Hunt et al., 2010); and mutations in GUCA1A encoding GCAP1 (Olshevskaya et al., 2004; Payne et al., 1998)) or functional impairment of cGMP-PDE (mutations in the different PDE subunits or in AIPL1 (Dvir et al., 2010; Huang et al., 1995; Kohl et al., 2012; McLaughlin et al., 1993; Ramamurthy et al., 2004; Thiadens et al., 2009)).

Collectively, we show compelling evidence of a direct interaction between RetGC1 and IMPDH1 at the rod outer segment compartment where phototransduction takes place, that is altered by mutations in IMPDH1 that cause

adRP or adLCA. This unanticipated connection between multienzyme complexes in nucleotide metabolism may serve to allow an integrated spatial modulation of purine synthesis according to the dark/light physiology requirements in these specialized cells. By bringing together inherited retinal dystrophy-causative genes so far considered unrelated, this finding opens a new conceptual framework to study the pathophysiology of these disorders.

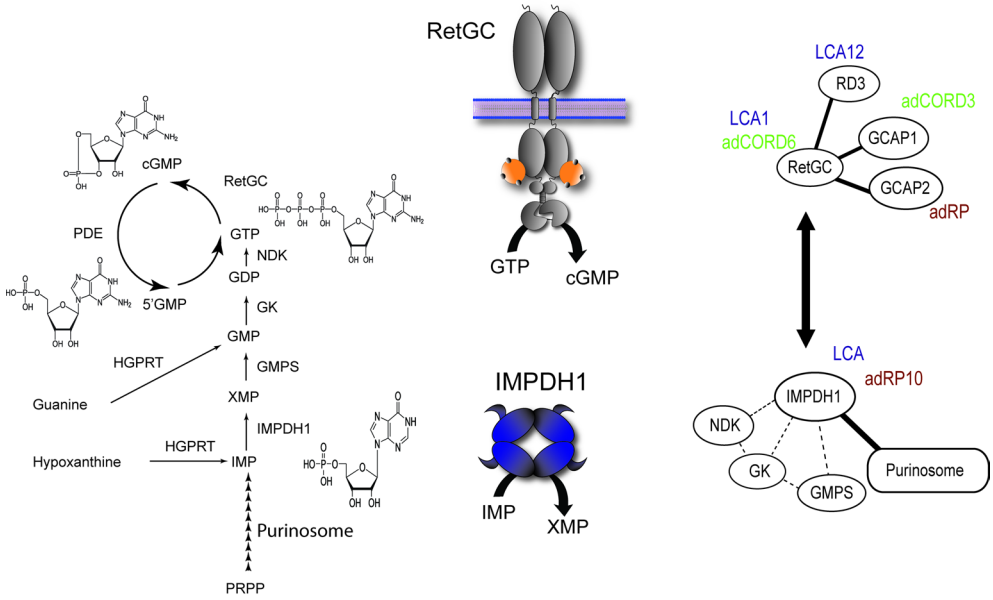

Figure IV.9. *RetGC1-IMPDH1 interaction points to an interplay between de novo synthesis of GTP and its conversion to cGMP that bridges blindness causative genes. RetGC1 and IMPDH1 are enzymes involved in guanine nucleotide metabolism, at different levels. IMPDH1 is involved in de novo synthesis of GTP (vertical pathway, each arrow representing an enzymatic activity), by catalyzing the production of XMP from IMP (the enzyme works in tetramers, in blue at inset). RetGC1 is an enzyme involved in cGMP turnover (cycle), being responsible for the synthesis of cGMP from GTP. RetGC1 is a membrane polypeptide that works in dimers (in grey at inset) in a Ca2+ regulated manner through the guanylate cyclase activating proteins (GCAPs, orange). GTP can also be produced by the salvage pathway (by HGPRT: hypoxanthine/guanine phosphorybosyl transferase), from guanine or hypoxanthine. The direct interaction between RetGC1 and IMPDH1 revealed in this study is shown by the thick arrow in the protein network at right, and reveals an interplay between the protein complexes responsible for de novo synthesis of GTP and for GTP conversion to cGMP, that functionally links distinct forms of inherited retinal blindness. Continuous lines linking circled proteins represent direct interactions that are well-established in the literature, while dashed lines represent expected functional associations. The implications of this new scenario are that a mutation at the level of IMPDH1 could putatively affect RetGC1 function, or vice versa. In addition, genes encoding other proteins in guanine metabolism might need to be considered as putative candidate blindness-causative or modifier genes. LCA, Leber Congenital Amaurosis; adRP, autosomal dominant retinitis pigmentosa; adCORD, autosomal dominant cone rod dystrophy.*

Chapter V: Localization of Brain-type Creatine Kinase in bovine retina

Chapter V: Characterization of RetGC1 association to Creatine Kinase-B in photoreceptor cells.

Contributions

We acknowledge the help of Sergi Tosal in the immunolocalization studies of Creatine kinase B, as well as the Proximity ligation assays on retinal sections. For Surface Plasmon Resonance studies, RetGC1 fusion proteins were purified by Anna Plana, and experiments were performance with the technical assistance of Dr. Marta Taulés at the molecular interaction analysis facility of CCiTUB..

My contribution to this Chapter was training and guiding Sergi Tosal with the immunolocalization analysis, as well as obtaining the frozen blocks of bovine retinas for analysis. I did the image acquisition and analysis. I did the biochemical characterization of the RetGC1- CK-B interaction.

Chapter V: Characterization of RetGC1 association to Creatine Kinase-B in photoreceptor cells.

5.1. Rationale

Among the 37 proteins identified in our GCAP1 pull-down assay with a fold-change$_{Ca2+/EGTA}$ > 3 (scatter plot in Figure IV.1, Chapter 4), was creatine kinase B (brain type). Creatine kinase B (CKB) was identified with 19 peptides (114 spectra) in the Ca2+-condition, and only one spectra in the EGTA condition (Table IV.1, Chapter 4). That is, it was one of the most abundant proteins among the proteins that bound to Ca2+-GCAP1. Creatine kinase B was not identified in the negative control pull-down assay with Ran, which indicates that creatine kinase B association to Ca2+-GCAP1 was also specific. Furthermore, CK-B has been found to associate to the DD-CD-C-terminus region of RetGC1, in pull-down assays performed with different regions of the RetGC1 cytosolic region (Figure IV.5, Chapter 4). That is, our proteomic results point to an association of CK-B to the RetGC/GCAPs complex. Creatine kinase (CK) catalyzes the reversible transphosphorylation from ATP to creatine (Cr) to yield phosphocreatine (PCr). The action of CK contributes to maintain the cellular energy homeostasis by guaranteeing stable and locally buffered ATP/ADP ratios (Andres et al., 2008; Wallimann et al., 1998), by generating an intracellular pool of PCr which represents a temporal energy buffer that prevents a fall on ATP levels in high cell energy requirements scenarios. Cytosolic and mitochondrial CK are specifically localized in those focus of high ATP consumption of the cell, like ATPases of different ions pumps, myosin ATPase of contractile muscle apparatus, or the calcium pumps in the sarcoplasmic reticulum. In that respect, the synthesis of cGMP by the RetGC/GCAPs complex is known to require ATP, in addition to the GTP substrate. The reason for this ATP requirement for RetGC1 catalytic activity is currently not understood, despite the fact that ATP has to be added to extracts when assaying retinal guanylyl cyclase activity in reconstituted systems.

To address whether there was a functional association between RetGC1 and CK-B at photoreceptor outer segments, as the robust proteomic data is indicating, we analyzed CK-B co-localization with GCAP1, as well as with RetGC1 and GCAP2, in bovine retinal sections. We also performed Proximity Ligation Assay, to determine whether at any particular cell compartment these proteins localize at a proximity of 40nm or less, which would be indicative of a putative interaction. Finally, we analyzed whether CK-B interacted directly with RetGC1 and we measured the affinity of the interaction by monitoring direct binding of RetGC1 and CK-B recombinant proteins.

5.2 Localization of CKB in bovine retinas

In order to characterize the precise localization of CKB in bovine retinas, bovine retinal cryosections were stained with different monoclonal and polyclonal antibodies against human CKB. A collection of antibodies against CKB was generously provided by Drs. Theo Wallimann (ETH Zurich) and Uwe Slachttner (University of Grenoble). Our results indicate that CKB is more abundantly expressed in cones than in rods (Figure 1.B), where it is enriched at the inner segment compartment and at the synaptic terminal (Figure V.1. B, E and H), but also clearly present at the cone outer segment compartment (Figure V.1 E). An identical pattern of CK-B staining was obtained with antibodies addressed to the C-terminal part of the protein (rabbit monoclonal EPR3927, GeneTex), or to the N-terminal part (mouse monoclonal 21E10, Sistermans et al. 1995). CK-B showed an almost complete co-localization with GCAP1 at all cellular compartments (Figure V.1 C, F, I), which would be consistent with a functional association of these proteins. Consistently, the proximity ligation assay performed with these same two antibodies to GCAP1 and CK-B, revealed that both proteins localize at a proximity of 40nm or less at the inner and outer segment of cones (Figure V.1.J-L). Surprisingly, a positive signal was also obtained at rod outer segments, which indicates that the proximity ligation assay amplification is more sensitive than regular indirect fluorescence detection (Figure V.1.J and L).

CK-B appears to be much more abundant at cones than at rods. When a co-immunolocalization study was carried between CK-B and GCAP2, CK-B highlighted cones while GCAP2 highlighted preferentially rods, therefore giving rise to a mutually exclusive staining pattern (Figure V.2).

Collectively, our results point to CK-B associating to either free GCAP1 or to the RetGC1/GCAP1 complex in cones. To address whether CK-B associated to RetGC1/GCAP1 complex in cones, we performed RetGC1 and CK-B co-immunostaining studies. These studies revealed that RetGC1 and CK-B co-localize at cone outer segments (Figure V.3, D, E and F). Furthermore, RetGC1 and CK-B yielded a positive PLA signal at cone outer segments (Figure V.3, H and K).

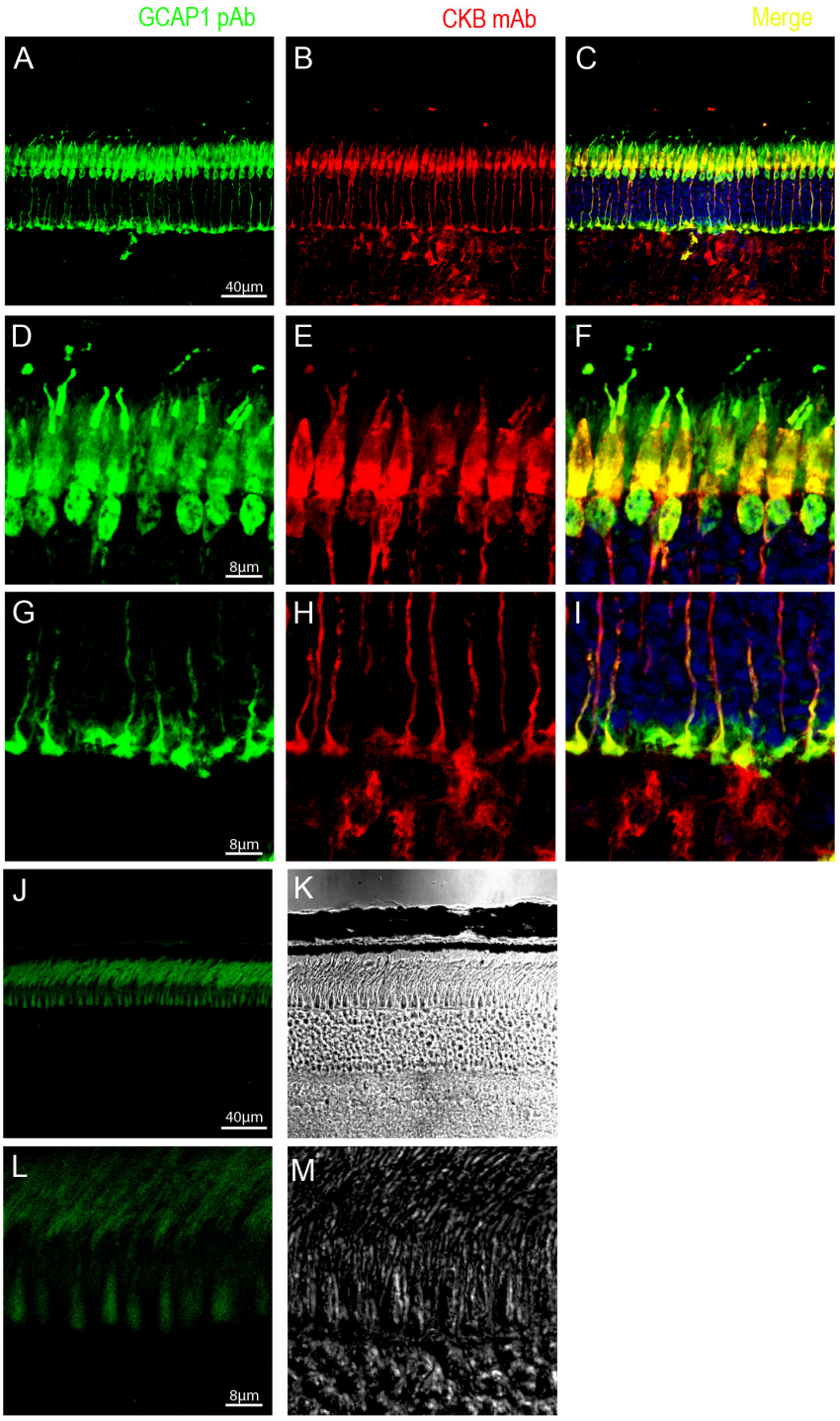
GCAP1 pAb
CKB mAb
Merge
A
B
C
40µm
D
E
F
8µm
G
H
I
8µm
J
K
40µm
L
M
8µm

Figure V.*1. Co-immunostaining of CK-B and GCAP1 in bovine retinal sections, and Proximity ligation assay. GCAP1 immunostaining by indirect immunofluorescence (green signal, panels A, D, G); and CK-B immunostaining by indirect immunofluorescence (red signal in B, E and H) show co-localization of GCAP1 and CK-B at outer segments , inner segments (D, E, F) and at synaptic terminals (G, H and I). The proximity ligation assay produced a positive signal at the inner and outer segments of cones, indicating that both protein are closer than 40nm in these compartments (J and L).*

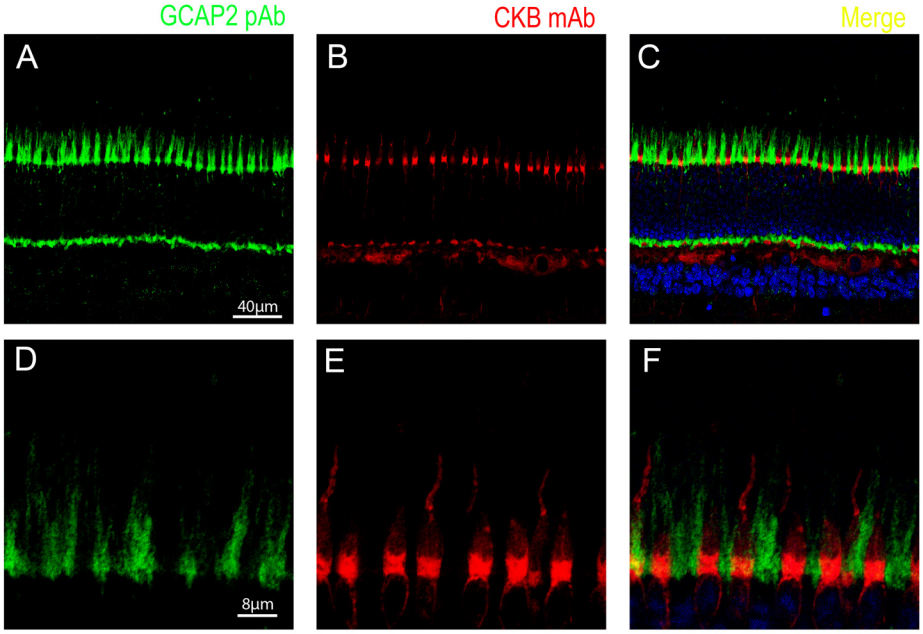

Figure V.2. Co-immunostaining of CKB with GCAP2. CKB indirect immunostaining (red signal in B and E), and GCAP2 indirect immunofluorescence (in green in A and D) shows that GCAP2 is much more abundant in rods than cones, whereas CK-B is predominant in cones. Therefore, a mutually exclusive pattern of localization is apparent (C and F).

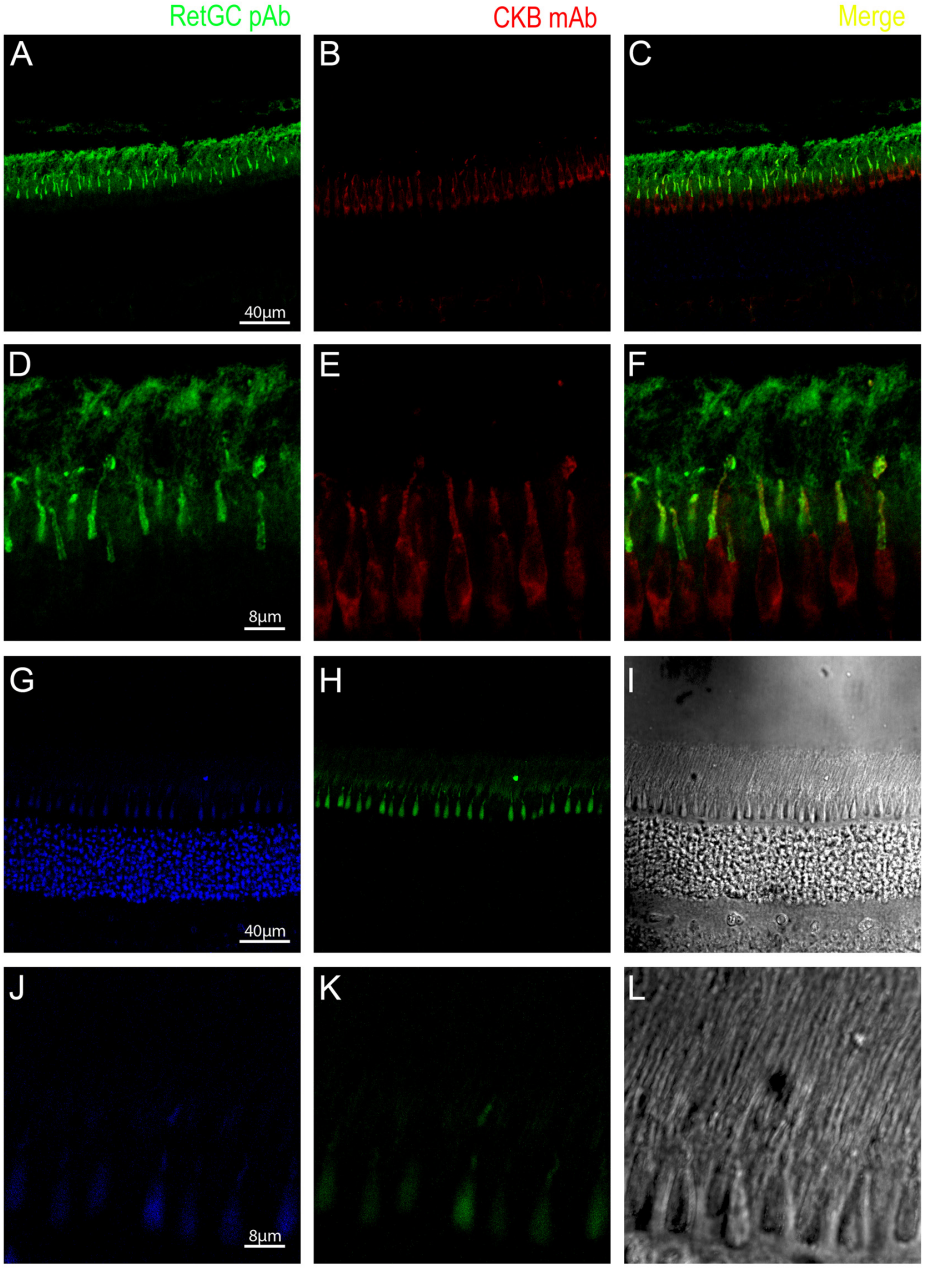

Figure V.3. Co-localization of CKB with RetGC and Proximity ligation assay. Indirect immunofluorescence of CKB (red signal in B and E), and indirect immunostaining of RetGC (in green in A and D) reveal colocalization of both proteins at the outer segment of cones.. A Proximity ligation assay positive signal is appreciated at cone inner and outer segments (H and K).

5.3. Monitoring recombinant RetGC1 and CK-B binding by Surface Plasmon Resonance (SPR).

Pull-down assays with different fragments of RetGC1 had already indicated an association of CK-B to the DD-CD-C-terminus part of RetGC1 cytosolic region (Chapter 4. Figure IV.6). In order to study whether this interaction is direct, and to measure its affinity, we performed steady-state binding measurements with a fixed concentration of RetGC (MBP-DD/CD/C-term) and a range of concentrations of CK-B.

RetGC and CKB presented a fast dynamic interaction with a Kd of 29,3 µM (Figure V.5).

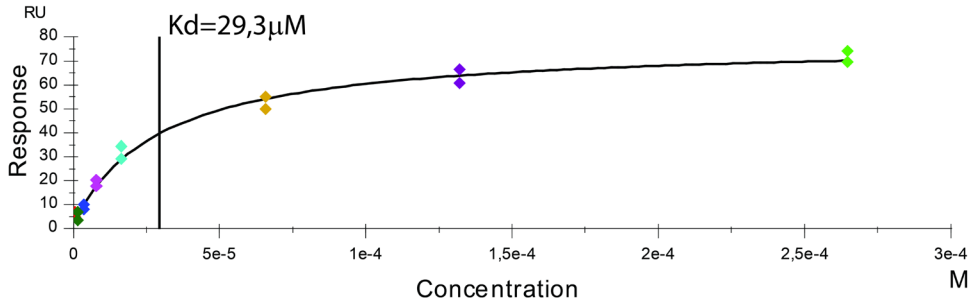

Figure V.5. CKB and RetGC1 show a direct interaction with micromolar affinity. Surface Plasmon Resonance (SPR) analysis of the interaction affinity. The RetGC1-DD/CD fragment of the cyclase were used as ligand covalently attached to the sensor chip; and the CKB protein was passed in the mobile phase as an analyte at 2-fold serial dilutions from a 264.8µM stock solution. The affinity of the interaction was determined from measurement of steady-state binding levels as a function of analyte concentration, from multi-cycle experiments performed with duplicates. For analysis of the steady-state binding data, a model of 1:1 binding was assumed (4-parameter fitting, T200 Biacore analysis software), and the chi-square value defining the closeness of the fit (describing the deviation between the experimental and fitted curves) was 8.68 RU^2 (R_{max} = 76.26 RU). Chi-square values are typically considered acceptable when they are less than 10% of the experimental maximal response.

This result indicates that CK-B establishes a direct interaction with RetGC1, in the micromolar range, which is in the physiological range of protein-protein interactions that could have physiological relevance. This result is consistent with previous pull-down assay results, with our GCAP1 pull-down assay and with the co-localization of these three proteins at cone outer segments. Collectively, our results

point to a role of CK-B at providing local ATP in the environment of the cyclase. However, the physiological relevance of this finding, and why this phenomenon appears to be much more relevant for cones than for rods is not clear yet, and awaits further investigation.

5.4. Discussion

Rods and cones must respond to a high range of light intensities. In darkness, both rods and cone have a similar darkness current, by what they have a similar ATP consumption, however their responses in light are different (Nikonov et al., 2006). Rods have higher light sensitivity than cones, responding to a very low light intensities but they are saturated at low light intensities.

On the other hand, cones present a higher dynamic range than rods, with a lower light sensitivity but a faster kinetic response and over a higher range of light intensity. In this way, energy requirements of cones are higher than rods. Therefore, cones may need a fast energetic system to maintain the energy requirements of the cell. CKB could supply the ATP needed for cones phototransduction, as coefficient diffusion of PCr is higher than ATP (Hubley et al., 1995), and maintain a high concentration of ATP locally.

Taken together, CKB could provide a fast energy supply in cones because of its higher energetic requirements than rods.

On basis of our results of Chapter IV and data collected from Surface plasmon resonance data (Figure V.5), CKB has been demonstrated to interact directly with RetGC, may supply the ATP required in maintaining the cGMP levels. In cones, the current through cGMP-gated channels never falls further of half of darkness even in bright light (Okawa et al., 2008), so cGMP levels must be maintained high.

Global discussion and future perspectives

Global discussion and future perspectives.

The overall goal of this study was to advance the knowledge of how the protein complex responsible for cGMP synthesis in rods and cones, the RetGC/GCAPs complex, is assembled, transported to rod outer segments, organized and regulated *in vivo*. Because cGMP is the second messenger in the light response, this protein complex plays a key role in the physiology of photoreceptors. Despite its extensive characterization *in vitro* by biochemical and structural studies, fundamental questions remain open on the function of this protein complex *in vivo*, in the context of the living cell: - How is the complex assembled? – How is the complex transported from the inner to the outer segment compartment where phototransduction takes place? – What confers this protein complex "ciliary destination" rather than "synapse fate", during vesicular polarized trafficking? – Is this protein complex anchored at rod outer segment disc membranes? – How is it organized, how does it fit in with other signaling complexes in the light response, to guarantee the rapid kinetics of the light response?

This study aimed at setting the ground to address some of these questions. We wanted to sustain this study on two main methodologies: i) proteomics and protein biochemistry, to identify new protein interactors of the complex that would give us clues as to its organization *in vivo*; and ii) genetics, to test the functional significance of identified interactions.

Because of the complexity of the visual system, and the extremely high compartmentalization of retinal photoreceptor cells, the use of cells in culture or reconstituted systems is of limited use. Because of our interest in doing the studies in living animals, we first put our effort into implementing mouse genetic techniques to transfect photoreceptor cells that by-passed conventional transgenic strategies. We focused on *in vivo* DNA electroporation. We set to implement the methodology developed by Connie Cepko at Harvard for *in vivo* DNA electroporation in the retina, and particularly in rod photoreceptors (Matsuda and Cepko, 2004). During the course of this study, we successfully implemented this methodology in the lab (Appendix I. Figure I).

This methodology was very useful to study how mutation in the GCAP proteins affected subcellular localization (chapter III). However, one limitation of this method is that it yields mosaic expression, and transfection levels are not enough to allow biochemical analysis of transfected tissue.

With the goal of exploiting the potential of *in vivo* DNA electroporation for the generation of stable transgenics, we tried to achieve the transfection of spermatogonial stem cells in mice, as described (Dhup and Majumdar, 2008). Conceptually, we thought it would be easier to transfect dividing stem cells than the highly differentiated neurons of the retina. However, after very extensive work at

developing injection and electroporation surgical procedures, and improving the transgene cassette design, we observed Sertoli and Leydig cell transfection, but not transfected spermatogonial or sperm cells. After optimizing the plasmid backbone, promoter and flanking DNA insulator sequences of the transgene expression cassette, the maximum transfection of sperm cells with a fluorescent reporter was determined to be 1.3% of cells analyzed by the cell sorter. This methodology was deemed unpractical (Figure II.10 and table II.8). One possible explanation for the failure of this technique may rely on the difficulty to modify the genome of stem or pluripotent cells. In this sense, it may be worth to try to modify the genome with the CRISPR/Cas9 system rather than trying to insert foreign DNA, in future studies.

By applying *in vivo* DNA electroporation after subretinal injection we were able to study the molecular determinants for GCAPs subcellular distribution (Chapter III). The most important conclusion of this study was its demonstration that GCAPs direct binding to RetGC1 is required for the GCAPs to distribute to the outer segment. This is in line with what was expected (Baehr et al., 2007; Karan et al., 2010; Peshenko et al., 2014), but it had not been demonstrated. In addition, we observed an effect of myristoylation in GCAP1 distribution. Myristoylation is also required for GCAP1 distribution to rod outer segments. This might be explained by the observation that myristoylated GCAP1 has a higher apparent affinity for the cyclase (so, unmyristoylated GCAP1 has a lower affinity for the cyclase); or it may imply an additional regulatory step in trafficking (Chapter III, Figure III.5). Future studies will be addressed at distinguishing these two alternatives.

On the other hand, GCAP2 subcellular distribution presents a more complex regulation because of its phosphorylation at the COOH-terminus (López-del Hoyo et al., 2014). About half the normal complement of GCAP2 is phosphorylated under standard light conditions in wildtype mice. Phosphorylation of GCAP2 at S201determines its binding to 14-3-3 and its sequestration at the inner segment. This appears to be a mechanism in place to regulate GCAP2 subcellular distribution (López-del Hoyo et al., 2014). However, when overly desregulated, like in the transgenic mouse model described in López-del Hoyo et al. 2014, that expresses a form of GCAP2 impaired to bind Ca2+, its massive phosphorylation and retention leads to a severe toxicity. By showing that the bG161R-GCAP2 is retained at the inner segment in a high fraction of transfected cells we are indicating that this pathway of toxicity is very likely to contribute to the pathophysiology of the hG157R-GCAP2 mutation linked to adRP in human patients.

In parallel to these genetic studies, we performed proteomic and biochemical analysis with the aim of identifying new protein interactors of the RetGC/GCAPs complex. We performed a comparative proteomic approach from a pull-down of bovine ROS preparations with GCAP1, either in Ca2+ or EGTA conditions. A rigorous label-free quantitative analysis, and a comparison of results with a negative control pull-down, allowed us to identify the “bonafide” putative candidates. Among

them, we first focused on inosine monophosphate dehydrogenase (IMPDH1), the rate limiting enzyme in *de novo* synthesis of GTP, as IMPDH1 is directly linked to inherited retinal dystrophies. The importance of this protein interaction was also highlighted by the fact that we identified two other proteins involved in de novo GTP synthesis (GUK1 and the product of the ATIC gene), Figure IV.1 and Table IV.1.

The question at stake was whether the *de novo* synthesis of GTP was linked to GTP conversion to cGMP in photoreceptor cells. To test that, we first showed that IMPDH1 associated not only to GCAP1 but also to RetGC1 in rod outer segment preparations, and that these proteins co-migrated by size-exclusion chromatography fractionation of ROS homogenates. We then established that the IMPDH1 interaction with RetGC1 was direct, with a dissociation constant in the micromolar range. In addition, we mapped the interaction and showed that it involved the dimerization of the cyclase. We showed the implication of IMPDH1 CBS domain at modulating this interaction, and how human mutations clustering in this domain altered the efficnity of the interaction. Our results showed that the adRP R224P mutant of IMPDH1 substantially decreased the interaction with RetGC (40% in relationship to WT), while the N198K mutation associated to adLCA enhanced the interaction (1.57 times more than WT) (Figure IV.7).

We conclude that the pathway of *de novo* GTP synthesis is coupled to the conversion of GTP to cGMP. This unanticipated connection between multienzyme complexes in nucleotide metabolism may serve to allow an integrated spatial modulation of purine synthesis according to the dark/light physiology requirements in these specialized cells. By bringing together inherited retinal dystrophy-causative genes so far considered unrelated, this finding opens a new conceptual framework to study the pathophysiology of these disorders (Figure 4.8). The implications of this new scenario are that a mutation at the level of IMPDH1 could putatively affect RetGC1 function, or vice versa. Another relevant implication is that specific inhibitors of IMPDH could be tested to treat the inherited retinal dystrophies associated to mutations that lead to constitutive guanylate cyclase activity (mutations in GUCY2D encoding RetGC1 associated to adCD (Hunt et al., 2010); and mutations in GUCA1A encoding GCAP1 (Olshevskaya et al., 2004; Payne et al., 1998)) or functional impairment of cGMP-PDE (mutations in the different PDE subunits or in AIPL1 (Dvir et al., 2010; Huang et al., 1995; Kohl et al., 2012; McLaughlin et al., 1993; Ramamurthy et al., 2004; Thiadens et al., 2009)).

Future experiments will be addressed at characterizing the precise contribution of the *de novo* and *salvage* pathways to GTP supply for phototransduction. By using IMPDH1-specific inhibitors, as well as inhibitors of the *salvage* pathway, we will try to determine the precise contribution of each route to photoreceptor cell physiology.

Another important question to address in the characterization of this assembly of protein complexes in a macromolecular multienzyme complex, is whether

assembly and dissociation of the partners in light dependent. - Is it regulated by light? - How? – What is the functional significance of this coupling?

On the other hand, we have also identified and characterized an interactor of RetGC1 that appears highly specific of cone cells: the Creatine Kinase Brain-type, CKB (Figure V.1, V.2, V.3). Creatine Kinase is an enzyme involved in energy metabolism that is abundantly expressed in tisssues with high energy demand, like muscle and brain. We here show that there is a clear colocalization of CKB with RetGC1, that is specific of cone outer segments.

- Why is CK-B so abundant at cone outer segment and why does it associate to RetGC/GCAP complexes? One explanation could be that cones presents a higher dynamic range than rods, with lower light sensitivity but faster response kinetics, and they respond to light over a higher range of ambient light intensities. In this way, the energy requirement of cones could be higher than that of rods. Therefore, cones may rely on a fast energy supply system to maintain the local ATP requirements of the cell. The coefficient diffusion of PCr is higher than ATP (Hubley et al., 1995), and PCr would help to maintain a high concentration of ATP locally.

Further experiments will be needed to elucidate the precise role of CKB at maintaining light response kinetics and light adaptation capacity. Future studies will base on using specific inhibitors of CKB on living mice while performing ERG recordings.

Conclusions

Conclusions

1. The transgenesis methodology based on *in vivo* DNA electroporation reported by Dhup & Majumdar, Nature Methods 2008, when strictly reproduced as reported, results in a maximum efficiency of 1.43% of spermatozoid transfection, which yields it unpractical.

2. In the absence of GCAP1 binding to RetGC1 there is no GCAP1 distribution to rod outer segments. Assembly of the RetGC1/GCAP1 complex precedes its transport.

3. GCAP1 myristoylation is required for GCAP1 distribution to rod outer segments.

4. The human G157R-GCAP2 mutation linked to autosomal dominant retinitis pigmentosa leads to abnormal protein retention at the inner segment, which results in cell toxicity by a mechanism independent of cGMP metabolism.

5. GCAP1 and RetGC1 pull-down assays, as well as size-exclussion fractionation from bovine rod outer segment preparations reveal an association of IMPDH1 to the RetGC/GCAPs complex.

6. Retinal Guanylate Cyclase 1 (RetGC1) establishes a direct interaction with Inosine Monophosphate Dehydrogenase 1 (IMPDH1), the first and rate-limiting step in de novo GTP synthesis. This interaction has a dissociation constant in the micromolar range.
7. The RetGC1 region involved in IMPDH1 interaction is the catalytic domain and C-terminal region of the protein. This interaction requires the dimerization domain of RetGC1.

8. The “Cystathione beta Synthase” domain of IMPDH1 regulates this interaction.

9. Mutation R224P in IMPDH1 linked to autosomal dominant Retinitis Pigmentosa 10 (RP10) decreases the RetGC1-IMPDH1 interaction.

10. Mutation N198K in IMPDH1 linked to rare Leber Congenital Amaurosis (ad rare LCA) enhances the RetGC1-IMPDH1 interaction.

11. RetGC1 and IMPDH1 co-localize at the connecting cilium of rods and cones, and at rod outer segments where phototransduction takes place.

12. Creatine kinase B associates to RetGC1 in cone outer segment compartments.

Conclusiones

1. Cuando estrictamente reproducimos la metodología de transgénesis basada en la electroporación de DNA *in vivo,* publicada por Dhup & Majumdar, Nature Methods 2008, resulta en una eficiencia máxima del 1,43% de espermatozoides transfectados, cuyo rendimiento es impráctico.

2. En ausencia de unión de GCAP1 a RetGC1, GCAP1 no se distribuye al segmento externo. El ensamblaje del complejo RetGC1/GCAP1 precede a su transporte.

3. La miristoilación de GCAP1 es necesaria para su distribución al segmento externo.

4. La mutación humana G157R_GCAP2, ligada a Retinitis Pigmentosa autosómica dominante conduce a una retención anormal de la proteína en el segmento interno, lo que resulta tóxico para la célula mediante un mecanismo independiente del metabolismo de cGMP.

5. Ensayos Pull-Down con GCAP1 y RetGC, así como cromatografía de exclusión de tamaño de preparaciones de segmentos externos de bastones, revelaron la asociación de IMPDH1 con el complejo RetGC/GCAPs.

6. La guanilato ciclasa de retina (RetGC1) establece una interacción directa con la inosina monofosfato deshidrogenasa 1 (IMPDH1), la enzima responsable del paso limitante de la síntesis *de novo* de GTP. Esta interacción tiene una constante de disociación en el rango micromolar.

7. La región del dominio catalítico y la del C-terminal de RetGC1 participan en la interacción con IMPDH1. Esta interacción requiere del dominio de dimerización de RetGC1.

8. El dominio “Cystathione-β-Synthase” de IMPDH1 regula esta interacción.

9. La mutación R224P de IMPDH1, ligada a Retinitis Pigmentosa autosómica dominante 10 (adRP10) disminuye la interacción de IMPDH1 con RetGC1.

10. La mutación N198K de IMPDH1, ligada a una forma rara de Amaurosis Congénita de Leber (adLCA) aumenta la interacción entre IMPDH1 y RetGC1

11. RetGC1 e IMPDH1 colocalizan en el cilio de conos y bastones y en el segmento externo, donde tiene lugar la fototransducción.

12. La isoforma cerebral de la creatina quinasa se asocia a RetGC1 en el compartimento sensorial de conos.

Chapter VII: Materials and Methods

Chapter VII: Materials and Methods

Pertaining to animal research, this study was conducted in accordance with the ARVO statement for the use of animals in ophthalmic and vision research and in compliance with acts 5/1995 and 214/1997 for the welfare of experimental animals of the autonomous community (Generalitat) of Catalonia, and approved by the ethics committee on animal experiments of the University of Barcelona.

7.1. Mouse Strains used and genotyping protocols.

The following mouse strains have been used in this work:

- C57Bl/6J (Charles River).
- GCAP1 and GCAP2 double knockout mice (Mendez et al., 2001) (from here on referred to as GCAPs-/-). This transgenic line lacks the expression of both GCAP1 and GCAP2.
- GCAPs-/- bGCAP2+ (Mendez et al., 2001)(also referred to as GCAP2 WT-E line). This transgenic line expresses bovine GCAP2 in the GCAPs-/-genetic background.

For genotyping of the different mouse strains, genomic DNA was obtained from a small piece of tail, by digesting the tissue at 55ºC overnight in 250µl of tailing buffer [50mM TrisHCl pH8.0; 100mM EDTA; 0.5% SDS] with 0,5mg/ml of Proteinase K. 125µl of 8M NH_4OAc and 750µl of 98% ethanol were added to precipitate DNA. After DNA precipitation and washing, the DNA pellet was further purified by standard phenol-chloroform (Phenol-Chlorophorm-Isoamylalcohol 25:24:1) extraction and ethanol precipitation, and quantified.

Polymerase Chain Reaction (PCR) genotyping was performed in 20µl reactions, by mixing 2µl of 10x PCR buffer with 0.16µl of deoxy nucleotide mix (dATP, dCTP, dGTP, dTTP, 25mM each), 0.6µl of 50mM MgCl2, 0.5µl of primer mix (forward and reverse primers at 20 pmol/µl each), 1µl of tail genomic DNA, and 0.12 µl of Taq DNA Polymerase. PCR cycles typically included one initial dissociation step at 95ºC for 3.5min; 30 cycles of amplification (94ºC 30sec; 63ºC 30sec; 72ºC 1min); and a final extension step of 72ºC for 10min. The annealing temperature was adjusted for each genotyping protocol depending on the pair of primers. The pair of primers used for genotyping of each strain is indicated in Appendix II). Amplified DNA bands were analyzed by electrophoresis in a 0.8% agarose gel in 1xTAE buffer.

7.2. Bacterial Strains used for cloning work and protein expression.

All bacterial strains used in this study were commercial modifications from *E. coli.*

7.2.1. Cloning strains:

- XL1-Blue. This strain was used for general cloning purposes and site-directed mutagenesis. Genotype: *recA1 endA1 gyrA96 thi-1 hsdR17 supE44 relA1 lac* [F′ *proAB lacI*qZΔ*M15* Tn*10* (Tetr)].
- DH10β. For general cloning purposes. Genotype: F^- *endA1 deoR*$^+$ *recA1 galE15 galK16nupG rpsL* Δ*(lac)X74* φ80*lacZΔM15 araD139* Δ*(ara,leu)7697 mcrA* Δ*(mrr-hsdRMS-mcrBC)* Str^R λ^-
- GT115 (*Invivogen)*. This strain was used for cloning and maintaining pCpG plasmids devoid of CpG dinucleotides. Genotype: *F- mcrA* Δ*(mrr-hsdRMS-mcrBC) φ80lacZ*Δ*M15* Δ*lacX74 recA1 rspL (StrA) endA1* Δ*dcm uidA*(Δ*MluI)::pir-116* Δ*sbcC-sbcD.*
- Dam-/Dcm- (*#C2925 from NEB*). Methyltransferase deficient *E. coli* cells suitable for growth of plasmids free of Dam and Dcm methylation. Genotype: *ara-14 leuB6 fhuA31 lacY1 tsx78 glnV44 galK2 galT22 mcrA dcm-6 hisG4 rfbD1 R(zgb210::Tn10)* Tet^S *endA1 rspL136* (Str^R) *dam13::Tn9* (Cam^R) *xylA-5 mtl-1 thi-1 mcrB1 hsdR2*

7.2.2. Protein expression strain:

- BL21(DE3). High-efficiency of protein expression under control of T7 promoter. This strain allows control of expression by IPTG. Genotype:F–, *omp*T, *hsd*S_B (r_B–, m_B–), *dcm*, *gal*, λ(DE3).

7.3. Competent bacterial cells for DNA transfection:

7.3.1. For DNA electroporation.

Molecular Cloning (Sambrook and Russel, 2001): chapter 1, protocol 26. Briefly, bacteria are grown to mid-log phase, chilled, centrifuged, and washed extensively with an ice-cold buffer or H_2O to reduce the ionic strength of the cell suspension, and then suspended in an ice-cold buffer containing 10% glycerol. We typically obtain a cloning efficiency of $10^{9\text{-}10}$transformants/µg of DNA with this protocol.

7.3.2. Chemically competent cells by TSS method.

Modified from Chung et al (Chung et al., 1989). This protocol typically yields an efficiency of 10^7transformants/µg of DNA. Briefly, TSS buffer is prepared (LB medium supplemented with 10% (w/v) PEG 8000, 30mM $MgCl_2$, 5% (v/v) DMSO. pH6,5), sterilized by filtration (0.22µm filter) and chilled in advance. 50ml of LB media are inoculated with 500ul of an overnight cell culture, and bacteria are grown

to mid-log phase. (OD600 of 0.2 - 0.5). Carry out all subsequent steps at 4ºC. Cell pellets are obtained by centrifugation for 10 minutes at 3000 rpm at 4ºC and resuspend in 5ml of TSS buffer. 100 µl aliquots into pre-chilled eppendorfs were stored at − 80ºC. For transformation, TSS cells were thawed on ice. DNA was added and the mix was incubated for 30min on ice. The mix was then incubated at 42ºC for 30sec (heat shock) and returned to ice for 2min. Cells were allowed to recover in SOC medium for 1h at 37°C under shaking, and plated.

7.4. cDNA cloning and generation of expression vectors.

7.4.1. Materials used in PCR work.

The following DNA polymerases were used, following manufacturer's instructions:

- PCR amplification in genotyping reactions: Taq polymerase (Invitrogen) or BioTaq (Bioline).
- PCR amplification for DNA cloning purposes: High-Fidelity PCR DNA polymerases: Pfu Ultra II Turbo HS (Agilent) or KOD polymerase (Millipore).

7.4.2. Total RNA extraction and cDNA synthesis from RNA.

Retinas for RNA extraction were dissected in ice-cold PBS. RNA was extracted by homogenizing each murine retina in 200µl of Trizol reagent (Invitrogen), adding 40µl of $CHCl_3$, vortexing for 1min and letting sit on ice for 15min. Samples were centrifuged at maximal speed for 15min at 4ºC, and the aqueous phase transferred to a new tube, where it was mixed with a volume of isopropanol and kept at -80ºC until use. RNA precipitation was performed by centrifugation at maximal speed for 30min at 4ºC. After washing and drying, the RNA was resuspended in 20µl of RNAase-free water. cDNA synthesis was performed with the High-capacity cDNA reverse transcription kit (#4368814.ThermoFisher Scientific), following manufacturer's instructions.

7.4.3. Generation of mammalian expression vectors for in vivo DNA electroporation.

For cloning of reporter genes into a plasmid completely devoid of CpG islets, the pCpG-free plasmid was purchased from Invivogen (#pcpgf-mcs) and the cDNA for the enhanced green fluorescent protein (EGFP) was amplified from the pL_UG plasmid (#L01GLUG001XA. SignalingGateway) with primers P5-P6 and cloned into the BglII and NheI sites of pCpG-free. The cDNA for Mito-DsRed (the reporter gene encoding the DsRed fluorescent protein fused to a mitochondrial localization signal) was amplified from pDsRed2-Mito (#632421. Clontech, a gift from Dr. Anna Aragay); with primers P4-P52, digested with BamHI/KpnI and cloned into the BglII/KpnI sites of pCpG-free.

For generation of the mammalian expression vectors based on the different versions of the Mouse Opsin Promoter (MOP), a deletion by PCR strategy was used (Imai et al., 1991), using MOP-I plasmid as the original template.

First, 2kb upstream of Enhancer was deleted by amplification of plasmid MOP-I as template, with primers P9-P10, and the fragment was self-ligated to generate 2Kb-MOP. The CpG island of pMOP was removed using the same strategy, using as template 2Kb-MOP and primers P11-P12, generating pMOPII. For generation of pMOP-III, primers P10&P11 were used and pMOP-I as template.

To generate pMOPII flanked by HS4 DNA barrier insulator sequences, two copies of HS4 were cloned upstream of the expression cassette. For this purpose, HS4 was amplified with primers P15-P16 from p1Fel (a gift from Dr. Lluis Montoliú) and inserted at the KpnI site of pMOPII. Clones with two tandem inserts in the same orientation were selected by restriction mapping analysis. One copy of HS4 was inserted into downstream of the expression cassette. HS4 was amplified from p1Fel with primers P17 -P18 and cloned into the EagI site of pMOPII.

For cloning the MOP-GCAP2-pA expression cassette into pCpG plasmid, the pCpG plasmid was amplified with primers P13-P14 to add KpnI and XbaI sites to the pCpG plasmid, and the fragment KpnI-MOP-GCAP-pA-XbaI inserted.

For generation of a mammalian expression vector of hGCAP1 under the MOP, hGCAP1 cDNA was amplified from pET21b-hGCAP1 plasmid (see below) with primers P19-P20 and inserted into the XhoI/BamHI sites of pMOP.

The collection of GCAP1 and GCAP2 mutants generated for subretinal injection and electroporation, presented in chapter III, were generated by site-directed mutagenesis using the Quick-Change kit (Stratagene) and primers P21 to P36 (Appendix II).

7.4.4. Generation of bacterial expression vectors for protein expression.

The plasmid for human GCAP1 expression in bacteria was originally developed in Dr. James Hurley´s laboratory, and contains the human GCAP1 cDNA into the NdeI and BamHI sites of pET21b (Novagen, Merck Millipore). Two different bacterial expression vectors for IMPDH1 were obtained based on the cDNA of the bovine IMPDH1 canonical isoform into different plasmids. The cDNA of IMPDH1 canonical isoform (514 aa, UniprotKB/Swiss-Prot: A0JNA3.2; GI:378548423) was obtained from total RNA from bovine retina using the High-capacity cDNA reverse transcription kit from ThermoFisher Scientific, and amplified by PCR using the KOD hot start DNA polymerase (Millipore), using either the pair of primers P1-P2 or P3-P4 (see Appendix II for primers sequences). Bovine IMPDH1 cDNA was introduced into the NdeI-BamHI sites of pET15b (Novagene, Merck Millipore, therefore creating a fusion protein with a His.tag at the NH2-terminus) or BglII- XhoI sites of pET32a-LIC (a gift from Dr. Cheryl Arrowsmith

obtained from Addgene, creating a fusion protein with Thioredoxin-His.tag at the NH2-terminus). The IMPDH1ΔCBS construct (which lacks the tandem repeats of the CBS domain at residues E111-K242) was generated from plasmid pET32a-LIC-bIMPDH1 by PCR deletion with primers P5-P6. Plasmid pET32a-LIC-bIMPDH1 was also used as template for generation of the R105W, N198K, R224P, and D226N individual mutants, by using the Site-directed mutagenesis kit from Agilent, and primers P7-P14. All cloning work in the generation of E. coli expression vectors was confirmed by sequencing. Human retinal guanylate cyclase bacterial expression vectors: RetGC-JMD/KHD (M496-K806), RetGC-DD/CD (N807-S1103), and RetGC-CD (G868-S1103) were a generous gift from Dr. Karl W. Koch (University of Oldenburg) and consisted of the corresponding cDNA fragments cloned into pDB.His.MBP (from the Berkeley Structural Genomics Center through the DNASU Plasmid Repository), that adds a His-tag and Maltose Binding Protein (MBP) at the NH2-terminus in frame with the gene of interest. Plasmid containing NH2-terminus fusion protein of His-tag with creatine kinase human isoform was purchased from DNASU (pMCSG7-hCKB, #HsCD00343148).

7.5. Bacterial Protein Expression.

For protein expression, chemical transformation was performed on E. coli BL-21(DE3) strain. Cells were grown at 37°C in 500 ml cultures in Luria Broth medium with antibiotic (100µg/ml Ampicillin or 50µg/ml Kanamycin) to an OD600 of 0.5, and protein expression was induced by addition of 1mM IPTG for 4h. For myristoylation of GCAP1, cells were cotransformed with pBB131 plasmid encoding N-myristoyl transferase (NMT) (a gift from Dr. J. Gordon, Washington University School of Medicine, Missouri, USA), and free myristic acid was added to a final concentration of 50µg/ml 30 min before of induction of expression. In the case of GCAP1 and the MBP-fused RetGC1 fragments the proteins were in the insoluble fraction of bacterial extracts, and had to be purified from inclusion bodies. Briefly, inclusion bodies were obtained in a series of steps of bacterial lysis by sonication followed by sedimentation, in lysis buffer (100mM Sodium phosphate pH8, 150mM NaCl, 1mM PMSF, 1mg/ml lysozyme). Purified inclusion bodies were solubilized in 6M Guanidinium-HCl in 100mM sodium phosphate pH8, 150mM NaCl, 25mM Imidazole, clarified by centrifugation at 30000g for 30min and loaded to a pre-equilibrated 5ml HisTrapTM Chelating HP Columns (GE Healthcare). A protocol for on-column refolding was then performed by first exchanging 6M urea for the 6M guanidinium-HCl in the running buffer (100mM sodium phosphate pH8, 150mM NaCl, 25mM Imidazole, pH8.0) and then subjecting the column to a decreasing gradient of urea (6M to 0M in running buffer, in 30 column volumes). Proteins were then eluted in 100mM sodium phosphate pH8, 150mM NaCl, 500mM imidazole, and concentrated with 10 kDa MWCO Amicon Ultra-15 centrifugation filter units

(Millipore) for the removal of imidazole. Protein stocks were either kept at -80ºC (GCAP1) or kept at 4ºC and used shortly after purification (RetGC1 fragments).

Bovine His.IMPDH1 expressed from plasmid pET15b in E coli BL21 was mostly insoluble and had to be purified from inclusion bodies and refolded. Inclusion bodies were obtained and solubilized in 6M guanidinium-HCl as indicated above. After clarification (12000rpm, 20min, 4ºC), the protein was purified by metal chelation with 5ml HisTrapTM Chelating HP Columns (GE Healthcare) in the presence of 6M Guanidinium-HCl (Running buffer: 20mM Hepes, 200mM NaCl, 6M Guanidinium-HCl, 10mM β-mercaptoethanol, 10mM imidazole, pH8.0) and eluted with 500mM imidazol in running buffer. His.IMPDH1 was refolded by three steps of dialysis, to gradually decrease the urea concentration: 1) against dialysis buffer (20mM Hepes pH 8.0; 200mM NaCl) with 6M urea; and 2) against dialysis buffer with 3M urea; and 3) against dialysis buffer with 1M urea and 0.4M arginine. The presence of 1M urea and 0.4M Arginine (Wang et al., 2011) was required to maintain the protein in soluble form. His.IMPDH1 was concentrated using 10 kDa MWCO Amicon Ultra-15 centrifugation filter units to obtain a protein stock at 2.5mg/ml (in 1M urea, 0.4M Arg), that was either used for injecting rabbits for antibody production, or crosslinked to an Aminolink Resin (ThermoFisher Scientific) to generate IMPDH1-immobilyzed resin for pull-down assays.

Thioredoxin-fused IMPDH1 (Trx.His.IMPDH1), IMPDH1ΔCBS and the four mutants (R105W, N198K, R224P, and D226N) were partially soluble when expressed from pET32a-LIC-bIMPDH1 plasmid in E coli BL21 strain. Proteins could be purified from the soluble fraction of bacterial extracts. Briefly, bacterial cells were lysed in Lysis Buffer (100mM Sodium phosphate pH8, 150mM NaCl, 25mM Imidazole, 1mM PMSF, 1mg/ml lysozyme, 5ug/ml DNaseI and 5ug/ml RNaseA) and sonicated (pulses) for 1min in ice. After clarification at 20000g for 30min at 4ºC, the soluble fractions were bound to TALON® Metal Affinity Resin by metal chelation to the His.tag (#635501, Clontech). Trx.His.IMPDH1-immobilized resin (wildtype protein and the four mutants) was kept and directly used in pull-down assays to test the effect of the mutation on the RetGC interaction. To obtain a soluble source of Trx.His.IMPDH1 for Surface Plasmon Resonance (SPR) binding studies, the protein was eluted in 20mM Hepes pH 8, 115mM KCl, 10mM NaCl, 10mM MgCl2, and 500mM Imizadole. The protein was kept at 4ºC and used shortly after purification. His.hCKB was purified from supernatant fractions as Trx.His.IMPDH1

7.6. Southern Blot

Southern transfer and hybridization (Southern, 1975) is typically used to study how genes are organized within genomes by mapping restriction sites in and around segments of genomic DNA for which specific probes are available. Genomic DNA is first digested with one or more restriction enzymes, and the resulting fragments

are separated according to size by electrophoresis through a standard agarose gel. The DNA is then denatured in situ and transferred from the gel to a solid support (usually a nylon or nitrocellulose membrane). The DNA attached to the membrane is hybridized to a labeled DNA, RNA, or oligonucleotide probe, and bands complementary to the probe are located by an appropriate detection system, for example, by autoradiography. By estimating the size and number of the bands generated after digestion of the genomic DNA with different restriction enzymes, singly or in combination, it is possible to place the target DNA within a context of restriction sites(Sambrook and Russel, 2001).

10µg of genomic DNA obtained from mouse tails were digested with affordable selected restriction enzyme, maintaining a ratio of 10u/µg of DNA. After complete digestion, loading buffer (0.04% xylene cyanol FF, 2.5% Ficoll (Type400) in H_2O) was added to the samples, and samples were run in a 1% agarose gel without Ethidium bromide or *Sybr Safe*. (No more than 10ng of an internal control of digested pMOP-I plasmid was added as internal reference of molecular weight). Immediately after the run, the gel was transferred to a glass baking dish, and a razor blade was used to trim away unused areas of the gel, including the section of gel above the wells. A small triangular piece from the bottom left-hand corner of the gel was cut off for orientation purposes. The gel was incubated for 10min in 0.2N HCl, and rinsed in ddH_2O several times. To denature the DNA, the gel was soaked in Denaturation Solution (1.5M NaCl, 0.5M NaOH) for 45min, and rinsed with ddH_2O. The gel was incubated for 45min in Neutralization Buffer (1M Tris-HCl pH7.4, 1.5M NaCl). A piece of nylon membrane (Byodyne B Nylon membrane. Pall) was cut about 1mm larger than gel. Two sheets of thick blotting paper (3MM Whatman) were cut to the same size as the membrane. The nylon membrane was floated on the surface of a dish of ddH_2O until it was completed wet, and then immersed in 5xSSPE [20x SSPE (3M NaCl, 0.2M NaH_2PO_4, 0.02M EDTA, pH7,4)] for at least 5min. The corner of the membrane was marked to match the corner cut from the gel. An upward capillary transfer system was assembled by placing a long Whatmann 3MM paper covering the support in direct contact with the inverted gel. The Nylon membrane was placed in direct contact with the gel avoiding any bubbles. The membrane was covered with some sheets of Whatmann 3MM and about a 5cm-thickness of paper towels. A weight was placed on top, to allow the transfer to proceed overnight.

Once the transfer was done, DNA in the membrane was cross-linked to it under UV light. The membrane was rinsed with ddH_2O, dried and kept until use.

For the labelling by hybridization, a probe was synthesized by radiolabeling of DNA fragments by extension of oligonucleotides [Molecular Cloning, Chapeter 9, protocol 1]. Briefly, 25ng of PCR-amplified DNA of the desired probe was mixed with 125 ng of random hexamers in 30µl of water (50µM), boiled for 2 minutes and placed on ice for 1 minute. To the 30µl mixture, the following reagents were added: 8µl of ddH_2O, 1µl dNTPs 5mM each excluding dCTP (dATP, dGTP, dTTP, without

dCTP), 5µl of 10x NEB2 Buffer (500mM NaCl, 100mM Tris-HCL pH 7.9, 100mM $MgCl_2$, 10mM DTT), 5 units of Klenow DNA polymerase and 5µl of 10mCi/ml α-^{32}P dCTP. After 1h incubation at RT (25ºC), 10µl of NA Stop/Storage Buffer was added (50mM Tris-Cl pH7.5, 50mM NaCl, 5mM EDTA, 0,5% (w/v) SDS). The labelled probe was purified with an Elutip-D Column (*Whatman*), and its activity measured at the scintillation counter. The membrane was hydrated with wash solution #1 (2xSSPE) and prehybridized for a minimum of 1h at 65ºC in pre-warmed hybridization solution (10% (w/v) dextran sulphate, 5xSSPE, 2% (w/v) SDS) at 65ºC containing 1xDenhardt's [50x Denhardt's Solution:1% (w/v) Ficoll 400, 1% (w/v) polyvinylpyrrolidone, 1% (w/v) Bovine serum albumin]and boiled salmon sperm DNA 10µg/ml (Agilent). For hybridization, the dsDNA probe was denatured by incubation at 95ºC for 5min and immediate placement on ice. Prehybridization solution was replaced with fresh hybridization solution containing 1xDenhardt's and boiled salmon sperm DNA and the probe. As little solution as possible was used. Hybridization was allowed to proceed overnight at 60ºC. Subsequently the membrane was carefully removed from the hybridization solution and placed into a clean container for washing. Membrane was washed twice at room temperature in Solution #1, twice for 15min at 55ºC with Solution #2 (2xSSPE, 1% (w/v) SDS) and twice for 15min at 55ºC with Solution #3 (0.1x SSPE). Membrane was exposed in darkroom to X-ray film for 24-48h at -80ºC.

7.7. In Vivo DNA electroporation in the retina

In vivo DNA electroporation in the retina following DNA injection in the subretinal space was developed by C. Cepko´s laboratory (Matsuda and Cepko, 2004) at Harvard in 2004. This technique allows transient expression of a gene of interest into photoreceptor cells, if a photoreceptor-specific promoter is used.

We have implemented Cepko´s procedures in the laboratory with minor modifications. The plasmid DNA was amplified in bacteria and purified by maxiprep (Qiagen plasmid maxi kit. Qiagen). A DNA solution (6µg/µl) in PBS and fast green 0,1% dye was prepared by mixing the expression vector of interest (circular plasmid) with a GFP encoding plasmid (pL_UG) at a molar ratio of 2:1. The plasmid encoding EGFP is added to easily identify the injection area at the step of analysis, 25 days later. For *in vivo* DNA electroporation, new born mouse pups at postnatal day 1 are used. Briefly, pups are anesthetized by submersion in ice for 4min. At a stereo microscope, an opening is performed with a scalpel following the natural line of the eyelid, after cleaning the zone with povidone-iodine solution. A small incision is then performed on the sclera, with a 30-gauge needle. For DNA injection, we used customized capillary glass pipettes [(#300048. Harvard Apparatus), pulled in a Puller P-97 from Sutter Instruments according to the following parameters: heat=650, Pull=60, Velocity=60, Time=200)]. The capillary glass pipettes were

attached to a nanoinjector (Drummond Nanoject) and were managed by a micromanipulator. After inserting the glass pipette in the eye, and carefully micromanipulating it to reach the subretinal space (reached when the pipette meets the resistance of the back of the eye upon touching the choroid), approximately 0,5-1µl of circular naked DNA were delivered. After DNA injection, tweezer-type electrodes briefly soaked in PBS were placed to softly hold the heads of the pups placing the positive electrode of the tweezer over the injected eye, and five square pulses of 80V of 50-ms duration with 950-ms intervals were applied by using a pulse generator (CUY21, Nepagene). Pups were left to recovery over a thermal blanket until the end of procedure, returned to their cage and raised in normal conditions. Mice were processed at postnatal day 25-30.

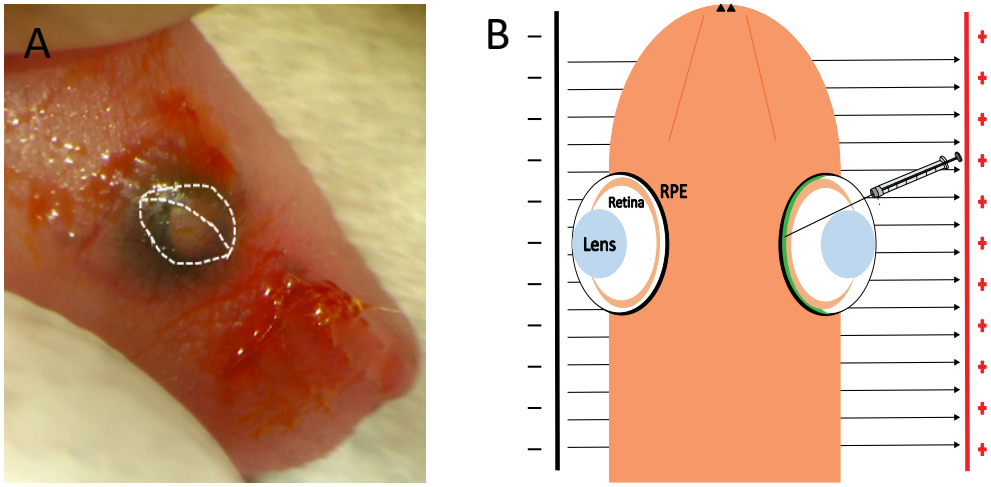

Figure VII.1. A. Image showing the eyelid and an outline of the incisura that will be cut with a scalpel, following that natural opening line of the eyelid. B. Schematic figure of injection and electroporation. Adapted from Matsuda & Cepko 2004.

7.8. In Vivo DNA electroporation into the male germ line of mice

C57Bl/6J males at 30 days-of-age were used in the electroporation procedures. Mice were anesthetized with ketamine (40mg/kg) and xylacine (check spelling) (5mg/kg) by intraperitoneal injection, and buprenorphine (0,012mg/kg) by subcutaneous injection. The area of the scrotum was shaved with an electric razor-blade, and cleaned with ethanol 70º and povidone-iodine solution. A small incision was performed following the scrotal raphe so that both testis were exposed.

In hemicastration procedures, the right testis was castrated by knotting the vas deferent and associated arteries and veins, and cutting through them. The left testis

was injected with a solution of DNA (0,5µg/µl) in PBS with Trypan Blue 0,04% as a tracer. In contrast to the procedure of DNA electroporation in the retina, in which circular plasmid DNAs are injected for transient transgenic expression, DNA injected in the testis proceeds from bacterial maxipreparations, but was purified by CsCl gradient (Sambrook and Russel, 2001) and linearized, given that what we pursue is DNA integration in the genome. Typically, DNA is linearized by overnight restriction digestion and subsequently purified by phenol-chlorophorm extraction and ethanol precipitation. About 25µl (12µg) of DNA solution is injected into each testis at three different locations, by using a 28gauge bevel-end needle coupled to a Hamilton syringe (#7636-01, Hamilton Company). It is crucial that the injection does not affect the internal pressure of the testis so it is important to do it slowly. After DNA injection, tweezer-type electrodes briefly soaked in PBS were placed over the testis and two rounds of four square pulses of 60V of 50-ms duration with 950-ms intervals alternating direction of electric field were applied by using a pulse generator (CUY21, Nepagene). The electroporated testis is repositioned into the scrotum and stitched with vicryl 5-0 sutures (J303H, Johnson and Johnson). After the surgery, and once the anaesthesia effect is extinguishing, meloxicam 5mg/kg (Metacam 5mg/ml. Boehringer Ingelheim) is applied by subcutaneous injection.

An alternative procedure for DNA injection avoiding surgery was also performed. In this procedure, mice were injected through the scrotum wall, by injecting each testis with 20-25 µl DNA solution. Both testis were held simultaneously with the electroporator tweezers and electroporation was performed as described above. Thirty-five days after injection, electroporated mice were mated with 2 females each of the same mouse strain, at postnatal day 50-60.

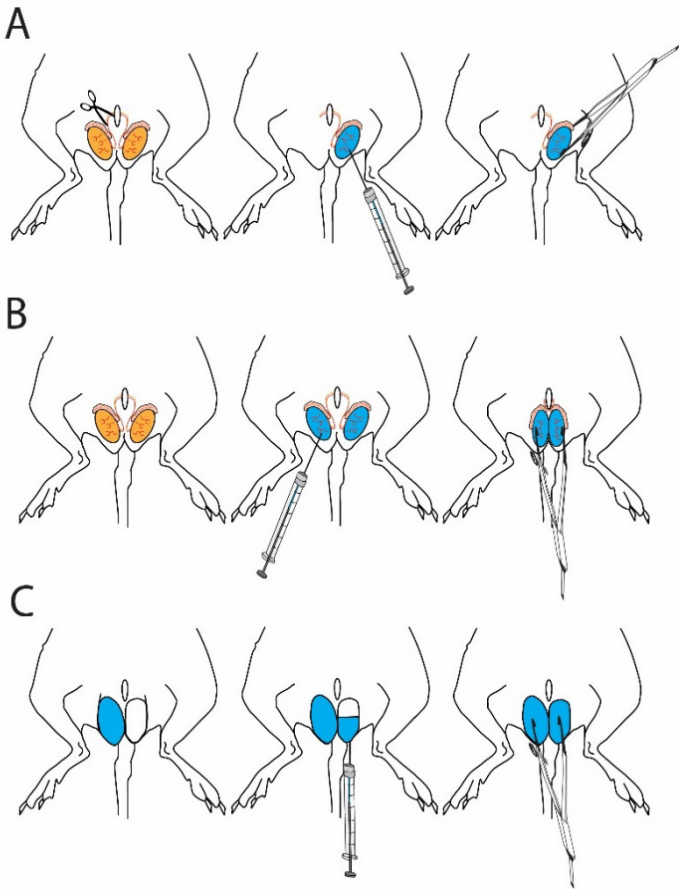

Figure VII.2. Schematic procedures for in vivo DNA electroporation at the gonad. A. Surgery with hemicastration (H) and DNA injection at remaining testis. B. Surgery with injection of both testis (S). C. Invasive injection trans-scrotum (T).

7.9. Immunofluorescence localization assays in bovine or murine retinas.

For immunofluorescence localization assays in bovine eyes, bovine eyes were obtained approximately 10min postmortem and were immediately processed on location. Mice were opened by a clean cut to remove the cornea, and submerged in fixative (4% paraformaldehyde in phosphate buffer saline pH7.4) for 2h at room temperature. For mice eyes, mice were sacrificed and eyes were marked at the superior center for orientation purposes. Immediately after enucleation the eyes were punctured with a needle and submerged in fixative (4% paraformaldehyde; 0.02% glutaraldehyde in phosphate buffer saline at pH7.4). The cornea was excised, and at

1h in fixative, the lens was removed and the eyecups were further fixed for a total of 2 h at room temperature. Eyecups were washed in PBS and then infiltrated in acrylamide (8.4% acrylamide, 0.014% bisacrylamide in PBS pH7.4 for 14 h before acrylamide polymerization was induced), included in OCT compound and frozen in liquid nitrogen. OCT blocks were stored at -80ºC until used. Cryosections along the vertical axis of the eyecup were obtained at 20 µm-thickness using a CM1510S Leica cryostat (Leica Microsystems).

Sections were incubated with blocking solution (3% normal goat serum, 1% BSA, 0,3% Triton-X100 in PBS pH7.4, 1 h at room temperature); first antibody (16h at 4ºC), secondary antibody (1h 30min at room temperature), and fixed for 15 min in 4% paraformaldehyde prior to being mounted with Mowiol [Calbiochem 475904].

Images were acquired at a laser scanning confocal microscope (Leica TCS-SL and TCS-SP2). Images were processed with Leica confocal software Lite and ImageJ.

7.10. Bovine Retinal Fractionation and preparations of bovine rod outer segments.

Bovine eyes were obtained at a local slaughterhouse at about 15min postmortem and were dark adapted for 1h in oxigenated Locke's Buffer (10mM HEPES pH7.4, 136mM NaCl, 3.6mM KCl, 2.4mM MgCl2, 1.2mM CaCl2, 20mM NaHCO2, 0.02mM EDTA, 10mM Glucose, 1mM PMSF) in ice. From that point on, the retinal dissection and tissue fractionation procedure were performed under dim-red light. Pools of ten retinas were collected in SS34 centrifuge tubes, in 15ml of Buffer A (100mM NaH2PO4.H2O pH6.5, 0,1mM EDTA, 2mM MgCl2) with 25% sucrose. Rod outer segments were gradually collected in five cycles of mechanical disruption of this organelle from the retinas by vortexing (2min vortex at 1800rpm in buffer A with 25% sucrose) followed by its collection from the supernatant fraction after centrifugation at 180g, 10min, 4ºC. The combined supernatant fractions from these cycles were diluted in 2 volumes of buffer A and rod outer segments were pelleted by centrifugation (40000g, 15min, 4ºC). The pellet was resuspended in 2ml of buffer A and loaded on top of a two-step 30%-35% sucrose cushion in buffer A (16ml:16ml), and centrifuged at 140000g for 90min at 4ºC. ROS were collected at the interface, diluted in buffer A and pelleted at 40000g, 15min and 4ºC. Pellets were resuspended in 20mM HEPES pH7.4 and stored in aliquots at -80°C. Rhodopsin concentration was calculated using as molar extinction coefficient ε_{500}=40600 M/cm.

7.11. Proteomic studies and protein biochemical analysis: immunoprecipitation and pull-down assays, liquid chromatography and mass spectrometry.

7.11.1. GCAP1 pull-down assays in the proteomic approach to identify new GCAP1 interacting proteins.

100µg of GCAP1 were crosslinked to 10mg of magnetic beads (Dynabeads® M-270 Epoxy, ThermoScientific) according to manufacturer's instructions. GCAP1-immobilized beads were divided into two equal aliquots to perform parallel pull-down assays in Ca2+ or EGTA conditions. Each aliquot was incubated for 1h at room temperature with 1.5mg of bovine ROS solubilized in 1% Triton X100 in binding buffer (20mM HEPES pH7.4, 135mM NaCl, 5mM KCl, 1mM NaF, 1mM PMSF, 1mM β-mercapto-ethanol, 1% Triton X-100, cOmplete™ Mini EDTA-free Protease Inhibitor Cocktail) containing either 5mM CaCl2 (Ca2+-condition) or 4mM EGTA/1.5mM MgCl2 (EGTA-condition). After the binding step the beads were washed and bound material was eluted with 0.2M Glycine-HCl pH 2.5. The beads were washed and used on two more 1h serial binding steps with the sample. Serial elution fractions were combined, neutralized, and concentrated by ethanol precipitation.

A parallel pull-down assay was performed with Ran (a cytosolic protein similar in size to GCAP1), under identical Ca2+ or EGTA conditions using the same bov ROS as starting material, as a negative control. For LC/MS-MS samples were treated and analyzed as previously detailed (López-del Hoyo et al., 2014), with the modifications here detailed. For LC/MS-MS analysis, samples were reduced; alkylated; precipitated; resuspended in 1.6M urea and digested with trypsin (37ºC, 14h). Tryptic peptides were separated by nano liquid chromatography [Proxeon EASY-nLC, EASY C18 trap column, EASY C18 analytical column (Thermo Fisher Scientific)]. A 0-40% buffer B linear gradient in 90min was employed, using solvent B (97% ACN, 0.1% formic acid) and solvent A (3% ACN, 0.1% formic acid). MS/MS analysis was performed using an LTQ Orbitrap Velos (Thermo Fisher Scientific) with a nano electrospray ion source with precursor ion selection in the Orbitrap at 30000 resolution, selecting the 20 most intense precursor ions in positive ion mode. MS/MS data acquisition was completed using Xcalibur 2.1 (Thermo Fisher Scientific). For identification of peptides, collision energy (CE) of 35% was the fragmentation method used. For protein identification, data was processed using Proteome Discoverer 1.4.1.14 (Thermo Fisher Scientific).

For database searching, raw mass spectrometry files were submitted to the in-house MOUSE-BOVIN_UP_SP_r_2014-5.fasta Swiss-Prot database (released February 2014; 22460 protein entries) using SEQUEST version 28.0 (Thermo Fisher Scientific). The criteria used to accept identification included a minimum of 2

peptides matched per protein, with a false discovery rate (FDR) of 1%. All proteins were treated as ungrouped.

For label-free quantitative proteomic analysis the "GCAP1-Ca2+" and "GCAP1-EGTA" protein lists were filtered to remove any duplications resulting from the use of bovine and mouse fasta sequence libraries, and only those proteins unequivocally assigned by at least a unique peptide were retained. The equation in Fig 1 was applied, where for each protein R_{SC} (Ratio from Spectral Count) is the $\log_2$ ratio of abundance between Samples 1 (Ca2+) and 2 (EGTA); n_1 and n_2 are spectral counts for the protein in Samples 1 and 2, respectively; t_1 and t_2 are total numbers of spectra over all proteins in the two samples; and f is a correction factor set to 0.5. This expression corrects for differences in sampling depth between both conditions, and avoids the discontinuity seen in simple count ratios when a protein shows spectral count = 0 in one of the samples.

7.11.2. Immunoprecipitation of GCAP1 and IMPDH1

For immunoprecipitation assays of GCAP1 or IMPDH1, 2µg of monoclonal Ab α-GCAP1 (MAI-724, Thermo Scientific) or purified polyclonal antibody α-IMPDH1 (generated in the lab) were incubated for 15min with 40µl of Dynabeads-Protein G (LifeTechnologies). Following washing and pre-equilibration in homogenization Buffer [20mM HEPES pH7.2, 115mM KCl, 10mM NaCl, 10mM $MgCl_2$, 1.3mM D(+)-Trehalose, 1mM *n*-Dodecyl β-D-maltoside (DDM), 1mM PMSF, 1mM NaF, 0.5mM $CaCl_2$, 1mM β-Glycerophosphate, 1mM ATP, 1mM IMP, 1mM NAD+, 0.2mM Mycophenolic acid (MPA)], the beads were incubated with 4mg of total bovine retinal extracts or 2mg of bovine ROS preparations in homogenization buffer with 20mM DDM and 1mM MPA for 1h at RT. The beads were washed and boiled in 1x Laemmli SDS sample buffer, for SDS-PAGE analysis. In a typical experiment, 2% of the input and flow through fractions were loaded adjacent to 100% of the bound fraction. Proteins in the gels were transferred to nitrocellulose membranes and immunoblotted with the different host antibodies listed in annex table II. Secondary antibodies were conjugated to fluorescent dyes for use in the Odyssey scan system. Images were acquired at the Odyssey Imaging System (LI-COR, Lincol, Nebraska USA).

7.11.3. IMPDH1 pull-down assays performed on whole retinal homogenates.

For IMPDH1 pull-down assays on whole retinal homogenates, a recombinant form of the bovine canonical IMPDH1 protein fused to a His tag (His.IMPDH1) was immobilized to Aminolink Plus Coupling Resin (#20501. ThermoFisher Scientific). IMPDH1-immobilized resin (corresponding to about 100µg of bovine His.IMPDH1 crosslinked to Aminolink resin) was used per pull-down assay, using 10mg of total

bovine retina extract or 2mg of bROS in the homogenization buffer used for immunoprecipitation assays.

7.11.4. IMPDH1 pull-down assays to study the effect of IMPDH1 blindness-associated mutations on the affinity of IMPDH1 for RetGC1.

For the pull-down assays comparing individual IMPDH1 mutants, mutant IMPDH1 protein was bound to TALON resin by metal chelation (based on the His tag in the recombinant proteins), and aliquots of IMPDH1-immobilized resin corresponding to an equal amount of IMPDH1 in each sample (wildtype and R105W, N198K, R224P, and D226N individual mutants) were used as bait in pull-down assays of 10mg of total bovine retinal extracts in homogenization buffer. For Western blot detection, nitrocellulose membranes were incubated with anti-RetGC1 pAb and IRDye 800CW Donkey anti-rabbit antibody (LI-COR Biosciences). Images were acquired and band densities were quantified with Odyssey application software 3.0. Statistical analysis was done with the GraphPad Prism 6, with one-way ANOVA by Dunnett's test (α=0.05). RectGC1 pull-down assays were performed with the truncated forms of the protein as detailed, using whole retinal homogenates as starting material.

7.11.5. Pull-down assays with the different RetGC fragments.

RectGC1 pull-down assays were performed with the truncated forms of the protein (write-down here the three fragments used in the RetGC pull-down figure) by binding the corresponding recombinant proteins to His-chelating columns (Ge Healthcare) , washing and pre-equilibrating, before performing the binding step with whole retinal homogenates. After extensive washing on the columns, acidic elution was performed with Glycine pH2.0. Bound proteins were identified by SDS-PAGE and Western Blot.

7.12. Size Exclusion Chromatography

A fraction corresponding to 1mg total protein of bov ROS was solubilized in solubilization buffer (20mM HEPES pH7.2, 115mM KCl, 10mM NaCl, 10mM $MgCl_2$, 1.3mM D(+)-Trehalose, 20mM DDM, 1mM PMSF, 1mM NaF, 1mM β-Glycerophosphate, 0.5mM $CaCl_2$ or 5mM EGTA), clarified and injected into a pre-equilibrated 3.5µm-bead size column with a separation range of 10kDa-1500kDa [XBridge Protein BEH SEC Column, 450Å, 3.5 µm, 7.8 mm X 300 mm (Waters Chromatography)] in Running Buffer (20mM HEPES pH7.2, 115mM KCl, 10mM NaCl, 10mM $MgCl_2$, 1.3mM D(+)-Trehalose, 1mM DDM, 1mM PMSF, 1mM NaF, 0.5mM $CaCl_2$ or 5mM EGTA) at a flow rate of 0.86ml/min. Fractions were collected every 30s from exclusion time 6min up to 15min, precipitated with 10

volumes of cold-acetone and resolved by 12% SDS-PAGE. Proteins were transferred to a nitrocellulose membrane, that was incubated with different antibodies as detailed in Appendix III.

7.12. Surface Plasmon Resonance Interaction Analysis.

A Biacore T200 system was used (GE Healthcare). The MBP.RetGC-DD/CD or MBP.RetGC-JMD/JHD fragments of the cyclase were covalently attached to two different channels of a CM5 sensor chip using amine coupling chemistry, to a theoretical response level of 200-400 resonance units (RU). Reference channels were activated and deactivated in the absence of ligand. The Thio.His.IMPDH1 protein was passed as an analyte at 2-fold serial dilutions from a 0.48mg/ml stock solution, at: 6.71; 3.36; 1.68; 0.84; 0.42; and 0.21 μM concentrations. The interaction affinity was determined from measurement of steady-state binding levels as a function of analyte concentration, from multi-cycle experiments performed with duplicates. For analysis of the steady-state binding data, a model of 1:1 binding was assumed (4-parameter fitting, T200 Biacore analysis software), and the chi-square value defining the closeness of the fit (describing the deviation between the experimental and fitted curves) was 1.57 RU^2 for RetGC-DD/CD (R_{max} = 44.1 RU) and 0.167 RU^2 for RetGC-JMD/KHD (R_{max} = 50.5 RU). Chi-square values are typically considered acceptable when they are less than 10% of the experimental maximal response.

Bibliography

Bibliography

Aherne, A., Kennan, A., Kenna, P.F., McNally, N., Lloyd, D.G., Alberts, I.L., Kiang, A.S., Humphries, M.M., Ayuso, C., Engel, P.C., Gu, J.J., Mitchell, B.S., Farrar, G.J., Humphries, P., 2004. On the molecular pathology of neurodegeneration in IMPDH1-based retinitis pigmentosa. Hum. Mol. Genet. 13, 641–650. doi:10.1093/hmg/ddh061

Alan F. Wright, C.F.C., Wright, A.F., Chakarova, C.F., Abd El-Aziz, M.M., Bhattacharya, S.S., 2010. Photoreceptor degeneration: genetic and mechanistic dissection of a complex trait. Nat. Rev. Genet. 11, 273–84. doi:10.1038/nrg2717

Ames, J.B., Dizhoor, A.M., Ikura, M., Palczewski, K., Stryer, L., 1999. Three-dimensional structure of guanylyl cyclase activating protein-2, a calcium-sensitive modulator of photoreceptor guanylyl cyclases. J. Biol. Chem. 274, 19329–37. doi:10.1074/jbc.274.27.19329

Ames, J.B., Ishima, R., Tanaka, T., 1997. Molecular mechanics of calcium – myristoyl switches. Nature 389, 198–202.

Ames, J.B., Lim, S., 2012. Molecular structure and target recognition of neuronal calcium sensor proteins. Biochim. Biophys. Acta 1820, 1205–13. doi:10.1016/j.bbagen.2011.10.003

Andres, R.H., Ducray, A.D., Schlattner, U., Wallimann, T., Widmer, H.R., 2008. Functions and effects of creatine in the central nervous system. Brain Res. Bull. 76, 329–343. doi:10.1016/j.brainresbull.2008.02.035

Azadi, S., Molday, L.L., Molday, R.S., 2010. RD3 , the protein associated with Leber congenital amaurosis type 12 , is required for guanylate cyclase traf fi cking in photoreceptor cells. Proc. Natl. Acad. Sci. U. S. A. 107, 1–6. doi:10.1073/pnas.1010460107/-/DCSupplemental.www.pnas.org/cgi/doi/10.1073/pnas.1010460107

Backliwal, G., Hildinger, M., Kuettel, I., Delegrange, F., Hacker, D.L., Wurm, F.M., 2008. Valproic acid: A viable alternative to sodium butyrate for enhancing protein expression in mammalian cell cultures. Biotechnol. Bioeng. 101, 182–189. doi:10.1002/bit.21882

Baehr, W., Karan, S., Maeda, T., Luo, D.-G.G., Li, S., Bronson, J.D., Watt, C.B., Yau, K.-W.W., Frederick, J.M., Palczewski, K., 2007. The function of guanylate cyclase 1 and guanylate cyclase 2 in rod and cone photoreceptors. J. Biol. Chem. 282, 8837–47. doi:10.1074/jbc.M610369200

Bell, A.C., West, A.G., Felsenfeld, G., 1999. The protein CTCF is required for the enhancer blocking activity of vertebrate insulators. Cell 98, 387–396. doi:10.1016/S0092-8674(00)81967-4

Bender, A.T., Beavo, J.A., 2006. Cyclic nucleotide phosphodiesterases: molecular regulation to clinical use. Pharmacol. Rev. 58, 488–520. doi:10.1124/pr.58.3.5

Bock, C., Walter, J., Paulsen, M., Lengauer, T., 2007. CpG island mapping by epigenome prediction. PLoS Comput. Biol. 3, e110. doi:10.1371/journal.pcbi.0030110

Bode, J., Stengert-Iber, M., Kay, V., Schlake, T., Dietz-Pfeilstetter, A., 1996. Scaffold/matrix-attached regions: topological switches with multiple regulatory functions. Crit. Rev. Eukaryot. Gene Expr. 6, 115–138.

Bowes, C., Li, T., Danciger, M., Baxter, L.C., Applebury, M.L., Farber, D.B., 1990. Retinal degeneration in the rd mouse is caused by a defect in the beta subunit of rod cGMP-phosphodiesterase. Nature 347, 677–680. doi:10.1038/347677a0

Bowne, S.J., Liu, Q., Sullivan, L.S., Zhu, J., Spellicy, C.J., Rickman, B., Pierce, E.A., Daiger, S.P., Rickman, C.B., Pierce, E.A., Daiger, S.P., 2006a. Why do mutations in the ubiquitously expressed housekeeping gene IMPDH1 cause retina-specific photoreceptor degeneration? Invest. Ophthalmol. Vis. Sci. 47, 3754–3765. doi:10.1167/iovs.06-0207

Bowne, S.J., Sullivan, L.S., Blanton, S.H., Cepko, C.L., Blackshaw, S., Birch, D.G., Hughbanks-Wheaton, D., Heckenlively, J.R., Daiger, S.P., 2002. Mutations in the inosine monophosphate dehydrogenase 1 gene (IMPDH1) cause the RP10 form of autosomal dominant retinitis pigmentosa. Hum. Mol. Genet. 11, 559–568.

Bowne, S.J., Sullivan, L.S., Mortimer, S.E., Hedstrom, L., Zhu, J., Spellicy, C.J., Gire, A.I., Hughbanks-Wheaton, D., Birch, D.G., Lewis, R.A., Heckenlively, J.R., Daiger, S.P., 2006b. Spectrum and Frequency of Mutations in IMPDH1 Associated with Autosomal Dominant Retinitis Pigmentosa and Leber Congenital Amaurosis. Investig. Opthalmology Vis. Sci. 47, 34. doi:10.1167/iovs.05-0868

Boye, S.E., 2015. Leber congenital amaurosis caused by mutations in GUCY2D. Cold Spring Harb. Perspect. Med. 5. doi:10.1101/cshperspect.a017350

Buey, R.M., Ledesma-Amaro, R., Velázquez-Campoy, A., Balsera, M., Chagoyen, M., de Pereda, J.M., Revuelta, J.L., 2015. Guanine nucleotide binding to the Bateman domain mediates the allosteric inhibition of eukaryotic IMP dehydrogenases. Nat. Commun. 6, 8923. doi:10.1038/ncomms9923

Burgoyne, R.D., 2007. Neuronal calcium sensor proteins: generating diversity in neuronal Ca2+ signalling. Nat. Rev. Neurosci. 8, 182–93. doi:10.1038/nrn2093

Burgoyne, R.D., Haynes, L.P., 2012. Understanding the physiological roles of the neuronal calcium sensor proteins. Mol. Brain 5, 2. doi:10.1186/1756-6606-5-2

Burns, M.E., Arshavsky, V.Y., 2005. Beyond counting photons: trials and trends in vertebrate visual transduction. Neuron 48, 387–401. doi:10.1016/j.neuron.2005.10.014

Capecchi, M.R., 1989. Altering the genome by homologous recombination. Science 244, 1288–92.

Cepko, C., 2014. Intrinsically different retinal progenitor cells produce specific types of progeny. Nat Rev Neurosci 15, 615–627.

Chaillet, J.R., Bader, D.S., Leder, P., 1995. Regulation of genomic imprinting by gametic and embryomc processes. Genes Dev. 9, 1177–1187.

Chang, B., Grau, T., Dangel, S., Hurd, R., Jurklies, B., Sener, E.C., Andreasson, S., Dollfus, H., Baumann, B., Bolz, S., Artemyev, N., Kohl, S., Heckenlively, J., Wissinger, B., 2009. A homologous genetic basis of the murine cpfl1 mutant

and human achromatopsia linked to mutations in the PDE6C gene. Proc. Natl. Acad. Sci. U. S. A. 106, 19581–19586. doi:10.1073/pnas.0907720106

Chang, C.-C., Lin, W.-C., Pai, L.-M., Lee, H.-S., Wu, S.-C., Ding, S.-T., Liu, J.-L., Sung, L.-Y., 2015. Cytoophidium assembly reflects upregulation of IMPDH activity. J. Cell Sci. 128, 3550–3555. doi:10.1242/jcs.175265

Chen, C., Chasin, L.A., 1998. Cointegration of DNA molecules introduced into mammalian cells by electroporation. Somat. Cell Mol. Genet. 24, 249–56.

Chung, C.T., Niemela, S.L., Miller, R.H., 1989. One-step preparation of competent Escherichia coli: transformation and storage of bacterial cells in the same solution. Proc. Natl. Acad. Sci. U. S. A. 86, 2172–5.

Cohen, G.B., Oprian, D.D., Robinson, P.R., 1992. Mechanism of activation and inactivation of opsin: role of Glu113 and Lys296. Biochemistry 31, 12592–601.

Cohen, S.N., Chang, A.C., Hsu, L., 1972. Nonchromosomal antibiotic resistance in bacteria: genetic transformation of Escherichia coli by R-factor DNA. Proc. Natl. Acad. Sci. U. S. A. 69, 2110–4.

Cong, L., Ran, F.A., Cox, D., Lin, S., Barretto, R., Habib, N., Hsu, P.D., Wu, X., Jiang, W., Marraffini, L. a, Zhang, F., 2013. Multiplex genome engineering using CRISPR/Cas systems. Science (80-.). 339, 819–23. doi:10.1126/science.1231143

Constantine, R., Zhang, H., Gerstner, C.D., Frederick, J.M., Baehr, W., 2012. Uncoordinated (UNC)119: coordinating the trafficking of myristoylated proteins. Vision Res. 75, 26–32. doi:10.1016/j.visres.2012.08.012

Cross, H.E., 2016. Hereditary Ocular Disease Database [WWW Document]. Hered. Ocul. Dis. Database. URL https://disorders.eyes.arizona.edu (accessed 6.3.16).

Cuenca, N., Lopez, S., Howes, K., Kolb, H., 1998. The localization of guanylyl cyclase-activating proteins in the mammalian retina. Invest. Ophthalmol. Vis. Sci. 39, 1243–1250.

Daiger, S.P., Bowne, S.J., Sullivan, L.S., 2015. Genes and Mutations Causing Autosomal Dominant Retinitis Pigmentosa. Cold Spring Harb. Perspect. Med. 5, 1–13. doi:10.1101/cshperspect.a017129

de Castro-Miró, M., Pomares, E., Lorés-Motta, L., Tonda, R., Dopazo, J., Marfany, G., Gonzàlez-Duarte, R., 2014. Combined Genetic and High-Throughput Strategies for Molecular Diagnosis of Inherited Retinal Dystrophies. PLoS One 9, e88410. doi:10.1371/journal.pone.0088410

Deaton, A., Bird, A., 2011. CpG islands and the regulation of transcription. Genes Dev. 25, 1010–1022. doi:10.1101/gad.2037511.1010

Dell'Orco, D., Sulmann, S., Zägel, P., Marino, V., Koch, K.-W.W., Z??gel, P., Marino, V., Koch, K.-W.W., 2014. Impact of cone dystrophy-related mutations in GCAP1 on a kinetic model of phototransduction. Cell. Mol. Life Sci. 71, 3829–3840. doi:10.1007/s00018-014-1593-4

den Hollander, A.I., Koenekoop, R.K., Mohamed, M.D., Arts, H.H., Boldt, K., Towns, K. V, Sedmak, T., Beer, M., Nagel-Wolfrum, K., McKibbin, M., Dharmaraj, S., Lopez, I., Ivings, L., Williams, G. a, Springell, K., Woods, C.G., Jafri, H., Rashid, Y., Strom, T.M., van der Zwaag, B., Gosens, I., Kersten, F.F.J., van Wijk, E., Veltman, J. a, Zonneveld, M.N., van Beersum,

S.E.C., Maumenee, I.H., Wolfrum, U., Cheetham, M.E., Ueffing, M., Cremers, F.P.M., Inglehearn, C.F., Roepman, R., 2007. Mutations in LCA5, encoding the ciliary protein lebercilin, cause Leber congenital amaurosis. Nat. Genet. 39, 889–95. doi:10.1038/ng2066

den Hollander, A.I., Roepman, R., Koenekoop, R.K., Cremers, F.P.M., 2008. Leber congenital amaurosis: genes, proteins and disease mechanisms. Prog Retin Eye Res 27, 391–419. doi:10.1016/j.preteyeres.2008.05.003

Dhup, S., Majumdar, S.S., 2008. Transgenesis via permanent integration of genes in repopulating spermatogonial cells in vivo. Nat. Methods 5, 601–603. doi:10.1038/nmeth.1225

Dizhoor, A.M., 2000. Regulation of cGMP synthesis in photoreceptors: role in signal transduction and congenital diseases of the retina. Cell Signal 12, 711–719. doi:10.1016/S0898-6568(00)00134-0

Dizhoor, A.M., Hurley, J.B., 1996. Inactivation of EF-hands makes GCAP-2 (p24) a constitutive activator of photoreceptor guanylyl cyclase by preventing a Ca2+-induced "activator-to-inhibitor" transition. J. Biol. Chem. 271, 19346–19350. doi:10.1074/jbc.271.32.19346

Dizhoor, A.M., Lowe, D.G., Olshevskaya, E. V., Laura, R.P., Hurley, J.B., 1994. The human photoreceptor membrane guanylyl cyclase, RetGC, is present in outer segments and is regulated by calcium and a soluble activator. Neuron 12, 1345–1352. doi:10.1016/0896-6273(94)90449-9

Dizhoor, A.M., Olshevskaya, E. V., Henzel, W.J., Wong, S.C., Stults, J.T., Ankoudinova, I., Hurley, J.B., 1995. Cloning, Sequencing, and Expression of a 24-kDa Ca2+-binding Protein Activating Photoreceptor Guanylyl Cyclase. J. Biol. Chem. 270, 25200–25206. doi:10.1074/jbc.270.42.25200

Doetschman, T., Gregg, R.G., Maeda, N., Hooper, M.L., Melton, D.W., Thompson, S., Smithies, O., 1987. Targetted correction of a mutant HPRT gene in mouse embryonic stem cells. Nature 330, 576–8. doi:10.1038/330576a0

Dokmanovic, M., Clarke, C., Marks, P. a, 2007. Histone deacetylase inhibitors: overview and perspectives. Mol. Cancer Res. 5, 981–9. doi:10.1158/1541-7786.MCR-07-0324

Dvir, L., Srour, G., Abu-Ras, R., Miller, B., Shalev, S.A., Ben-Yosef, T., 2010. Autosomal-recessive early-onset retinitis pigmentosa caused by a mutation in PDE6G, the gene encoding the gamma subunit of rod cGMP phosphodiesterase. Am. J. Hum. Genet. 87, 258–264. doi:10.1016/j.ajhg.2010.06.016

Ermilov, A.N., Olshevskaya, E. V, Dizhoor, A.M., 2001. Instead of binding calcium, one of the EF-hand structures in guanylyl cyclase activating protein-2 is required for targeting photoreceptor guanylyl cyclase. J. Biol. Chem. 276, 48143–8. doi:10.1074/jbc.M107539200

Fain, G.L., 2006. Why photoreceptors die (and why they don't). Bioessays 28, 344–354. doi:10.1002/bies.20382

Fain, G.L., Matthews, H.R., Cornwall, M.C., Koutalos, Y., 2001. Adaptation in vertebrate photoreceptors. Physiol. Rev. 81, 117–151. doi:10.1016/0896-6273(93)90123-9

Farber, D.B., 1995. From mice to men: the cyclic GMP phosphodiesterase gene in

vision and disease. The Proctor Lecture. Invest. Ophthalmol. Vis. Sci. 36, 263–75.

Felisbino, M.B., Tamashiro, W.M.S.C., Mello, M.L.S., 2011. Chromatin remodeling, cell proliferation and cell death in valproic acid-treated HeLa cells. PLoS One 6, e29144. doi:10.1371/journal.pone.0029144

Fesenko, E.E., Kolesnikov, S.S., Lyubarsky, A.L., 1985. Induction by cyclic GMP of cationic conductance in plasma membrane of retinal rod outer segment. Nature 313, 310–313.

French, J.B., Zhao, H., An, S., Niessen, S., Deng, Y., Cravatt, B.F., Benkovic, S.J., 2013. Hsp70/Hsp90 chaperone machinery is involved in the assembly of the purinosome. Proc. Natl. Acad. Sci. U. S. A. 110, 2528–2533. doi:10.1073/pnas.1300173110

Fu, Y., Yau, K.W., 2007. Phototransduction in mouse rods and cones. Pflugers Arch. Eur. J. Physiol. 454, 805–819. doi:10.1007/s00424-006-0194-y

Gaj, T., Gersbach, C. a, Barbas, C.F., 2013. ZFN, TALEN, and CRISPR/Cas-based methods for genome engineering. Trends Biotechnol. 31, 397–405. doi:10.1016/j.tibtech.2013.04.004

Gaszner, M., Felsenfeld, G., 2006. Insulators: exploiting transcriptional and epigenetic mechanisms. Nat. Rev. Genet. 7, 703–13. doi:10.1038/nrg1925

Gillespie, P.G., Beavo, J.A., 1988. Characterization of a bovine cone photoreceptor phosphodiesterase purified by cyclic GMP-sepharose chromatography. J. Biol. Chem. 263, 8133–41.

Gorczyca, W.A., Gray-Keller, M.P., Detwiler, P.B., Palczewski, K., 1994. Purification and physiological evaluation of a guanylate cyclase activating protein from retinal rods. Proc. Natl. Acad. Sci. U. S. A. 91, 4014–8. doi:10.1073/pnas.91.9.4014

Gross, O.P., Pugh, E.N., Burns, M.E., 2015. cGMP in mouse rods: the spatiotemporal dynamics underlying single photon responses. Front. Mol. Neurosci. 8, 1–10. doi:10.3389/fnmol.2015.00006

Gross, O.P., Pugh, E.N., Burns, M.E., 2012. Spatiotemporal cGMP dynamics in living mouse rods. Biophys. J. 102, 1775–1784. doi:10.1016/j.bpj.2012.03.035

Hamel, C.P., 2007. Cone rod dystrophies. Orphanet J. Rare Dis. 2, 1–7. doi:10.1186/1750-1172-2-7

Havugimana, P.C., Hart, G.T., Nepusz, T., Yang, H., Turinsky, A.L., Li, Z., Wang, P.I., Boutz, D.R., Fong, V., Phanse, S., Babu, M., Craig, S.A., Hu, P., Wan, C., Vlasblom, J., Dar, V.-N., Bezginov, A., Clark, G.W., Wu, G.C., Wodak, S.J., Tillier, E.R.M., Paccanaro, A., Marcotte, E.M., Emili, A., 2012. A census of human soluble protein complexes. Cell 150, 1068–1081. doi:10.1016/j.cell.2012.08.011

Hedstrom, L., 2009. IMP Dehydrogenase: Structure, Mechanism, and Inhibition. Chem. Rev. 109, 2903–2928. doi:10.1021/cr900021w

Hibbitt, O., Coward, K., Kubota, H., Prathalingham, N., Holt, W., Kohri, K., Parrington, J., 2006. In vivo gene transfer by electroporation allows expression of a fluorescent transgene in hamster testis and epididymal sperm and has no adverse effects upon testicular integrity or sperm quality. Biol. Reprod. 74, 95–101. doi:10.1095/biolreprod.105.042267

Howes, K.A., Pennesi, M.E., Sokal, I., Church-kopish, J., Schmidt, B., Margolis, D., Frederick, J.M., Rieke, F., Palczewski, K., Wu, S.M., Detwiler, P.B., Baehr, W., 2002. GCAP1 rescues rod photoreceptor response in GCAP1 / GCAP2 knockout mice 21, 1545–1554.

Huang, S.H., Pittler, S.J., Huang, X., Oliveira, L., Berson, E.L., Dryja, T.P., 1995. Autosomal recessive retinitis pigmentosa caused by mutations in the alpha subunit of rod cGMP phosphodiesterase. Nat. Genet. 11, 468–71. doi:10.1038/ng1295-468

Huang, Z., Tamura, M., Sakurai, T., Chuma, S., Saito, T., Nakatsuji, N., 2000. In vivo transfection of testicular germ cells and transgenesis by using the mitochondrially localized jelly ¢ sh £ uorescent protein gene 487, 248–251.

Huangfu, D., Maehr, R., Guo, W., Eijkelenboom, A., Snitow, M., Chen, A.E., Melton, D. a, 2008. Induction of pluripotent stem cells by defined factors is greatly improved by small-molecule compounds. Nat. Biotechnol. 26, 795–7. doi:10.1038/nbt1418

Hubley, M.J., Rosanske, R.C., Moerland, T.S., 1995. Diffusion coefficients of ATP and creatine phosphate in isolated muscle: pulsed gradient 31P NMR of small biological samples. NMR Biomed. 8, 72–8.

Hunt, D.M., Buch, P., Michaelides, M., 2010. Guanylate cyclases and associated activator proteins in retinal disease. Mol. Cell. Biochem. 334, 157–168. doi:10.1007/s11010-009-0331-y

Hwang, J.-Y., Koch, K.-W., 2002. The myristoylation of the neuronal Ca2+-sensors guanylate cyclase-activating protein 1 and 2. Biochim. Biophys. Acta - Proteins Proteomics 1600, 111–117. doi:10.1016/S1570-9639(02)00451-X

Hwang, J., Koch, K., 2002. Calcium- and Myristoyl-Dependent Properties of Guanylate Cyclase-Activating Protein-1 and Protein-2 †. Biochemistry 41, 13021–13028. doi:10.1021/bi026618y

Imai, Y., Matsushima, Y., Sugimura, T., Terada, M., 1991. A simple and rapid method for generating a deletion by PCR. Nucleic Acids Res. 19, 2785.

Jacobson, S.G., Cideciyan, A. V, Peshenko, I. V, Sumaroka, A., Olshevskaya, E. V, Cao, L., Schwartz, S.B., Roman, A.J., Olivares, M.B., Sadigh, S., Yau, K.-W., Heon, E., Stone, E.M., Dizhoor, A.M., 2013. Determining consequences of retinal membrane guanylyl cyclase (RetGC1) deficiency in human Leber congenital amaurosis en route to therapy: residual cone-photoreceptor vision correlates with biochemical properties of the mutants. Hum. Mol. Genet. 22, 168–183. doi:10.1093/hmg/dds421

Jaenisch, R., Mintz, B., 1974. Simian virus 40 DNA sequences in DNA of healthy adult mice derived from preimplantation blastocysts injected with viral DNA. Proc. Natl. Acad. Sci. U. S. A. 71, 1250–4.

Jiang, J., Promchan, K., Jiang, H., Awasthi, P., Marshall, H., Harned, A., Natarajan, V., 2016. Depletion of BBS Protein LZTFL1 Affects Growth and Causes Retinal Degeneration in Mice. J. Genet. Genomics 43, 381–391. doi:10.1016/j.jgg.2015.11.006

Jiang, L., Frederick, J.M., Baehr, W., 2014. RNA interference gene therapy in dominant retinitis pigmentosa and cone-rod dystrophy mouse models caused by GCAP1 mutations. Front. Mol. Neurosci. 7, 25. doi:10.3389/fnmol.2014.00025

Jiang, L., Wheaton, D., Bereta, G., Zhang, K., Palczewski, K., Birch, D.G., Baehr, W., 2008. A novel GCAP1(N104K) mutation in EF-hand 3 (EF3) linked to autosomal dominant cone dystrophy. Vision Res. 48, 2425–2432. doi:10.1016/j.visres.2008.07.016

Jinek, M., East, A., Cheng, A., Lin, S., Ma, E., Doudna, J., 2013. RNA-programmed genome editing in human cells. Elife 2, e00471. doi:10.7554/eLife.00471

Kamenarova, K., Corton, M., García-Sandoval, B., Fernández-San Jose, P., Panchev, V., Ávila-Fernández, A., López-Molina, M.I., Chakarova, C., Ayuso, C., Bhattacharya, S.S., 2013. Novel GUCA1A mutations suggesting possible mechanisms of pathogenesis in cone, cone-rod, and macular dystrophy patients. Biomed Res. Int. 2013. doi:10.1155/2013/517570

Karan, S., Frederick, J.M., Baehr, W., 2010. Novel functions of photoreceptor guanylate cyclases revealed by targeted deletion. Mol. Cell. Biochem. 334, 141–55. doi:10.1007/s11010-009-0322-z

Kawamura, S., Tachibanaki, S., 2008. Rod and cone photoreceptors: Molecular basis of the difference in their physiology. Comp. Biochem. Physiol. - A Mol. Integr. Physiol. 150, 369–377. doi:10.1016/j.cbpa.2008.04.600

Kennan, A., Aherne, A., Palfi, A., Humphries, M., McKee, A., Stitt, A., Simpson, D. a C., Demtroder, K., Orntoft, T., Ayuso, C., Kenna, P.F., Farrar, G.J., Humphries, P., 2002. Identification of an IMPDH1 mutation in autosomal dominant retinitis pigmentosa (RP10) revealed following comparative microarray analysis of transcripts derived from retinas of wild-type and Rho(-/-) mice. Hum. Mol. Genet. 11, 547–557.

Koch, K.-W., Dell'orco, D., 2013. A calcium-relay mechanism in vertebrate phototransduction. ACS Chem. Neurosci. 4, 909–17. doi:10.1021/cn400027z

Koch, K.-W., Stryer, L., 1988. Highly cooperative feedback control of retinal rod guanylate cyclase by calcium ions. Nature 334, 64–66.

Kohl, S., Coppieters, F., Meire, F., Schaich, S., Roosing, S., Brennenstuhl, C., Bolz, S., van Genderen, M.M., Riemslag, F.C.C., European Retinal Disease Consortium, Lukowski, R., den Hollander, A.I., Cremers, F.P.M., De Baere, E., Hoyng, C.B., Wissinger, B., 2012. A nonsense mutation in PDE6H causes autosomal-recessive incomplete achromatopsia. Am. J. Hum. Genet. 91, 527–532. doi:10.1016/j.ajhg.2012.07.006

Kojima, Y., Hayashi, Y., Kurokawa, S., Mizuno, K., Sasaki, S., Kohri, K., 2008. No evidence of germ-line transmission by adenovirus-mediated gene transfer to mouse testes. Fertil. Steril. 89, 1448–1454. doi:10.1016/j.fertnstert.2007.04.062

Kojima, Y., Sasaki, S., Umemoto, Y., Hashimoto, Y., Hayashi, Y., Kohri, K., 2003. Effects of Adenovirus Mediated Gene Transfer to Mouse Testis In Vivo on Spermatogenesis and Next Generation. J. Urol. 170, 2109–2114. doi:10.1097/01.ju.0000092898.91658.08

Kolandaivelu, S., Huang, J., Hurley, J.B., Ramamurthy, V., 2009. AIPL1, a protein associated with childhood blindness, interacts with alpha-subunit of rod phosphodiesterase (PDE6) and is essential for its proper assembly. J. Biol. Chem. 284, 30853–30861. doi:10.1074/jbc.M109.036780

Koller, B.H., Hagemann, L.J., Doetschman, T., Hagaman, J.R., Huang, S.,

Williams, P.J., First, N.L., Maeda, N., Smithies, O., 1989. Germ-line transmission of a planned alteration made in a hypoxanthine phosphoribosyltransferase gene by homologous recombination in embryonic stem cells. Proc. Natl. Acad. Sci. U. S. A. 86, 8927–31.

Krizaj, D., Copenhagen, D.R., 2002. Calcium regulation in photoreceptors. Front. Biosci. 7, d2023. doi:10.2741/krizaj

Krylov, D.M., Niemi, G.A., Dizhoor, A.M., Hurley, J.B., 1999. Mapping Sites in Guanylyl Cyclase Activating Protein-1 Required for Regulation of Photoreceptor Membrane Guanylyl Cyclases. J. Biol. Chem. 274, 10833–10839. doi:10.1074/jbc.274.16.10833

Kumar, R., Chen, S., Scheurer, D., Wang, Q.L., Duh, E., Sung, C.H., Rehemtulla, a, Swaroop, a, Adler, R., Zack, D.J., 1996. The bZIP transcription factor Nrl stimulates rhodopsin promoter activity in primary retinal cell cultures. J. Biol. Chem. 271, 29612–8.

Kwok, M.C.M., Holopainen, J.M., Molday, L.L., Foster, L.J., Molday, R.S., 2008. Proteomics of photoreceptor outer segments identifies a subset of SNARE and Rab proteins implicated in membrane vesicle trafficking and fusion. Mol. Cell. Proteomics 7, 1053–1066. doi:10.1074/mcp.M700571-MCP200

Laura, R.P., Dizhoor, A.M., Hurley, J.B., 1996. The Membrane Guanylyl Cyclase, Retinal Guanylyl Cyclase-1, Is Activated through Its Intracellular Domain. J. Biol. Chem. 271, 11646–11651. doi:10.1074/jbc.271.20.11646

Lem, J., Applebury, M.L., Falk, J.D., Flannery, J.G., Simon, M.I., 1991. Tissue-specific and developmental regulation of rod opsin chimeric genes in transgenic mice. Neuron 6, 201–210. doi:10.1016/0896-6273(91)90356-5

Lim, S., Dizhoor, A.M., Ames, J.B., 2014. Structural diversity of neuronal calcium sensor proteins and insights for activation of retinal guanylyl cyclase by GCAP1. Front. Mol. Neurosci. 7, 19. doi:10.3389/fnmol.2014.00019

Lim, S., Peshenko, I. V, Dizhoor, A.M., Ames, J.B., 2013. Structural Insights for Activation of Retinal Guanylate Cyclase by GCAP1. PLoS One 8, e81822. doi:10.1371/journal.pone.0081822

Lois, C., Hong, E.J., Pease, S., Brown, E.J., Baltimore, D., 2002. Germline transmission and tissue-specific expression of transgenes delivered by lentiviral vectors. Science (80-.). 295, 868–72. doi:10.1126/science.1067081

López-del Hoyo, N., 2014. Role of Guanylate Cyclase Activating Proteins in photoreceptor cells of the retina in health and disease. Doctoral Thesis. Universitat de Barcelona. doi:http://hdl.handle.net/10803/283566

López-del Hoyo, N., Fazioli, L., López-Begines, S., Fernández-Sánchez, L., Cuenca, N., Llorens, J., de la Villa, P., Méndez, A., 2012. Overexpression of guanylate cyclase activating protein 2 in rod photoreceptors in vivo leads to morphological changes at the synaptic ribbon. PLoS One 7, e42994. doi:10.1371/journal.pone.0042994

López-del Hoyo, N., López-Begines, S., Rosa, J.L., Chen, J., Méndez, A., 2014. Functional EF-hands in neuronal calcium sensor GCAP2 determine its phosphorylation state and subcellular distribution in vivo, and are essential for photoreceptor cell integrity. PLoS Genet. 10, e1004480. doi:10.1371/journal.pgen.1004480

Lowe, D.G., Dizhoor, A.M., Liu, K., Gu, Q., Spencer, M., Laura, R., Lu, L.,

Hurley, J.B., 1995. Cloning and expression of a second photoreceptor-specific membrane retina guanylyl cyclase (RetGC), RetGC-2. Proc. Natl. Acad. Sci. U. S. A. 92, 5535–9.

Lucas, K.A., Pitari, G.M., Kazerounian, S., Ruiz-Stewart, I., Park, J., Schulz, S., Chepenik, K.P., Waldman, S.A., 2000. Guanylyl cyclases and signaling by cyclic GMP. Pharmacol. Rev. 52, 375–414.

Makino, C.L., Wen, X.-H., Olshevskaya, E. V, Peshenko, I. V, Savchenko, A.B., Dizhoor, A.M., 2012. Enzymatic relay mechanism stimulates cyclic GMP synthesis in rod photoresponse: biochemical and physiological study in guanylyl cyclase activating protein 1 knockout mice. PLoS One 7, e47637. doi:10.1371/journal.pone.0047637

Mali, P., Yang, L., Esvelt, K.M., Aach, J., Guell, M., DiCarlo, J.E., Norville, J.E., Church, G.M., 2013. RNA-guided human genome engineering via Cas9. Science 339, 823–6. doi:10.1126/science.1232033

Marchion, D.C., Bicaku, E., Daud, A.I., Sullivan, D.M., Munster, P.N., 2005. Valproic Acid Alters Chromatin Structure by Regulation of Chromatin Modulation Proteins Valproic Acid Alters Chromatin Structure by Regulation of Chromatin Modulation Proteins 3815–3822.

Marie, S., Heron, B., Bitoun, P., Timmerman, T., Van Den Berghe, G., Vincent, M.F., 2004. AICA-ribosiduria: a novel, neurologically devastating inborn error of purine biosynthesis caused by mutation of ATIC. Am J Hum Genet 74, 1276–1281.

Matsuda, T., Cepko, C.L., 2004. Electroporation and RNA interference in the rodent retina in vivo and in vitro. Proc. Natl. Acad. Sci. U. S. A. 101, 16–22. doi:10.1073/pnas.2235688100

Mazelova, J., Astuto-Gribble, L., Inoue, H., Tam, B.M., Schonteich, E., Prekeris, R., Moritz, O.L., Randazzo, P. a, Deretic, D., 2009. Ciliary targeting motif VxPx directs assembly of a trafficking module through Arf4. EMBO J. 28, 183–92. doi:10.1038/emboj.2008.267

McCue, H. V, Haynes, L.P., Burgoyne, R.D., 2010. The diversity of calcium sensor proteins in the regulation of neuronal function. Cold Spring Harb. Perspect. Biol. 2, a004085. doi:10.1101/cshperspect.a004085

McLaughlin, M.E., Sandberg, M.A., Berson, E.L., Dryja, T.P., 1993. Recessive mutations in the gene encoding the beta-subunit of rod phosphodiesterase in patients with retinitis pigmentosa. Nat. Genet. 4, 130–4. doi:10.1038/ng0693-130

McLean, J.E., Hamaguchi, N., Belenky, P., Mortimer, S.E., Stanton, M., Hedstrom, L., 2004. Inosine 5'-monophosphate dehydrogenase binds nucleic acids in vitro and in vivo. Biochem J 379, 243–251.

Mendez, A., Burns, M.E., Sokal, I., Dizhoor, A.M., Baehr, W., Palczewski, K., Baylor, D.A., Chen, J., 2001. Role of guanylate cyclase-activating proteins (GCAPs) in setting the flash sensitivity of rod photoreceptors. Proc. Natl. Acad. Sci. 98, 9948–9953.

Mendez, A., Chen, J., 2002. Mouse models to study GCAP functions in intact photoreceptors. Adv. Exp. Med. Biol. 514, 361–388.

Molday, L.L., Djajadi, H., Yan, P., Szczygiel, L., Boye, S.L., Chiodo, V. a, Gregory-Evans, K., Sarunic, M. V, Hauswirth, W.W., Molday, R.S., 2013.

RD3 gene delivery restores guanylate cyclase localization and rescues photoreceptors in the Rd3 mouse model of Leber congenital amaurosis 12. Hum. Mol. Genet. 22, 3894–905. doi:10.1093/hmg/ddt244

Molday, L.L., Jefferies, T., Molday, R.S., 2014. Insights into the role of RD3 in guanylate cyclase trafficking, photoreceptor degeneration, and Leber congenital amaurosis. Front. Mol. Neurosci. 7, 1–6. doi:10.3389/fnmol.2014.00044

Mortimer, S.E., Hedstrom, L., 2005. Autosomal dominant retinitis pigmentosa mutations in inosine 5'-monophosphate dehydrogenase type I disrupt nucleic acid binding. Biochem J 390, 41–47. doi:10.1042/BJ20042051

Newbold, R.J., Deery, E.C., Payne, A.M., Wilkie, S.E., Hunt, D.M., Warren, M.J., 2002. Guanylate cyclase activating proteins, guanylate cyclase and disease. Adv. Exp. Med. Biol. 514, 411–438.

Newbold, R.J., Deery, E.C., Walker, C.E., Wilkie, S.E., Srinivasan, N., Hunt, D.M., Bhattacharya, S.S., Warren, M.J., 2001. The destabilization of human GCAP1 by a proline to leucine mutation might cause cone-rod dystrophy. Hum. Mol. Genet. 10, 47–54.

Nie, Z., Chen, S., Kumar, R., Zack, D.J., 1996. RER, an evolutionarily conserved sequence upstream of the rhodopsin gene, has enhancer activity. J. Biol. Chem. 271, 2667–75.

Nikonov, S.S., Kholodenko, R., Lem, J., Pugh, E.N., 2006. Physiological Features of the S- and M-cone Photoreceptors of Wild-type Mice from Single-cell Recordings. J. Gen. Physiol. 127, 359–374. doi:10.1085/jgp.200609490

Nishiguchi, K., Sokal, I., Yang, L., Roychowdhry, N., Palczewski, K., Berson, E.L., Dryja, T., Baehr, W., 2004. A Novel Mutation (I143NT) in Guanylate Cyclase-Activating Protein 1 (GCAP1) Associated with Autosomal Dominant Cone Degeneration. Invest. Ophthalmol. Vis. Sci. 45, 3863–3870. doi:10.3851/IMP2701.Changes

Okabe, M., Ikawa, M., Kominami, K., Nakanishi, T., Nishimune, Y., 1997. "Green mice" as a source of ubiquitous green cells. FEBS Lett. 407, 313–319.

Okawa, H., Sampath, A.P., Laughlin, S.B., Fain, G.L., 2008. ATP Consumption by Mammalian Rod Photoreceptors in Darkness and in Light. Curr. Biol. 18, 1917–1921. doi:10.1016/j.cub.2008.10.029

Old, W.M., Meyer-Arendt, K., Aveline-Wolf, L., Pierce, K.G., Mendoza, A., Sevinsky, J.R., Resing, K.A., Ahn, N.G., 2005. Comparison of label-free methods for quantifying human proteins by shotgun proteomics. Mol. Cell. Proteomics 4, 1487–1502. doi:10.1074/mcp.M500084-MCP200

Olshevskaya, E. V., Boikov, S., Ermilov, a., Krylov, D., Hurley, J.B., Dizhoor, a. M., 1999. Mapping Functional Domains of the Guanylate Cyclase Regulator Protein, GCAP-2. J. Biol. Chem. 274, 10823–10832. doi:10.1074/jbc.274.16.10823

Olshevskaya, E. V, Calvert, P.D., Woodruff, M.L., Peshenko, I. V, Savchenko, A.B., Makino, C.L., Ho, Y.-S.Y.-S.S., Fain, G.L., Dizhoor, A.M., 2004. The Y99C mutation in guanylyl cyclase-activating protein 1 increases intracellular Ca2+ and causes photoreceptor degeneration in transgenic mice. J. Neurosci. 24, 6078–6085. doi:10.1523/JNEUROSCI.0963-04.2004

Olshevskaya, E. V, Hughes, R.E., Hurley, J.B., Dizhoor, a M., 1997. Calcium

binding, but not a calcium-myristoyl switch, controls the ability of guanylyl cyclase-activating protein GCAP-2 to regulate photoreceptor guanylyl cyclase. J. Biol. Chem. 272, 14327–33.

Otto-Bruc, a E., Fariss, R.N., Van Hooser, J.P., Palczewski, K., 1998. Phosphorylation of photolyzed rhodopsin is calcium-insensitive in retina permeabilized by alpha-toxin. Proc. Natl. Acad. Sci. U. S. A. 95, 15014–9. doi:10.1073/pnas.95.25.15014

Palczewski, K., Sokal, I., Baehr, W., 2004. Guanylate cyclase-activating proteins: structure, function, and diversity. Biochem. Biophys. Res. Commun. 322, 1123–30. doi:10.1016/j.bbrc.2004.07.122

Palczewski, K., Subbaraya, I., Gorczyca, W.A., Helekar, B.S., Ruiz, C.C., Ohguro, H., Huang, J., Zhao, X., Crabb, J.W., Johnson, R.S., Walsh, K.A., Gray-Keller, M.P., Detwiler, P.B., Baehr, W., 1994. Molecular cloning and characterization of retinal photoreceptor guanylyl cyclase-activating protein. Neuron 13, 395–404. doi:10.1016/0896-6273(94)90355-7

Palmiter, R.D., Brinster, R.L., Hammer, R.E., Trumbauer, M.E., Rosenfeld, M.G., Birnberg, N.C., Evans, R.M., 1982. Dramatic growth of mice that develop from eggs microinjected with metallothionein-growth hormone fusion genes. Nature 300, 611–5.

Pannbacker, R., 1973. Control of guanylate cyclase activity in the rod outer segment. Science (80-.). 182, 1138–1140.

Parrington, J., Coward, K., Gadea, J., 2011. Sperm and testis mediated DNA transfer as a means of gene therapy. Syst. Biol. Reprod. Med. 57, 35–42. doi:10.3109/19396368.2010.514022

Payne, A.M., Downes, S.M., Bessant, D.A., Taylor, R., Holder, G.E., Warren, M.J., Bird, A.C., Bhattacharya, S.S., 1998. A mutation in guanylate cyclase activator 1A (GUCA1A) in an autosomal dominant cone dystrophy pedigree mapping to a new locus on chromosome 6p21.1. Hum. Mol. Genet. 7, 273–7.

Peng, G.-H., Chen, S., 2011. Active opsin loci adopt intrachromosomal loops that depend on the photoreceptor transcription factor network. Proc. Natl. Acad. Sci. U. S. A. 108, 17821–6. doi:10.1073/pnas.1109209108

Perrault, I., Estrada-Cuzcano, A., Lopez, I., Kohl, S., Li, S., Testa, F., Zekveld-Vroon, R., Wang, X., Pomares, E., Andorf, J., Aboussair, N., Banfi, S., Delphin, N., den Hollander, A.I., Edelson, C., Florijn, R., Jean-Pierre, M., Leowski, C., Megarbane, A., Villanueva, C., Flores, B., Munnich, A., Ren, H., Zobor, D., Bergen, A., Chen, R., Cremers, F.P.M., Gonzalez-Duarte, R., Koenekoop, R.K., Simonelli, F., Stone, E., Wissinger, B., Zhang, Q., Kaplan, J., Rozet, J.-M., 2013. Union makes strength: a worldwide collaborative genetic and clinical study to provide a comprehensive survey of RD3 mutations and delineate the associated phenotype. PLoS One 8, e51622. doi:10.1371/journal.pone.0051622

Perrault, I., Rozet, J.M., Calvas, P., Gerber, S., Camuzat, A., Dollfus, H., Châtelin, S., Souied, E., Ghazi, I., Leowski, C., Bonnemaison, M., Le Paslier, D., Frézal, J., Dufier, J.L., Pittler, S., Munnich, A., Kaplan, J., 1996. Retinal-specific guanylate cyclase gene mutations in Leber's congenital amaurosis. Nat. Genet. 14, 461–4. doi:10.1038/ng1296-461

Peshenko, I. V., Olshevskaya, E. V., Dizhoor, A.M., 2015. Dimerization domain of

retinal membrane guanylyl cyclase 1 (RetGC1) is an essential part of guanylyl cyclase-activating protein (GCAP) binding interface. J. Biol. Chem. 290, 19584–19596. doi:10.1074/jbc.M115.661371

Peshenko, I. V., Olshevskaya, E. V., Dizhoor, A.M., 2004. Ca2+-dependent conformational changes in guanylyl cyclase-activating protein 2 (GCAP-2) revealed by site-specific phosphorylation and partial proteolysis. J. Biol. Chem. 279, 50342–50349. doi:10.1074/jbc.M408683200

Peshenko, I. V., Olshevskaya, E. V., Lim, S., Ames, J.B., Dizhoor, A.M., 2014. Identification of Target Binding Site in Photoreceptor Guanylyl Cyclase-activating Protein 1 (GCAP1). J. Biol. Chem. 289, 10140–54. doi:10.1074/jbc.M113.540716

Peshenko, I. V., Olshevskaya, E. V., Lim, S., Ames, J.B., Dizhoor, A.M., 2012. Calcium-myristoyl Tug is a new mechanism for intramolecular tuning of calcium sensitivity and target enzyme interaction for guanylyl cyclase-activating protein 1: dynamic connection between N-fatty acyl group and EF-hand controls calcium sensitivity. J. Biol. Chem. 287, 13972–84. doi:10.1074/jbc.M112.341883

Peshenko, I. V, Dizhoor, A.M., 2007. Activation and inhibition of photoreceptor guanylyl cyclase by guanylyl cyclase activating protein 1 (GCAP-1): the functional role of Mg2+/Ca2+ exchange in EF-hand domains. J. Biol. Chem. 282, 21645–52. doi:10.1074/jbc.M702368200

Peshenko, I. V, Dizhoor, A.M., 2004. Guanylyl cyclase-activating proteins (GCAPs) are Ca2+/Mg2+ sensors: implications for photoreceptor guanylyl cyclase (RetGC) regulation in mammalian photoreceptors. J. Biol. Chem. 279, 16903–6. doi:10.1074/jbc.C400065200

Peshenko, I. V, Olshevskaya, E. V, Dizhoor, A.M., 2015. Evaluating the Role of Retinal Guanylyl Cyclase 1 (RetGC1) Domains In Binding Guanylyl Cyclase Activating Proteins (GCAP)., The Journal of biological chemistry. doi:10.1074/jbc.M114.629642

Peshenko, I. V, Olshevskaya, E. V, Dizhoor, A.M., 2012. Interaction of GCAP1 with retinal guanylyl cyclase and calcium: sensitivity to fatty acylation. Front. Mol. Neurosci. 5, 19. doi:10.3389/fnmol.2012.00019

Peshenko, I. V, Olshevskaya, E. V, Savchenko, A.B., Karan, S., Palczewski, K., Baehr, W., Dizhoor, A.M., 2011. Enzymatic properties and regulation of the native isozymes of retinal membrane guanylyl cyclase (RetGC) from mouse photoreceptors. Biochemistry 50, 5590–5600. doi:10.1021/bi200491b

Pimkin, M., Markham, G.D., 2008. The CBS subdomain of inosine 5'-monophosphate dehydrogenase regulates purine nucleotide turnover. Mol. Microbiol. 68, 342–59. doi:10.1111/j.1365-2958.2008.06153.x

Posokhova, E., Song, H., Belcastro, M., Higgins, L., Bigley, L.R., Michaud, N.A., Martemyanov, K.A., Sokolov, M., 2011. Disruption of the chaperonin containing TCP-1 function affects protein networks essential for rod outer segment morphogenesis and survival. Mol. Cell. Proteomics 10, M110.000570. doi:10.1074/mcp.M110.000570

Preising, M.N., Hausotter-Will, N., Solbach, M.C., Friedburg, C., Ruschendorf, F., Lorenz, B., 2012. Mutations in RD3 are associated with an extremely rare and severe form of early onset retinal dystrophy. Invest. Ophthalmol. Vis. Sci. 53,

3463–3472. doi:10.1167/iovs.12-9519

Pugh, E.N., Lamb, T.D., 1990. Cyclic GMP and calcium: the internal messengers of excitation and adaptation in vertebrate photoreceptors. Vision Res. 30, 1923–48.

Qi, L.S., Larson, M.H., Gilbert, L.A., Doudna, J.A., Weissman, J.S., Arkin, A.P., Lim, W.A., 2013. Repurposing CRISPR as an RNA-Guided Platform for Sequence-Specific Control of Gene Expression. Cell 152, 1173–1183. doi:10.1016/j.cell.2013.02.022

Quiambao, A.B., Peachey, N.S., Mangini, N.J., Rohlich, P., Hollyfield, J.G., al-Ubaidi, M.R., 1997. A 221-bp fragment of the mouse opsin promoter directs expression specifically to the rod photoreceptors of transgenic mice. Vis Neurosci 14, 617–625.

Ramamurthy, V., Niemi, G.A., Reh, T.A., Hurley, J.B., 2004. Leber congenital amaurosis linked to AIPL1: a mouse model reveals destabilization of cGMP phosphodiesterase. Proc Natl Acad Sci U S A 101, 13897–13902.

Rodieck, R.W., 1998. The First Steps in Seeing, 1st ed. Sinauer Associates, Inc., Sunderland, MA.

Sakamoto, K., McCluskey, M., Wensel, T.G., Naggert, J.K., Nishina, P.M., 2009. New mouse models for recessive retinitis pigmentosa caused by mutations in the Pde6a gene. Hum Mol Genet 18, 178–192.

Sambrook, J., Russel, D.W., 2001. Molecular Cloning. A laboratory Manual. Cold Spring Harbor Laboratory Press.

Sato, M., Nakazawa, M., Usui, T., Tanimoto, N., Abe, H., Ohguro, H., 2005. Mutations in the gene coding for guanylate cyclase-activating protein 2 (GUCA1B gene) in patients with autosomal dominant retinal dystrophies. Graefes Arch. Clin. Exp. Ophthalmol. 243, 235–42. doi:10.1007/s00417-004-1015-7

Scholten, A., Koch, K.-W., 2011. Differential Calcium Signaling by Cone Specific Guanylate Cyclase-Activating Proteins from the Zebrafish Retina. PLoS One 6, e23117. doi:10.1371/journal.pone.0023117

Schröder, T., Lilie, H., Lange, C., Schro, T., 2011. The myristoylation of guanylate cyclase-activating protein-2 causes an increase in thermodynamic stability in the presence but not in the absence of Ca^{2+}. Protein Sci. 20, 1155–1165. doi:10.1002/pro.643

Shang, T., Zhang, X., Wang, T., Sun, B., Deng, T., Han, D., 2011. Toll-like receptor-initiated testicular innate immune responses in mouse Leydig cells. Endocrinology 152, 2827–36. doi:10.1210/en.2011-0031

Sharma, R.K., Duda, T., 2014. Membrane guanylate cyclase, a multimodal transduction machine: history, present, and future directions. Front. Mol. Neurosci. 7, 56. doi:10.3389/fnmol.2014.00056

Sheffield, V.C., 2010. The blind leading the obese: the molecular pathophysiology of a human obesity syndrome. Trans. Am. Clin. Climatol. Assoc. 121, 172–182.

Shin, J.-B., Streijger, F., Beynon, A., Peters, T., Gadzala, L., McMillen, D., Bystrom, C., Van der Zee, C.E.E.M., Wallimann, T., Gillespie, P.G., 2007. Hair bundles are specialized for ATP delivery via creatine kinase. Neuron 53, 371–86. doi:10.1016/j.neuron.2006.12.021

Shyjan, A.W., de Sauvage, F.J., Gillett, N.A., Goeddel, D. V, Lowe, D.G., 1992. Molecular cloning of a retina-specific membrane guanylyl cyclase. Neuron 9, 727–37.

Sistermans, E.A., de Kok, Y.J., Peters, W., Ginsel, L.A., Jap, P.H., Wieringa, B., 1995. Tissue- and cell-specific distribution of creatine kinase B: a new and highly specific monoclonal antibody for use in immunohistochemistry. Cell Tissue Res. 280, 435–446.

Sokal, I., Alekseev, A., Palczewski, K., 2003. Photoreceptor guanylate cyclase variants: cGMP production under control. Acta Biochim Pol 50, 1075–1095.

Sokal, I., Li, N., Surgucheva, I., Warren, M.J., Payne, A.M., Bhattacharya, S.S., Baehr, W., Palczewski, K., 1998. GCAP1 (Y99C) mutant is constitutively active in autosomal dominant cone dystrophy. Mol. Cell 2, 129–33.

Southern, E.M., 1975. Detection of specific sequences among DNA fragments separated by gel electrophoresis. J. Mol. Biol. 98, 503–17.

Spellicy, C.J., Daiger, S.P., Sullivan, L.S., Zhu, J., Liu, Q., Pierce, E. a, Bowne, S.J., 2007. Characterization of retinal inosine monophosphate dehydrogenase 1 in several mammalian species. Mol. Vis. 13, 1866–1872.

Stephen, R., Bereta, G., Golczak, M., Palczewski, K., Sousa, M.C., 2007. Stabilizing function for myristoyl group revealed by the crystal structure of a neuronal calcium sensor, guanylate cyclase-activating protein 1. Structure 15, 1392–402. doi:10.1016/j.str.2007.09.013

Stief, A., Winter, D.M., Stratling, W.H., Sippel, A.E., Edgeworth, J., Freemont, P., Hogg, N., 1989. A nuclear DNA attachment element mediates elevated and position-independent gene activity. Nature 341, 343–345. doi:10.1038/340301a0

Stone, E.M., 2007. Leber Congenital Amaurosis-A Model for Efficient Genetic Testing of Heterogeneous Disorders: LXIV Edward Jackson Memorial Lecture. Am. J. Ophthalmol. 144, 791–811. doi:10.1016/j.ajo.2007.08.022

Tam, L.C.S., Kiang, A.-S., Campbell, M., Keaney, J., Farrar, G.J., Humphries, M.M., Kenna, P.F., Humphries, P., 2010. Prevention of autosomal dominant retinitis pigmentosa by systemic drug therapy targeting heat shock protein 90 (Hsp90). Hum. Mol. Genet. 19, 4421–4436. doi:10.1093/hmg/ddq369

Tam, L.C.S., Kiang, A.S., Kennan, A., Kenna, P.F., Chadderton, N., Ader, M., Palfi, A., Aherne, A., Ayuso, C., Campbell, M., Reynolds, A., Mckee, A., Humphries, M.M., Farrar, G.J., Humphries, P., 2008. Therapeutic benefit derived from RNAi-mediated ablation of IMPDH1 transcripts in a murine model of autosomal dominant retinitis pigmentosa (RP10). Hum Mol Genet 17, 2084–2100. doi:10.1093/hmg/ddn107

Thiadens, A.A., den Hollander, A.I., Roosing, S., Nabuurs, S.B., Zekveld-Vroon, R.C., Collin, R.W., De Baere, E., Koenekoop, R.K., van Schooneveld, M.J., Strom, T.M., van Lith-Verhoeven, J.J., Lotery, A.J., van Moll-Ramirez, N., Leroy, B.P., van den Born, L.I., Hoyng, C.B., Cremers, F.P., Klaver, C.C., 2009. Homozygosity mapping reveals PDE6C mutations in patients with early-onset cone photoreceptor disorders. Am J Hum Genet 85, 240–247.

Thomas, E.C., Gunter, J.H., Webster, J. a, Schieber, N.L., Oorschot, V., Parton, R.G., Whitehead, J.P., 2012. Different characteristics and nucleotide binding properties of inosine monophosphate dehydrogenase (IMPDH) isoforms.

PLoS One 7, e51096. doi:10.1371/journal.pone.0051096
Thomas, K.R., Capecchi, M.R., 1987. Site-directed mutagenesis by gene targeting in mouse embryo-derived stem cells. Cell 51, 503–12.
Tsang, S.H., Gouras, P., Yamashita, C.K., Kjeldbye, H., Fisher, J., Farber, D.B., Goff, S.P., 1996. Retinal degeneration in mice lacking the gamma subunit of the rod cGMP phosphodiesterase. Science 272, 1026–9.
Tummala, P., Mali, R.S., Guzman, E., Zhang, X., Mitton, K.P., 2010. Temporal ChIP-on-Chip of RNA-Polymerase-II to detect novel gene activation events during photoreceptor maturation. Mol. Vis. 16, 252–71.
Usmani, A., Ganguli, N., Sarkar, H., Dhup, S., Batta, S.R., Vimal, M., Ganguli, N., Basu, S., Nagarajan, P., Majumdar, S.S., 2013. A non-surgical approach for male germ cell mediated gene transmission through transgenesis. Sci. Rep. 3, 3430. doi:10.1038/srep03430
Wallimann, T., Dolder, M., Schlattner, U., Eder, M., Hornemann, T., O'Gorman, E., Rück, a, Brdiczka, D., 1998. Some new aspects of creatine kinase (CK): compartmentation, structure, function and regulation for cellular and mitochondrial bioenergetics and physiology. Biofactors 8, 229–34.
Wang, H., Yang, H., Shivalila, C.S., Dawlaty, M.M., Cheng, A.W., Zhang, F., Jaenisch, R., 2013. One-Step Generation of Mice Carrying Mutations in Multiple Genes by CRISPR/Cas-Mediated Genome Engineering. Cell 153, 910–918. doi:10.1016/j.cell.2013.04.025
Wang, X.T., Mion, B., Aherne, A., Engel, P.C., 2011. Molecular recruitment as a basis for negative dominant inheritance? Propagation of misfolding in oligomers of IMPDH1, the mutated enzyme in the RP10 form of retinitis pigmentosa. Biochim. Biophys. Acta - Mol. Basis Dis. 1812, 1472–1476. doi:10.1016/j.bbadis.2011.07.006
Weichman, K., Chaillet, J.R., 1997. Phenotypic variation in a genetically identical population of mice. Mol. Cell. Biol. 17, 5269–74.
Wen, X.-H., Dizhoor, A.M., Makino, C.L., 2014. Membrane guanylyl cyclase complexes shape the photoresponses of retinal rods and cones. Front. Mol. Neurosci. 7, 45. doi:10.3389/fnmol.2014.00045
Wensel, T.G., 2008. Signal transducing membrane complexes of photoreceptor outer segments. Vis. Res 48, 2052–2061. doi:10.1016/j.visres.2008.03.010
Wilkie, S.E., Newbold, R.J., Deery, E., Walker, C.E., Stinton, I., Ramamurthy, V., Hurley, J.B., Bhattacharya, S.S., Warren, M.J., Hunt, D.M., 2000. Functional characterization of missense mutations at codon 838 in retinal guanylate cyclase correlates with disease severity in patients with autosomal dominant cone-rod dystrophy. Hum. Mol. Genet. 9, 3065–73. doi:10.1093/hmg/9.20.3065
Wilmut, I., Schnieke, A.E., McWhir, J., Kind, A.J., Campbell, K.H., 1997. Viable offspring derived from fetal and adult mammalian cells. Nature 385, 810–3. doi:10.1038/385810a0
Woodruff, M.L., Olshevskaya, E. V, Savchenko, A.B., Peshenko, I. V, Barrett, R., Bush, R.A., Sieving, P.A., Fain, G.L., Dizhoor, A.M., 2007. Constitutive excitation by Gly90Asp rhodopsin rescues rods from degeneration caused by elevated production of cGMP in the dark. J Neurosci 27, 8805–8815.
Xu, D., Cobb, G., Spellicy, C.J., Bowne, S.J., Daiger, S.P., Hedstrom, L., 2008.

Retinal isoforms of inosine 5???-monophosphate dehydrogenase type 1 are poor nucleic acid binding proteins. Arch. Biochem. Biophys. 472, 100–104. doi:10.1016/j.abb.2008.02.012

Yang, H., Wang, H., Shivalila, C.S., Cheng, A.W., Shi, L., Jaenisch, R., 2013. One-step generation of mice carrying reporter and conditional alleles by CRISPR/Cas-mediated genome engineering. Cell 154, 1370–9. doi:10.1016/j.cell.2013.08.022

Yang, R.B., Foster, D.C., Garbers, D.L., Fülle, H.J., 1995. Two membrane forms of guanylyl cyclase found in the eye. Proc. Natl. Acad. Sci. U. S. A. 92, 602–6.

Yau, K.W., Hardie, R.C., 2009. Phototransduction Motifs and Variations. Cell 139, 246–264. doi:10.1016/j.cell.2009.09.029

Yu, C., Zhao, H., Pugh, R.J., Pedley, A.M., French, J., Jones, S. a, Zhuang, X., Jinnah, H., Huang, T.J., Benkovic, S.J., 2014. Purinosome formation as a function of the cell cycle. Proc. Natl. Acad. Sci. 112, 1368–1373. doi:10.1073/pnas.1423009112

Zack, D.J., Bennett, J., Wang, Y., Davenport, C., Klaunberg, B., Gearhart, J., Nathans, J., 1991. Unusual topography of bovine rhodopsin promoter-IacZ fusion gene expression in transgenic mouse retinas. Neuron 6, 187–199. doi:10.1016/0896-6273(91)90355-4

Zeuner, M., Bieback, K., Widera, D., 2015. Controversial role of toll-like receptor 4 in adult stem cells. Stem Cell Rev. Reports 11, 621–634. doi:10.1007/s12015-015-9589-5

Zhang, H., Constantine, R., Frederick, J.M., Baehr, W., 2012. The prenyl-binding protein PrBP/δ: A chaperone participating in intracellular trafficking. Vision Res. 75, 19–25. doi:10.1016/j.visres.2012.08.013

Zhang, H., Constantine, R., Vorobiev, S., Chen, Y., Seetharaman, J., Huang, Y.J., Xiao, R., Montelione, G.T., Gerstner, C.D., Davis, M.W., Inana, G., Whitby, F.G., Jorgensen, E.M., Hill, C.P., Tong, L., Baehr, W., 2011. UNC119 is required for G protein trafficking in sensory neurons. Nat. Neurosci. 14, 874–80. doi:10.1038/nn.2835

Zhang, Q., Nishimura, D., Vogel, T., Shao, J., Swiderski, R., Yin, T., Searby, C., Carter, C.S., Kim, G., Bugge, K., Stone, E.M., Sheffield, V.C., 2013. BBS7 is required for BBSome formation and its absence in mice results in Bardet-Biedl syndrome phenotypes and selective abnormalities in membrane protein trafficking. J. Cell Sci. 126, 2372–2380. doi:10.1242/jcs.111740

Zhao, H., Chiaro, C.R., Zhang, L., Smith, P.B., Chan, C.Y., Pedley, A.M., Pugh, R.J., French, J.B., Patterson, A.D., Benkovic, S.J., 2015. Quantitative analysis of purine nucleotides indicates that purinosomes increase de Novo purine biosynthesis. J. Biol. Chem. 290, 6705–6713. doi:10.1074/jbc.M114.628701

Zhao, H., French, J.B., Fang, Y., Benkovic, S.J., 2013. The purinosome, a multi-protein complex involved in the de novo biosynthesis of purines in humans. Chem. Commun. 49, 4444. doi:10.1039/c3cc41437j

Zulliger, R., Naash, M.I., Rajala, R.V.S., Molday, R.S., Azadi, S., 2015. Impaired association of retinal degeneration-3 with guanylate cyclase-1 and guanylate cyclase-activating protein-1 leads to leber congenital amaurosis-1. J. Biol. Chem. 290, 3488–99. doi:10.1074/jbc.M114.616656

Acknowledgements

Acknowledgements

First, I would like to express my sincere gratitude to my advisor Dra. Ana Méndez for the continuous support of my Ph.D study and related research, for his patience, motivation, and immense knowledge. His guidance helped me in all the time of research and writing of this thesis.

Special mention is deserved my labmates during these hard years of work. Years of hard work but also fun and talks. Thanks to Natalia, Lucrezia and Anna, with labmates as well, with its extraordinary capacity for sacrifice and work, everything has been easier. We also thank the master students: Amélia, Sergi, Ari and Francesc, who despite of his short stay, they have helped me in uncountless experiments.

I cannot forget my other lab partners, the whole group of Dr. Gorostiza: Merce, Nuria, Silvia, Aida, Miquel, Maria Isabel, Ariadna and Antonio, and their latest additions, Alex and Rosalba. My sincere congratulations for your work and thanks for making it easier and bearable the toughest stages of research.

I would also like to thank all members of the Department of Experimental Therapeutics and Pathology and the Department of Physiological Sciences, who along with those named above are my little scientific family in Barcelona.

This work has not been possible without the assistance of members of CCiTUB. I acknowledge the expert assistance with size exclusion chromatography of Drs. Isidre Casal and Esther Miralles at the Separative techniques Unit; expert assistance with proteomics analysis of Drs. Josep Maria Estanyol and María José Fidalgo at Proteomic Unit; and the expert assistance with the Biacore system of Dr. Marta Taulés at the Citometry Unit of the Scientific and Technological Services of the University of Barcelona (CCiT-UB). We kindly acknowledge the excellent technical assistance of Dr. Benjamín Torrejón with image acquisition at the Leica TCS-SL at the CCiT-UB. We are in debt with Dr. Alvaro Gimeno at the Vivarium facility for his assistance with the rabbit immunization protocol for generation of antibodies and his training and expertise in surgery protocols for mice. We are very grateful to the kind veterinarian staff at Mercabarna, for giving us access to their laboratory space for bovine eye *in situ* processing immediately postmortem.

I cannot express in words everything that I owe my life mate Loreto, *la que jala de mi cuando caigo,* for their understanding, support, patience and intellectual stimulation throughout all these years. Without her everything would have been more difficult.

Last but not the least, I would like to thank my family: my parents and to my sisters, Angela and Celia, for supporting me spiritually throughout writing this thesis and my life in general. Also thank to all my family and friends that one way or another have helped me in all my life to get here.

Appendix

Appendix

Appendix I. Transfected cells by subretinal electroporation

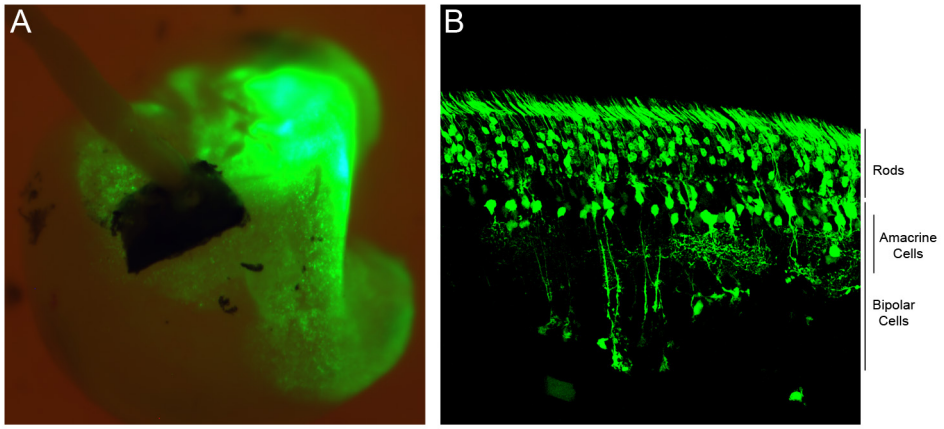

Figure Appendix I.1. Representative efficiency of transfection obtained by subretinal electroporation. A. Eye-cup of an electroporated retina with GFP coding plasmid under UV-light. B. Cross-section of a retina electroporated with a plasmid encoding GFP. Photoreceptor cells layer, bipolar cells prolongations and amacrine cells are distinguishable.

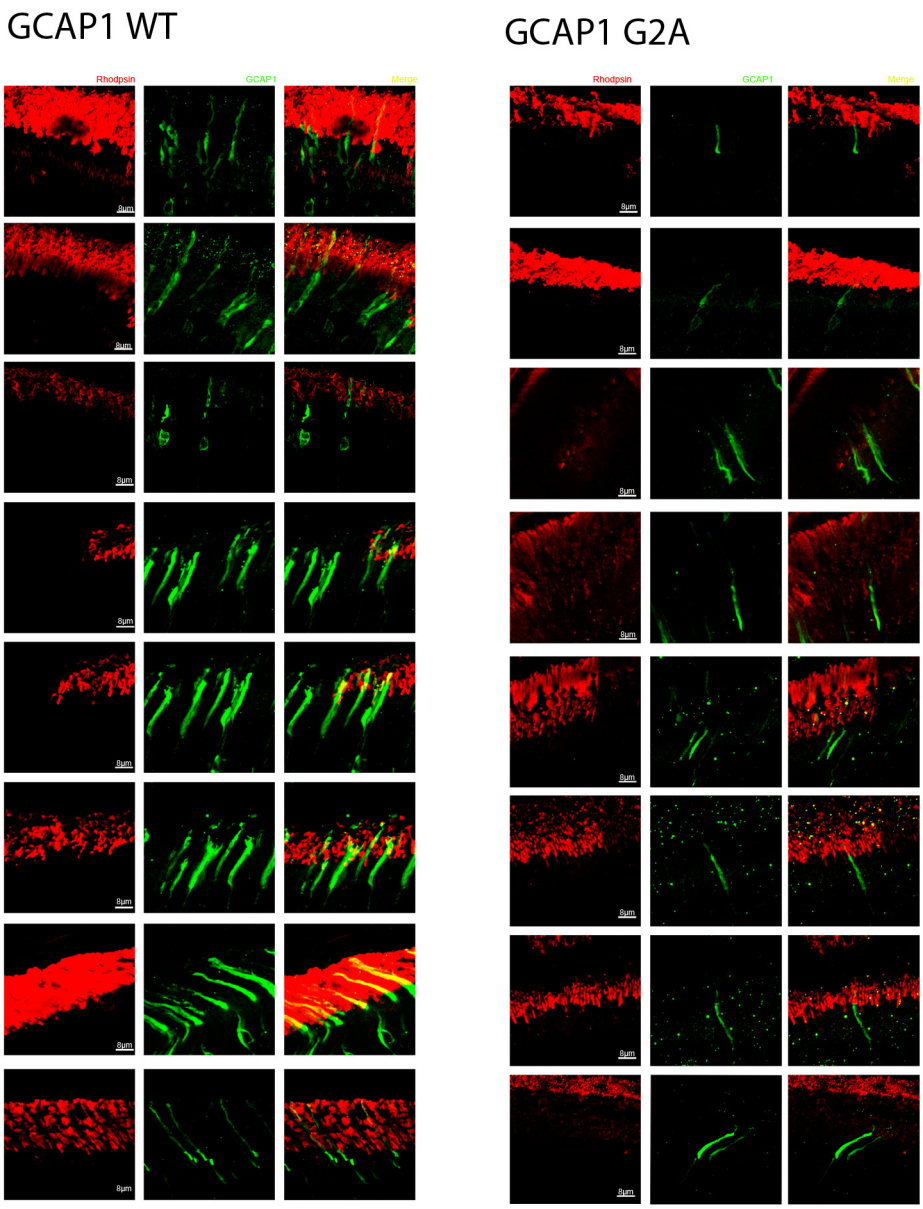

Figure Appendix I.2. Analyzed cells for GCAP1_WT and G2A.

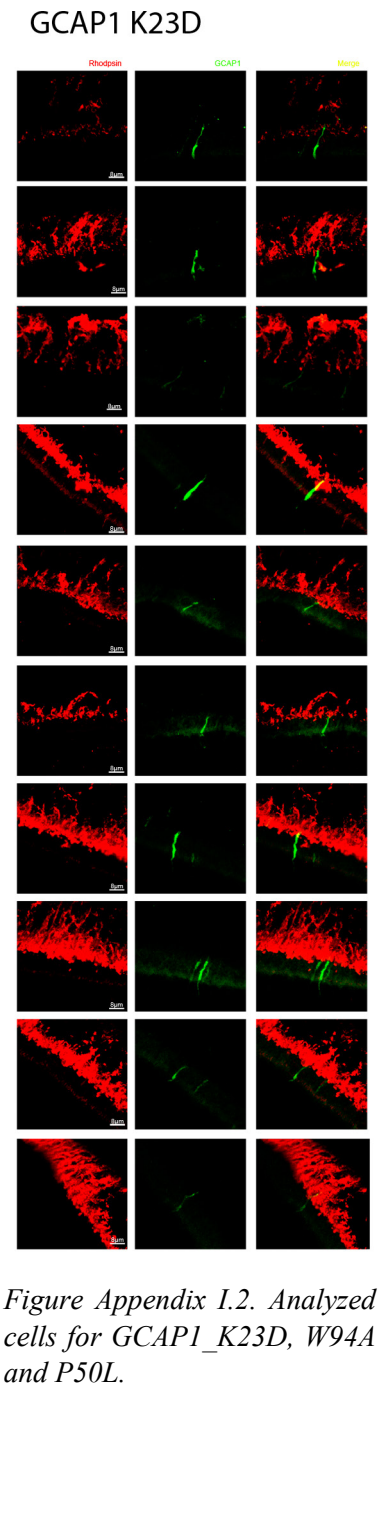

Figure Appendix I.2. Analyzed cells for GCAP1_K23D, W94A and P50L.

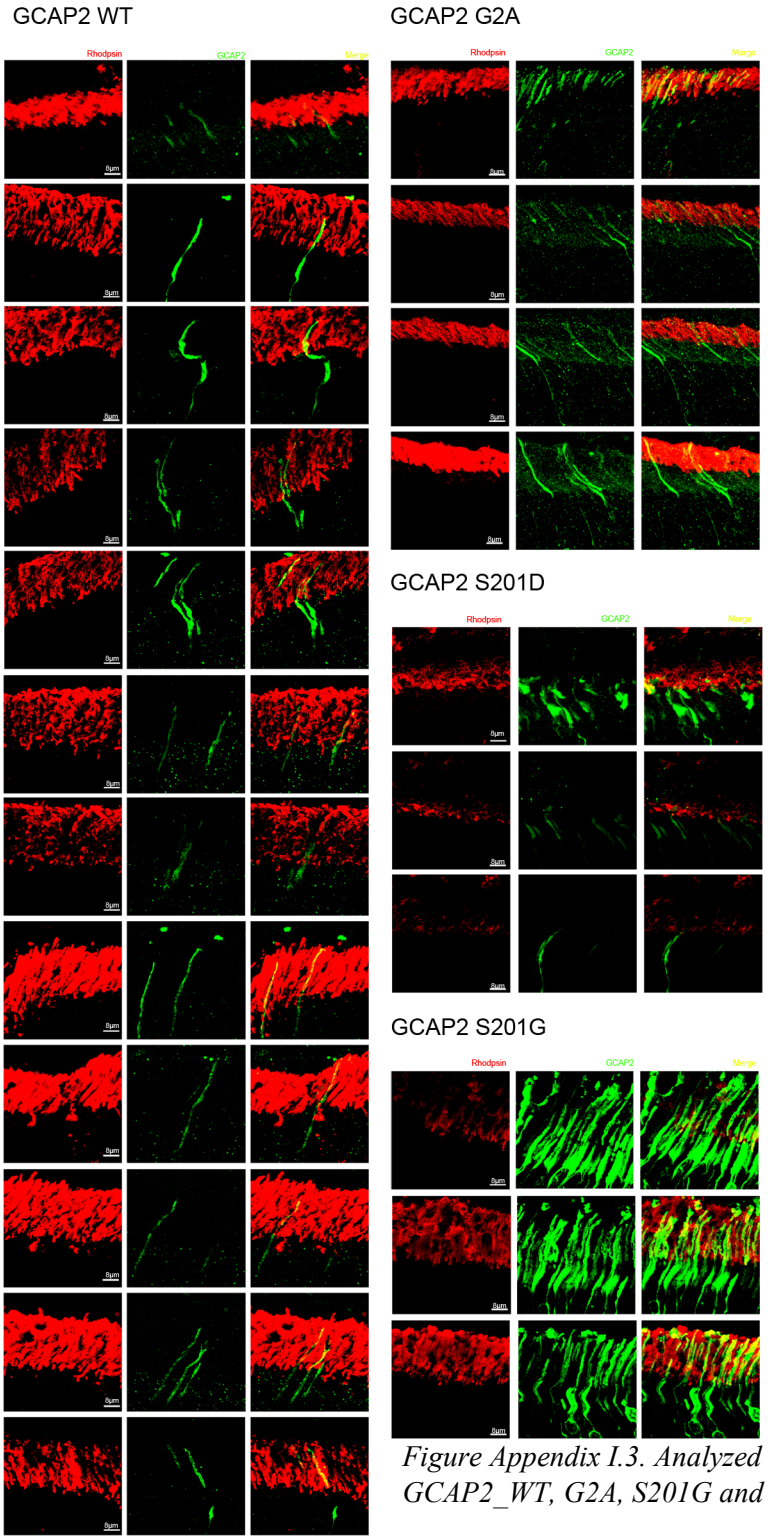

Figure Appendix I.3. Analyzed cells for GCAP2_WT, G2A, S201G and S201D.

GCAP2 G161R

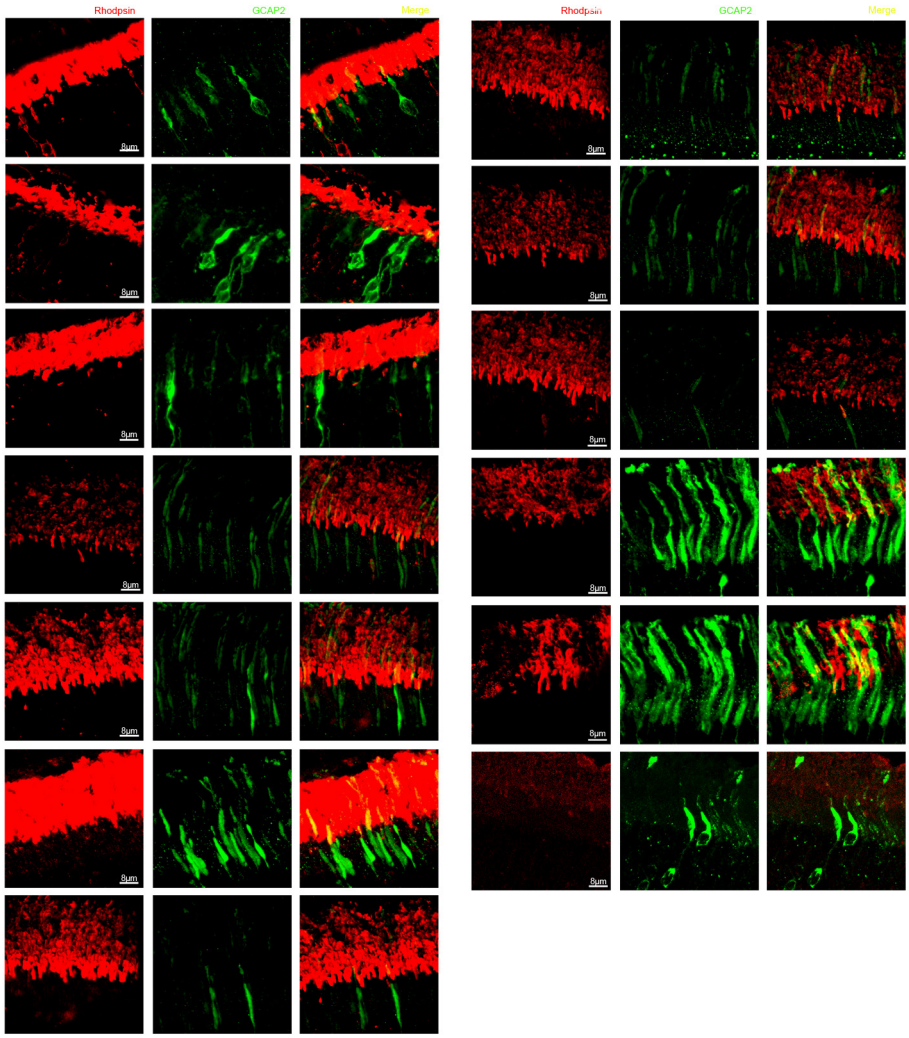

Figure Appendix I.4. Analyzed cells for GCAP2_G161R.

Appendix II. Primer List

Appendix II. Primers List		
ID	**Name**	**Sequence**
P1	Rh1.1	GTGCCTGGAGTTGCGCTGTGGG
P2	p24_rv	TGGCCTCCTCGTTGTCCGGGACCTT
P3	pL_UG_Fw	GGGGTTGGCGAGTGTGTTTTGTGA
P4	pL_UG_Rv	GGTGGTGCAGATGAACTTCAGGGT
P5	EGFP_NheI_Fw	GCGATCAGATCTATGGTGAGCAAGGG CGAGGAGCTG
P6	EGFP_BglII_Rv	GCGATCGCTAGCTTACTTGTACAGCTC GTCCATGCC
P8	DsRed_KpnI_Rv	GCATGCGGTACCCTAAGACAGGAACA GGTGGTGGCG
P9	2Kb_ups_MOP_del_Fw	CCATTCTCTCCCTGGGTCAGCC
P10	T7_Rv	GGTACCCTATAGTGAGTCGTATTA
P11	CpG_MOP_Del_Fw	GGAGAAGTGAATTTAGGGCCCAAGGG
P12	CpG_MOP_Del_Rv	GCAGGAGGGGCGTAAGAAGTTTTGC
P13	Fw_CpG_KpnI	GCGATCGGTACCTTTTAATCTGCTGTTT GCTCACAT
P14	Rv_CpG_XbaI	GCGATCTCTAGACAGTCAATATGTTCA CCCCAAAAA
P15	KpnI_HS4_Fw	GCGCCCGGTACC CTGTCATTCTAAATCTCTCTTTCA
P16	KpnI_HS4_Rv	GCATATGGTACCTCGACTCTAGAGGGA CAGCCCCCC
P17	EagI_HS4_Fw	GCGCCCCGGCCGCTGTCATTCTAAATC TCTCTTTCA
P18	EagI_HS4_Rev	GCATATCGGCCGTCGACTCTAGAGGG ACAGCCCCCC
P19	hGCAP1_Fw	GCATGCCTCGAGATGGGCAACGTGAT GGAGGGAAAGTCAGTG
P20	hGCAP1_Rv	GCATGCGGATCCTCAGCCGGCTGCCT CAGCGGCCTCGTCAGC

P21	GCAP2_G2A_Fw	GGGCCAGGATGGCGCAGCAGTTCAG
P22	GCAP2_G2A_Rv	CTGAACTGCTGCGCCATCCTGGCCC
P23	GCAP2_G161R_Fw	CCTTCTGGTGGATGAAAATCGAGATGG TCAGCTG
P24	GCAP2_G161R_Rv	CAGCTGACCATCTCGATTTTCATCCAC CAGAAGG
P25	GCAP2_S201G_Fw	GATCTCTCAGCAGAGGCGGAAAGATG CCATGTTCTGAG
P26	GCAP2_S201G_Rv	CTCAGAACATGGCATCTTTCCGCCTCT GCTGAGAGATC
P27	GCAP2_S201D_Fw	CTCAGCAGAGGCGGAAAGGTGCCATG TTC
P28	GCAP2_S201D_Rv	GAACATGGCACCTTTCCGCCTCTGCTG AG
P29	GCAP1_G2A_Fw	CCTCCATCACGTTGGCCATCTCGAGGC TG
P30	GCAP1_G2A_Rv	CAGCCTCGAGATGGCCAACGTGATGG AGG
P31	GCAP1_K23D_Fw	GAGTGCCACCAGTGGTACGACAAGTTC ATGACTGAGTGC
P32	GCAP1_K23D_Rv	GCACTCAGTCATGAACTTGTCGTACCA CTGGTGGCACTC
P33	GCAP1_P50L_Fw	AAGAACCTGAGCCTGTCGGCCAGCCA G
P34	GCAP1_P50L_Rv	CTGGCTGGCCGACAGGCTCAGGTTCTT
P35	GCAP1_W94A_Fw	GTGGAACAGAAGCTCCGCGCGTACTTC AAGCTCTATGA
P36	GCAP1_W94A_Rv	TCATAGAGCTTGAAGTACGCGCGGAGC TTCTGTTCCAC
P37	Fw_bIMPDH1_NdeI	GCATGCCATATGGCGGACTACCTGATC AGCGGCGGC
P38	Rv_bIMPDH1_BamHI	GGCTTGGGATCCTCAGTACAGCCGCTT CTCGTAAG
P39	Fw_BglII_pET32_bIMPDH1_5	GCATGC CAGATCTG GCGGACTACCTGATCAGCGGCGGC

P40	Rv_XhoI_pET32_bIMPDH1_5	GGCTTG CTCGAG TCAGTACAGCCGCTTCTCGTAAG
P41	Fw_bIMPDH1-CBS deletion	CAGCTGCTGTGCGGGGCGGCTGTG
P42	Rv_bIMPDH1-CBS deletion	AAATTTCTTGACCTTCCGCACCTC
P43	bIMPDH1_N198K_Rv	CTGCGCTGCAGAATCTCCTTTGCCTCTTTCAATGTT
P44	bIMPDH1_R105W_Fw	TCCAGGCCAATGAGGTGTGGAAGGTCAAGAAATTT
P45	bIMPDH1_N198K_Fw	AACATTGAAAGAGGCAAAGGAGATTCTGCAGCGCAG
P46	bIMPDH1_R105W_Rv	AAATTTCTTGACCTTCCACACCTCATTGGCCTGGA
P47	bIMPDH1_R224P_Fw	TGGCCATCATTGCCCCCACTGACCTGAAGAAGAACC
P48	bIMPDH1_R224P_Rv	GGTTCTTCTTCAGGTCAGTGGGGGCAATGATGGCCA
P49	bIMPDH1_D226N_Fw	TGGCCATCATTGCCCGCACTAACCTGAAGAAGAACC
P50	bIMPDH1_D226N_Rv	GGTTCTTCTTCAGGTTAGTGCGGGCAATGATGGCCA
P51	T3	ATTAACCCTCACTAAAG
P52	T7	TAATACGACTCACTATAGGG
P53	T7_terminator	GCTAGTTATTGCTCAGCGG
P54	SP6	ATTTAGGTGACACTATAG
P55	CpG-CMV-Fv	CAATAGGGACTTTCCATTG

Appendix III. List of Antibodies used

Appendix III. List of Antibodies used						
Primary Antibodies						
Protein	**Reference**	**Brand**	**Clonal**	**Host**	**Dilution WB**	**Dilution IHC**
GCAP1	MA1-724	Thermo Scientific	monoclonal	mouse	1:2000	1:500
GCAP2	MA1-725	Thermo Scientific	monoclonal	mouse	1:2000	1:500
GCAP1			polyclonal	rabbit	1:2000	1:100
GCAP2			polyclonal	rabbit	1:2000	1:100
Rhodopsin			Monoclonal 1D4	mouse	1:10000	1:8000
IMPDH1	MABN291	Millipore	monoclonal	mouse	1:2000	DW
IMPDH1			polyclonal	rabbit	1:5000-10000	1:500
CKB	HM2110	Hycult	Monoclonal 21E10	mouse	1:10000	1:5000
CKB	GTX62373	Genetex	Monoclonal EPR3927	rabbit	1:2000	1:500
RetGC			polyclonal	rabbit	1:2000	1:200
RetGC			polyclonal	rabbit	1:2000	1:200
GFP	11 814 460 001	Roche	Monoclonal 7.1&13.1	mouse	1:2000	NT
Tranducin alpha			polyclonal	rabbit	1:5000	**NT**
HSP90	PA3-013	ThermoScientific	polyclonal	rabbit	1:2000	DW
14-3-3	ab14110	Abcam	Monoclonal 3F7			
NT: Non Tested. DW: Don't Work						

Secondary Antibodies				
Host	***Specificity***	***Ligand***	***Dilution***	***Brand***
Donkey	*rabbit*	*IRDye680*	*1:5000-25000*	*LI-COR Biosciences*
Donkey	*rabbit*	*IRDye800*	*1:5000-25000*	*LI-COR Biosciences*
Goat	*mouse*	*IRDye680*	*1:5000-25000*	*LI-COR Biosciences*
Goat	*mouse*	*IRDye800*	*1:5000-25000*	*LI-COR Biosciences*
	Protein G	*IRDye800*	*1:5000*	*Rockland Immunochemicals*
Donkey	*rabbit*	*Alexa488*	*1:500*	*LifeTechnologies*
Donkey	*rabbit*	*Alexa555*	*1:500*	*LifeTechnologies*
Donkey	*rabbit*	*Alexa647*	*1:500*	*LifeTechnologies*
Goat	*mouse*	*Alexa488*	*1:500*	*LifeTechnologies*
Goat	*mouse*	*Alexa555*	*1:500*	*LifeTechnologies*
Goat	*mouse*	*Alexa647*	*1:500*	*LifeTechnologies*

Appendix IV. List of Abbreviations

Abbreviations

A	
AICART	Aminoimidazolecarbox- Amide Ribonucleotide Transformylase
AIRS	Aminoimidazole Ribonucleotide Synthetase
AMP	Adenosine Monophosphate
ASL	Adenylosuccinate Lyase
ATIC	Bifunctional enzyme composed of AICART And IMPCH
ATP	Adenosine Triphosphate
B	
BBSome	Complex of Seven Bardet–Biedl Syndrome (BBS) Proteins
BSA	Bovine Serum Albumin
C	
Ca2+	Calcium Ion
CAIRS	Carboxyaminoimidazole Ribonucleotide Synthase (CAIRS)
CBS	Cystathione-B-Synthase Domain
CC	Connecting Cilium
CD	Cyclase Domain
CD	Cone Dystrophy
cDNA	Complementary DNA
CEP290	Centrosomal Protein 290kda
cGMP	Cyclic Guanosine Monophosphate
CKB	Creatine Kinase Brain-Type
CKM	Creatine Kinase Muscle-Type
CORD	Cone-Rod Dystrophy
CpG	Regions of DNA where a cytosine nucleotide is followed by a guanine nucleotide
Cr	Creatine
CRISPR/Cas9	Clustered Regularly Interspaced Short Palindromic Re peats/Cas9 Nuclease
Crx	Cone-Rod Homeobox Gene
C-Term	Carboxyl-Terminal

D	
DD	Dimerization Domain Of Retgc1
Dsred	*Discosoma* Sp. Red Fluorescent Protein
DTT	Dithiothreitol
E	
ECD	Extracellular Domain Of Retgc1
EDTA	Ethylene Diamine Tetra acetic Acid
EGTA	Ethylene Glycol Tetra acetic Acid
F	
FGAMS	Formylglycinamidine Ribonucleotide Synthase
G	
GAP	GTP-ase-Activating Proteins
GARS	Glycinamide Ribonucleotide Synthetase
GCAP1	Guanylyl Cyclase Activating Protein 1
GCAP2	Guanylyl Cyclase Activating Protein 2
GCAPs	Guanylyl Cyclase Activating Proteins
GDP	Guanosine Diphosphate
GEF	Guanine Nucleotide Exchange Factors
GMP	Guanosine Monophosphate
GRK1-7	Rhodopsin Kinase
GTP	Guanosine Triphosphate
Gαβγ	A, β and γ subunits of Transduncin
Gβ5	Atypical G Protein β Subunit
H	
HDAC	Histone Deacetylase
HEPES	2-[4-(2-Hydroxyethyl)Piperazin-1-Yl]Ethanesulfonic Acid
HGPRT	Hypoxanthine Guanine Phophoribosyl Transferase
HS4	Felsenfeld Insulator At The 5' End Of The Chicken Beta Globin Locus
I	
ICFO	Institut De Ciencies Fotoniques
IMP	Inosine Monophosphate
IMPCH	Inosine Monophosphate Cyclohydrolase
IMPDH1	Inosine Monophosphate Dehydrogenase 1

IS	Inner Segment
J	
JMD	Junction Membrane Domain
K	
Kd	Dissociation Constant
KDa	Kilo Dalton
KHD	Kinase-Homolog Domain
KO	Knock-Out
L	
LCA	Leber Congenital Amaurosis
LCA5	Lebercilin
M	
MAR	Matrix-Attachment Region
Mg2+	Magnesium
mM	Mili Molar
MOP	Mouse Opsin Promoter
Myr	Myristoyl Group
N	
Na+	Sodium
Na2CO3	Sodium Bicarbonate
Nacl	Sodium Chloride
NAD+	Nicotinamide Adenine Dinucleotide
NaFl	Sodium Flouride
NaH2PO4	Sodium Phosphate
NCS	Neuronal Calcium Sensor
nM	Nanomolar
Nrl	Neural Retina Leucine Zipper
O	
ONL	Outer Nuclear Layer
OPL	Outer Plexiform Layer
OS	Outer Segment

P	
PAICS	Bifunctional Enzyme (PAICS) which is composed of Carboxyaminoimidazole Ribonucleotide Synthase (CAIRS) and Succinoaminoimidazolecarboxamide Ribonucleotide Synthetase (SAICARS)
PBS	Phosphate Buffered Saline
PCr	Phosphocreatine
PCR	Polymerase Chain Reaction
PDE	Phosphodiesterase
PDE6	Phosphodiesterase 6
PLA	Proximity Ligation Assay
PMSF	Phenylmethanesulfonylfluoride
PPAT	Phosphoribosylpyrophosphate Amido- Transferase
PPRP	Phophoribosyl Pirophosphate
PrBP/δ	Gene Product of PDE6
R	
R9AP	RGS9 Anchoring Protein
RD3	Retinal Degeneration 3
RER	Rhodopsin Enhancer Region
RetGC1	Retinal Guanylate Cyclase 1
RGS9	Regulator Of G-Protein Signaling 9
ROI	Region of Interest
RP	Retinitis Pigmentosa
RPE	Retinal Pigmented Epithelium
RPGR	Retinitis Pigmentosa GTP-ase Regulator
RPGRIP1	Retinitis Pigmentosa GTP-ase Regulator Interacting Protein 1
RPPR	Rhodopsin Proximal Promoter Region
S	
SAICARS	Succinoaminoimidazolecarboxamide Ribonucleotide Synthetase
sGC	Soluble Guanylate Cyclase
SMGT	Sperm-Mediated Gene Transfer
SP	Signal Peptide
SPR	Surface Plasmon Resonance
T	
TALEN	Transcription Activator-Like Effector Nucleases

TM	Transmembrane Domain
TMGT	Testi-Mediated Gene Transfer
TOPORS	TOP1 Binding Arginine/Serine Rich Protein
TrifGART	Trifunctional Enzyme (TGART) which is composed of Glycinamide Ribonucleotide Synthetase (GARS), GAR Formyltransferase (GART) And Aminoimidazole Ribonucleotide Synthetase (AIRS)
Trx	Thioredoxin
TSS	Transcription Start Site
TULP1	Tubby Like Protein 1
U	
uMT-CK	Ubiquitous Mitochondrial Creatine Kinase
UNC119	Protein Unc-119 Homolog
UV	Ultraviolet Light
V	
VPA	Valproic Acid
W	
WB	Western Blot
WT	Wildtype
X	
XlRP	Chromosome X-Linked Retinitis Pigmentosa
XMP	Xanthine Monophosphate
Z	
ZFN	Zinc-Finger Nuclease